

LIBRARY
Michigan State
University

This is to certify that the
dissertation entitled

**ENZYMES AND GENES INVOLVED IN BIOSYNTHESIS OF
PLANT LIPID POLYESTERS**

presented by

MARIA ISABEL MOLINA

has been accepted towards fulfillment
of the requirements for the

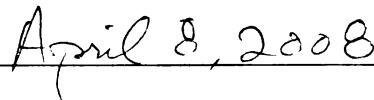
PH.D.

degree in

Plant Biology



Major Professor's Signature



Date

PLACE IN RETURN BOX to remove this checkout from your record.
TO AVOID FINES return on or before date due.
MAY BE RECALLED with earlier due date if requested.

DATE DUE	DATE DUE	DATE DUE

**ENZYMES AND GENES INVOLVED IN BIOSYNTHESIS OF PLANT LIPID
POLYESTERS**

By

Maria Isabel Molina

A DISSERTATION

**Submitted to
Michigan State University
in partial fulfillment of the requirements
for the degree of**

DOCTOR OF PHILOSOPHY

Department of Plant Biology

2008

ABSTRACT

ENZYMES AND GENES INVOLVED IN BIOSYNTHESIS OF PLANT LIPID POLYESTERS

By

Maria Isabel Molina

All higher plants depend on extra cellular lipophilic barriers that control the movement of water, solutes, and gases, and that provide an interface with the biotic and abiotic environment. Cutin and suberin are polyesters of fatty acids that constitute the polymeric matrices of these barriers. Because of their structural complexity and intractability, progress in understanding the structure, enzymology and genetics of lipid polyesters has been limited. Overall, the goal of this study was to identify genes and enzymes involved in the biosynthesis of these biopolymers using the model plant, *Arabidopsis thaliana*. To aid this goal, a new method was developed for the quantitative analysis of lipid polyester monomers in seeds. Monomers typical of both cutin and suberin were found and most of these monomers are deposited in the seed coat. Distinct temporal patterns of accumulation of individual monomers were observed at different stages of Brassica seed development. Promoter-YFP fusions of cutin and suberin associated genes revealed distinct spatial patterns of expression in seed coat cell layers. Evidence from these studies support the presence of a suberized layer deposited on the outer integument, and of a cutin-like polyester layer associated with the inner integument of the seed coat.

The method developed for seed polyester analysis allowed a reverse-genetics approach that was suitable for screening for genes involved in either cutin or/and suberin biosynthesis. Candidate genes were selected using bioinformatic approaches including transcript co-expression analysis. Among the mutants of preferred genes, a knockout mutant of a cytochrome P450-dependent ω -oxidase gene, *cyp86A1*, showed major reductions in ω -oxidized suberin monomers thereby demonstrating its involvement in suberin biosynthesis. This finding was further substantiated by TEM analysis of suberized cell walls. Furthermore, this approach was useful to identify a novel acyl-transferase of the BAHD family that is involved in the deposition of ferulate in Arabidopsis suberin. The monomer phenotype of this mutant suggests that the disrupted gene encodes a feruloyl-CoA transferase, the first such enzyme discovered in plants.

In addition, this research work used *in planta* overexpression approaches to explore the function of two orthologous P450 enzymes; ATT1 from Arabidopsis and PH1 from petunia stigmas. The interchange of these genes was expected to complement the *att1* mutant and increase the production of ω -hydroxy fatty acids in tobacco stigma polyesters. However, transgenic plants failed to accumulate higher levels of ω -hydroxy fatty acids. Although the current assumption is that ATT1 catalyzes the ω -hydroxylation step leading to synthesis of cutin precursors, results suggest that they may be able to catalyze further oxidation steps to produce dicarboxylic acids. The hypothesis of the existence of a “metabolon” for polyester synthesis was tested. The combination of these results has provided new insights on how CYP86A enzymes may function *in vivo*.

Copyright by
Maria Isabel Molina
2008

ACKNOWLEDGEMENTS

The accomplishment of this dissertation was possible thanks to the many people both from the scientific community and outside of the academic environment. I thank my advisor, John Ohlrogge, for accepting me into his lab, and for his unconditional support over the years. He has been a fantastic mentor, both scientifically and personally. I consider myself very fortunate for having another great mentor, Mike Pollard. Mike devoted hours and hours of his time to teach me about lipid biochemistry. Through challenging questions, he taught me how to think as a scientist. From John and Mike I learnt how to approach problems related to plant biology from different but complementary perspectives, and this combination is reflected throughout this dissertation. Besides my advisors, I would like to thank the rest of my thesis committee: Christoph Benning, Kevin Walker, and Ray Hammerschmidt. They have given their time to read this manuscript and have also offered valuable advice during my graduate career at MSU.

Colleagues at the Ohlrogge lab have immensely collaborated with my research, generously sharing their scientific expertise with me and offering critical comments and suggestions that helped me establish the overall direction of my work. Besides being great scientific collaborators, I truly enjoyed the time we spent together. For this, I thank Katrin Weber, Fred Beisson, Yonghua Li, Phil Bates, Doug Allen, Tim Durrett, Jilian Fan, Deborah dos Santos, Mi Chang Suh, Weili Yang, Shannon Bell, Greg Tilton, Kjell Stalverg, Ajay Tumaney, Joerg

Schwender, and Dezi Elzinga. My thanks also to a former member of the lab, Gustavo Bonaventure, for co-authoring my first paper. To Alicia Pastor, and Melinda Frame, for their invaluable assistance with the Electron and Laser Confocal microscopes.

I specially thank my husband, Alejandro, for his patience, support, and constant encouragement. He gave me the strength and confidence to continue in this journey even in the difficult times. My thanks to my family in Argentina and friends at MSU. In particular, I want to express my gratitude to Carol Ohlrogge and Nori Pollard for making us feel part of their families.

Finally, I would like to acknowledge Phytochemistry and The Plant Journal for their permission for reproducing previously copyrighted material in Chapters 2 and 3, respectively. Research in this thesis has partly been supported by the Fulbright Association, the Department of Plant Biology at MSU, the Graduate School at MSU and a USDA grant. Their support is gratefully acknowledged.

TABLE OF CONTENTS

LIST OF TABLES.....	XI
LIST OF FIGURES	XII
CHAPTER 1	1
INTRODUCTION.....	1
Objectives	5
The biopolymers cutin and suberin	6
Structure, functions, and location	6
Chemical composition.....	9
Depolymerization and analysis of monomers	13
Biosynthesis	18
A. Biosynthesis and assembly of aliphatic polyesters	18
B. Bioynthesis and assembly of the suberin polyaromatic domain....	28
Cutin and suberin: major questions	29
Seed coats	30
Seed coats structure in Brassicaceae	30
Functions of the seed coat.....	33
Lipid polyesters in seed coats.....	34
Lipid polyesters in stigma exudates	35
CHAPTER 2	39
THE LIPID POLYESTER COMPOSITION OF <i>ARABIDOPSIS THALIANA</i> AND <i>BRASSICA NAPUS</i> SEEDS	39
ABSTRACT.....	40
INTRODUCTION	41
RESULTS AND DISCUSSION	44
Monomer analysis methods – introduction	44
Characterization of monomer analysis methods.....	46
Monomer analysis methods - identification and quantification of monomers.....	56
Identification of 9,10,18-trihydroxyoctadecenoate	62
Identification of branched-chain monomers	63
Analysis of <i>Arabidopsis thaliana</i> seeds	70
Analysis of Brassica napus Wild Type Seeds.....	72
Distribution of Monomers between Seed Coat and Embryo in <i>Brassica</i> <i>napus</i> seeds	75
CONCLUSION.....	79
EXPERIMENTAL PROCEDURES	80

Plant material.....	80
Sample delipidation of seeds.....	81
Methanolysis with sodium methoxide	82
Additional depolymerization methods	82
Hydrogenation	83
Preparation of trimethylsilyl and acetyl derivatives	84
GC-MS and GC-FID analysis	84
TAG separation and analysis.....	85
Identification of branched alcohols	86
CHAPTER 3	87
LIPID POLYESTER DEPOSITION AND LOCALIZATION IN DEVELOPING SEEDS	
OF <i>BRASSICA NAPUS</i> AND <i>ARABIDOPSIS THALIANA</i>	87
ABSTRACT.....	88
INTRODUCTION	89
RESULTS	92
Lipid polyester monomers are deposited from mid-maturation onwards	
in developing <i>Brassica napus</i> seeds	92
Extractable wax accumulation in developing <i>Brassica napus</i> seeds	97
Localization of polyesters in chalazal and non-chalazal regions of	
<i>Brassica</i> seeds	99
Analysis of the <i>ap2-7</i> <i>Arabidopsis</i> mutant distinguishes outer and inner	
integument polyester monomer contributions	99
Seeds of the <i>Arabidopsis thaliana</i> mutants <i>fatB</i> , <i>gpat5</i> and <i>att1</i> have	
abnormal lipid polyester monomer loads compared to wild type seeds	
.....	101
Lipid polyesters, but not extractable waxes, influence seed coat	
permeability to tetrazolium salts	107
Promoter-YFP reporter analysis of biosynthetic genes suggest different	
localization of polyester layers in the developing seed coat	110
DISCUSSION	115
Seed structure and development.....	117
Suberin monomers are preferentially localized to the outer integument	
of the seed coat	118
Cutin monomers are preferentially localized to the inner integument of	
the seed coat	122
EXPERIMENTAL PROCEDURES.....	124
Plant material.....	124
Lipid analysis	125
Tetrazolium salt penetration assay	126
Construct design and <i>Arabidopsis</i> transformation	127
Microscopy	128
CHAPTER 4	130

IDENTIFICATION AND FUNCTIONAL ANALYSIS OF CANDIDATE GENES FOR	
LIPID POLYESTER BIOSYNTHESIS	130
ABSTRACT.....	131
INTRODUCTION	132
RESULTS AND DISCUSSION	134
Identification of candidate genes for polyester biosynthesis	134
P450-Fatty acid oxidases	140
Acyl-CoA-utilizing acyltransferases	158
Characterization of at5g41040 knockouts.....	162
Long chain acyl-CoA synthetases (LACS).....	175
CONCLUSIONS	181
EXPERIMENTAL PROCEDURES.....	182
Plant materials and growth conditions	182
Bioinformatics	183
Mutant isolation	184
Reverse Transcription Polymerase Chain Reaction (RT-PCR)	185
YFP reporter construct design and plant transformation	187
Transmission electron microscopy	187
 CHAPTER 5	 189
<i>IN PLANTA</i> HETEROLOGOUS EXPRESSION APPROACH TO UNDERSTAND THE	
FUNCTION OF CYP86A PROTEINS	189
ABSTRACT.....	190
INTRODUCTION	191
Plant fatty acid omega-hydroxylases	192
Soluble lipid polyesters from “wet” stigmas.....	196
RESULTS	201
Characterization of Arabidopsis <i>att1</i> mutants	201
Complementation of <i>att1</i> mutants with the ω -hydroxylase PH1 from	
Petunia stigmas	210
Lipid polyester phenotype of transgenic lines.....	213
Over-expression of At4g00360 (ATT1) in stigmas of <i>Nicotiana tabacum</i>	
.....	215
Analysis of Petunia PH1-RNAi lines. Is there a metabolon involved in	
stigma polyester assembly?	219
DISCUSSION	225
What is the biochemical reaction catalyzed by ATT1?	227
EXPERIMENTAL PROCEDURES.....	234
Binary constructs for tobacco transformation.....	234
Binary constructs for complementation of <i>att1</i> mutants	237
<i>Agrobacterium</i> transformation	238
Generation of transgenic tobacco lines by <i>Agrobacterium</i> transformation	
.....	238
Transformation of <i>A. thaliana att1</i> mutants.....	239
Reverse Transcription Polymerase Chain Reaction (RT-PCR)	239

Stigma fatty acid analysis	240
Cutin analysis	241
Analysis of Petunia RNAi stigma lipids	241
CHAPTER 6	243
CONCLUSIONS AND FUTURE DIRECTIONS	243
Conclusions on seed lipid polyester characterization	244
Directions for further research on seed coat extracellular lipids	248
Conclusions on the role of P450 monooxygenases on lipid polyester monomer modification	249
Directions for further research on P450 monooxygenases	252
Conclusions on preliminary characterization of a mutant of the BAHD family involved in suberin synthesis.....	254
Directions for further research on acylCoA-utilizing acyltransferases.....	256
APPENDICES.....	262
APPENDIX A.....	263
Additional components released by transmethylation of <i>B. napus</i> and Arabidopsis delipidated samples	263
APPENDIX B.....	266
Correlated expression between lipid polyester related genes and candidate genes	266
APPENDIX C.....	268
Developing seeds microarray expression data.....	268
APPENDIX D.....	269
Fatty acid elongases	269
LITERATURE CITED	273

LIST OF TABLES

TABLE 1. COMPOSITIONAL COMPARISON BETWEEN CUTIN AND SUBERIN.	11
TABLE 2. MONOMER COMPOSITION FOR THE DEPOLYMERIZATION OF SOLVENT-EXTRACTED WILD TYPE <i>ARABIDOPSIS THALIANA</i> SEED RESIDUES BY NaOMe-CATALYZED TRANSMETHYLATION	51
TABLE 3. MASS SPECTRAL DATA FOR REPRESENTATIVE MAJOR MONOMERS IN <i>ARABIDOPSIS</i> SEED POLYESTERS.....	58
TABLE 4. MONOMER COMPOSITION AFTER DEPOLYMERIZATION OF SOLVENT-EXTRACTED <i>BRASSICA NAPUS</i> SEED RESIDUES BY NaOMe-CATALYZED TRANSMETHYLATION..	65
TABLE 5. MINOR COMPONENTS OF PURIFIED HYDROXY FATTY ACID METHYL ESTER AND DIMETHYL DICARBOXYLATE FRACTIONS ISOLATED FROM <i>ARABIDOPSIS THALIANA</i> SEED POLYESTERS.	68
TABLE 6. <i>ARABIDOPSIS</i> CANDIDATE GENES SELECTED ON BASIS OF GENE CO-RELATIONS AND/OR TRANSCRIPT UP-REGULATION IN EPIDERMAL OR CORK MICROARRAYS....	137
TABLE 7. SUMMARY OF MUTANTS CHARACTERIZED IN THIS WORK.	141
TABLE 8. PRIMER SEQUENCES USED IN WORK DESCRIBED IN CHAPTER 4.	186
TABLE 9. OLIGONUCLEOTIDES FOR AMPLIFICATION OF STIGMA-SPECIFIC PROMOTERS AND <i>ATT1</i> cDNA.....	236
TABLE 10. PEARSON PAIRWISE CORRELATION COEFFICIENTS (R^2) BETWEEN BAIT GENES AND CANDIDATE GENES FOR LIPID POLYESTER SYNTHESIS.....	266

LIST OF FIGURES

NOTE: IMAGES IN THIS DISSERTATION ARE PRESENTED IN COLOR.

FIGURE 1. DIAGRAMMATIC (LEFT) AND SCANNING ELECTRON MICROSCOPIC (RIGHT) VIEWS OF <i>ARABIDOPSIS</i> STEM EPIDERMIS AND CUTICLE.....	7
FIGURE 2. SCHEMATIC (A) AND TRANSMISSION ELECTRON MICROSCOPIC (B) VIEWS OF <i>ARABIDOPSIS</i> SUBERIZED ROOT CELLS.	8
FIGURE 3. PROPOSED MACROMOLECULAR STRUCTURE OF POTATO SUBERIN.	14
FIGURE 4. METHODS FOR CHEMICAL DEPOLYMERIZATION OF POLYESTERS AND SYLILATION OF ALCOHOL FUNCTIONS WITH BFTSA.....	16
FIGURE 5. PROPOSED BIOSYNTHETIC ROUTES FOR THE C16 AND C18 FAMILIES OF CUTIN MONOMERS, AND THEIR INCORPORATION TO THE POLYESTER (INSET).	20
FIGURE 6. (A) SCHEME OF <i>ARABIDOPSIS</i> SEED ANATOMY AND (B) SCHEMATIC DRAWING OF THE GENERAL ORGANIZATION OF THE DEVELOPING AND MATURE SEED COAT...	32
FIGURE 7. STRUCTURE AND MOLECULAR WEIGHT DISTRIBUTION OF LIPID POLYESTERS FOUND IN STIGMA EXUDATES.	37
FIGURE 8. STANDARDIZATION OF THE NAOME-MEOH-MEOAc TRANSMETHYLATION REACTION FOR DEPOLYMERIZATION OF EXHAUSTIVELY EXTRACTED <i>ARABIDOPSIS</i> SEED RESIDUES.....	49
FIGURE 9.. COMPARISON OF THE MAJOR MONOMER COMPOSITION AFTER DEPOLYMERIZATION OF SOLVENT-EXTRACTED <i>ARABIDOPSIS THALIANA</i> SEED RESIDUES BY BASE (NAOMe) (A) AND ACID (H ₂ SO ₄) (B) CATALYZED TRANSMETHYLATION REACTIONS RUN FOR 48 HOURS.	55
FIGURE 10. CHROMATOGRAM FOR GC ANALYSIS (DB-5 COLUMN) OF MONOMERS RELEASED BY DEPOLYMERIZATION OF SOLVENT-EXTRACTED <i>ARABIDOPSIS</i> SEED RESIDUES WITH NAOMe-CATALYZED TRANSMETHYLATION AND THEN ACETYLATION.	60
FIGURE 11. ELECTRON IMPACT MASS SPECTRA FOR DIMETHYL 2-METHYLHENEICOSANE-1,21-DIOATE (A) AND DIMETHYL DOCOSANE-1,22-DIOATE (B).	69
FIGURE 12. COMPARISON OF THE MAJOR MONOMER COMPOSITION AFTER DEPOLYMERIZATION OF SOLVENT-EXTRACTED <i>ARABIDOPSIS THALIANA</i> AND <i>BRASSICA NAPUS</i> SEED RESIDUES BY NAOMe-CATALYZED TRANSMETHYLATION..	72

FIGURE 13. COMPARISON OF <i>ARABIDOPSIS THALIANA</i> AND <i>BRASSICA NAPUS</i> SEED MONOMER CLASSES (A) AND TOTAL MONOMER CHAIN LENGTH DISTRIBUTIONS (B).	74
FIGURE 14. THE DISTRIBUTION OF MONOMER CLASSES IN WHOLE SEED, SEED COAT AND EMBRYO OF <i>BRASSICA NAPUS</i> MATURE SEEDS (A), AND THE DISTRIBUTION OF INDIVIDUAL MONOMERS IN WHOLE SEED, SEED COAT AND EMBRYO OF <i>BRASSICA NAPUS</i> MATURE SEEDS (B).....	77
FIGURE 15. STAGES OF DEVELOPMENT AND ANALYSIS OF TOTAL LIPID POLYESTER MONOMER CONTENT AND TOTAL OIL CONTENT IN DEVELOPING SEEDS OF <i>BRASSICA NAPUS</i>	93
FIGURE 16. VARIATION IN LIPID POLYESTER MONOMER COMPOSITION DURING DEVELOPMENT OF <i>BRASSICA NAPUS</i> SEEDS.	94
FIGURE 17. DEPOSITION OF CHLOROFORM-EXTRACTABLE WAXES IN <i>BRASSICA NAPUS</i> SEEDS.	98
FIGURE 18. POLYESTER MONOMERS IN THE CHALAZAL AND NON-CHALAZAL REGIONS OF <i>BRASSICA NAPUS</i> SEEDS.	100
FIGURE 19. POLYESTER MONOMER COMPOSITION OF <i>AP2-7 ARABIDOPSIS THALIANA</i> MUTANTS.	102
FIGURE 20. COMPARISON OF SEED MONOMER COMPOSITION BETWEEN WILD TYPE AND MUTANT <i>ARABIDOPSIS</i> LINES.	103
FIGURE 21. TETRAZOLIUM UPTAKE ASSAYS.	108
FIGURE 22. TISSUE SPECIFICITY OF GENE EXPRESSION IN LIVING DEVELOPING SEEDS.	113
FIGURE 23. PUTATIVE PATHWAYS FOR THE SYNTHESIS OF ALIPHATIC POLYESTERS. ..	138
FIGURE 24. COMPARISON OF <i>ATT1</i> AND <i>GPAT4</i> PROMOTER ACTIVITIES.	144
FIGURE 25. MICROSCOPICAL ANALYSIS OF SURFACE LIPIDS IN <i>ATT1</i> MUTANTS.	145
FIGURE 26. (A) GENOMIC ORGANIZATION OF THE <i>CYP86A1</i> SALK LINES AND (B) CONFIRMATION OF SILENCED LINES BY RT-PCR.	148
FIGURE 27. LOAD AND MONOMER COMPOSITION OF (A) 7-WEEK OLD ROOT AND (B) MATURE SEED POLYESTERS FROM WT AND <i>CYP86A1</i> MUTANTS.	150
FIGURE 28. ANALYSIS OF eYFP EXPRESSION IN <i>ARABIDOPSIS</i> PLANTS TRANSFORMED WITH <i>PRO_{CYP86A1}::eYFP</i>	152

FIGURE 29. TRANSMISSION ELECTRON MICROSCOPY OF SUBERIZED PERIDERMAL CELLS IN 7-WEEK OLD ROOTS.	154
FIGURE 30. LOAD AND COMPOSITION OF ALIPHATICS RELEASED BY TRANSMETHYLATION OF 6-WEEK <i>LCR-2</i> MUTANTS AND <i>COL0</i> WILD-TYPE LEAF RESIDUE.	155
FIGURE 31. LOAD AND COMPOSITION OF ALIPHATICS RELEASED BY TRANSMETHYLATION OF <i>ATT1-2</i> AND <i>CYP86A4</i> SINGLE MUTANTS, <i>ATT1-2/CYP86A4</i> DOUBLE MUTANT, AND <i>COL0</i> WILD-TYPE STEM RESIDUES.	157
FIGURE 32. PHYLOGENETIC ANALYSIS OF THE <i>ARABIDOPSIS</i> BAHD FAMILY.	160
FIGURE 33. (A) GENOMIC ORGANIZATION OF THE <i>AT5G41040</i> SALK LINES AND (B) RT- PCR ANALYSIS OF <i>AT5G41040</i> TRANSCRIPTS ISOLATED FROM ROOTS OF WILD TYPE AND <i>AT5G41040-1</i> MUTANTS.	163
FIGURE 34. COMPARISON OF SEED LIPID POLYESTER MONOMER COMPOSITION BETWEEN WILD-TYPE AND <i>AT5G41040</i> KNOCKOUTS.	165
FIGURE 35. SEED SOLUBLE LIPID POLYESTER MONOMERS.	168
FIGURE 36. SEED COAT PERMEABILITY TO TETRAZOLIUM SALTS.	170
FIGURE 37. ROOT POLYESTER AND WAX PHENOTYPES.	171
FIGURE 38. TRANSMISSION ELECTRON MICROGRAPHS OF <i>ARABIDOPSIS</i> ROOTS IN THE LATER STAGES OF SECONDARY THICKENING.	174
FIGURE 39. LIPID POLYESTER MONOMER LOAD AND COMPOSITION IN LEAVES OF <i>LACS</i> SINGLE (A) AND MULTIPLE (B) MUTANTS.	178
FIGURE 40. SEED LIPID POLYESTER MONOMER LOAD AND COMPOSITION IN WILD-TYPE AND <i>LACS2</i> , <i>LACS1-2</i> AND <i>LACS3</i> KNOCKOUTS.	179
FIGURE 41. SCHEMATIC REPRESENTATION OF THE ENZYMATIC REACTION CATALYZED BY PLANT ω -HYDROXYLASES.	193
FIGURE 42. PHYLOGENETIC TREE FOR FATTY ACID ω -HYDROXYLASES FROM PLANTS AND OTHER KINGDOMS.	194
FIGURE 43. STRUCTURAL COMPARISON OF SOLUBLE AND INSOLUBLE LIPID POLYESTERS.	198
FIGURE 44. EXPRESSION ANALYSIS OF THE <i>ARABIDOPSIS</i> CYP86A SUBFAMILY.	203

FIGURE 45. (A) SCHEMATIC REPRESENTATION OF THE GENOMIC ORGANIZATION OF ATT1 MUTANTS AND (B) RT-PCR FROM LEAVES AND STEMS OF ATT1-2 AND WT PLANTS.	204
FIGURE 46. PERMEABILITY OF <i>ATT1</i> CUTICLES TO TOLUIDINE BLUE.....	205
FIGURE 47. COMPARISON OF THE MONOMER COMPOSITION AFTER DEPOLYMERIZATION OF SOLVENT-EXTRACTED <i>ARABIDOPSIS THALIANA</i> WILD TYPE AND ATT1 MUTANTS BY NAOME-CATALYZED TRANSMETHYLATION.	208
FIGURE 48. DEDUCED AMINO ACID SEQUENCE ALIGNMENT OF <i>ARABIDOPSIS THALIANA</i> CYP86A2 AND <i>PETUNIA HYBRIDA</i> PH1 OMEGA-HYDROXYLASES.	210
FIGURE 49. BINARY CONSTRUCTS FOR COMPLEMENTATION OF <i>ARABIDOPSIS</i> ATT1 MUTANTS WITH <i>PETUNIA</i> ω -HYDROXYLASE (PH1) cDNA.	212
FIGURE 50. LIPID POLYESTER PHENOTYPE OF PH1-TRANSFORMED <i>ATT1-1</i> LINES.	214
FIGURE 51. BINARY CONSTRUCTS USED FOR OVEREXPRESSION OF At4G00360 (ATT1) IN STIGMAS OF <i>NICOTIANA TABACUM</i>	216
FIGURE 52. LIPID ANALYSIS IN WHOLE STIGMAS OF TOBACCO TRANSGENIC LINES.	218
FIGURE 53. ANALYSIS OF POLY-HYDROXY FATTY ACIDS IN <i>PETUNIA</i> RNAi LINES TO TEST THE “METABOLON” HYPOTHESIS:	222
FIGURE 54. ANALYSIS OF SOLVENT-EXTRACTED STIGMA LIPIDS OF <i>PETUNIA</i> PH1 RNAi LINES.	223
FIGURE 55. POSSIBLE BIOSYNTHETIC PATHWAYS FOR THE SYNTHESIS OF ACYL- GLYCEROL UNITS.	229
FIGURE 56. HYPOTHETICAL REACTIONS CATALYZED BY CYP86A2 (ATT1) IN THE ROUTE OF BIOSYNTHESIS OF DICARBOXYLIC ACIDS IN <i>ARABIDOPSIS</i> EPIDERMAL CELLS. .	231
FIGURE 57. SURFACE LIPID LOAD AND DISTRIBUTION IN <i>ARABIDOPSIS THALIANA</i> SEEDS.	246
FIGURE 58. SCHEMATIC DIAGRAM OF THE PROPOSED ENZYMATIC REACTION CATALYZED BY ENZYME ENCODED BY At5G41040.	258
FIGURE 59. MS SPECTRA OF THE LIGNAN MOLECULE RELEASED BY TRANSESTERIFICATION OF SEED RESEDUES.	264
FIGURE 60. MS SPECTRUM OF 1-PHENANTHRENECARBOXYLIC ACID, TETRADECAHYDRO- 1, 4A-DIMETHYL-7-(1-METHYLETHYL)-, METHYL ESTER.	265

FIGURE 61. GENE EXPRESSION IN ARABIDOPSIS DEVELOPING SEEDS FOR SELECTED CANDIDATE GENES.....	268
FIGURE 62. LOAD AND MONOMER COMPOSITION OF SEED POLYESTERS FROM WT AND <i>AT1G04220</i> MUTANT.	271

CHAPTER 1

INTRODUCTION

Plant lipids comprise an extremely diverse group of molecules, and their biosynthesis involves different pathways and several cellular compartments. Among these lipids, glycerolipids derived from the glycerol and fatty acid biosynthetic pathways are the most abundant class in plant cells (Ohlrogge and Browse, 1995). Glycerolipids perform unique functions as main components of the membranes that define the cell and its compartments. Those functions include photosynthetic processes in leaf mesophyll cells. However, some plant cells synthesize higher amounts of lipids than leaf mesophyll cells. For example, cells from seeds can produce not only membrane lipids but also storage lipids and epidermal cells synthesize cutin monomers and waxes, which provide the protective and waterproofing barrier that covers the surface of plants. For epidermal cells, flux into extracellular lipids can exceed that for membrane lipid synthesis (Suh et al., 2005). In other cells, such as those in peridermis and wounded tissues, suberin monomers and waxes are produced to form a barrier in response to stresses from the environment, or during development (Kolattukudy, 2001a).

Suberin and cutin, collectively called lipid polyesters, are two distinct types of plant insoluble polymers derived from fatty acids. Cutin constitutes the matrix

of the plant cuticle (Esau, 1977) whereas suberin is a heteropolymer co-deposited with waxes inside the cell wall (Bernards, 2002). While cutin is usually composed largely of C16 and C18 hydroxy and hydroxy epoxy fatty acids, suberin consists of aliphatic domains where C16 and C18 dicarboxylic acids, very long chain fatty acids and alcohols are found, as well as aromatic domains derived from hydroxycinnamic acids (Kolattukudy, 2001a). Glycerol is a common component in both polyesters (Moire et al., 1999; Graça and Pereira, 2000; Graça et al., 2002). Interestingly, the recent finding that unsaturated dicarboxylic acids are major monomers in *Arabidopsis* and *Brassica napus* cutin (Bonaventure et al., 2004; Franke et al., 2005) raised new questions: Does the long-standing classification of cutin and suberin monomers require revision? or, Does *Arabidopsis* have a different type of polyester network?. Since these polymers are difficult to isolate, neither cutin nor suberin is easy to study. Indeed, although cutin constitutes one of the largest interfaces between the biosphere and the atmosphere (Bargel et al., 2006), this biopolymer remains poorly understood at the structural, biochemical and genetic levels.

The identification of genes encoding enzymes involved in polyester biosynthesis is now possible, given the molecular genetic tools available for *Arabidopsis thaliana*. Both forward and reverse genetic screens require robust chemical analyses to complement assays of functional properties such as cuticle permeability, organ fusion phenotypes, or pathogen susceptibility. Such analyses have only recently been published (Bonaventure et al., 2004; Xiao et al., 2004;

Franke et al., 2005). However, a reliable method for seed polyester analysis has not previously been available. Because the seed coat provides the interface between the embryo and its environment, it has essential functions in the plant life cycle. The specialized cells forming the seed coat layers play fundamental and different roles throughout seed development and even at maturity, when they are dead. During seed development, dormancy, and germination, the seed coat imparts protection against pathogens and adverse conditions, allowing survival of the offspring. Besides its protective functions, it is involved in embryo nutrition during development, and has functions in establishing and maintaining seed dormancy, facilitating seed dispersal, and promoting germination under favorable conditions (Haughn and Chaudhury, 2005). Two major groups of seed coat mutants have been described. One group is affected in flavonoid pigmentation (e.g. *transparent testa* and *transparent testa galabra* mutants) and the other group is affected in seed coat structure (e.g. *aberrant testa shape* mutants) (Bentsink and Koornneeff, 2002). However, seed coat knockout mutants with altered cutin/suberin composition have so far not been characterized. One advantage of using *Arabidopsis* as a model is that economically important oilseed crops such as *Brassica napus* are members of the same family.

In most plant cuticles, waxes play a critical role as a barrier for water passage. In seed coats, however, waxes are minor components (Beisson et al., 2006; Shao et al., 2007), suggesting that polyesters may be the main agents regulating seed coat permeability. It has recently been shown that polyesters

contribute to seed coat permeability and seed dormancy in soybean and *Arabidopsis* (Beisson et al., 2006; Shao et al., 2007), and they also may influence pathogen resistance. Given the importance of these polyester barriers, one aim of the present work was to investigate the chemical composition of the lipid polyester monomers present in seed coats of *Arabidopsis thaliana* and *Brassica napus*.

A third type of lipid polyester, rich in hydroxy fatty acids, is very abundant in the exudates from stigmas of solanaceous plants (Cresti et al., 1986). Stigma polyesters are structurally related to cutin, but they are soluble in organic solvents, a property that makes them a potentially powerful system for studying biosynthesis and assembly of hydroxy fatty-acid-based polyesters. Thus, developing stigmas offer a promising tool to study the enzymology of cutin biosynthesis. Both stigma polyesters and cutin are located at the plant surface and, therefore, play an important role in the interaction of the plant with its environment. Stigma polyesters are essential for pollen-stigma interactions, while cutin provides a barrier for defense against pathogens, preserves organ identity, and controls water and gas exchanges. Because of their significance in crop physiology, lipid polyesters are agriculturally important. To test the utility of the stigma exudates as a model to study polyester biosynthesis, another goal of the present work was to investigate if the biosynthesis of cutin and stigma hydroxy fatty acids occurs through similar pathways.

OBJECTIVES

In summary, the **overall objectives** of the work presented in this thesis were:

- Develop a method for analysis of seed polyesters (Presented in Chapter 2).
- Apply method to characterize lipid polyesters in seeds of Brassicaceae (Presented in Chapters 2 and 3).
- Apply method to mutant screening to gene discovery (Presented in Chapters 3 and 4).
- Understand the role of cytochrome P450 ω -hydroxylase gene products in the biosynthesis of plant soluble (stigma) and insoluble (cutin) lipid polyesters. (Presented in Chapter 5).

This objective was approached by analyzing hydroxy fatty acid-containing lipid products in:

- a. stigmas of transgenic tobacco plants over-expressing an *Arabidopsis* ω -hydroxylase gene (ATT1);
- b. leaves/stems of an *Arabidopsis* knockout mutant (*att1*) complemented with an homologous gene from *Petunia hybrida*.

An overview of the current knowledge on different aspects of plant lipid polyesters is given below.

THE BIOPOLYMERS CUTIN AND SUBERIN

Structure, functions, and location

Land plants have developed an outer skin that protects them from desiccation and acts as a defensive barrier against pathogens (Holloway, 1994). This non-cellular thin coat, the cuticle, covers the external surface of the epidermal cells of aerial organs. Internal cuticles occur in seed coats and juice sacs of grapefruit (Espelie et al., 1980), and line the substomatal cavity (Pesacreta and Hasenstein, 1999). The cuticle is composed of polymers (cutin and cutan), waxes, and polysaccharides (Jeffree, 1996). Cutin is a polyester of hydroxy and hydroxy epoxy fatty acids, providing a framework for the cuticle. Cutan is less understood. This biomacromolecule is mostly linked by ether bonds and therefore remains as a non-depolymerizable fraction after ester-bond hydrolysis (Mosle et al., 1997; Villena et al., 1999).

The cuticle. Cuticles have several layers (**Figure 1**), which are defined on the basis of their position and chemical composition: an “inner cuticle”, attached to the cell wall, that contains polymers, waxes, and polysaccharides; the “cuticle proper” comprised of polymers with embedded waxes, and epicuticular wax layer (Heredia, 2003; Bargel et al., 2006). The thickness of these layers depends on the species, anatomical location and developmental stage. The overall cuticular thickness is therefore variable, ranging from 0.1 to 14 μm in leaves, and

containing <20 to 600 μg of cutin per cm^2 surface area (Kolattukudy, 2001b). In fruits the cutin content can reach 1.5 mg/cm^2 . Cutin is believed to be the most abundant lipid polyester among plants (Heredia, 2003).

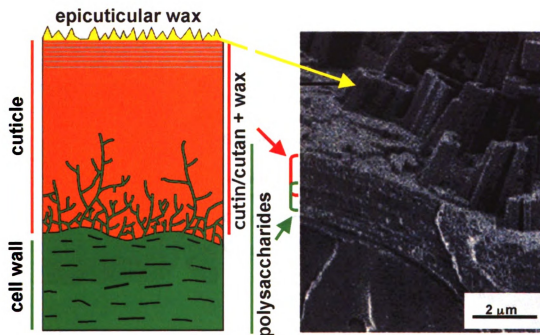


Figure 1. Diagrammatic (left) and scanning electron microscopic (right) views of *Arabidopsis* stem epidermis and cuticle.
Modified from Kunst et al.(2005) and Bargel et al. (2006).

Waxes embedded in cutin make the cuticle an efficient barrier against water loss and gas exchange (Kolattukudy, 1984). The cuticle constitutes the interface between the plant and its environment and thus functions as a barrier to protect leaves, fruits, and other aerial organs from pathogen attack. It controls the diffusion of molecules into plant tissues and plays a role in maintaining the separation of organs during organogenesis.

Suberized cell walls. While the cuticle lies on the outer face of the primary cell wall, suberin is located on the inside of the primary cell wall close to the plasma membrane (Kolattukudy, 1980a) (**Figure 2**). Suberin consists of a polymeric material with embedded waxes. Its ultrastructure is frequently lamellar when observed by transmission electron microscopy (TEM), showing alternating light and dark bands (Bernards and Lewis, 1997).

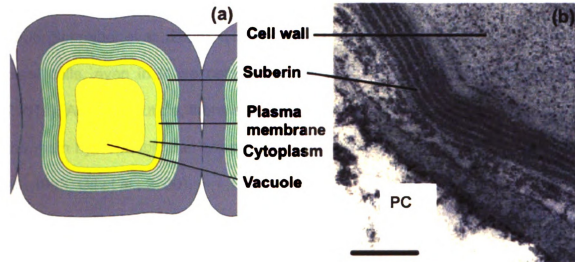


Figure 2. Schematic (a) and transmission electron microscopic (b) views of *Arabidopsis* suberized root cells.

Suberized peridermal and endodermal cells present the typical lamellar deposition within the cell walls (arrow heads). The TEM image was adapted from Franke et al. (2005). PC, peridermal cell. Bar: 100 nm.

Typically, the function of suberin is to control the movement of water and solutes from various tissues, and to contribute to the strength of the cell wall (Nawrath, 2002). It is synthesized during normal development or as a result of environmental stresses (Dean and Kolattukudy, 1976). Suberin is found in peridermis of shoots (e.g. cork) and of underground organs (e.g. potato) (Bernards and Lewis, 1997). In primary roots, it is found in endodermal,

rhizodermal and hypodermal cells (Ma and Peterson, 2003). It may be deposited surrounding the bundle sheaths of monocot leaves, between seed coats and in vascular tissue during seed development (Espelie, 1980), at the boundary between secretory organs and the rest of the plant (Thomson et al. 1979), as well as in trichomes of certain varieties of cotton (Yatsu, 1983). Exposure to cold, mineral stress and fungal infection are some examples where suberization occurs as a response to external factors (Kolattukudy, 2001a; Ghanati et al., 2005; Schreiber et al., 2005). It is also deposited as a wound response by injured plant cells, even in those cells which normally synthesize cutin (Kolattukudy, 2001a). As in the cuticle, there is evidence that waxes deposited with suberin are the main hydrophobic barriers protecting cell walls (Soliday et al., 1979; Vogt et al., 1983; Gil et al., 2000).

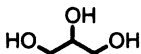
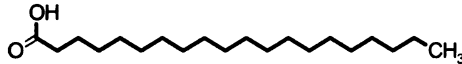
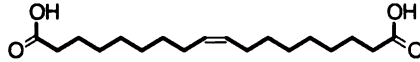
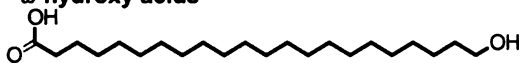
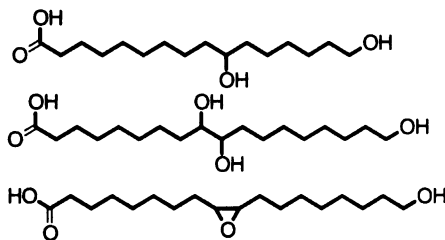

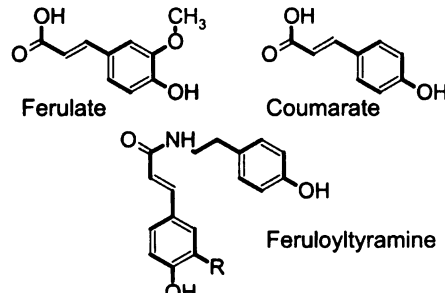
Chemical composition

The cuticle. The two major hydrophobic constituents of the plant cuticle are the insoluble polymers and soluble waxes (Bargel et al., 2006). The chemistry of these soluble lipids is varied, and in general, they are not biosynthetically related to cutin. Waxes are composed of aliphatics and aromatics. The former group includes long-chain alkanes and substituted derivatives such as fatty acids, primary and secondary alcohols, aldehydes and ketones. The cutin polyester is usually composed of esterified hydroxy- and hydroxy epoxy fatty acids, which are derived from C16 saturated and C18

unsaturated fatty acids, the most abundant in plant cells (**Table 1**) (Kolattukudy, 1996). In C16-rich cutins, 16-hydroxy- and 10,16-dihydroxy-palmitic acids are usually dominant, while in C18-rich cutins 9,10,18-trihydroxystearic acid and 9,10-epoxy-18-hydroxystearic acid monomers and the corresponding octadecenoic acids are common. In addition, glycerol has been found esterified to cutin aliphatic monomers (Graça et al., 2002) while minor amounts of hydroxycinnamic acids have been reported as aromatic structural components of cutin (Kolattukudy, 1977; Fang et al., 2001). Interestingly, although dicarboxylic acids have in the past been reported as only minor components of cutin, it is now known that these structures are major monomers found in *Arabidopsis thaliana* leaf and stem cuticles (Bonaventure et al., 2004; Franke et al., 2005). The native polymeric structure of cutin remains unresolved, and proposed three-dimensional arrangements based on monomer composition remain largely speculative. Likewise, it is still unclear if the insolubility of the polyester is a consequence of covalent linkage to the cell wall or cutan, or of the high MW of the polymer (Pollard et al., submitted).

Suberin. Whereas aromatic constituents of cutin are minor (<5%), in suberin these monomers are abundant (**Table 1**). Although both cutin and the poly(aliphatic) domains of suberin have structural similarities and analogous functions in the protection of plant organs, they are distinguished by their characteristic monomer composition (Bernards et al., 2004). The aliphatic polymer of suberin is composed mainly of C16 to C28 ω -hydroxy fatty acids and

Table 1. Compositional comparison between cutin and suberin.

Monomer	Cutin	Suberin
Glycerol 	Substantial	Substantial
Unsubstituted acids 	Minor (C16-C18)	Minor (C16-C26)
α,ω-dicarboxylic acids (C16-C26) 	Minor ^a	Common and substantial
ω-hydroxy acids 	Major (C16-C18)	Common and substantial (C16-C26)
Substituted ω-hydroxy acids (C16-C18) 	Major	Minor ^b
Primary alcohols (C18-C26) 	Rare and minor	Common and Substantial
Phenolics 	Low	High

^a C16-C18 dicarboxylates are major monomers in *Arabidopsis* and *Brassica napus* cutin; ^b In some cases is substantial (Kolattukudy, 1980a). Substituted dicarboxylic acids and α,ω -diols are also frequently found in suberins.

C16 to C26 α,ω -dicarboxylic acids, the latter of which are diagnostic monomers. A characteristic feature of suberin is the presence of monobasic monomers of very long chain fatty acids and alcohols (C20 to C32, with C22 and C24 being the most common). The aromatic network is a hydroxycinnamate-derived polymer, primarily comprised of ferulic acid, N-feruloyltyramine, cinnamic acid, p-coumaric acid or caffeic acid (Bernards et al., 1995). Glycerol is another major compound of this polyester, constituting up to 20% of total monomer mass of suberin in oak, cotton, and potato (Moire et al., 1999; Graca and Pereira, 2000; Graça and Pereira, 2000). Unlike cuticular waxes, suberin-associated waxes resemble the structural constituents of the polyester and seem to be biosynthetically related (Li et al., 2007).

Models to explain the macromolecular structure of suberin are based on the use of degradative techniques for chemical analyses and further reconstruction of the original structures, in combination with ultrastructural data. Bernards (2002) described suberin as a hydroxycinnamic acid-monolignol polyphenolic domain embedded in the primary cell wall and covalently linked to a glycerol-based polyaliphatic domain (**Figure 3**). The aliphatic monomers are linearly arranged, forming the electron-translucent bands. The thickness of this layer has been shown to be defined by the length of the carbon chain of these monomers (Schmutz et al., 1996). The nature of the opaque bands is less understood. According to this model, it corresponds to glycerol, esterified phenolics, and possibly waxes. The presence of other electron-rich molecules

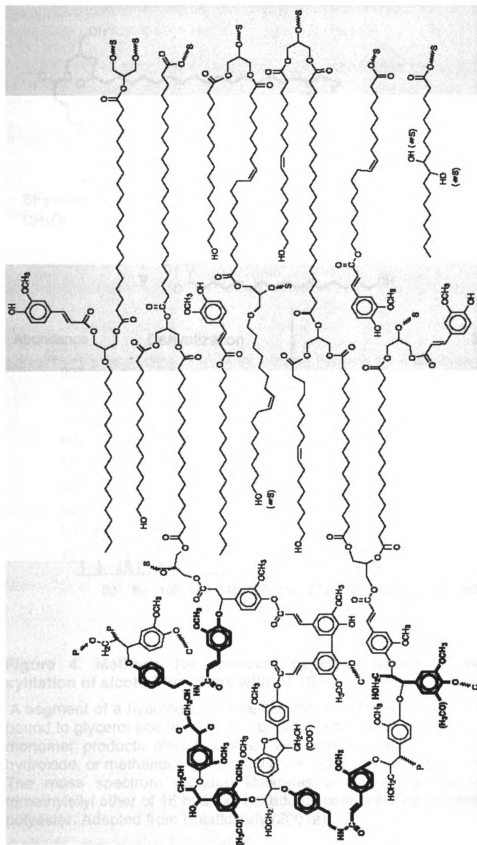
such as polysaccharides or proteins that could serve as a scaffold cannot be ruled out. Graça and Santos (2007) proposed a similar structural arrangement. In both models ferulic acid has been suggested to be the linker between polyaromatics and the suberin polyester. It is important to bear in mind that these models were largely based on potato periderm and cork. More work is needed to extrapolate the proposed macromolecular organization to other species and different organs.

Depolymerization and analysis of monomers

Cutin. After solvent extraction of soluble lipids with chloroform and methanol, the lipid polyester remaining in the residue can be chemically depolymerized by hydrogenolysis with lithium aluminium hydride, by alkaline hydrolysis or by methanolysis catalyzed by boron trifluoride or sodium methoxide (Walton and Kolattukudy, 1972; Kolattukudy, 1981). These methods cleave ester bonds. The released monomers are then usually derivatized with BFTSA (*N,O*-bis(trimethylsilyl)-trifluoroacetamide) or other silylating reagents to convert them to the corresponding trimethylsilyl derivatives, and these are subjected to gas chromatography/mass spectrometry (GC-MS). **Figure 4** summarizes the steps for chemical depolymerization of lipid polyesters and subsequent analysis. Monomers are identified according to their characteristic fragmentation spectra. Alternatively, the depolymerization step can be performed enzymatically with

Figure 3. Proposed macromolecular structure of potato suberin.

The poly-aromatic domain is shown attached to carbohydrates in primary cell wall. The polyester domain is based on glycerol and aliphatics, and a minor proportion of aromatics (ferulate). The light and dark bands depicted in the model correspond to the electro-translucent and electro-opaque bands observed by TEM. Aliphatics constitute the light bands, whereas phenolics form the dark zones. The thickness light plus dark bands is about 3-4 nm in this model. C=carbohydrates ; S= suberin; P= phenolic. Taken from Bernards (2002).



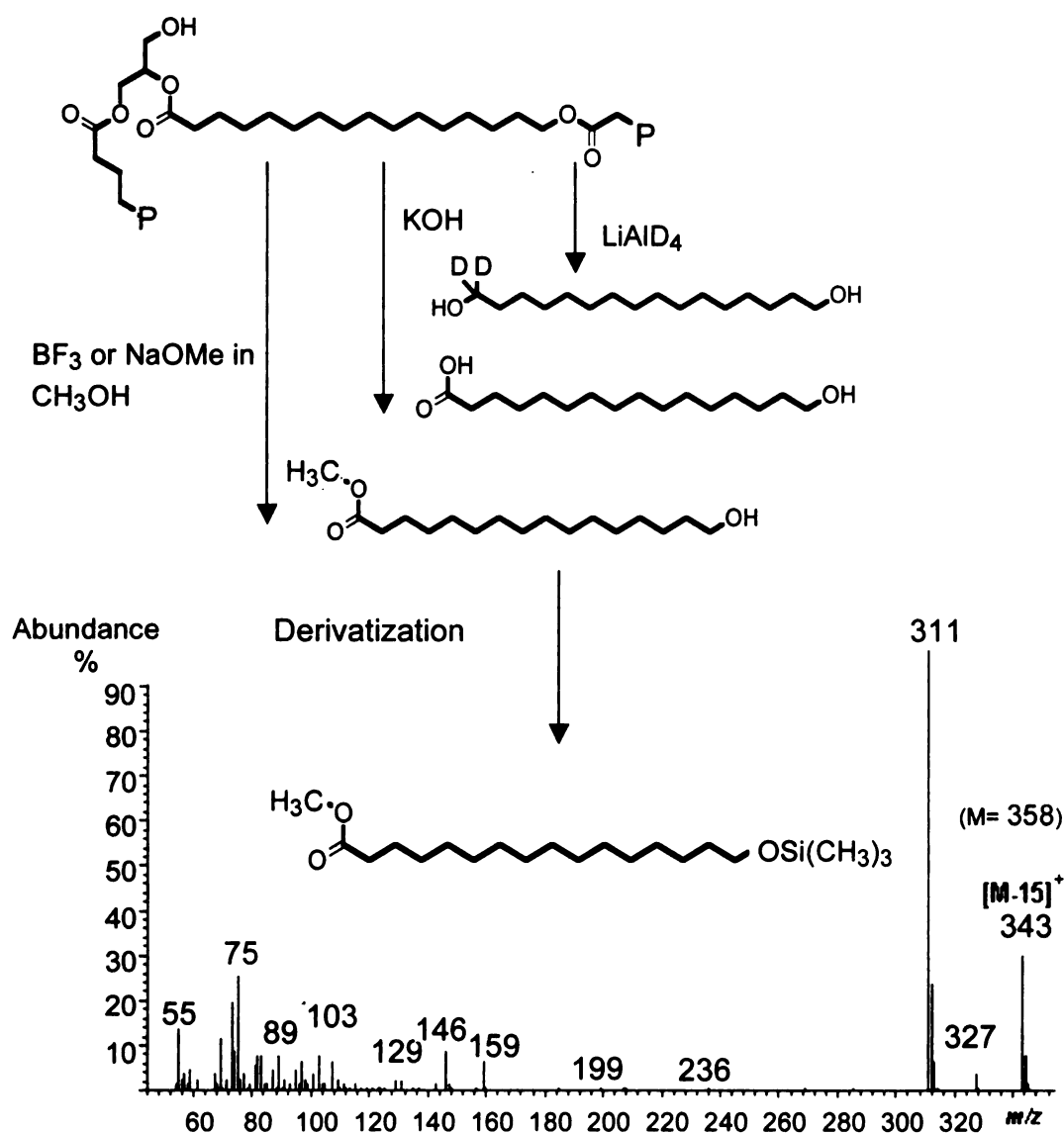


Figure 4. Methods for chemical depolymerization of polyesters and silylation of alcohol functions with BFTSA.

A segment of a hypothetical polyester containing 16-hydroxy hexadecanoic acid bound to glycerol and to another monomer in the polymer (P) (left) gives different monomer products after hydrolysis with lithium aluminium hydride, potassium hydroxide, or methanol catalyzed by boron trifluoride or sodium methoxide (right). The mass spectrum (bottom) illustrates a typical fragmentation pattern of trimethylsilyl ether of 16-hydroxy hexadecanoate obtained by methanolysis of the polyester. Adapted from Kolattukudy (2001a).

lipases or cutinases. The resulting oligomers can be subjected to electron impact (EI) and liquid secondary ionization (LSI) mass spectrometry (MS) and NMR spectroscopy, thereby obtaining structural information (Ray et al., 1998; Ray and Stark, 1998).

Suberin. The depolymerization methods described above can also be applied to analyze the aliphatic domains in suberized cell walls. Moreover, a fraction of the aromatic monomers can be released in these analyses. However, some C-C and C-O-C cross-linking in the aromatic domains of suberin make this polymer more difficult to depolymerize and more severe treatments are required (Kolattukudy, 1993, 2001a). Some examples of these procedures are thioacidolysis, CuO oxidation, and nitrobenzene oxidation. Application of the lignin-specific methods thioacidolysis (Lapierre et al., 1986; Monties, 1989) and DFRC (derivatization followed by reductive cleavage) (Lu and Ralph, 1997) have revealed that monolignols are a minor fraction of suberin aromatics (Bernards, 2002). On the other hand, alkaline nitrobenzene oxidation is exhaustive and yields total aromatic content, at the expense of losing chemical information. Only after NMR analysis of potato tissues treated with C¹³-labeled phenylalanine it became clear that most of the aromatic constituents of suberin are phenylpropanoids (Bernards et al., 1995).

Cutan and suberin. After depolymerization of cutin and suberin with methods that cleave ester bonds, a non-hydrolyzable fraction remains in the

matrix of the residue. This non-ester bound polymers are often called "cutan" and "suberan", respectively. Cutan has been analyzed by pyrolysis-coupled gas-liquid chromatography and mass spectrometry, resulting in C16 and C18 fatty acids plus C19-C26 hydrocarbons. More recently, using ^{13}C -nuclear magnetic resonance (NMR) and Fourier transform infrared (FT-IR), calorimetry, X-ray diffraction, and ozonolysis (Villena et al., 1999) have characterized this fraction in leaves of *Agave americana*, showing that cutan consists of an ether-bound three-dimensional network containing double bonds and free carboxylic acid functions. The occurrence of cutan in desert plants has been interpreted as a plant adaptation to cope with drought climate (Boom et al., 2005). It is still unclear if cutin and cutan are different polymers rather than one polymer formed by ester and non-ester bonds (Kolattukudy, 1996).

Biosynthesis

A. Biosynthesis and assembly of aliphatic polyesters

Suberin contains those monomers typically found in cutin, namely fatty acids, ω -hydroxylated monomers, and also alcohols and α,ω -dicarboxylic acids that are considered diagnostic of suberin (**Table 1**). Textbooks and reviews usually describe the synthesis of cutin and suberin aliphatic monomers as distinct pathways, with chain elongation and conversion of ω -hydroxy acids to dicarboxylic acids being specific for suberin monomers. However, data from *Arabidopsis* has shown that dicarboxylates are not exclusively found in suberin,

and that the same gene families seem to be involved in the synthesis of both type of polyesters. Chain-elongation then can be considered solely for suberin, and will be introduced in **Appendix D**. Primary alcohols may derive from the wax biosynthetic pathway, by action of a NADPH-dependent alcohol-forming reductase (FAR) on acyl-CoA intermediates (Metz et al., 2000). In the next paragraphs, the current knowledge on the synthesis and assembly of both cutin and suberin aliphatics is summarized together.

Synthesis of aliphatic monomers. Early radiolabeling experiments performed by Kolattukudy in the 1970's gave insight into the pathways involved in the biosynthesis of C16 and C18 monomer classes. Based on those biochemical assays, a pathway for the biosynthesis of cutin monomers was proposed and is schematized in **Figure 5**. Similarly, the biosynthetic routes for the major aliphatic monomers of suberin have been studied in the past using incorporation of labeled oleic acid or acetate in wound-healed potato slices (Dean and Kolattukudy, 1977).

Polyester monomers are derived from 16:0 and 18:1 fatty acyl-CoAs. Monomer hydroxylation and/or epoxydation steps require NADPH and O₂ as co-factors and are inhibited by CO, thereby suggesting the involvement of a CytP450-type enzyme (Soliday and Kolattukudy, 1977; Kolattukudy, 2001a). Possible alternative routes for the biosynthesis of oleic acid-derived cutin monomers were proposed by Blee and Schuber, 1993. The authors used a cell

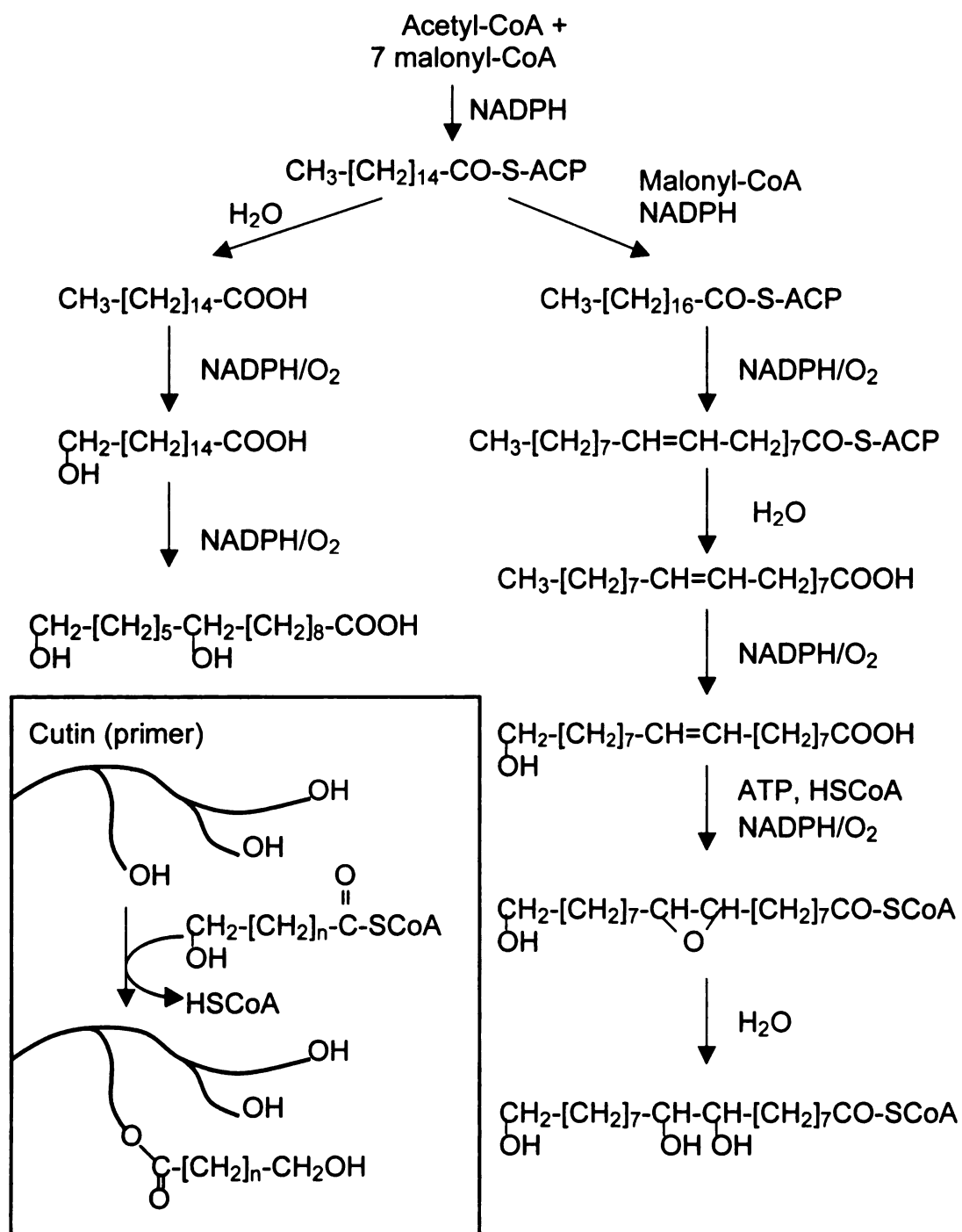


Figure 5. Proposed biosynthetic routes for the C16 and C18 families of cutin monomers, and their incorporation to the polyester (inset).

Adapted from Kolattukudy (2001a).

free system to demonstrate that a pathway involving lipoxygenase, peroxygenase and epoxide hydrolase activities, along with a cytochrome p450 hydroxylase, produced C18 cutin acids *in vitro*. In this system, the peroxygenase cloned from soybean seedlings preferred oleic acid rather than the hydroxylated monomer as substrate. Furthermore, the soluble epoxide hydrolase purified from soybean seedlings preferred the non-hydroxylated monomer (cis-epoxide). Hence, the cytochrome p450 activity was required downstream of the epoxydation step. Kolattukudy (2001a) argued against this assumption, reasoning that if this mechanism occurred in cutin, then mid-chain non- ω -hydroxylated functional molecules should be found in the polyester, and this is not the case. The involvement of the peroxygenase pathway in cutin biosynthesis was later confirmed by *in planta* inhibition of this enzyme, which resulted in a thinner cuticle and increased susceptibility of maize leaves to infection by fungi (Lequeu et al., 2003).

Since biochemical approaches to isolate enzymes involved in biosynthesis of cutin/suberin monomers have not been successful, genetic approaches have been attempted to dissect biosynthetic pathways. Several cutin mutants have been identified in part because they resemble transgenic plants that over-express fungal cutinase (Sieber et al., 2000), which show alterations in the structure of the cuticle and organ fusions, or because they present increased susceptibility to pathogens (Xiao et al., 2004). Such forward genetics screenings have identified two mutants of the Arabidopsis CYP86A subfamily of putative ω -

hydroxylases (Duan and Schuler, 2005). Characterization of the *Arabidopsis att1* mutant (Xiao et al., 2004) has shown that *ATT1* (encoding CYP86A2) is functionally implicated in cutin biosynthesis *in planta*. Although a 70% reduction in cutin monomers was reported, the reaction catalyzed by ATT1 in *Arabidopsis* epidermal polyesters is still unknown (discussed in Chapter 5). In addition, the *lacerata (lcr)* mutant (*cyp86a8*) has a pleiotropic phenotype consistent with a defective cuticle, showing organ fusion, leaf deformation and pollen germination on the surface of leaves (Wellesen et al., 2001). Although this enzyme catalyzes ω -hydroxylation of fatty acids in yeast, the direct role of the enzyme in cuticle synthesis cannot be inferred since the polyester composition of this mutant was not reported.

By similar forward genetics screens, other *Arabidopsis* genes potentially involved in cutin biosynthesis were also identified: *HOTHEAD (HTH,)* and *BODYGUARD (BDG, see next section)* (Lolle et al., 1992; Yephremov et al., 1999; Pruitt et al., 2000; Wellesen et al., 2001; Kurdyukov et al., 2006a; Kurdyukov et al., 2006b). They encode putatives oxidoreductase and carboxyesterase/synthase, respectively, which are involved in lipid metabolism. Their respective mutants present organ fusions in flowers and/or leaves. Although they have been shown to influence the formation of the cuticle, the precise function of the encoded proteins in cuticle biosynthesis is unclear and needs biochemical confirmation.

HOTHEAD was proposed to catalyze the synthesis of ω -oxo acids that are intermediates in synthesis of dicarboxylic acids (Kurdyukov et al., 2006b). This mechanism has been biochemically demonstrated in earlier studies using potato periderm (Agrawal and Kolattukudy, 1977; Agrawal and Kolattukudy, 1978) and cell-free extracts of bean epidermis (Kolattukudy et al., 1975). However, reports on tobacco CYP95A5 (Le Bouquin et al., 2001) and Arabidopsis CYP94C1 (Kandel et al., 2007) have shown that cytochrome P450 may also be involved in the conversion of fatty acids to dicarboxylic acids. Thus, different pathways from alcohol to acid have been proposed, and are discussed in Chapter 5.

The family of acyl-CoA synthetases (LACS) is also required for polyester biosynthesis. The finding that knockout mutants of *LACS2* had a defective cuticle (Schnurr et al., 2004; Bessire et al., 2007; Tang et al., 2007) indicated that free fatty acids are probably intermediates in cutin synthesis and need to be activated by LACS2. *In vitro* assays demonstrated that this enzyme can use both fatty acids and ω -hydroxylated fatty acids as substrates (Schnurr et al., 2004). However it is unclear where in the pathway this activation step takes place.

Polyester assembly. The key enzyme responsible for the assembly of the three-dimensional polyester network remains elusive. Such an enzyme would presumably function by transferring ω -hydroxy-acyl-CoAs to free hydroxy groups in the polyester acceptor (catenation reaction) (**Figure 5, inset**) (Croteau and Kolattukudy, 1973; Kolattukudy, 1981). This assumption was based on early *in*

vitro reactions using ω -hydroxy-acyl-CoAs and an extracellular insoluble acceptor. But only secondary hydroxyl groups were acylated in these experiments, and it is therefore unlikely that *in vivo* catenation proceeds in the same way. One protein purified and sequenced that may be involved in this process is a putative acyl-CoA transferase from *Agave americana* epidermis (Reina and Heredia, 2001). This protein contained an HxxxE motif, which is conserved in other acyl-transferases.

Qualitative and quantitative analyses of lipid polyester monomers in *Arabidopsis* are now routine (Bonaventure et al., 2004), allowing the use of reverse genetic approaches to discover new genes involved in cutin and suberin synthesis. Identification of candidate genes for such studies has been aided by the availability of epidermis and phellem (cork) transcriptomes (Suh et al., 2005; Soler et al., 2007), as well as public repositories for microarray data. In fact, these strategies have facilitated the identification of three enzymes of the GPAT family of putative glycerol-3-phosphate-acyltransferases that have key roles in cutin and suberin synthesis. Since glycerol has an important function in cross-linking the monomers, as evidenced by partial depolymerization analyses (Graça and Pereira, 2000; Graça et al., 2002; Graça and Santos, 2006) an acyl-transferase activity is needed to assemble the polymer. *GPAT5* was the first gene identified that is involved in the transfer of suberin aliphatics. *gpat5* alleles (Beisson et al., 2007) showed reduced saturated long-chain fatty acid composition in seed coats and roots, consistent with defective suberin

deposition. *GPAT4* and *GPAT8* were shown to have similar function in cutin monomer acyl transfer reactions (Li et al., 2007a). Thus, this new evidence suggests that the building blocks that constitute the higher order polyesters in *Arabidopsis* are acyl-glycerols. It is unknown how acyl-glycerols are transported and assembled into the insoluble polyester.

Glycerol esterified to ω -hydroxy fatty acid, caffeic acid and fatty acid has been found in suberin waxes from green cotton (Schmutz et al., 1993). Ferulic acid esters of very long chain fatty alcohols also occur in suberin waxes. Such structures may represent intermediates that could be further incorporated to the suberin polymer by a peroxidase (Kolattukudy, 2001a), accounting for polyester insolubility. Although this assumption was reinforced by the finding that ferulate esterified to glycerol and to ω -hydroxy fatty acids was released by partial depolymerization, this hypothesis requires confirmation.

The biochemical mechanism of the polymerization reaction, and whether it takes places within the cell or in extracellular locations remain enigmatic. Lipases have been proposed to act as polyester synthases. Kurdyukov et al. (2006a) have suggested that a lipolytic enzyme, the *BDG* gene product, acts as an extracellular synthase required for polymerization processes in the cuticle. However, *bdg* mutants showed a complex pleiotropic phenotype, with defects in growth, morphology, and cell differentiation. Thus, a more general function in cell proliferation/differentiation cannot be ruled out (Kurdyukov et al., 2006a).

Furthermore, a different hydrolase that belongs to the family of GDGL-motif putative lipases has been identified in *Agave Americana* leaves and has been suggested to be involved in both hydrolysis and transfer of activated monomers in cutin synthesis (Reina et al., 2007).

Transport processes. Little is known about how cutin precursors are transported from their intracellular site of synthesis to the polyester deposition site. Understanding how polyester monomers, oligomers, or domains are transported to their deposition site will be crucial to gain insight into the polymerization mechanism. Vesicle-mediated transport has been suggested based on ultrastructural analysis of rapidly expanding rice internodes (Hoffmann-Benning et al., 1994). Other transport mechanisms include ATP binding cassette (ABC) transporters and LTPs (lipid transporter proteins). Type I LTPs and ABC transporters from the with-brown complex (WBC) subfamily have been found up-regulated in stem epidermis (Suh et al., 2005); ABC transporters of the WBC and ATH subfamilies were up-regulated in cork (Soler et al., 2007). The finding that a knockout of the plasma membrane-localized ABC transporter *WBC11* had lower loads of wax and cutin (Bird et al., 2007; Panikashvili et al., 2007) suggested that this mechanism could be involved in transport of cutin building blocks (in any of the discussed forms) and waxes, but this needs biochemical confirmation. LTPs are small, soluble extracellular proteins that may mediate the transport of monomers or acylglycerols through the hydrophilic cell walls to the site of

polymerization, although there is not direct evidence for such role (reviewed by Yeats and Rose, 2007).

Regulation of polyester synthesis. Lipid polyesters are synthesized during normal development and in response to various stress conditions, in coordination with wax biosynthetic pathways. Consequently, these highly orchestrated processes need tight regulation. A transcription factor of the ethylene response family (WIN1/SHN1) caused wax accumulation when ectopically expressed (Aharoni et al., 2004; Broun et al., 2004). It was demonstrated that, directly or indirectly, this transcription factor triggers the expression of cutin-synthesizing genes (i.e. *LACS2*, *CYP86A4*, *CYP86A7*, *GPAT4*). Using a similar gain-of-function approach, AtMYB41 has been recently identified as a regulator of cuticle deposition and cell expansion that is only expressed under stress conditions (i.e. ABA, draught, and salt treatments) (Cominelli et al., 2007). The regulatory mechanisms that control the tissue-specific and developmental deposition of suberin are unknown. It is clear that the biosynthetic machinery responds to environmental stimuli, and that the regular pattern observed in the suberin lamellae must result from some specific mechanism that has not been elucidated. Based on their expression profiles, Aharoni et al. (2004) speculated that members of the ERF transcription factors could be involved in regulation of suberization. Candidate genes for cork regulation include members of the *R2R3 MYB*, *APETALA1* and *WRKY* families (Soler et al., 2007).

B. Bioynthesis and assembly of the suberin polyaromatic domain

The poly(phenolic) domain of suberin is a polymer of crosslinked hydroxycinnamic acids and their derivatives, and monolignols (Bernards et al., 2004). Phenylalanine is the common intermediate, synthesized via the shikimate pathway. In potato tubers, where an anionic peroxidase associated with the crosslinking of aromatic monomers is induced upon wounding (Borchert, 1974, 1978; Espelie and Kolattukudy, 1985; Espelie et al., 1986), it has been shown that the purified enzyme has preference for hydroxycinnamic acids over monolignols (Bernards et al., 1999). Although the *in planta* function of the acidic peroxidase in potato remains to be proven, it is believed that the enzyme is required for suberinization (Bernards et al., 2004). A plasma membrane-associated NADPH-dependent oxidase is activated during the suberization process. This enzyme produces H_2O_2 , which is used for polymerization of aromatics into the polyaromatic domain catalyzed by the peroxidase (one or several isoforms). In tomato fungal resistant lines, an anionic peroxidase is expressed upon fungal induction of suberization (Mohan et al., 1993). However, downregulation of two tomato genes encoding anionic peroxidases failed to suppress deposition of suberin (Sherf et al., 1993). Hence, other peroxidases (e.g. cationic peroxidases) can catalyze the incorporation of aromatic monomers into suberin domains (Kolattukudy, 2001a). Alternatively, laccases (multi-copper containing glycoproteins) may have a role in these processes. Although evidence for the *in vivo* function of this 17-member family in *Arabidopsis* is scarce, it is

known that 16 of those genes are expressed in roots, and they respond to salt stress (Cai et al., 2006). Furthermore, laccases, but not peroxidases, are up-regulated in the phellem transcriptome (Soler et al., 2007)

Cutin and suberin: major questions

At present, thirty years after the pioneering studies performed by Kolattukudy, many questions regarding polyester biosynthesis, assembly, and structure remain still unanswered: Which specific enzymes/genes are involved in monomer synthesis and polyester assembly?, How are they regulated?, What is the order of the biosynthetic reactions?, What species are transported to the site of polyester assembly? Where does the polymerization reaction occur?. What is the three dimensional structure of the polyester? Because of new analytical tools and Arabidopsis functional genomics strategies, it is now possible to design new and robust experiments to approach these questions. In particular, this dissertation work deals with establishing analytical techniques for chemical analysis of lipid polyesters, and identifying enzymes involved in their synthesis. Chapter 2 describes the development of an analytical method that is used to characterize wild-type Arabidopsis and Brassica seeds. Chapter 3 demonstrates that the assay is useful to reveal compositional differences in mutants affected in cutin and/or suberin. Chapter 4 uses a bioinformatics approach to generate a list of prioritized candidates, which are further tested by mutant analysis. Finally,

Chapter 5 focuses on the Arabidopsis *CYP86A2* gene product and its role the synthesis of the major Arabidopsis cutin monomer, C18:2 dicarboxylic acid.

The following paragraphs introduce the rationale behind the studies presented in each chapter.

SEED COATS

In seeds of angiosperms, three main components are distinguished: the embryo, the endosperm, and the seed coat. Embryo and endosperm have both maternal and paternal origin, whereas seed coats differentiate from the ovule integuments and therefore have maternal origin (Boesewinkel and Bouman, 1995). The specialized cells forming the seed coat layers play fundamental and different roles throughout seed development and even at maturity, when the seed coat cells are dead. During seed development, dormancy, and germination, the seed coat imparts protection against pathogens and adverse conditions, allowing survival of the offspring. Besides its protective functions, it is involved in embryo nutrition during development, and has functions in establishing and maintaining seed dormancy, facilitating seed dispersal, and promoting germination under favorable conditions (Haughn and Chaudhury, 2005)

Seed coats structure in Brassicaceae

In seed coats of mature seeds, several structures are recognized: the testa and tegmen, which develop from the outer and inner integument respectively (Corner, 1976), and the hilum, raphe, chalaza, and micropyle. The terms integument(s) and seed coat are assigned to the same organ when it is in the immature or mature state, respectively (Werker, 1997). The basic cellular layers that form the seed coat in Brassicaceae are similar among members of this family (Moise et al., 2005). In the mature seed coat of *Arabidopsis*, the testa arises from the outer integument (oi), formed by a superficial epidermal layer containing mucilage (oi2) and a palisade layer (oi1) (Beeckman et al., 2000) (**Figure 6a-b**). A subepidermal layer in the middle of the testa is absent in *Arabidopsis*, although it is found in other species of the family. The cells in the mature epidermal layer have thick inner tangential (parallel to the seed surface) and radial (perpendicular to the seed surface) walls and are devoid of cytoplasm. During development, mucilage is deposited between the primary cell wall and the protoplasm on the outer side of the outer cell layer. The cytoplasm is displaced, forming a column in the center of the cell, and a secondary cell wall is produced forming the columella, which, at maturity, consists of a reinforced cellulosic column. A dry thin mucilage layer is compressed under the outer tangential cell wall (Western et al., 2000; Windsor et al., 2000). The palisade layer also has reinforced cell walls and is compressed against the outer layer in the mature seed coat (Windsor et al., 2000). The tegmen originates from a three-layered (ii1-ii3) inner integument (ii), but the middle layer (ii2) surrounds only part of the embryo, resulting in only two layers in the zone of the chalazal and micropyle

(Figure 6) (Beeckman et al., 2000). At maturity, the three layers die and are highly compressed forming the pigmented tegmen. In addition, one or two layers of endosperm remain attached to the seed coat. In summary, in the mature seed coat of *A. thaliana* all the cell layers are dead and pressed together. Only the epidermis, which contains the thick-walled collumella and the mucilage, preserves its structure (Haughn and Chaudhury, 2005).

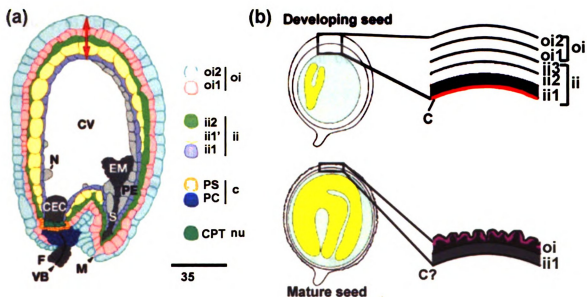


Figure 6. (a) Scheme of Arabidopsis seed anatomy and (b) Schematic drawing of the general organization of the developing and mature seed coat.

C = cuticle CEC, chalazal endosperm cyst; CPT, chalazal proliferating tissue; CV, central vacuole; EM, embryo; F, funiculus; ii, inner integument; M, micropyle; N, nodule; Nu, nucellus; oi, outer integument; PC, placentochalaza; PE, peripheral endosperm; PS, pigment strand; S, suspensor; VB, vascular bundle. (a) was adapted from Lepiniec et al. (2006); (b) was adapted from Nakaune et al. (2005).

Van Caeseele et al. (1981, 1982) have studied in detail the seed coats of *B. campestris* where, unlike *Arabidopsis*, the mucilaginous epidermal layer is compressed. Another difference is that the palisade layer presents secondary thickening in both the inner tangential and radial cell walls and is not collapsed at maturity. Neither cuticles nor suberized cell walls have been described in mature seed coats of *B. campestris*. In *A. thaliana* seeds, analysis by transmission electron microscopy revealed the presence of a cuticle on the inner cell layer of the inner integument facing the embryo in all developmental stages until maturity (**Figure 6**) (Beeckman et al., 2000). This cuticle could still be present in the mature seed but its visualization is difficult because the adjacent pigmented layers are fused together.

Functions of the seed coat

The seed coat envelops the embryo, and thus has functions associated with nutrition, protection, dispersal, promotion and maintenance of dormancy, and germination (Boesewinkel and Bouman, 1995). Flavonoid compounds synthesized by the inner integument have important functions including protection against radiation and defense through their antimicrobial activity (Winkel-Shirley, 2001). These compounds are also involved in the induction of dormancy (Debeaujon et al., 2000). The secondary thickening in the two outer layers of the testa is believed to impart support, defense, and impermeability to water and oxygen (Haughn and Chaudhury, 2005). The mucilage is a pectic

polysaccharide that swells upon seed imbibition, breaking the outer epidermal cell wall, and therefore contributing to germination particularly in dry environments (Penfield et al., 2001).

Analyses of a series of seed coat mutants have been useful to study *Arabidopsis* seed coat functions (Debeaujon and Koornneef, 2000; Debeaujon et al., 2000; Penfield et al., 2001; Clercx et al., 2004; Haughn and Chaudhury, 2005). From such studies, it was concluded that permeability to water and gases is mainly restricted by mucilage, secondary wall thickening, and flavonoid accumulation. These structures are also responsible for protecting the embryo and maintaining seed dormancy. In addition, the recent characterization of a suberin mutant, *gpat5*, demonstrated that lipid polyesters deposited in the seed coat play a critical role in preventing the passage of dyes (Beisson et al., 2007).

Lipid polyesters in seed coats

Seed coat imposed dormancy results from impermeability of the seed coat to water or gases, mechanical impediment of radicle protrusion, or prevention of inhibitors from leaving the embryo (Boesewinkel and Bouman, 1995). At maturity, closure of all seed coat openings and coating with water repellent substances are two requisites for seed coats becoming impermeable.

In the mature seed coat, the epidermal tissues derived from the ovule are capable of forming a cuticle, which is not necessarily on the outer surface of the organ (Martin and Juniper, 1970). Inner cuticles can develop between the seed coat and the remains of the nucellus or endosperm. In soybean, for example, the thick cuticle covering the palisade layer is the only structural feature that correlates with seed coat permeability (Ma et al., 2004). Early in the development of citrus seeds, cuticle-free channels to the embryo sac exist at the chalazal region and are later sealed with suberin polymers (Espelie et al., 1980). This has also been observed in wheat grains (Zee and O'Brien, 1970) and barley seeds (Cochrane, 1983). Suberized cell walls also occur in the epidermis of cotton seeds (Ryser, 1992). Although several cytological studies have been performed in the Brassicaceae, cuticles and/or suberized cell walls have not been reported (Van Caeseele et al., 1981, 1982). In *A. thaliana* seeds, the presence of a cuticle on the inner cell layer of the inner integument facing the embryo was described in immature seeds (Beeckman et al., 2000).

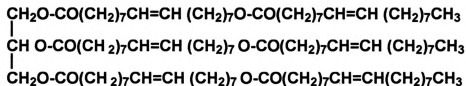
LIPID POLYESTERS IN STIGMA EXUDATES

Wet stigmas of solanaceous plants such as petunia (*Petunia hybrida*) and tobacco (*Nicotiana tabacum*) are covered with a sticky exudate, a mixture of lipid polyesters, proteins, and carbohydrates (Cresti et al., 1986). This fluid is essential for pollen growth in vivo. Moreover, it has been shown that the lipid fraction is sufficient and essential for this function (Wolters-Arts et al., 2002).

Stigma lipid polyesters are poly- ω -hydroxy fatty acids esterified to glycerol. In *N. tabacum*, tetra- to hepta-acylglycerols occur (**Figure 7**), with no free hydroxyl groups at the ends, meaning that all the polyester chains are end-capped with a non-hydroxy fatty acid (Matsuzaki et al., 1983a) (**Figure 7a**). The major ω -hydroxy fatty acids found in stigmas of solanaceous species are 18-hydroxyoleate and 18-hydroxylinoleate. Interestingly, these compounds are not found in the membrane of the stigmas or other tissues (Matsuzaki et al., 1983b), and have been reported as components of cutin and suberin (Kolattukudy, 1975).

Petunia stigmas contain 96% ω -hydroxy fatty acids, while tobacco stigmas contain 60% ω -hydroxy fatty acids (Koiwai and Matsuzaki, 1988). Recent studies performed using gel permeation chromatography showed that the petunia polyester fraction has about 50 acyl groups per molecule, whereas tobacco stigma exudate has 5-6 acyl groups per molecule (**Figure 7**) (Wang et al., 2003). As in cutin, more polar monomers (e.g. 9(10)-hydroxy-, 9(10),18-dihydroxy- and 9,10,18-trihydroxy-C18 fatty acids) have also been found in tobacco fractions. An important experimental difference with cutin is that stigma polyesters are extractable by organic solvents. Although cutin and stigma exudates have common characteristics, it is uncertain whether they are assembled by similar biosynthetic pathways and involve related genes.

(a) HEXAACYLGLYCEROL (TAG 6)



(b)

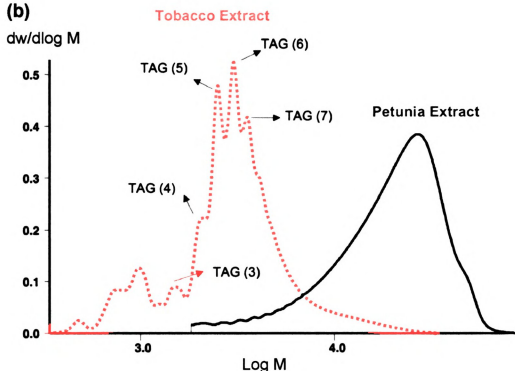


Figure 7. Structure and molecular weight distribution of lipid polyesters found in stigma exudates.

(a) Example of one of the possible isomers of hexaacylglycerol (TAG 6) found in tobacco stigmas. **(b)** Molecular weight distribution of stigma poly-acylglycerols determined by Gel Permeation Chromatography.

Less is known about the biosynthesis of stigma lipids. In petunia, a ω -hydroxylase gene (PH1, *petunia hydroxylase 1*) was identified using an EST-based approach. This gen is exclusively expressed in developing stigmas. Petunia plants transformed with RNAi constructs for the PH1 gene showed a dry stigma phenotype and arrested biosynthesis of ω -hydroxy fatty acids. These results suggested that PH1 has a crucial function in stigma lipid biosynthesis in petunia (Han et al., 2005). No related research has been performed for other species.

Phylogenetic analysis indicated that PH1 is related to the Arabidopsis CYP86A subfamily of ω -hydroxylases (Han et al., 2005). Moreover, its closest orthologous is CYP86A2 (*ATT1*), which is known to have a role in Arabidopsis cutin monomer oxidation (Xiao et al., 2004). Based on the evidence of these enzyme functions, in Chapter 5 I used an *in planta* transgenic approach to test the hypothesis that a “cutin” hydroxylase (*ATT1*) can hydroxylate stigma polyester monomers and, conversely, a stigma hydroxylase (PH1) can use leaf cutin monomers as substrates.

CHAPTER 2

THE LIPID POLYESTER COMPOSITION OF *ARABIDOPSIS THALIANA* AND *BRASSICA NAPUS* SEEDS

Maria Isabel Molina, Gustavo Bonaventure, John Ohlrogge, Mike Pollard
Department of Plant Biology, Michigan State University, East Lansing, MI
48824-1312, USA
Phytochemistry (2006), **67**, 2597-2610

Acknowledgements

This work was supported by the National Research Initiative of the USDA Cooperative State Research, Education and Extension Service, grant number 2005-35318-15419, and by a Fulbright Scholarship to Isabel Molina. We are grateful to Dr. Fred Beisson, Department of Plant Biology, Michigan State University, for helpful discussions and for a critical reading of the manuscript.

ABSTRACT

Mature seeds of *Arabidopsis thaliana* and *Brassica napus* contain a complex mixture of aliphatic monomers derived from the non-extractable lipid polyesters deposited by various seed tissues. Methods of polyester depolymerization of solvent-extracted seeds and analysis of aliphatic monomers were compared. Sodium methoxide-catalyzed depolymerization followed by GC analysis of the acetylated monomers was developed for routine quantitative analysis suitable for 0.5 g seed samples. In *Arabidopsis* seeds the major C16 and C18 monomers identified included ω -hydroxy fatty acids and α,ω -dicarboxylic acids derived from palmitate, oleate and linoleate, and 9,10,18-trihydroxyoctadecenoic acid. Among monomers which can collectively be considered derived from suberin, docosan-1-ol, docosane-1,22-diol, 22-hydroxydocosanoic acid, 24-hydroxytetracosanoic acid, tetracosane-1,24-dioic acid and ferulic acid were the major species. Compared to *Arabidopsis*, *Brassica* seeds showed a roughly similar proportion of monomer classes, with the exception that alkan-1-ols were 3-fold higher. Also, there were much less C24 aliphatic species and significant amounts of C14-C16 alkan-1-ols, including *iso*- and *anteiso*-methyl branched compounds. Dissection and analysis of mature *Brassica* seeds showed that the trihydroxy C18:1 fatty acid was found mainly in the embryo, while ferulate, fatty alcohols and C22 and C24 species were specific to the seed coat plus endosperm.

INTRODUCTION

Plants synthesize two distinct types of insoluble polymers derived from fatty acids: cutin and suberin (collectively called lipid polyesters). Cutin is the structural component of the plant cuticle, the outermost layer of aerial organs of higher plants (Kolattukudy, 2001a,b; Kolattukudy and Espelie, 1985). Waxes embedded in the cutin make the cuticle an efficient barrier against desiccation and gas exchange (Riederer and Schreiber, 2001). The cuticle constitutes the immediate contact zone between the plant and its environment and can function as a barrier to protect against pathogen attack. It controls the diffusion of molecules into plant tissues and plays a role in maintaining the separation of organs during organogenesis. While the cuticle lies on the outer face of the primary cell wall, suberin is located between the inner face of the primary cell wall and the plasma membrane (Kolattukudy, 1980). Typically, suberin acts as a barrier to control the movement of water and solutes, and to contribute to the strength of the cell wall (Nawrath, 2002). Suberin is typically found in outer bark, and in the epidermis and endodermis of roots. It is also deposited as a wound response by injured plant cells (Kolattukudy, 2001a). Suberized cells also occur in other plant tissues, such as bundle sheaths of grasses, in the chalazal region of seed coats (Espelie, 1980), at the boundary between the plant and its secretory organs (Thompson et al., 1979), as well as in fibers of cotton (Yatsu et al., 1983; Schmutz et al., 1996).

Cutin polyester is typically composed of esterified hydroxy- and polyhydroxy-C16 and C18 fatty acids (Heredia, 2003; Holloway, 1984; Kolattukudy, 1980a,b). In C16-rich cutins 16-hydroxy- and 10,16-dihydroxy-palmitic acids are usually dominant, while in C18-rich cutins 9,10,18-trihydroxystearic acid and 9,10-epoxy-18-hydroxystearic acid monomers and the corresponding octadecenoic acids are common. In addition, glycerol has been found esterified to cutin aliphatic monomers (Graça et al., 2002) while minor amounts of hydroxycinnamic acids and carbohydrates have been reported as structural components of cutin (Fang et al., 2001; Kolattukudy, 1977). Suberin, on the other hand, contains both aliphatic and aromatic monomers (Bernards et al., 1995; Kolattukudy, 2001a; Bernards, 2002; Holloway, 1984). The aliphatic polymer is composed mainly of C16 to C28 ω -hydroxy fatty acids and C16 to C26 α,ω -dioic acids, the latter of which are diagnostic for suberin. There is little mid-chain oxygen functionality. A characteristic feature is the presence of monobasic monomers of very long chain fatty acids and alcohols (C20 to C32, with C22 and C24 being the most common). The aromatic network is a hydroxycinnamate-derived polymer, primarily comprised of ferulic acid, N-feruloyltyramine, cinnamic acid, p-coumaric acid or caffeic acid (Bernards et al., 1995). Glycerol is another major compound of this polyester, constituting up to 20% by weight of suberin in oak, cotton and potato (Graça and Pereira, 2000a,b; Moire et al., 1999). The current model describes suberin as a hydroxycinnamic acid-monolignol polyphenolic domain embedded in the primary cell wall and covalently linked to a glycerol-based polyaliphatic domain (Bernards, 2002).

The chemistry of cutin, which varies both with species and organ analyzed (Espelie et al., 1979; Kolattukudy and Espelie, 1985), has been studied largely in leaves and fruits (Martin and Juniper, 1970; Kolattukudy, 1980b). Less is known about the composition of polyesters associated with seeds, in part because a reliable protocol for their analysis has not been developed. The seed coat plays an essential role in seed survival by providing mechanical and chemical protection, acting as a barrier to gas and water exchange, and maintaining seed dormancy (Boesewinkel and Bouman, 1995). The maternally-derived epidermal tissues in the seed (i.e. the seed coat) are capable of forming a cuticle, which is not necessarily on the outer surface of the organ (Martin and Juniper, 1970). A cuticle, which may originate from the ovule, can also develop between the seed coat and the remains of the nucellus or endosperm. Early in the development of citrus seeds, cuticle-free channels to the embryo sac exist at the chalazal region and are later sealed with suberin polymers (Espelie et al., 1980). This has also been observed in wheat grains (Zee and O'Brien, 1970) and barley seeds (Cochrane, 1983). Suberized cell walls have also been described in the epidermis of cotton seeds (Ryser, 1992). The basic cellular layers that form the seed coat in Brassicaceae, which includes the genera *Arabidopsis* and *Brassica*, are similar among species in this family (Moise et al., 2005). Although several cytological studies have been performed (Van Caeseele et al., 1981,1982; Beeckman et al., 2000), no evidence of cuticles and/or suberized cell walls in the mature seeds of *Brassica* species were reported. Such features may have been overlooked

Plant lipid polyesters are poorly understood at the structural, biosynthetic and genetic levels. However, the molecular genetic tools available for *Arabidopsis thaliana* should change this picture. Both forward and reverse genetic screens require robust chemical analyses to complement assays of functional properties such as cuticle permeability, organ fusion phenotypes, or pathogen susceptibility. Such analyses have only recently been published (Bonaventure et al., 2004; Xiao et al., 2004; Franke et al., 2005). However, a reliable method for seed polyester analysis is currently lacking. In this work we report the development of a quantitative method to analyze the polyester monomer content and composition in whole seeds of *Arabidopsis thaliana* and *Brassica napus*.

RESULTS AND DISCUSSION

Monomer analysis methods – introduction

The analysis of cutin and suberin monomer composition and content requires a depolymerization step to cleave ester bonds. Typically, this is achieved by one of four methods; saponification, acid-catalyzed transmethylation, base-catalyzed transmethylation, or hydrogenolysis (Holloway, 1984; Kolattukudy, 2001). Analysis of the extracted monomers by GC or GC-MS is usually undertaken after derivatization to produce TMSi ethers and esters,

since they give very diagnostic mass spectra. Saponification and transmethylation will also cleave amides, producing fatty acids or their methyl esters respectively. In choosing between the various methods, there is a trade-off between ease and reliability of the assay, and the loss or overlap of specific components. Our aim was to produce a robust method that could be used routinely for GC analysis of total seed polyesters. Apart from instrument availability, one reason for using a GC method for a quantitative screen is that the FID detector offers a very linear response over a very wide mass range and a simple theoretical correction factor when compared to total ion current quantification by GC-MS. Previously we used hydrogenolysis in conjunction with deuteriolysis (Walton and Kolattukudy, 1972) to analyze the polyesters present in the epidermal layer of Arabidopsis leaf and stem (Bonaventure et al., 2004). A drawback of this method is that it requires GC-MS analysis to distinguish the degree of deuteration of fatty polyols, in order to make assignments of structure. For example a 1, ω -diol hydrogenolysis product may be derived from 1, ω -diol, ω -hydroxy fatty acid and/or 1, ω -dicarboxylate monomers. The isotopomer analysis may introduce errors especially if it is conducted on weak molecular ion multiplet peaks. This is particularly problematic for lower abundance fatty polyol products. In our hands O-TMS esters also were quantitatively problematic, giving variable response factors significantly lower than theoretical, probably because of injector decomposition. Thus for this study we preferred transmethylation with fatty acid methyl ester analysis over saponification and silylation of hydroxyl and carboxylate groups. For GC analysis method we used acetylation, which

provides a more stable derivative of hydroxyl groups; silylation was used for identification purposes in setting up the method.

Although base-catalyzed transmethylation will not destroy epoxy fatty acids, the subsequent acetylation will rapidly convert epoxides to their corresponding vicinal diol diacetates. This was an acceptable trade-off since in *Arabidopsis* 9,10,18-triol C18 fatty acid monomers are considerably more abundant than the 18-hydroxy-9,10-epoxy C18 fatty acid monomers, both of which give 9,10,18-triacetoxy-fatty acid methyl ester products. In practice transmethylation with sodium methoxide in methanol always produced variable amounts of saponified products, indicating water in the system, despite our attempts to thoroughly dry the extracted and finely ground seed residues. To combat this we used methyl acetate as a co-solvent at 15% volume (Christie, 1982). Any water in the system will produce NaOH from NaOMe. This NaOH will be rapidly removed by saponification of methyl acetate to produce sodium acetate and methanol. A small fraction of the free hydroxyl groups in the monomers released will be acetylated by the equilibrium transesterification reaction $\text{ROH} + \text{MeOAc} \leftrightarrow \text{ROAc} + \text{MeOH}$, but this does not matter, since for the routine analysis the transmethyated sample is fully acetylated prior to GC separation.

Characterization of monomer analysis methods

The whole mature *Arabidopsis* seed (about 18 μg dry weight) contains about 6-7 μg of lipid, mainly triacylglycerol (Li et al., 2006), but only about 45 ng of total polyester monomers. Finely ground seeds are quenched in hot isopropanol to inactivate any degradative enzymes. When this is followed by multiple extractions with chloroform-methanol mixtures almost all the soluble endogenous lipid is removed (> 99.5%), but there are still some levels (15-20 ng/seed) of normal fatty acids and also sinapic acid released in the polyester analysis. This is reduced 10-fold when the extraction protocol also includes additional methanol and aqueous washes, as described in "Experimental procedures." These washes reduced the dry weight of the recovered seed residues from about 50% to 31% of the initial seed mass, yet gave similar or higher monomer recovery on a per seed basis. Triacylglycerol was recovered from these washes, indicating physical trapping as a dominant source of the excess normal fatty acids.

A 48 hr time course was run for the NaOMe-MeOH-MeOAc reaction, with two internal standards, namely methyl heptadecanoate acting as a mass standard and ω -pentadecalactone acting as a control for both transmethylation and acetylation reactions (**Figure 8**, upper panel). This showed that most of the polyester monomers were released in the first 30 minutes of the transmethylation reaction. The rapid depolymerization is expected (Holloway, 1984). However, with the exception of tetracosanoate, the normal fatty acids were transmethyated more slowly. We expect that most of the C16-C20 fatty acids (which represent

9.75 mole % of total monomers - **Table 2**) originate from “physically trapped” triacylglycerol. In support of this interpretation we analyzed the *fae1* mutant line, which is blocked in accumulation of C20 and C22 fatty acids in the seed triacylglycerols (Kunst et al., 1992; James et al., 1995). The effect of the *fae1* mutation on seed polyester monomers was minimal, with the exception that eicosenoate showed a 90% reduction (from 1.4 ± 0.4 to 0.12 ± 0.05 mole %) consistent with its origin from triacylglycerols. The C18 unsaturated fatty acids (5.5 ± 1.5 mole % in wild type) are therefore likely to be derived mainly from trapped triacylglycerols. The one fatty acid that is rapidly transmethyated is tetracosanoate, a behavior groups it with other polyester monomers.

Figure 8. Standardization of the NaOMe-MeOH-MeOAc transmethylation reaction for depolymerization of exhaustively extracted Arabidopsis seed residues.

Products were analyzed by FID-GC after acetylation, with the TIC of peaks of interest normalized against the TIC peak area for the recovery of methyl heptadecanoate internal standard. The upper panel shows the time course for appearance of total normal fatty acid methyl esters, total α,ω -dicarboxylate dimethyl diesters, total ω -hydroxy fatty acid methyl esters, methyl tetracosanoate and methyl trihydroxyoctadecenoate products. The lower panel shows the amount of total monomers recovered when 25 to 400 mg of seed residues was added to the reagent and transmethyated for 2 hr at 60°C. Each data point is the average of duplicates.

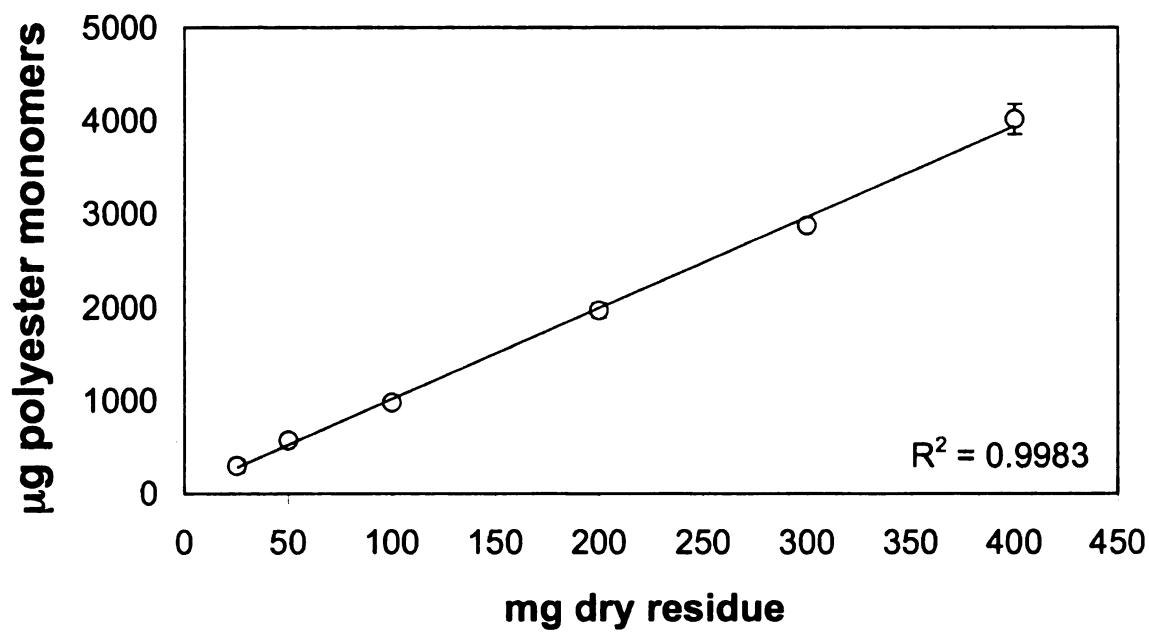
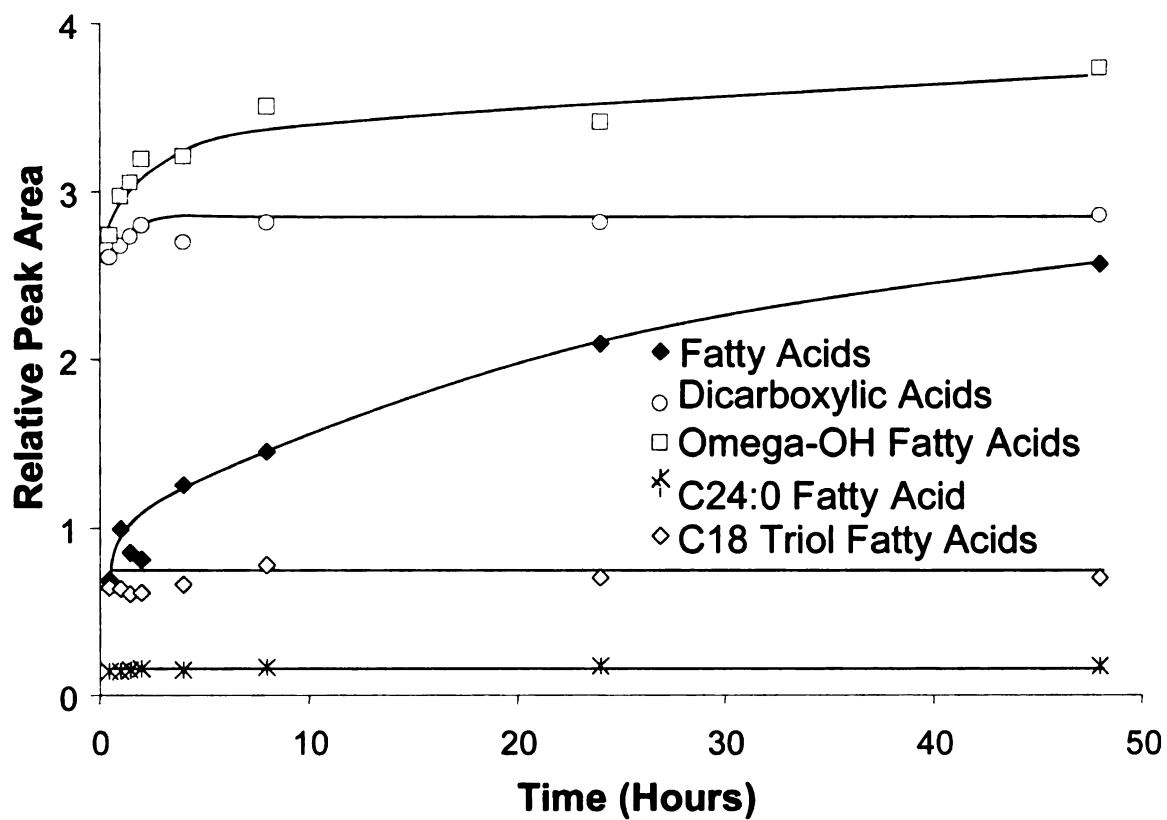


Figure 8.

Table 2. Monomer composition for the depolymerization of solvent-extracted wild type *Arabidopsis thaliana* seed residues by NaOMe-catalyzed transmethylation

#, Polyester Monomer (mole %)	Relative Amount	
1. Octadecan-1-ol	1.5	± 0.1
2. Eicosan-1-ol	1.5	± 0.1
3. Docosan-1-ol	2.8	± 0.25
4. Nonadecan-1-ol, branched	0.3	± 0.05
5. Tricosan-1-ol, branched	0.35	± 0.05
<i>Total Alkan-1-ols</i>		<i>6.5 ± 0.45</i>
6. 16-Hydroxyhexadecanoic Acid	1.75	± 0.1
7. 18-Hydroxyoctadecadienoic Acid	4.55	± 0.6
8. 18-Hydroxyoctadecenoic Acid	3.45	± 0.25
9. 18-Hydroxyoctadecanoic Acid	0.25	± 0.05
10. 20-Hydroxyeicosanoic Acid	0.65	± 0.1
11. 22-Hydroxydocosanoic Acid	4.2	± 0.25
12. 22-Hydroxydocosanoic Acid, branched	0.7	± 0.05
13. 23-Hydroxytricosanoic Acid	0.55	± 0.05
14. 24-Hydroxytetracosanoic Acid	12.6	± 0.45
15. 24-Hydroxytetracosanoic Acid, branched	0.4	± 0.05
16. 25-Hydroxypentacosanoic Acid	0.3	± 0.05
17. 26-Hydroxyhexacosanoic Acid	0.2	± 0.05
<i>Total ω-Hydroxy Fatty Acids</i>		<i>29.6 ± 1.95</i>
18. 1,16-Hexadecane Dioic Acid	1.8	± 0.1
19. 1,18-Octadecadiene Dioic Acid	8.9	± 0.75
20. 1,18-Octadecene Dioic Acid	3.4	± 0.2
21. 1,18-Octadecane Dioic Acid	0.5	± 0.05
22. 1,22-Docosane Dioic Acid	1.65	± 0.1
23. 1,24-Tetracosane Dioic Acid	8.5	± 0.4
<i>1,ω-Dicarboxylic Acids</i>		<i>24.75 ± 1.6</i>
24. 1,20-Eicosane Diol	0.3	± 0.05
25. 1,22-Docosane Diol	2.4	± 0.2
<i>Total 1,ω-Alkane Diols</i>		<i>2.7 ± 0.25</i>

Table 2. (Continued)

26. Hexadecanoic Acid	2.0	± 0.25	
27. Octadecanoic Acid	0.35	± 0.1	
28. C18:1, C18:2, C18:3 Acids	5.5	± 1.5	
29. Eicosanoic Acid	0.5	± 0.05	
30. Eicosenoic Acid	1.4	± 0.4	
31. Docosanoic Acid	0.5	± 0.05	
32. Tetracosanoic Acid	1.5	± 0.1	
33. Hexacosanoic Acid	0.55	± 0.05	
34. Hexacosenoic Acid	0.45	± 0.1	
35. Octacosenoic Acid	0.15		
36. Octacosenoic Acid	0.3	± 0.05	
37. Dotriacontanoic Acid	0.1		
38. Dotriacontenoic Acid	0.15		
39. Tetratriacontenoic Acid	0.15		
<i>Total Fatty Acids</i>			<i>13.6 ± 2.9</i>
40. 2-Hydroxytetracosanoic Acid	0.4	± 0.15	
41. 10,16-Dihydroxyhexadecanoic Acid	0.55	± 0.25	
42. 9,10,18-Trihydroxyoctadecenoic Acid	4.8	± 0.85	
<i>Secondary Hydroxy-Containing Species</i>			<i>5.75 ± 1.25</i>
43. Ferulate	15.2	± 1.3	
44. Sinapate	1.4	± 0.5	
45. C29:1 Sterol (sitosterol?)	0.5	± 0.05	
<i>Other</i>			<i>17.1 ± 1.9</i>

Three extractions of bulked *Arabidopsis thaliana* seed (ecotype Col0) batches were performed and each seed residue was analyzed in triplicate, to give 9 determinations, reported as the average ± SD. GC analyses were undertaken on acetyl derivatives. Peaks that were identified and that are at least 1% of the peak area of the greatest peak, 24-hydroxytetracosanoate, were summed to give 100 mole %. Unidentified peaks represented 18% of the identified peak-by-peak area. Numbers correspond to the peaks of the chromatogram in Figure 2.

In addition to the time course, various amounts of the exhaustively extracted seed residue were transmethylated with the NaOMe-MeOH-MeOAc reagent under the standard conditions (60°C for 2 hr) and polyester monomer content determined. The response was linear over the 25 to 400 mg sample range tested (**Figure 8**, lower panel). Particular attention was paid to the recovery of aromatic components. Spiking seed residues with methyl coumarate, ferulate or sinapate gave essentially quantitative recovery (> 90%) of these components for the transmethylation-acetylation protocol. Spiked tyramine recovery was lower (ca. 30%) and not enhanced by additional extractions under alkaline conditions. Thus the lack of tyramine observed in seed residue depolymerizations, even when run with either basic and acidic transmethylations over extended periods to allow for complete amide bond cleavage, is taken as an indication that tyramine adducts are not part of the seed polyester matrix unless they have been cross-linked through phenol coupling reactions.

A comparison of recently published monomer compositions from *Arabidopsis* leaf, stem and cuticle preparations obtained by four depolymerization methods (Nawrath, 2006) shows that there is a substantial discrepancy over the presence of C22:0, C24:0, C24:1 and C26:0 2-hydroxy fatty acids reported in some studies (Franke et al., 2005; Kurdyukov et al., 2006b), and their absence in others (Bonaventure et al., 2004; Xiao et al., 2004; Suh et al., 2005). We compared depolymerization by acid and base catalyzed transmethylation on the same batch of seed residues for 1 and 48 hours of

reaction, using only organic solvents or the combined organic and aqueous extractions to produce delipidated seed residues. The data set for the 48 hour depolymerizations are shown in **Figure 9**. Both acid and base-catalyzed transmethyations when run for extended times give 2-hydroxy fatty acid methyl ester products. However, the acid-catalyzed reaction is much faster, producing observable 2-hydroxy fatty acid methyl esters within the first hour, whereas the base-catalyzed reaction does not. At 48 hours of transmethylation the acid-catalyzed method produced 8.2 ± 1.23 mg of total monomers/g seed residue, of which 0.75 ± 0.08 mg/g (9.1%) was 2-hydroxy fatty acid, whereas the base catalyzed method produced 7.5 ± 0.84 mg/g of total monomers, of which 0.44 ± 0.1 mg/g (5.9%) was 2-hydroxy fatty acid. The monomer distribution between the two methods was similar (**Figure 9**). The aqueous extractions did not remove significant 2-hydroxy fatty acids from the seed residues.

In setting up our method we have chosen depolymerization by NaOMe-catalyzed transmethylation reaction over a short time to minimize the contribution of the 2-hydroxy fatty acids. We suspect that the 2-hydroxy fatty acids and low levels of very long-chain fatty acids (e.g. C26:0, C26:1, C28:0, C28:1) are derived from the N-acyl groups of sphingolipids, since these acyl compositions are characteristic of sphingolipids (Ohnishi et al., 1983; Imai et al., 1995; Markham et al., 2006). Additional reasons for this conclusion are as follows. First, if 2-hydroxy fatty acids were present in the insoluble matrix as O-acyl esters, then

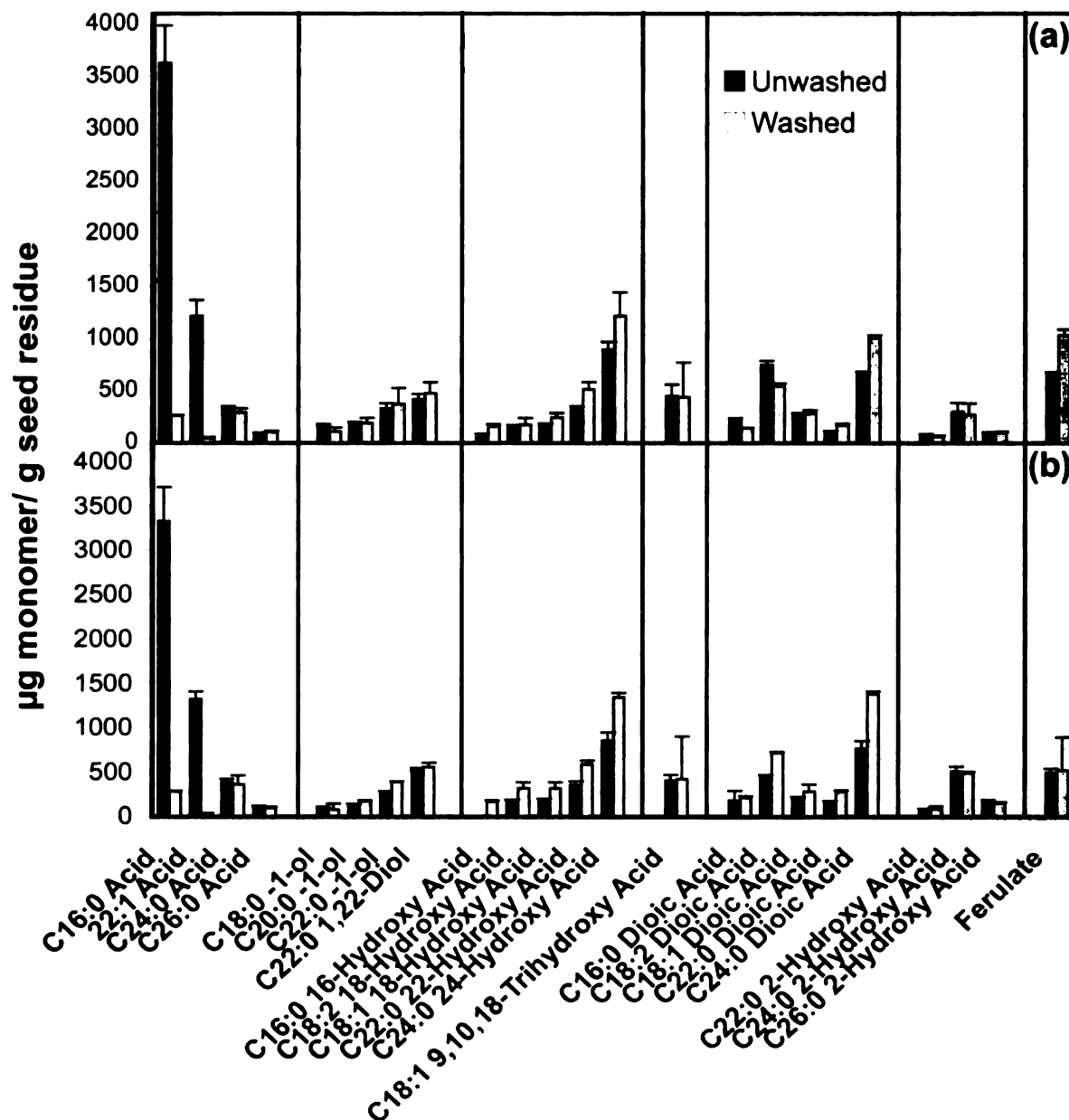


Figure 9. Comparison of the major monomer composition after depolymerization of solvent-extracted *Arabidopsis thaliana* seed residues by base (NaOMe) (a) and acid (H_2SO_4) (b) catalyzed transmethylation reactions run for 48 hours.

GC-MS analysis was conducted on TMSi derivatives, and monomers are quantified based on peak total ion current. Data are reported for the average of triplicate determinations \pm SD.

reaction with LiAlH_4 should produce 1,2-diol products. However, although hydrogenolysis of the seed residues with LiAlH_4 produces quantitative recovery of alcohol products corresponding to all other aliphatic components, 1,2-diols are absent. Hydrogenolysis will not cleave amide linkages, but instead reduce amides to amines, thus producing products that are not observed in the GC-MS analysis. Secondly, the slow kinetics of 2-hydroxy fatty acid transmethylation is consistent with their presence as amides, not esters. And thirdly, the bulk of sphingolipids in plants are not readily extractable in organic solvents (Sperling et al., 2005; Markham et al., 2006). These are the glycosylated inositol phosphoceramides, which may not be extracted in our protocol. Thus any 2-hydroxy fatty acids recovered by transmethylation will likely represent bulk seed sphingolipids. That is not to say that sphingolipids may not play a role in either the biogenesis of the cuticle, or the cuticle itself. However, leaf and stem, where cuticles can be isolated, seem a better system to investigate this possibility than seed.

Monomer analysis methods - identification and quantification of monomers

The basis of the identification of the products released by sodium-methoxide catalyzed transmethylation was mass spectrometry of TMSi derivatives of the transmethylation products. These were compared to a set of standard compounds, data from mass spectral libraries and the literature (Heller and Milne, 1978; Murphy, 1993; Bonaventure et al., 2004). Additional evidence of

structure came from the retention times of homologous series when compared to known standards before and after TLC fractionation, and from catalytic hydrogenation of the transmethylated sample prior to silylation and GC-MS analysis. The results from transmethylation were also compared with the composition obtained from hydrogenolysis, and from analysis of the molecular ion clusters of mono-, di-, tri- and tetraol-products of deuterium incorporation after deuteriolysis. Close correspondence of the major components by hydrogenolysis/deuteriolysis and transmethylation indicates that they are present mainly if not exclusively as esters, not amides in the solvent-insoluble residue. Diagnostic MS ions for the major monomers obtained by transmethylation and silylation of Arabidopsis seed residues are given in **Table 3**. In addition, a lignan and two diterpene acids were persistent minor components, tentatively identified as described in **Appendix A**. One important criterion for ensuring good reproducibility is to harvest fully mature seed. The deposition of Brassica seed polyesters occurs fairly late in seed maturation and compositional changes occur right up to seed maturity. In particular, the deposition of 10,16-dihydroxypalmitate is a very late event (see Chapter 3, **Figure 16**). Presumably the same occurs in Arabidopsis.

Table 3. Mass spectral data for representative major monomers in Arabidopsis seed polyesters

Docosan-1-ol, TMSi ether

383 [M-15]⁺ (100), 367 [M-31]⁺ (2), 103 (11), 75 (24), 73 (11)

Docosan-1,22-diol, bis-TMSi ether

471 [M-15]⁺ (1), 455 [M-31]⁺ (4), 396 [M-90]⁺ (4), 381 [M-105]⁺ (9), 165 (7), 149 (100), 147 (33), 111 (13), 103 (23), 97 (27), 83 (26), 75 (39), 73 (32)

Methyl 24-hydroxytetracosanoate, TMSi ether

455 [M-15]⁺ (57), 439 [M-31]⁺ (5), 423 [M-47]⁺ (100), 348 [M-122]⁺ (5), 159 (11), 146 (16), 103 (12), 75 (27), 73 (15)

Methyl 2-hydroxytetracosanoate, TMSi ether

470 [M]⁺ (3), 455 [M-15]⁺ (40), 427 [M-43]⁺ (4), 412 [M-58]⁺ (33), 411 [M-59]⁺ [M-COOMe]⁺ (100), 159 (9), 129 (12), 103 (15), 89 (17), 75 (17), 73 (41)

Dimethyl tetracosane-1,24-dioate

395 [M-31]⁺ (28), 362 [M-64]⁺ (4), 353 [M-73]⁺ (12), 321 [M-105]⁺ (12), 320 [M-106]⁺ (12), 154 (12), 112 (33), 98 (100), 97 (25), 87 (39), 84 (32), 74 (60), 69 (31)

Methyl 18-hydroxyoctadecenoate, TMSi ether

384 [M]⁺ (15), 369 [M-15]⁺ (38), 353 [M-31]⁺ (11), 337 [M-47]⁺ (71), 262 (6), 159 (29), 146 (19), 129 (20), 123 (20), 109 (56), 103 (30), 96 (55), 95 (63), 82 (50), 81 (70), 75 (100), 73 (80)

Methyl 18-hydroxyoctadecadienoate, TMSi ether

382 [M]⁺ (2), 367 [M-15]⁺ (7), 351 [M-31]⁺ (3), 335 [M-47]⁺ (10), 271 (13), 183 (27), 149 (27), 135 (56), 129 (45), 121 (81), 107 (42), 95 (76), 94 (62), 93 (72), 81 (76), 80 (88), 79 (69), 75 (68), 73 (100)

Dimethyl octadecene-1,18-dioate

340 [M]⁺ (5), 309 [M-31]⁺ (29), 308 [M-32]⁺ (30), 290 [M-50]⁺ (10), 277 [M-63]⁺ (33), 276 [M-64]⁺ (57), 248 (8), 109 (29), 98 (56), 95 (57), 87 (43), 81 (82), 74 (54), 69 (55), 67 (67), 55 (100)

Dimethyl octadecadiene-1,18-dioate

307 [M-31]⁺ (28), 306 [M-32]⁺ (57), 290 [M-50]⁺ (10), 275 [M-63]⁺ (25), 274 [M-64]⁺ (27), 208 (16), 194 (19), 180 (24), 149 (33), 135 (53), 121 (49), 107 (36), 95 (53), 94 (57), 93 (58), 81 (89), 80 (58), 79 (92), 74 (31), 67 (100)

Table 3. (Continued)

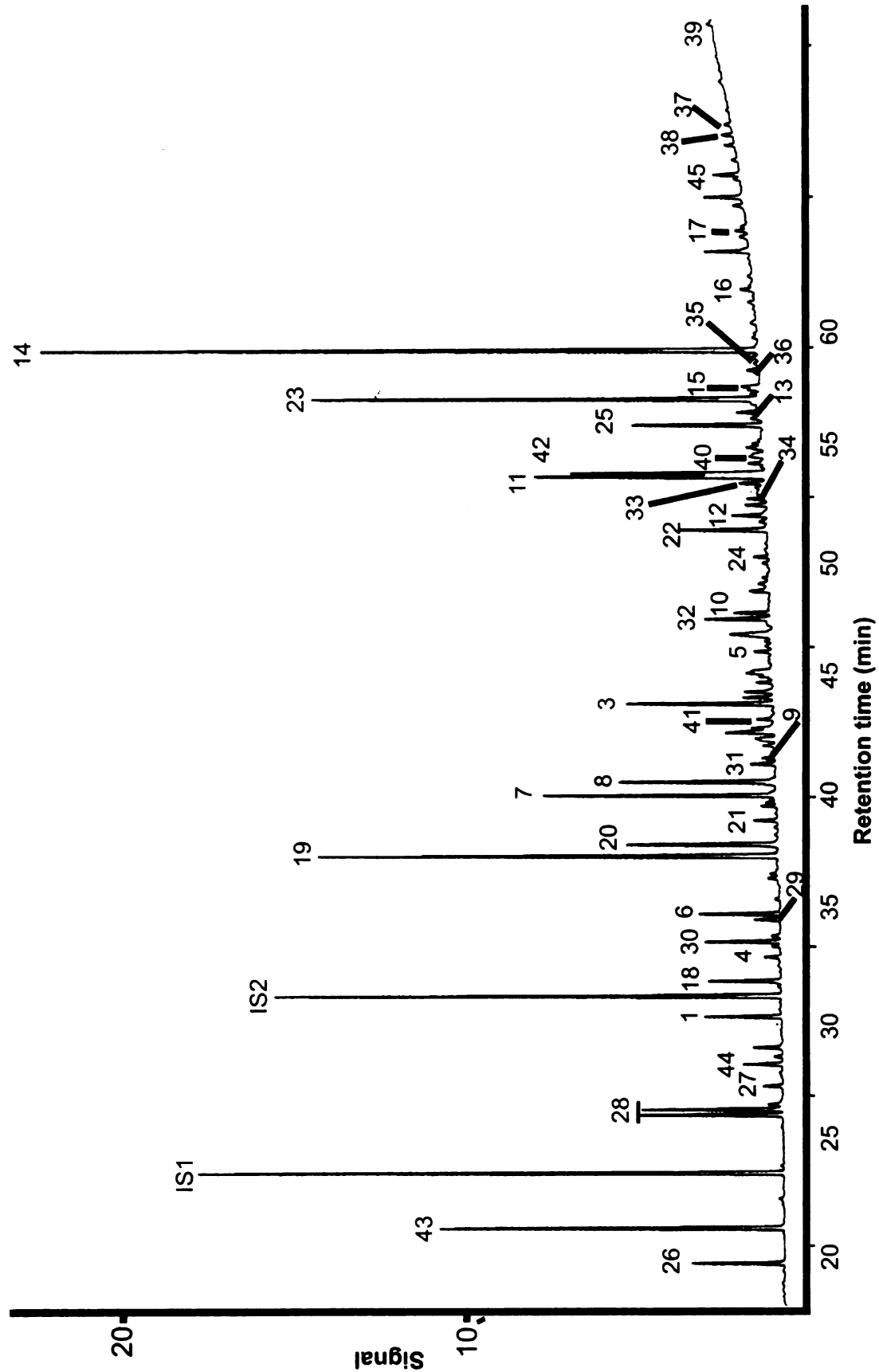
Methyl 10,16-dihydroxyhexadecanoate, bis-TMSi ether (9,16- minor isomer)
431 [M-15]⁺ (3), 415 [M-31]⁺ (2), 399 [M-47]⁺ (1), 309 (4), 275 (42), 274 (21), 273 (100), 259 (3), 244 (12), 185 (4), 169 (9), 147 (12), 129 (21), 103 (18), 95 (26), 75 (24), 73 (51)

Methyl 9,10,18-trihydroxyoctadecenoate, tris-TMSi ether
545 [M-15]⁺ (2), 529 [M-31]⁺ (1), 411 (2), 332 (9), 301 (11), 271 (56), 259 (100), 243 (10), 211 (8), 191 (14), 155 (26), 147 (37), 129 (29), 103 (13) 75 (18), 73 (85)

Methyl ferulate, TMSi ether
280 [M]⁺ (50), 265 [M-15]⁺ (16), 250 [M-30]⁺ (100), 219 [M-61]⁺ (22), 117 (5), 102 (6), 89 (4), 73 (14)

Figure 10 shows a typical chromatogram for the Arabidopsis seed monomers from methanolysis followed by acetylation. The only significant peak overlap is of eicosan-1-ol with dimethyl octadecadiene-1,18-dioate. As a screening tool this is unlikely to cause a problem because octadecan-1-ol contributes almost the same mole % as eicosan-1-ol (**Table 2**), allowing an approximate subtraction of the combined eicosan-1-ol/18:2 dicarboxylate peak. An exact quantification can be determined by one of several methods, which include hydrogenation or TLC separation to give an accurate measurement of eicosan-1-ol versus octacosan-1-ol, or by the simple expedient of using TMSi derivatives, when they separate well.

Figure 10. Chromatogram for GC analysis (DB-5 column) of monomers released by depolymerization of solvent-extracted Arabidopsis seed residues with NaOMe-catalyzed transmethylation and then acetylation. The internal standards methyl heptadecanoate (IS1) and methyl 15-acetoxypentadecanoate (IS2) are indicated. The numbers on the peaks correspond to the monomers detailed in Table 1.



Identification of 9,10,18-trihydroxyoctadecenoate

Methyl trihydroxyoctadecenoate was identified as the major polyester monomer of mature Brassica embryos dissected from seeds. It was therefore important to define its structure. The mass spectrum of the TMSi derivative from transmethylation showed a strong cleavage of the C(9)-C(10) bond with ionization towards the carboxyl end to give $m/z = 259$ ion (60%), and in the other direction a weaker $m/z = 301$ ion (5%). These ions define the C(9)-C(10) vicinal diol structure and place the double bond beyond C(11) (Eglinton and Hunneman, 1968). Cleavage at the C(10)-C(11) bond with ionization towards the carboxyl end gave a $m/z = 361$ ion (9%), which on further loss of TMSiOH produced the $m/z = 271$ ion (34%). Cleavage at the C(10)-C(11) bond is presumably driven by the proximal Δ^{12} double bond, which will produce the C(1)-C(10) fragment as the cation and the C(11)-C(18) fragment as an allylic-stabilized radical fragment. A small peak at $m/z = 545$ corresponding to (M-15) was also observed. After hydrogenation the corresponding saturate had diagnostic $m/z = 259$ (100%) and 303 (30%) ions. Comparison of the retention times of the hydrogenated trihydroxy methyl ester with the products from apple peel cutin suggested the major isomer corresponds to that of apple peel cutin and therefore has the erythro configuration (Eglinton and Hunneman, 1968). Hydrogenolysis and deuterolysis produced octadecen-1,9,10,18-tetraol (Walton and Kolattukudy, 1972). Mass spectroscopy of the TMSi derivative showed cleavage of the C(9)-C(10) bond with ionization towards the carboxyl end to give a diagnostic $m/z =$

303 ion (8%), and in the other direction a weak $m/z = 301$ ion (2%). Cleavage at the C(10)-C(11) bond with ionization towards the carboxyl end gave a $m/z = 405$ ion (2%), which with further loss of TMSiOH gives the $m/z = 315$ ion (4%). On deuteriolysis the ions were 301, 305, 317 and 407 respectively, indicating that the precursor is indeed the trihydroxy fatty acid and not the 18-hydroxy-9,10-epoxy fatty acid and again placing the double bond at the distal end of the molecule. Since we have little of this material further experiments to define regio- and stereo-chemistry were not undertaken, but it is reasonable to assume that this main fatty acid polyol is derived from linoleate and therefore has a 12-cis double bond. As further evidence of this possibility we note that labeled linoleic acid has been shown to be a precursor of 9,10,18-trihydroxyoctadecenoic acid (Kolattukudy et al., 1973). Analysis of spectra for the minor C18 tetraol peak after hydrogenolysis and deuterolysis indicated that both 9,10,18-trihydroxy-octadecenoate and 9,10-dihydroxy-1,18-octadecene dicarboxylate were precursors.

Identification of branched-chain monomers

Iso- and *anteiso*- methyl-branched alkanes have occasionally been reported as constituents of epicuticular waxes (Kolattukudy, 1980b; Kolattukudy and Espelie, 1985), but such branched structures are rarely if ever observed for polyester monomers. In this work branched-chain aliphatic monomers were identified as minor and sometimes significant components in seed polyesters. In

Brassica seed there were substantially more branched-chain monomers present than in Arabidopsis seed, most notably as C14 (2.1 mole %) and C15 (4.9 mole %) saturated alkan-1-ols. After enrichment by preparative TLC the branched-chain primary alcohols were identified using GC-MS of their TMSi ethers. Their mass spectra were very similar to mass spectra for straight-chain primary fatty alcohols. Their retention times relative to straight-chain fatty alcohols were 13.6 and 14.75 for the C14 and C15 compounds respectively. This compares to reductions of 0.37-0.44 and 0.27-0.31 ECL units respectively for *iso*- and *anteiso*-methyl-branches relative to straight-chain compounds on non-polar GC columns (Body, 1984). And finally, the C15 component co-eluted with the *anteiso*- and not the *iso*-pentadecan-1-ol standard. Thus the compounds were identified as 12-methyltridecan-1-ol (*iso*-tetradecan-1-ol) and 12-methyltetradecan-1-ol (*anteiso*-pentadecan-1-ol). They presumably arise from primers for fatty acid synthesis derived from valine and isoleucine respectively. Arabidopsis seed contained small amounts of C18, C19, C22 and C23 branched-chain alkan-1-ols (**Table 2**).

Turning to the ω -hydroxy fatty acid methyl esters, this fraction isolated by preparative TLC from Brassica seed transmethylation products did not contain branched-chain hydroxy fatty acid methyl esters although it did contain odd-chain hydroxy fatty acid methyl esters (**Table 4**). However, in Arabidopsis seeds the most abundant branched-chain compounds were identified by the mass spectra of their OTMSi-ether derivatives as methyl branched-chain hydroxy-docosanoate and hydroxy-tetracosanoate respectively (0.7 and 0.4 mole %, **Table 2**). They

Table 4. Monomer composition after depolymerization of solvent-extracted *Brassica napus* seed residues by NaOMe-catalyzed transmethylation.

Polyester Monomer	Relative Amount (mole %)
Tetradecan-1-ol	5.95 ± 0.23
Hexadecan-1-ol	5.71 ± 0.13
Octadecan-1-ol	1.05 ± 0.05
Eicosan-1-ol ^a	
Docosan-1-ol	0.63 ± 0.04
Tetradecan-1-ol, branched	2.4 ± 0.08
Pentadecan-1-ol, branched	4.9 ± 0.19
<i>Total Alkan-1-ols</i>	<i>20.38 ± 0.71</i>
16-Hydroxyhexadecanoic Acid	9.15 ± 0.16
18-Hydroxyoctadecadienoic Acid	1.01 ± 0.06
18-Hydroxyoctadecenoic Acid	4.90 ± 0.07
18-Hydroxyoctadecanoic Acid	0.81 ± 0.04
20-Hydroxyeicosanoic Acid	0.76 ± 0.05
22-Hydroxydocosanoic Acid	5.60 ± 0.19
23-Hydroxytricosanoic Acid	0.32 ± 0.10
24-Hydroxytetracosanoic Acid	1.15 ± 0.07
25-Hydroxypentacosanoic Acid	0.09 ± 0.09
<i>Total ω-Hydroxy Fatty Acids</i>	<i>23.8 ± 0.6</i>
1,16-Hexadecane Dioic Acid	3.83 ± 0.17
1,18-Octadecadiene Dioic Acid	2.78 ± 0.07
1,18-Octadecene Dioic Acid	3.97 ± 0.08
1,18-Octadecane Dioic Acid	1.07 ± 0.11
1,22-Docosane Dioic Acid	3.20 ± 0.09
1,24-Tetracosane Dioic Acid	0.81 ± 0.08
<i>α,ω-Dicarboxylic Acids</i>	<i>15.66 ± 1.6</i>
1,20-Eicosane Diol	0.06 ± 0.07
<i>Total α,ω-Alkane Diols</i>	<i>0.06 ± 0.07</i>
Tetradecanoic acid	2.04 ± 0.13
Pentadecanoic acid	1.42 ± 0.2
Hexadecanoic Acid	3.68 ± 0.35

Table 4. (Continued)

Octadecanoic Acid	0.92 ± 0.14	
C18:1, C18:2, C18:3 Acids	6.34 ± 1.21	
Eicosanoic Acid	0.59 ± 0.05	
Eicosenoic Acid	0.63 ± 0.49	
Docosanoic Acid	0.98 ± 0.04	
Tetracosanoic Acid	0.64 ± 0.15	
Hexacosanoic Acid	0.18 ± 0.04	
Hexacosenoic Acid	0.05 ± 0.05	
Octacosenoic Acid	0.15 ± 0.06	
<i>Total Fatty Acids</i>		<i>17.73 ± 2.59</i>
2-Hydroxytetracosanoic Acid	0.06 ± 0.17	
10,16-Dihydroxyhexadecanoic Acid	1.19 ± 0.92	
9,10,18-Trihydroxyoctadecenoic Acid	2.56 ± 0.54	
<i>Secondary Hydroxy-Containing Species</i>		<i>3.81 ± 1.62</i>
Ferulate	12.52 ± 0.77	
Sinapate	5.10 ± 1.21	
C29:1 Sterol (sitosterol?)	0.94 ± 0.19	
<i>Other</i>		<i>18.57 ± 2.17</i>

Bulked *Brassica napus* seed (cv Westar) was solvent extracted and polyester monomers analyzed in triplicate. The data are reported as the average ± SD. GC analyses were undertaken on acetyl derivatives. Peaks that were identified and that are at least 1% of the peak area of the greatest uncorrected peak, 16-hydroxyhexadecanoate, were summed to give 100 mole %.

run before the corresponding straight-chain compounds by 0.55 and 0.60 ECL units respectively on the DB-5 column. The question arises as to the exact structure of these compounds. Chromatographic data describes the behavior of *iso*- and *anteiso*-methyl-branched chains, which cause reductions of 0.4 and 0.3ECL units respectively compared to straight chains (Body, 1984). Also for comparison, on a non-polar column methyl 17-acetoxystearate elutes before methyl 18-acetoxystearate by 0.75 ECL units (Tulloch, 1964). As the compounds

are even-carbon we can rule out *anteiso*-branching derived from isoleucine precursor. Considering the branched-chain methyl hydroxy-docosanoate (the same reasoning applies to the tetracosanoate homolog) we have to distinguish between (i) 21-hydroxydocosanoate, (ii) other positional isomers that give secondary alcohols of the straight-chain compound, (iii) 21-hydroxy-20-methylhenicosanoate, and (iv) other positional isomers of 20-methylhenicosanoate containing a secondary hydroxyl group. There are no authentic hydroxy fatty acid standards available to test these possibilities.

When the very long-chain hydroxy fatty acids and dicarboxylic acid esters were fractionated by preparative TLC it became clear that each class of compounds contained a similar profile of minor components, which eluted in a similar order by GC (**Table 5**). The odd-chain and branched-chain components in the dicarboxylate fraction are at lower levels than for the ω -hydroxy fatty acids and thus would be under the GC integration thresholds set for the analysis given in **Table 2**. On preparative silica TLC the branched-chain hydroxy fatty acids esters and dicarboxylate diesters each ran very slightly ahead of the corresponding straight-chain esters or diester. This is the expected chromatographic behavior on introducing a methyl group in the α -position to the ester or primary alcohol functional group. The mass spectra of straight-chain saturated dimethyl diesters was dominated by ions at $m/z = 98$ (100%), with additional diagnostic ions at $m/z = 74$ and 112, and a relatively abundant ($M - 31$) ion. However, the branched-chain dicarboxylates, while retaining the $m/z =$

74, 112 and 98 ions, had as their base peak $m/z = 88$. The mass spectra are shown in **Figure 11**. The $m/z = 88$ ion is the expected ion arising from McLafferty fragmentation of a 2-methyl fatty acid methyl ester, and confirms the structures of the branched chain components as dimethyl 2-methyl-heneicosane-1,21-dioate and dimethyl 2-methyl-tricosane-1,23-dioate, respectively. The mass spectra of the branched-chain hydroxy-fatty acid methyl ester TMS ethers were essentially identical with the spectra of the straight-chain compounds. If (ω -n) hydroxy groups were present they should give distinctive CHROTMSi fragments (eg. $m/z = 117$ for the (ω -1)-hydroxy group), but no such distinctive fragments were observed.

Table 5. Minor components of purified hydroxy fatty acid methyl ester and dimethyl dicarboxylate fractions isolated from *Arabidopsis thaliana* seed polyesters.

Chain	ω -Hydroxy Fatty Acid	Dicarboxylic Acid
C20	0.11	0.01
C21	0.01	nd
C22 branched	0.07	0.02
C22	0.39	0.17
C23	0.06	0.02
C24 branched	0.035	0.02
C25	1.0	1.0
C26	0.03	0.01

For each fraction these components are shown normalized to the mass of the straight-chain C24 compound (1.0).

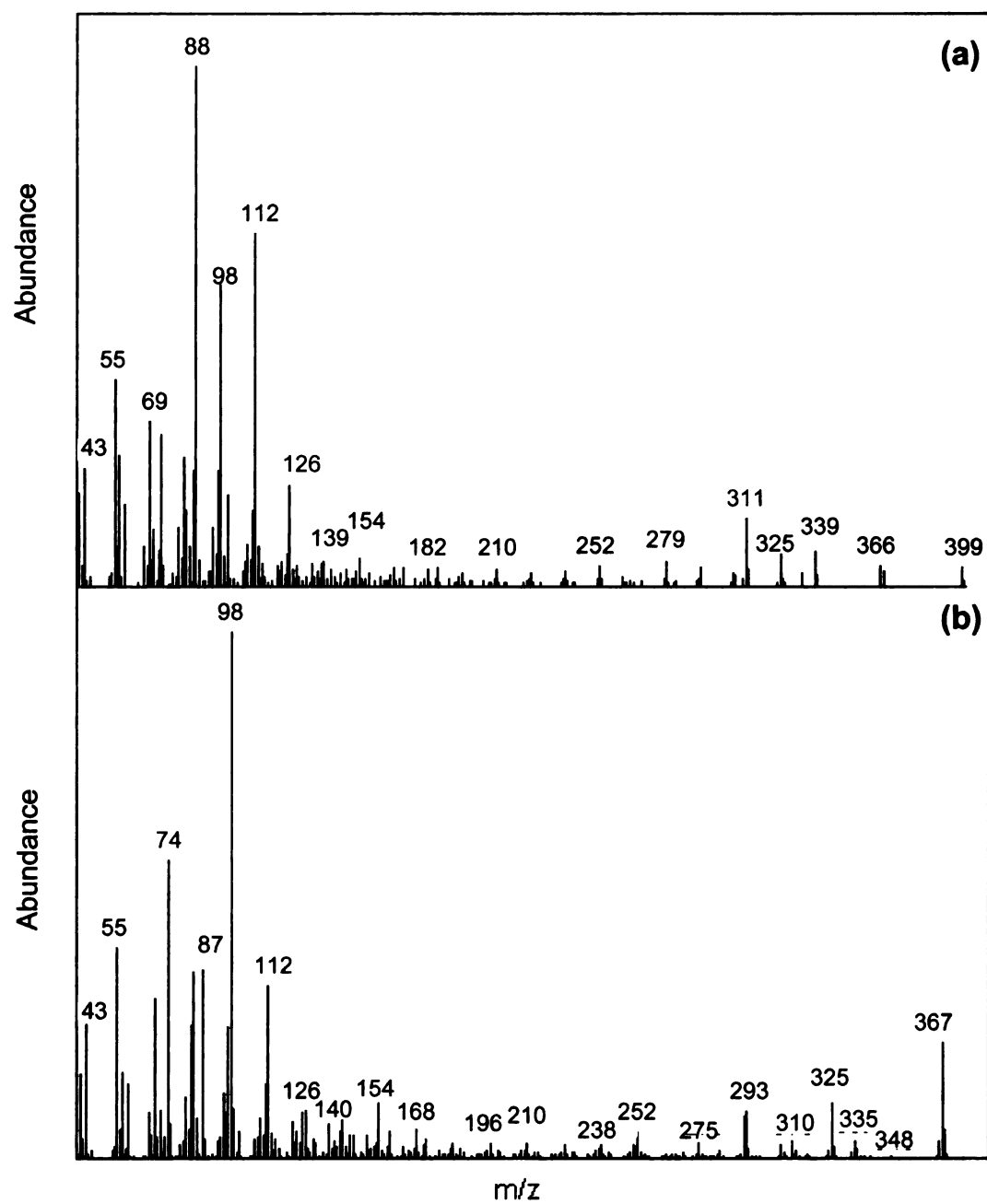


Figure 11. Electron impact mass spectra for dimethyl 2-methylheneicosane-1,21-dioate (a) and dimethyl docosane-1,22-dioate (b).

Our identification of 21-hydroxy-20-methylheneicosanoate and 23-hydroxy-22-methyltricosanoate methyl esters, and 2-methyl-branched even carbon number dicarboxylates in *Arabidopsis* seed polyesters lacks stereochemical definition, as it is based solely on mass spectral and chromatographic R_f and R_t data. However, it is consistent with the presence of odd-chain and *iso*- and *anteiso*-methyl branching found in Brassica seed polyester alkan-1-ols. Although these novel compounds are minor components, they provide biochemical insight by showing that the oxidation systems producing ω -hydroxy and carboxylate functional groups can readily accommodate a 2-methyl group.

Analysis of Arabidopsis thaliana seeds

Table 2 shows the monomers released by transmethylation from *Arabidopsis thaliana* (ecotype Col0) seed residues that had been extracted with organic and aqueous solvents. The identified components give a total of 8.6 ± 0.5 mg/g seed residue (26.1 ± 1.5 μ moles/g seed residue). This value results in an estimate of 46 ng monomers/seed, which corresponds to about 12 μ g monomers/cm² seed surface area. The mass per unit seed area does not represent an actual thickness of a specific polyester layer, since the location of the polyesters in the various seed tissues has not been determined and since other components may be present in such layers. However the mass/area value

is given to make comparisons with reported values for the *Arabidopsis* polyester monomers of about $1.5 \mu\text{g}/\text{cm}^2$ for leaf and $3\text{--}9 \mu\text{g}/\text{cm}^2$ for stem (Suh et al., 2005) and with *Brassica* seeds (see below). Only 18% of the total integrated peaks were unknown compounds, none of which was greater than 1%. Trace amounts of expected monomers not reported in **Table 2** such as tetracosane-1,24-diol, 18-hydroxy-octadecanoic acid, and tricosane-1,23-dioic acid were observed. In addition hydrogenation and deuterolysis studies suggested that there are trace amounts of both 9-hydroxy and 9,10-dihydroxy C18 1,18-dicarboxylic acids; the former may be derived from the epoxide. Previously, high dicarboxylic acid concentrations were generally considered to be indicative of suberin like polyesters. However, the presence of high proportions of C16 and C18 dicarboxylic acids in the leaf and stem epidermal layers (Bonaventure et al., 2004), and the presence of these in the isolated cuticles (Franke et al., 2005), suggest that this generalization is not appropriate for *Arabidopsis*. However, *Arabidopsis* seeds contain high amounts of 1, ω -bifunctional long-chain aliphatic compounds (primarily C22:0 and C24:0), to a total of 36.8 mole %, plus ferulate at 15 mole %. The co-occurrence of these monomers is indicative of suberin in the seeds. Branched- and odd-carbon components make up 1.5 mole % of the total. Normal fatty acids constitute 13.6 mole %, but as stated earlier much of this may be derived from physically trapped triacylglycerols. Also, the very long-chain saturated and monounsaturated fatty acids, and 2-hydroxytetracosanoate (total of 2.2 mole %) may be derived from N-acyl groups of residual sphingolipids, and

specifically the polar, highly glycosylated inositolphosphoceramides, which we assume are incompletely extracted by the protocol.

Analysis of *Brassica napus* Wild Type Seeds

The total seed polyester composition of *Brassica napus* was determined. The major components are shown in **Figure 12**, in comparison with *Arabidopsis thaliana*. A full tabulation for *Brassica napus* seeds is given in **Table 4**.

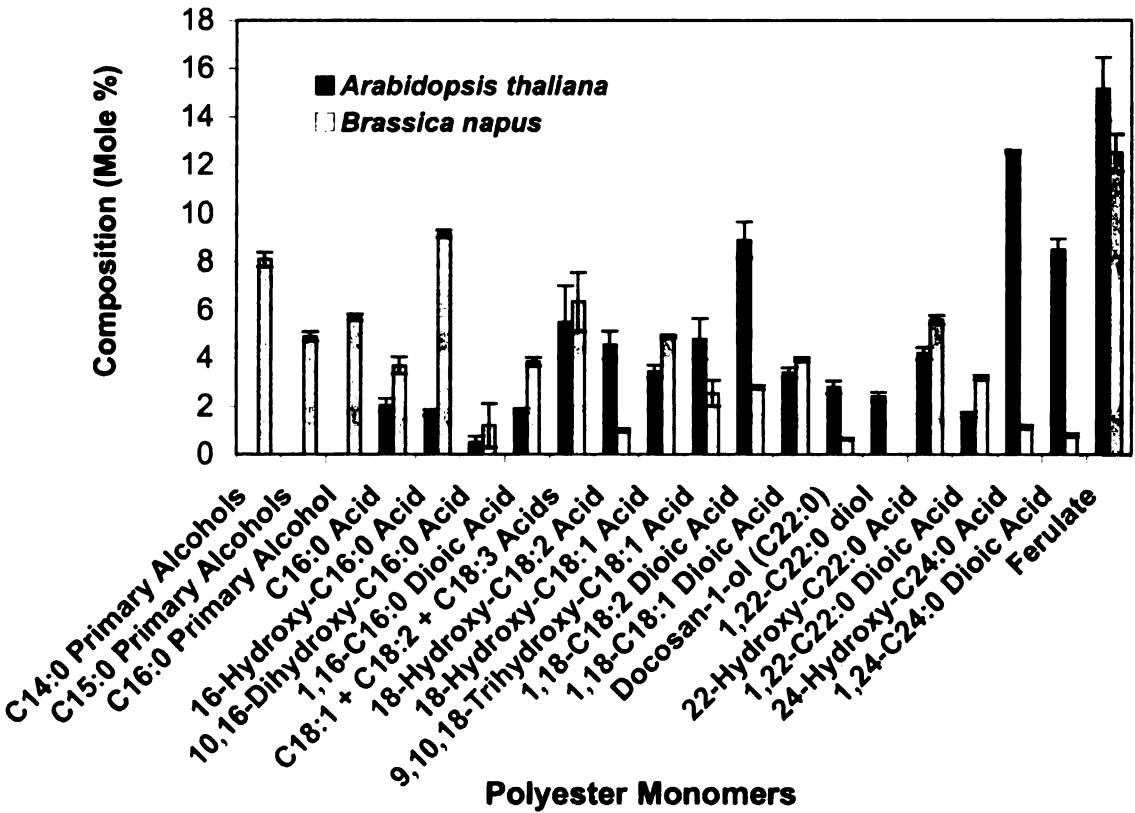


Figure 12. Comparison of the major monomer composition after depolymerization of solvent-extracted *Arabidopsis thaliana* and *Brassica napus* seed residues by NaOMe-catalyzed transmethylation.

Standard deviations for triplicate determinations are shown

A canola variety of rapeseed, *Westar*, was used to minimize the C20 and C22 fatty acid contamination from the seed oil residues. The same classes of monomers found in *Arabidopsis* are also present in the Brassica seeds, but there are several important quantitative and qualitative differences (**Figure 13**). First, Brassica has significantly more 1-alkanols than *Arabidopsis* (20.4 versus 6.5 mole %). These are gained mainly at the expense of dicarboxylic acids. Second, the Brassica seed has a much higher content of shorter chain length (\leq C16) aliphatics (40.0 versus 6.1 mole %), and a reduction in C24 aliphatics (2.6 versus 22.9 mole %). In particular, the C14 - C16 alkan-1-ols and 16-hydroxypalmitate are significant components of the depolymerized Brassica seeds when compared to *Arabidopsis* seeds, whereas 24-hydroxytetracosanoate and 1,24-tetracosanedioate are largely absent. Also, Brassica contains significantly more branched- and odd-carbon components than *Arabidopsis* (8.9 versus 3.2 mole % of the total). We expect that the considerable differences in monomer composition between *Arabidopsis* and Brassica seeds reflect genetics and seed size, but cannot rule out environment as a contributor to the variance. One of the reasons we conducted the analysis on Brassica seeds was to see if the polyester monomer compositions were similar enough between species to use Brassica instead of *Arabidopsis* in studies on seed development and seed tissue localization. Despite the species differences this appears to be a reasonable assumption.

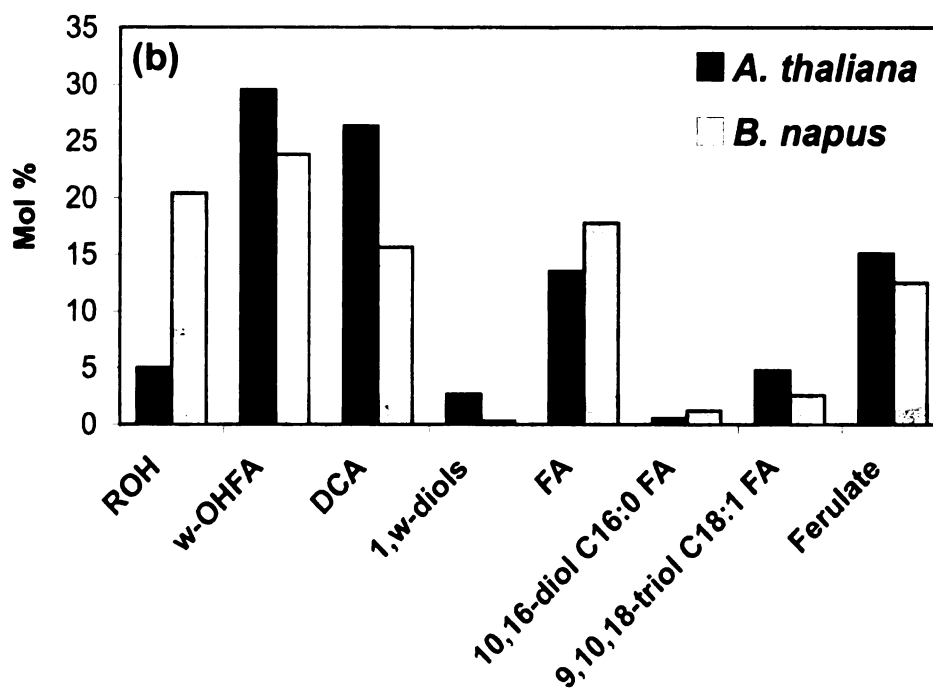
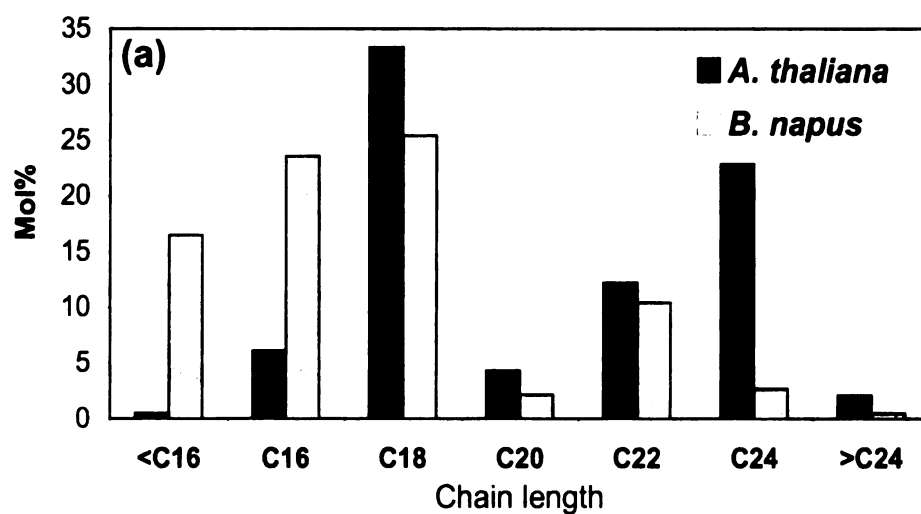


Figure 13. Comparison of *Arabidopsis thaliana* and *Brassica napus* seed monomer classes (a) and total monomer chain length distributions (b).

For Brassica seeds the identified components give a total of 1.94 ± 0.28 mg/g seed residue (6.8 ± 1.0 μ moles/g seed residue). This value results in an estimate of 0.66 mg monomers/g seed, which, using the data set of (Li et al., 2006) (Brassica seed wt. 4.2 mg, seed surface area 12 mm^2), gives an estimate of $23.1 \text{ } \mu\text{g monomers/cm}^2$ seed surface area. This is twice the value obtained for Arabidopsis and may be related to the fact that the seed coat is $\sim 50 \text{ } \mu\text{m}$ thick in *B. napus* and $20 \text{ } \mu\text{m}$ thick in Arabidopsis.

Distribution of Monomers between Seed Coat and Embryo in *Brassica napus* seeds

Seeds are complex organs so it is expected that the polyesters may originate from a variety of distinct cell layers. To further investigate the specific location of polyester monomers within the seed, *B. napus* mature dry seeds were manually dissected into seed coats and embryos. The endosperm layer remained attached to the seed coats, as shown by the high content of the endosperm-specific $\omega 7$ monounsaturated fatty acids (Li et al., 2006) in extractable lipids from this fraction (data not shown). **Figure 14** (upper panel) shows the distribution of polyester monomer classes in seed coat/endosperm and embryo fractions in comparison to whole seeds. With the exception of the 9,10,18-trihydroxyoctadecenoic fatty acid the composition of whole seeds reflects the composition of the seed coats (85% of total monomers). In embryos the

C18:1 trihydroxy fatty acid is dominant (about 60%) but C16:0, C18:1, and C18:2 ω -hydroxy fatty acids and α,ω -dicarboxylic acids are also present (**Figure 14a**). Typical suberin monomers were not found in the embryo fraction, indicating no contamination by seed coat. 9,10,18-Trihydroxyoctadecenoic acid is considered an indicator of cutin, although the embryo “cutin” monomer composition differs significantly from the C18:2 dicarboxylic acid-rich polyester found in the epidermis of leaves and stems of *Arabidopsis* (Bonaventure et al., 2004; Franke et al., 2005) and in *Brassica napus* (data not shown).

Ferulate and C20-C24 saturated fatty alcohol and α,ω -bifunctional monomers, which are considered indicative of suberin especially when they occur together, are clearly specific to the seed coat (**Figure 14**). If the C18:1 trihydroxy fatty acid was completely embryo-specific there might be about 10-15% contamination of the seed coat fraction by embryos. Visually inspected, there was very much less mass contamination, but surface layer cross-contamination remains a possibility. In this context, the cuticle found in grapefruit inner-seed coats was rich in C18 triol fatty acids (Espelie, 1980), suggesting that internal cuticles could have common features with “embryo-enriched” monomers reported here. However, as the mass of seed coat monomers dominates, any cross-contamination by the embryo cuticle will be very minor. Although C16:0 and C18:1 ω -hydroxy fatty acids and C16:0, C18:1 and C18:2 α,ω -dicarboxylic acids are found in the embryo, the dominant part of their masses are present in the seed coat.

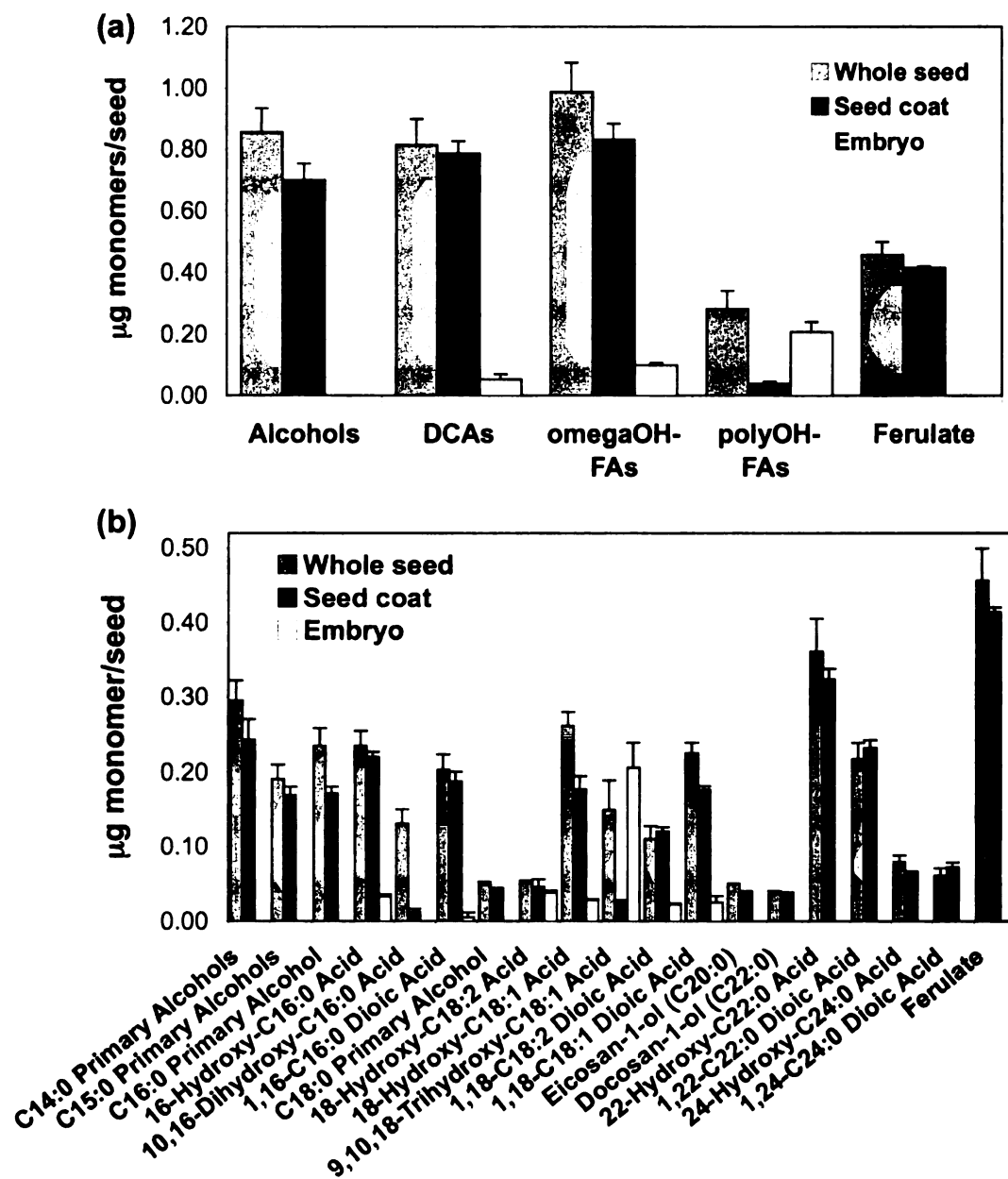


Figure 14. The distribution of monomer classes in whole seed, seed coat and embryo of *Brassica napus* mature seeds (a), and the distribution of individual monomers in whole seed, seed coat and embryo of *Brassica napus* mature seeds (b).

Standard deviations for triplicate determinations are shown.

Seed coat-enriched and embryo-enriched fractions obtained from *Arabidopsis* fractured mature seeds separated by floatation gave similar monomer distributions as for *B. napus* (data not shown) but the distinctions between the two fractions were not so clear, presumably because of greater cross-contamination. Based on analysis of *gpat5* mutant, which are suberin-associated acyltransferase mutants of *Arabidopsis* (presented in Chapter 3), we believe that much of the C22 and C24 ω -hydroxy fatty acid and dicarboxylate deposition is associated with late stage suberization of the chalazal region. This is a conclusion that agrees with analyses of grapefruit seed polyesters (Espelie, 1980). High levels of α,ω -dicarboxylic acids have generally been considered indicative of suberin. However, the presence of high proportions of C16 and C18 dicarboxylic acids, and particularly of the unique octadecadiene-1,18-dioate in the leaf and stem epidermal layers of *Arabidopsis* (Bonaventure et al., 2004) and *Brassica napus* (data not shown), and the presence of these in the isolated *Arabidopsis* leaf cuticles (Franke et al., 2005), suggest that this generalization may not be appropriate for *Arabidopsis*. Thus it is difficult to classify the remaining polyester monomers found in the seed coat as derived from suberin or cutin, or some intermediate or other form of polyester. Further work will require histochemical, electron microscopic and gene expression analyses to help classify polyester structures in the seed.

CONCLUSIONS

The genetics underlying plant polyester biosynthesis is largely unknown. However, the power of both forward and reverse genetic approaches in *Arabidopsis* allows for the identification of genes that affect the monomer composition of cutins and suberins. Such approaches first require identification and then facile but quantitative analysis of the polyester monomers. Such analyses of *Arabidopsis* cutins and suberins have only recently been reported (Bonaventure et al., 2004; Xiao et al., 2004; Franke et al., 2005). Genes have been identified through forward (Xiao et al., 2004; Kurdyukov et al., 2006) and reverse (Bonaventure et al., 2004) genetic screens. With catalogs of the genes involved in *Arabidopsis* lipid metabolism (Beisson et al., 2003) and of genes which are highly expressed in *Arabidopsis* stem epidermis, the site of cutin synthesis (Suh et al., 2005), it seems likely that reverse genetic approaches will accelerate. The juxtaposition of putative suberin and cutin monomers in the seed may allow for effective reverse genetic screening in a single sample for genes involved in either or both polyesters. The seeds of *Arabidopsis* contain the major polyester monomers found in the leaf and stem cuticle, namely 16-hydroxypalmitate, 10,16-dihydroxypalmitate, hexadecane-1,16-dioate, 18-hydroxyoleate, octadecene-1,18-dioate, 18-hydroxylinoleate and octadecadiene-1,18-dioate. In addition, there is a significant amount of 9,10,18-trihydroxyoctadecenoate, which is associated largely with the embryo, and a large proportion of monomers, including docosan-1-ol, docosane-1,22-diol, 22-

hydroxydocosanoate, docosane-1,22-dioate, 24-hydroxy-tetracosanoate, tetracosane-1,24-dioate and ferulate, which collectively are characteristic of suberin and which are associated entirely with the seed coat. Sufficient seeds can be obtained from a single plant, to which are applied the solvent extraction/homogenization/drying steps then transmethylation, acetylation and GC analysis. The slow step is thorough solvent and aqueous washing to delipidate the seed. However, the aqueous washes might be omitted, as it is not important to gather data on normal fatty acids and sinapate. A single GC analysis can be run with sample from less than 100 mg of seeds. Currently, we have successfully used the method to identify compositional changes in KO lines for three genes that are consistent with the loss of specific gene function, and are using it to screen additional KO mutant lines.

EXPERIMENTAL PROCEDURES

Plant material

Wild-type *Arabidopsis thaliana* (ecotypes Columbia and Wassilewskija-2) were grown on a mixture of soil:vermiculite:perlite (1:1:1 v/v/v) under white fluorescent light ($80\text{-}100\ \mu\text{E m}^{-2}\ \text{s}^{-1}$) in a 18-h-light/6-h-dark photoperiod. The temperature was set at 20-22°C and the relative humidity at 60-70%. Seeds were always stratified four d at 4°C. Seeds of *Brassica napus* cv *Westar* were planted

in 30 cm plastic pots in a (2:1 v/v) mixture of soil:vermiculite and grown in an air-conditioned greenhouse under natural light supplemented with lamps to provide 18-h-light/6-h-dark photoperiod.

Sample delipidation of seeds

Whole seeds of *A. thaliana* or *B. napus* were ground in liquid N₂ using mortar and pestle, immersed in boiling isopropanol (25 ml/g fresh tissue) and heated for 10 min at 80°C. After cooling the tissue was finely ground with a Polytron and extracted for at least 4 h at room temperature by shaking at 300 r.p.m. in isopropanol. The extract was centrifuged 10 min at 800 x g and the insoluble residue was re-extracted by shaking overnight at 300 r.p.m. with 25ml/g isopropanol. After centrifugation, the tissue was re-extracted with (2:1 v/v) chloroform:methanol at room temperature by shaking for approximately 8 h. The residue was re-extracted with (1:2 v/v) chloroform:methanol overnight and filtered through Whatman N°1 filter paper. Additional steps were performed after air-drying the solvent extracted tissues and re-grinding the residue to achieve a smaller particle size. The residue was extracted successively with methanol (30 min), water (30 min), 2 M NaCl (1 h), water (30 min), methanol (30 min), (1:2 v/v) chloroform:methanol (overnight) and (1:2 v/v) chloroform:methanol (overnight). All extraction steps were performed in a shaker (300 rpm) at room temperature and the residue was separated from the solvent by centrifugation (10 min at 800

x g), except for the last step where the sample was filtered. The residue was air-dried and then placed under vacuum over anhydrous CaCl_2 until constant weight was reached. Residue yields after extraction, as percentage of initial seed weight, were: *A. thaliana* Col0 -31%; WS-32%; *B. napus*- 37.1%.

Methanolysis with sodium methoxide

Approximately 0.1 g of solvent-extracted *Arabidopsis* residue, dried to constant weight, was heated at 60°C with periodic vortexing in 6 ml of methanol containing 15% (v/v) methyl acetate and 6% (w/v) sodium methoxide. Methyl heptadecanoate (Sigma, USA) and ω - pentadecalactone (Fluka, Switzerland) were added as internal standards at 1 mg/g dry residue each. Different incubation times were applied for the time-course analysis (0.5 to 48 h), with 2 h selected as the reaction time for the optimized protocol. The reaction mixtures were acidified with glacial acetic acid to pH 4-5, saline added and the fatty acid methyl esters extracted with methylene dichloride (10 ml). The organic phase was washed three times with dilute saline solution (0.5 M NaCl) and dried over anhydrous sodium sulfate. The solvent was evaporated to dryness under nitrogen and the product silylated to convert hydroxyl groups to their TMSi ethers or acetylated to produce the corresponding acetyl derivatives.

Additional depolymerization methods

The hydrogenolysis/deuterolysis protocol used for the analysis of Arabidopsis polyester monomers was described by Bonaventure et al. (2004). Methyl-heptadecanoate and ω -pentadecalactone were added as internal standards in the same amounts as indicated above. The polyol derivatives were silylated to convert free alcohols to their TMSi ethers. For acidic transmethylation several catalysts can be used, such as BF_3 , HCl , or H_2SO_4 in methanol (Christie, 2003; Holloway, 1984). Based on the remarks of Christie (2003) we opted for a sulphuric acid-methanol reagent. Dry seed residue (0.1g) and the internal standards were heated at 80°C with 4 ml of 5% (v/v) sulfuric acid in methanol plus 2 ml of toluene as a co-solvent for 48 h. To recover the fatty acid methyl esters, 3 ml 0.9% NaCl (w/v aq) and 10 ml methylene chloride were added, followed by centrifugation for 5 min at $800 \times g$ to facilitate phase separation. The organic extract was washed several times with dilute saline, dried over dry sodium sulfate and evaporated under a stream of nitrogen.

Hydrogenation

To confirm structures, samples of polyester monomers obtained after methanolysis were hydrogenated by stirring in methanol at room temperature for 2 h with platinum (IV) oxide catalyst in a hydrogen atmosphere at slightly greater than atmospheric pressure. This resulted in complete reduction of the double bonds. After addition of saline the product was extracted into diethyl ether and

the ether phase was washed several times with dilute saline. Finally, the ether solution was dried under nitrogen stream and the sample was silylated for GC-MS analysis.

Preparation of trimethylsilyl and acetyl derivatives

The products of hydrogenolysis or methanolysis were heated at 100 °C for 10 min in 0.1 ml pyridine and 0.1 ml BSTFA (*N,O*-bis(trimethylsilyl)-trifluoroacetamide). After cooling, the solvent was evaporated under nitrogen and the product was dissolved in 0.5 ml heptane:toluene (1:1 v/v) for GC-MS analysis. To obtain the acetyl derivatives, the fatty acid methyl esters were dissolved in 0.1 ml pyridine and 0.1 ml acetic anhydride and incubated 1 h at 60°C. The reagents were then removed under nitrogen gas and the dry samples were dissolved in 0.5 ml heptane:toluene (1:1 v/v) for GC or GC-MS analysis.

GC-MS and GC-FID analysis

GC (FID) analysis used a DB-5 capillary column (J&W Scientific, CA, USA; 30 m x 0.25 mm x 0.25 µm film thickness) with helium carrier gas at 1.5 ml/min constant flow and temperature programmed from 140°C to 310°C at 3°C/min, and then held for an additional 10 min at 310°C. Samples were injected in split mode (30:1 ratio, 310°C injector temperature) and peaks were quantified

on the basis of their FID ion current. Peak areas (pA.sec) were converted to relative weights by applying FID theoretical correction factors; that is, by assuming the FID response is proportional to carbon mass for all carbons bonded to at least one H-atom (Christie, 1991). The S/N threshold was set as 1% of the major peak. Unknowns were estimated as their total peak area against known peaks, taking the total peak area of the latter as 100%. The retention time of fatty acid standards was determined under the same conditions and used to verify the predominant fatty acids. For GC-MS a column of the same characteristics was used with helium carrier gas at 2 ml min^{-1} and oven temperature programmed from 110°C to 300°C at 10°C/min . Splitless injection was used and the mass spectrometer run in scan mode over 40-500 amu (electron impact ionization), with peaks quantified on the basis of their total ion current. For analysis of the molecular ion cluster, the detector was operated in single ion monitoring mode for ions (M-1) to (M+n+1), where M is the m/z value of the major natural isotopic abundance molecular ion and n represents the highest possible isotopic enrichment.

TAG separation and analysis

To analyze the lipid fractions eliminated in the additional washing steps, 3 g of Arabidopsis seeds were delipidated as described above. The solvent fractions from the additional washing steps were pooled and extracted with chloroform. The dried extract was dissolved in heptane and separated by TLC on

K6 silica plates (Whatman, Clifton, PA). The plate was developed with 80:20:1 (v/v/v) hexane:ether:acetic acid, and lipids were detected by exposure to iodine vapors. Triolein (1mg/ml) was used as standard.

Identification of branched alcohols

Approximately 20 mg of fatty acid methyl esters prepared by NaOMe catalyzed transesterification of *B. napus* seeds were separated by preparative TLC. The plate was developed with 80:20:1 (v/v/v) hexane:ether:acetic acid and the lipids were detected by spraying with 0.2% (w/v) 2',7'-dichlorofluorescein/ethanol. Nine different bands were identified under UV light, individually eluted with chloroform, and dried under N₂ stream. TMS derivatives were analyzed by GC-MS. Methyl 13-methyltetradecanoate (*iso*-pentadecanoate) and methyl 12-methyltetradecanoate (*anteiso*-pentadecanoate) standards were purchased from Matreya Inc. and reduced to the corresponding fatty alcohols with LiAlH₄.

CHAPTER 3

LIPID POLYESTER DEPOSITION AND LOCALIZATION IN DEVELOPING SEEDS OF *BRASSICA NAPUS* AND *ARABIDOPSIS THALIANA*

Maria Isabel Molina, John B. Ohlrogge, Mike Pollard

Department of Plant Biology, Michigan State University, East Lansing, MI 48824,
USA

The Plant Journal, (2008) **53**: 437-449

Acknowledgements

This work was supported by the National Research Initiative of the USDA Cooperative State Research, Education and Extension Service, grant number 2005-35318-15419, and by a Fulbright Foundation fellowship awarded to Isabel Molina. We thank George Haughn and Ljerka Kunst, Department of Botany, University of British Columbia, for providing us with the *ap2-7* line of *Arabidopsis* and Jian-Min Zhou, Department of Plant Pathology, Kansas State University, for the *att1-1* and *att1-2* lines of *Arabidopsis*. We also thank Dr. Fred Beisson for a critical reading of the manuscript. CLSM analyses were performed in the Center for Advanced Microscopy, MSU.

ABSTRACT

Mature seeds of *Arabidopsis thaliana* and *Brassica napus* contain complex mixtures of aliphatic monomers derived from non-extractable lipid polyesters. Most of the monomers are deposited in the seed coat, and their compositions suggest the presence of both cutin and suberin layers. The location of these polyesters within the seed coat, and their contributions to seed coat permeability and other functional properties are unknown. Polyester deposition was followed over *Brassica* seed development and distinct temporal patterns of monomer accumulation were observed. Octadecadiene-1,18-dioate, the major leaf cutin monomer, was transiently deposited. In contrast, the saturated dicarboxylates maintained a constant level during seed desiccation, whereas the fatty alcohols and saturated ω -hydroxy fatty acids continually increased. Dissection and analysis of *Brassica* seed coats showed that suberization is not specific to the chalaza. Analysis of the *Arabidopsis ap2-7* mutant suggested that suberin monomers are preferentially associated with the outer integument. Several *Arabidopsis* knockout mutant lines for genes involved in polyester biosynthesis (*att1*, *fatB* and *gpat5*) were examined for seed monomer load and composition. The variance in polyester monomers of these mutants is correlated with dye penetration assays. Furthermore, stable transgenic plants expressing *promoter::YFP* fusions showed *ATT1* promoter activity in the inner integument, whereas *GPAT5* promoter is active in the outer integument. Together, the *Arabidopsis* data indicated that there is a suberized layer associated with the

outer integument and a cutin-like polyester layer associated with the inner seed coat.

INTRODUCTION

In seeds of angiosperms the seed coat differentiates from the ovule integuments, which are derived from the epidermis and are maternal in origin (Boesewinkel and Bouman, 1995). The specialized cells forming the seed coat layers play a variety of roles during seed development and also at seed maturity, when the seed coat cells are dead. The seed coat imparts protection against pathogens and adverse conditions, allowing survival of the offspring. It is also involved in embryo nutrition during development, and has functions in establishing and maintaining seed dormancy, facilitating seed dispersal, and promoting germination under favorable conditions (Haughn and Chaudhury, 2005). In *Arabidopsis* the seed coat constitutes about 20% of mature dry seed weight (Li et al., 2006) and is associated with complex physiological processes such as seed dormancy and germination (Bewley, 1997). The cellular layers that form the seed coat in Brassicaceae are similar among members of this family (Moise et al., 2005). Analyses of seed coat mutants have been useful to study *Arabidopsis* seed coat functions. For instance, mutants with altered flavonoid production, such as *ban* (Albert et al., 1997), and those defective in the secondary cell walls of the outer layers, such as *ap2* (Western et al., 2001), show increased seed coat permeability to tetrazolium salts (Debeaujon et al., 2000).

High permeability correlates with decreased dormancy and capacity to germinate after storage. Another example of functional seed coat chemistry is seed mucilage, a pectic polysaccharide that swells upon seed imbibition, breaking the outer epidermal cell wall, and therefore contributing to germination, particularly in dry environments (Penfield et al., 2001; Beeckman et al., 2000; Western et al., 2000; Windsor et al., 2000). In addition, the recent characterization of a suberin mutant, *gpat5*, demonstrated that lipid polyesters deposited in the seed coat play important roles in dormancy and in controlling permeability to tetrazolium dyes (Beisson et al, 2007).

At maturity, closure of all seed coat openings and coating with water repellent substances are requisites for seed coat impermeability (Boesewinkel and Bouman, 1995). Suberized cell walls and cuticles are highly hydrophobic barriers often found in seed coats, and therefore play an important role in these processes. Cutin monomers have been identified in a variety of mono- and dicot seeds (Espelie et al., 1979). Ultrastructural analyses also suggested suberin in the internal layers of seed coats (Ballard, 1973; Johann, 1942; Zee and O'Brien, 1970). The most thorough characterization of polyesters in seed coats has been carried out using grapefruit seeds (Espelie et al., 1980). These seeds contain a cuticle in the inner seed coat except in the chalaza. By contrast, the chalazal region of the inner seed coat revealed suberin by both chemical and microscopic analyses. In addition, waxes were an important constituent of the permeability barrier in both the internal cuticle and suberized chalazal cells. The inner seed

coat cuticle appeared to be the major barrier controlling water uptake during imbibition. In *A. thaliana* seeds, analysis by TEM revealed the presence of a cuticle on the inner cell layer of the inner integument facing the embryo in all developmental stages until maturity (Beeckman et al., 2000). This cuticle could still be present in the mature seed but its visualization is difficult because the adjacent pigmented layers are fused together. Although several cytological studies have been performed on Brassica seed coats, cuticles and/or suberized cell walls have not been described in the mature seed coat (Van Caeseele et al., 1981, 1982) and may have been overlooked.

Previously, we reported on the analysis of the non-extractable polyester monomers in *Arabidopsis thaliana* and *Brassica napus* seeds (Molina et al., 2006). In *Arabidopsis* seeds the major C16 and C18 monomers were ω -hydroxy fatty acids and α,ω -dicarboxylic acids derived from palmitate, oleate and linoleate, and 9,10,18-trihydroxyoctadecenoic acid. Among the C20-C26 monomers, which can be considered to be derived from suberin, docosan-1-ol, docosane-1,22-diol, 22-hydroxydocosanoic acid, 24-hydroxytetracosanoic acid and tetracosane-1,24-dioic acids were the major species. Ferulic acid was also identified. Analysis of *Brassica napus* seeds revealed the same classes of monomers. Dissection and analysis of mature Brassica seeds showed that the trihydroxy oleate was found mainly in the embryo, while ferulate, fatty alcohols and C22 and C24 species were specific to the seed coat plus endosperm fraction. In the present study we report the timing of deposition of lipid polyester monomers in *Brassica napus*

developing seeds. Furthermore, analyses of the dye permeability of *Arabidopsis thaliana* knockout mutants and of promoter::YFP fusions of different genes of lipid polyester biosynthesis give insights into the localization of specific polyester layers within the seed coat.

RESULTS

Lipid polyester monomers are deposited from mid-maturation onwards in developing *Brassica napus* seeds

Because of their size *Brassica napus* seeds are preferred over *Arabidopsis* seeds to measure lipid polyester monomer deposition during development. The deposition of polyester monomers was assayed in seeds at six different stages: 1 (12-20 DAF), 2 (20-25 DAF), 3 (25-30 DAF), 4 (30-35 DAF), 5 (35-40 DAF) and 6 (mature dry). As shown in **Figure 15**, at stage 1 the seed coat was translucent and had expanded to about 80% of its eventual diameter. The “globular” to “heart” staged embryos occupied up to 10% of the seed volume. Stage 3 (25-30 DAF) corresponded to “mid-maturation stage,” during which triacylglycerol synthesis was maximal and the embryo would best be described as “green cotyledon.”

The onset of polyester monomer accumulation lagged slightly behind triacylglycerol accumulation. The maximum load was reached at stage 4 and maintained thereafter (**Figure 15a**). However, total monomer content was

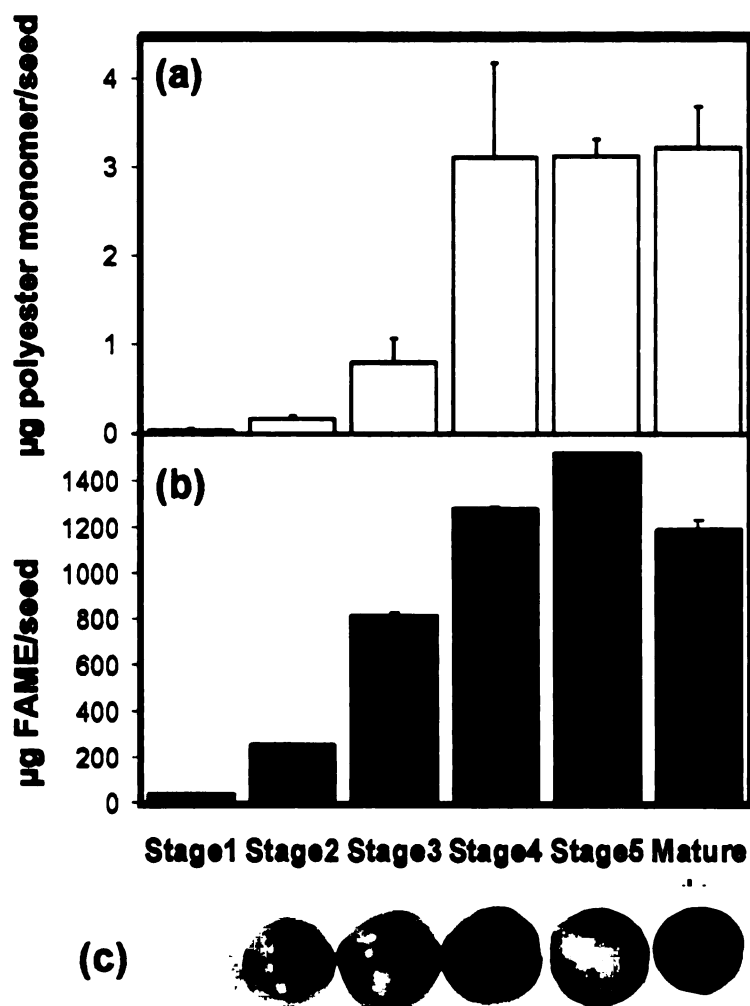


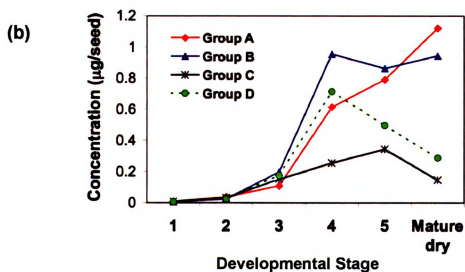
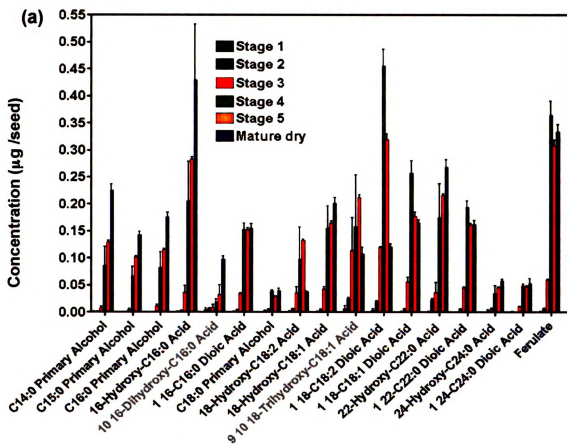
Figure 15. Stages of development and analysis of total lipid polyester monomer content and total oil content in developing seeds of *Brassica napus*.

(a) Total polyester monomers released by transmethylation. **(b)** Total oil, determined as total fatty acids in pooled solvent extractions from the same samples. **(c)** Seeds representing each developmental stage (see the first section in Results for details such as days after flowering ranges). Data are reported for the average of triplicate determinations \pm SD.

somewhat deceptive because various monomer species were lost while the deposition of others continued (**Figure 16a**). Monomers could be classified as

Figure 16. Variation in lipid polyester monomer composition during development of *Brassica napus* seeds.

(a) Deposition of individual monomers, **(b)** specific groupings of monomers. Four groups were defined according to the timing of deposition. Group A: C14:0, C15:0, C16:0 alcohols/C16:0, C22:0 and C24:0 ω -hydroxy fatty acids/ 10,16-dihydroxy palmitate; Group B: C16:0, C22:0 and C24:0 dicarboxylates/octadecan-1-ol/C18:1 and C18:0 ω -hydroxy fatty acids/ferulate; Group C: 9,10,18-trihydroxy oleate; Group D: C18:1/C18:2 dicarboxylates. Error bars indicate standard deviation from three determinations.



belonging to one of four groups as defined by the kinetics of their deposition (**Figure 16b**). Unsaturated C18 dicarboxylates peaked early (stage 4) and then decreased to 50% of their maximum value in mature seeds. 9,10,18-Trihydroxyoctadecenoate, which is predominantly an embryo-associated monome (Chapter 2, and Molina et al., 2006), increased slowly until stage 5 and diminished in mature seeds. In contrast, saturated dicarboxylates, octadecan-1-ol, ferulate and 18-hydroxyoleate increased until stage 4 and then remained approximately constant through seed desiccation. And finally, primary alcohols (C14-C16), saturated ω -hydroxy fatty acids and 10,16-dihydroxypalmitate deposition continued until the seed reached a mature dry state. The appearance of 10,16-dihydroxypalmitate is particularly late, and may explain its greater variability in seed polyester analysis.

Clearly, although the seed coat reaches its maximum diameter and thus surface area by stage 2-3, the deposition of aliphatic polyesters continues to occur throughout all later stages of seed coat development. The kinetics of ferulate deposition correlated with saturated dicarboxylates (**Figure 16b**, Group B) rather than fatty alcohols and ω -hydroxy fatty acids (**Figure 16b**, Group A). This seems rather surprising, given that alkyl ferulates and ω -feruloyloxyfatty acids are known natural products (Bernards and Lewis, 1992; del Rio et al., 2004; Byla and Herz, 1996), and because ferulates are expected to be esterified at their carboxylate functional group, to allow oxidative coupling of their phenolic group to produce the polyaromatic domain of suberin (Bernards et al., 1995).

However, we expect much of the ferulate to be cross-linked, and therefore hidden from analysis. This makes any changes in measured ferulate content hard to interpret. Ferulate deposition might continue throughout seed desiccation but ferulate oxidative coupling might remove monomers that would otherwise be released by transesterification.

Extractable wax accumulation in developing *Brassica napus* seeds

Waxes, including alkanes, have been noted in the inner seed coat of grapefruit (Espelie, 1980) and reported as surface components of *Arabidopsis* seeds (Beisson et al., 2007). Thus we analyzed the accumulation of waxes extracted by rapid chloroform dipping of developing *Brassica napus* seed over the six stages described in **Figure 15**. Total wax loads and wax composition for the mature seeds are shown in **Figure 17**. The wax composition of *Brassica* seeds mirrors that of *Arabidopsis* seeds, being dominated by nonacosane and its 15-hydroxy and oxo derivatives. The seed wax compositions are similar to the composition of *Arabidopsis* stem waxes (Rashotte et al., 2001). Unlike lipid polyesters, wax deposition was already significant at the earliest stage, and wax load was maintained at a fairly constant level from stages 2 through 5 at about $0.3\text{-}0.4\ \mu\text{g}/\text{cm}^2$. This value is comparable to epicuticular wax loads in *Arabidopsis* leaves (Suh et al., 2005) and is in agreement with the wax content reported for *Arabidopsis* seeds (Beisson et al., 2007). At the last stage there is an increase in recoverable waxes. We do not know if this increase represents a biosynthetic

pulse or if the desiccation of the seed leads to fracturing of the outermost integument layer and increased penetration of the chloroform solvent, allowing greater extractability of waxes.

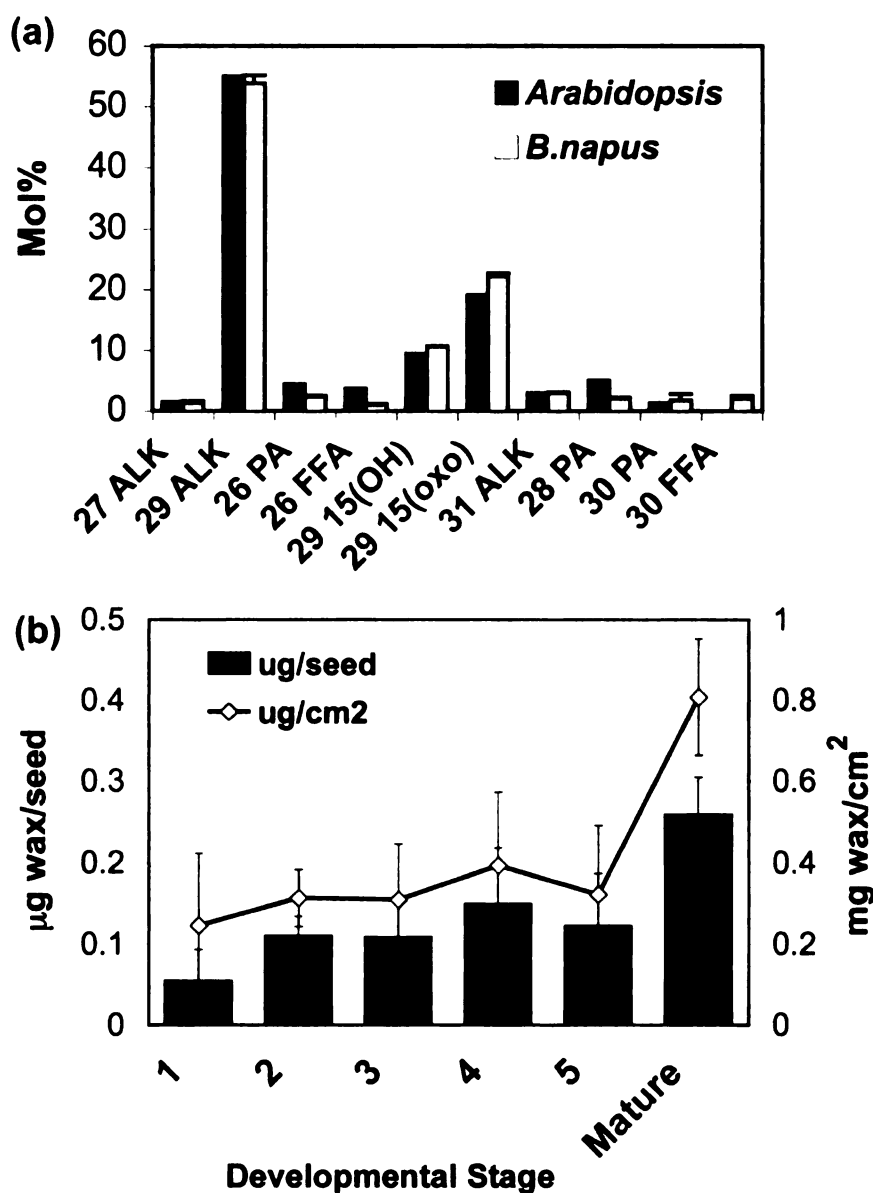


Figure 17. Deposition of chloroform-extractable waxes in *Brassica napus* seeds.

(a) Comparison between *Arabidopsis* and *B. napus* wax components extracted from mature seeds. **(b)** Total wax loads in *B. napus* developing seeds.

Localization of polyesters in chalazal and non-chalazal regions of *Brassica* seeds

The chalaza is the region where the funiculus attaches to the seed coat. It is the channel through which nutrients are transported to the endosperm and embryo, and it is sealed late in seed development. Stage 5 *Brassica napus* seeds were dissected to isolate the chalazal region, which includes the scar of the funiculus (or hilum) and the micropyle (**Figure 18a**). The chalazal sample included up to 20% of the seed mass. Monomer compositions and contents for the chalazal and the rest of the seed are presented in **Figure 18b**. Inspection of **Figure 18b** shows that substantial amounts of all the monomers are found in the non-chalazal fraction. Since these include fatty alcohols, ferulate and saturated C22 and C24 α,ω -bifunctional monomers which are typical of suberin, we infer that suberization is present over the entire seed coat. There are no monomers which can be considered chalazal-specific.

Analysis of the *ap2-7* Arabidopsis mutant distinguishes outer and inner integument polyester monomer contributions

APETALA2 (At4g36920) encodes a putative transcription factor. One function of this gene is to control seed coat development (Haughn and

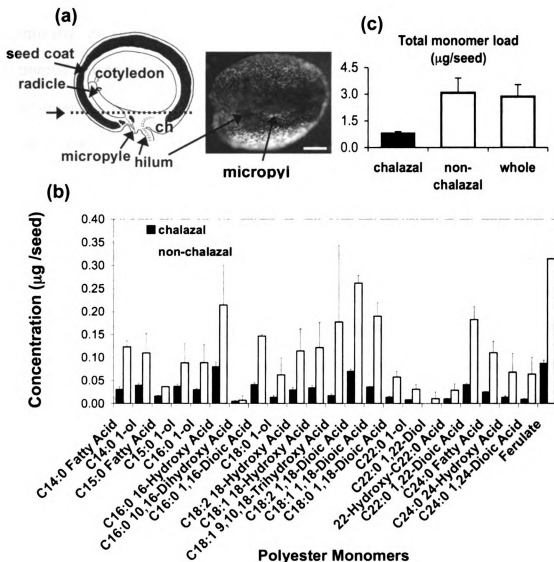


Figure 18. Polyester monomers in the chalazal and non-chalazal regions of *Brassica napus* seeds.

(a) Schematic representation of the seed of *B. napus* (left) and bright field micrograph taken from the chalazal end (ch), where the microphylla and the scar of the funiculus (hilum) converge (right). The arrow indicates the plane where seeds were dissected. The non-chalazal region contains most or all of the embryo. **(b)** Analysis of lipid polyester monomers released by transmethylation from stage 5 dissected seeds. The composition of the chalazal and non-chalazal regions is expressed in μg monomer/seed. Error bars indicate standard deviation from three determinations. **(c)** Total monomer loads in dissected and whole seeds. Scale bar = 0.5 mm.

Chaudhury, 2005). It is required for the differentiation of both layers of the outer integument. In “strong” mutant alleles the arrested development results in loss of epidermal mucilage and columella, leaving only remnants of the undifferentiated outer integument in mature seed coats (Western et al., 2001). *ap2-7* is one such allele, and we have performed a polyester monomer analysis on this line (**Figure 19**). Octadecadiene-1,18-dioate, a major component of the seed polyesters and the major component of Arabidopsis leaf and stem polyesters (Bonaventure et al., 2004; Franke et al., 2005), is largely unaffected. By contrast, the saturated C22 and C24 α,ω -bifunctional monomers are all substantially reduced, as is the ferulate. This implies that most of the suberin deposition is dependent on fully developed outer integument cell layers. It is not clear whether the remaining ferulate and C22-C24 aliphatic suberin monomers seen in *ap2-7* seeds represent a residual deposition in the remnants of the outer integument, or are associated with the chalaza or the inner integument, or are induced by the loss of the hydrophobic barrier properties of the outer integument.

Seeds of the *Arabidopsis thaliana* mutants *fatB*, *gpat5* and *att1* have abnormal lipid polyester monomer loads compared to wild type seeds

The sodium methoxide-based transmethylation method developed for the analysis of lipid polyester monomers in Arabidopsis seeds (Molina et al., 2006) was applied to three mutants in which changes in seed polyester content and composition are known or might be expected. The monomer compositions are

shown in **Figure 20** and compared to their respective wild-type backgrounds. The compositional changes reported below for the mutants are consistent with the loss of specific gene function.

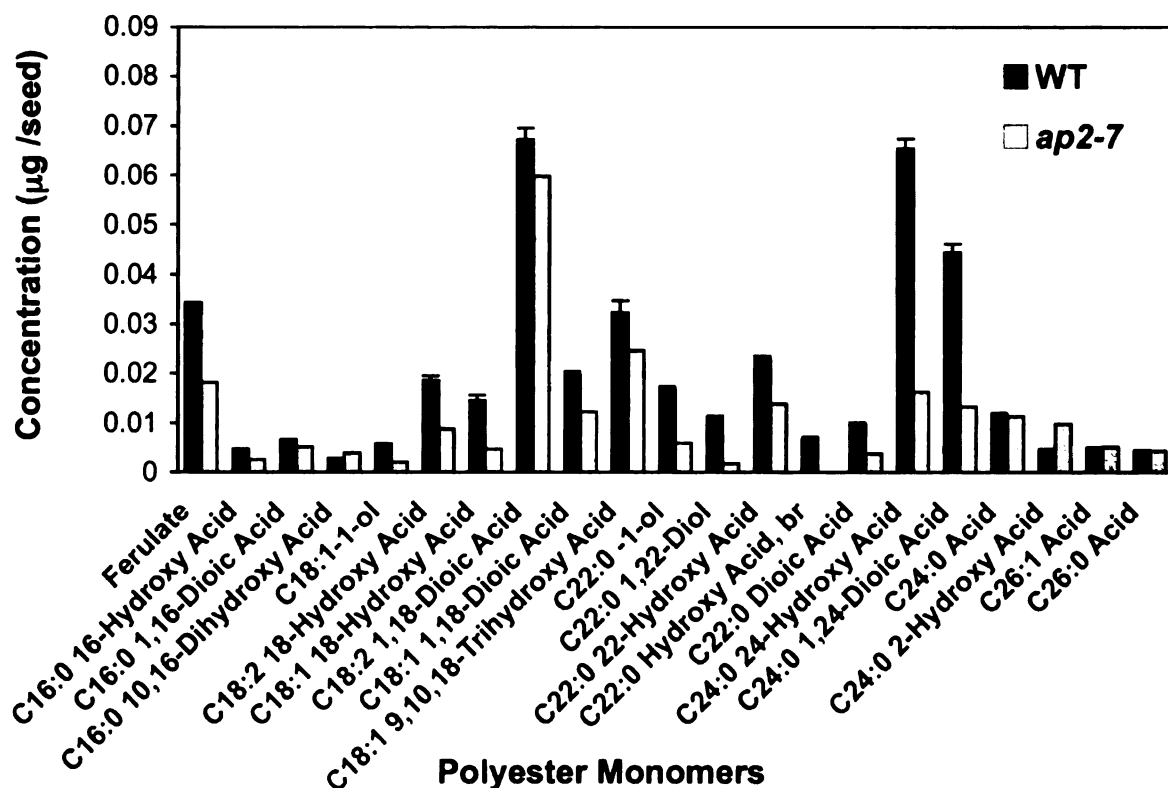


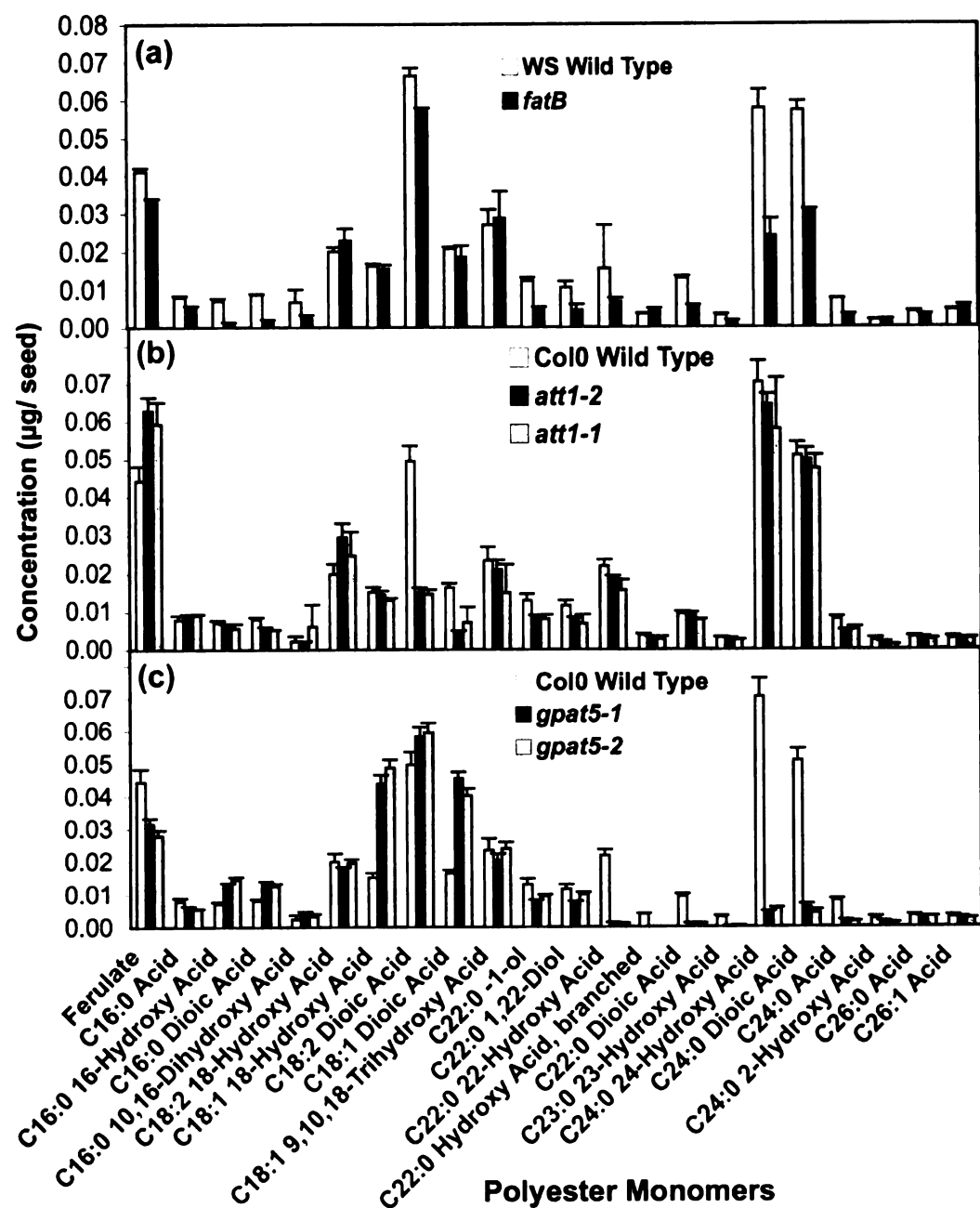
Figure 19. Polyester monomer composition of *ap2-7 Arabidopsis thaliana* mutants.

Comparison of monomers released by transmethylation of delipidated residues of *ap2-7* mutant and wild type seeds. No replicate analyses are available for *ap2-7* seeds (see Experimental Procedures). br: branched-chain monomers.

The *FATB* gene (At1g08510) encodes a plastid-localized acyl-ACP thioesterase with high activity towards palmitoyl-ACP (Salas and Ohlrogge, 2002). A knock out of this gene reduces the cytosolic supply of palmitate, altering

Figure 20. Comparison of seed monomer composition between wild type and mutant Arabidopsis lines.

(a) Polyester monomers in *fatB* and WS wild type seeds **(b)** Polyester monomers in *gpat5-1*, *gpat5-2* and **(c)** *att1-1*, *att1-2* mutants compared to Col-0 wild type seeds. Total polyester monomer loads (mg/g dry residue) were as follows: WS wild type: 7.81 ± 0.5 ; *fatB*: 4.78 ± 0.22 ; Col0 wild type: 7.88 ± 0.5 ; *att1-1*: 7.03 ± 0.56 ; *att1-2*: 7.53 ± 0.22 ; *gpat5-1*: 5.13 ± 0.28 ; *gpat5-2*: 6.56 ± 0.38 . Data are reported for the average of triplicate determinations \pm SD



phospholipid acyl composition and reducing leaf and stem epicuticular wax loads (Bonaventure et al., 2003). In addition, leaf C16 cutin monomers were reduced in this mutant (Bonaventure et al., 2004). Similar reductions (65-85%) were found in 16-hydroxy- and 10,16-dihydroxy-palmitate and 1,16-hexadecane dioate in the seed polyesters (**Figure 20a**). Furthermore, there were 45-65% reductions in the levels of straight-chain C20-24 components, which is consistent with the role of FATB in providing precursors for these very long chain saturated monomers.

The *ATT1* gene encodes a cytochrome P450 (CYP86A2, At4g00360) that is a member of the ω -hydroxylase gene family (Duan and Schuler, 2005; Xiao et al., 2004). The *att1* mutation causes a reduction in the monomer content of the isolated cuticle in leaves/stem (Xiao et al., 2004). As shown in **Figure 20b**, in seeds the primary effect of the *att1* mutations is a reduction in the content of 1,18-octadecadiene dioate and 1,18-octadecene dioate by about 70% each, and a smaller reduction (30%) in 1,16-hexadecane dioate. There is not a decrease in the corresponding 18-hydroxy acids content; in fact, 18-hydroxy-octadecadienoate increases by 30-45% while 18-hydroxy-octadecenoate is essentially unaltered. The seed phenotype of *att1* is completely consistent with the leaf and stem polyester phenotypes (**Chapter 5, Figure 47a-b**). These observations imply that ATT1 is important for C18 unsaturated dicarboxylate production. The ratio of C18:1 to C18:2 in the combined ω -hydroxy acid plus dicarboxylate fraction remained constant at 3:7 in spite of the *att1* mutation. This suggests that there is no selectivity between C18:1 and C18:2 substrate supply

for oxidation. Because *att1* causes a major reduction in C18 unsaturated dicarboxylate production, without a concomitant decrease in ω -hydroxy fatty acids the actual oxidation catalyzed *in vivo* by CYP86A2 remains obscure (fatty acid oxidation to ω -hydroxy or to dicarboxylic acid, or ω -hydroxy fatty acid oxidation to dicarboxylic acid?). Another important observation is that the *att1* mutation has minimal effect on the levels of C22:0 and C24:0 dicarboxylates and more generally causes only very slight reductions in the levels of C20 - C24 monomers. However, as ATT1 is expressed primarily in a non-suberized tissue layer (see below) we cannot infer any ATT1 acyl chain-length specificity from the monomer distribution of the mutant.

GPAT5 (At3g11430) belongs to an eight member gene family annotated as glycerol-3-phosphate acyltransferases (Zheng et al., 2003), and is predominantly expressed in seeds, roots and anthers. Mutations in *GPAT5* (Beisson et al., 2007) and ectopic expression of this gene (Li et al., 2007b) show that it encodes an acyltransferase involved in suberin biosynthesis. The *gpat5-2* mutation (**Figure 20c**) gives a dramatic reduction (from 3.25 to 0.30 mg/g dry seed residue) for all the C20-C26 monomers that are anticipated to be suberin constituents and which carry at least one COOH group. However, the C18 to C23 primary alcohols and 1, ω -diols, which contain no COOH group for an acyl transferase to act upon, do not significantly change. This would seem to confirm *GPAT5* as a functional acyltransferase with capacity to utilize very long-chain saturated acyl groups (> C18). However, we do not know whether *GPAT5* acts

upstream or downstream of the oxidation steps. The reduction in the C20-C26 ω -hydroxy fatty acid and dicarboxylic acid monomer load is partly compensated by an increase in C16:0, C18:1 and to a lesser extent C18:2 ω -hydroxy fatty acid and dicarboxylic acids, which rise from 2.14 to 3.92 mg/g dry seed residue. Thus the reduction of suberin-like monomers of 2.95 mg/g dry seed residue is largely offset by the increase in C16-C18 monomers of 1.78 mg/g dry seed residue. The data trends are consistent with a set of seed analyses previously performed on both *gpat5* alleles (Beisson et al., 2007). However, a comparison of the two independently obtained data sets for seeds shows some significant quantitative differences for certain monomers. The origin of these differences is unknown.

Lipid polyesters, but not extractable waxes, influence seed coat permeability to tetrazolium salts

To evaluate the influence of lipid polyesters on seed coat permeability we compared the kinetics of tetrazolium salt uptake by mature seeds of wild-type *Arabidopsis* and mutants with altered polyester monomer composition (**Figure 21a**). Tetrazolium salts are amphipathic cations, which, after penetrating the dead cells of the seed coat, are reduced to red-colored formazans by NADH-dependant reductases in the embryo (Berridge et al., 1996). Whereas wild-type seeds remained impermeable for several days, embryos of both *fatb* and *gpat5* mutants showed perceptible red staining after 2 h incubation. After 24 h of incubation, a 14-fold increase in formazans was observed in *fatb* seeds and a

Figure 21. Tetrazolium uptake assays.

(a) Time course of formazans produced by reduction of tetrazolium salts by the embryos of *Arabidopsis* WT and mutants, measured by absorbance at 485 nm. Data are reported for the average of duplicate determinations \pm SD. **(b-m)** Staining pattern in seeds incubated with tetrazolium salt: **(b, c)** *gpat5* seeds incubated for 6 h (arrows indicate red staining in radicle and cotyledon tips); **(d, e)** *gpat5* seeds (48 h); **(f, g)** *fatB* seeds (6 h); **(h, i)** *fatB* seeds (48 h); **(j, k)** WT seeds (48 h); **(l, m)** *ap2-7* seeds (6h); **(n, o)** *ap2-7* seeds (12h). Scale bars = 1 mm (b, d, f, h, j), 0.25 mm (c, e, g, i, k, m, o), and 0.5 mm (l, n).

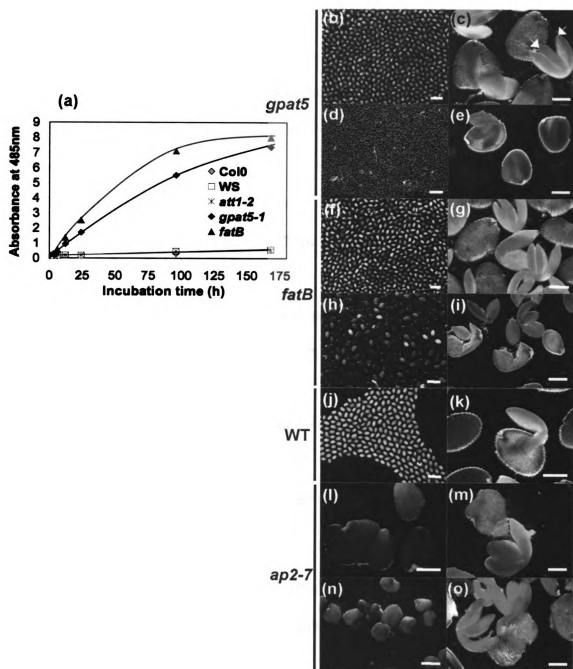


Figure 21.

10-fold increase in *gpat-5* seeds, compared to WS and Col0 wild type lines respectively. In addition, seed samples were observed under inverted microscope (**Figure 21b-o**). The pattern of dye penetration differed between the two mutants. *gpat5* embryos first became colored only in the radicle and cotyledon tips (next to the chalazal end) (**Figure 21b-c**), as noted previously by Beisson et al. (2007), whereas *fatB* embryos stained evenly over the entire embryo surface (**Figure 21f-g**). Similar to wild-type (**Figure 21j-k**), *att1* mutant seeds remained impermeable even after 48 h incubation. When *ap2-7* seeds were examined, embryos in seeds incubated for 6 hours stained evenly over the entire embryo surface (**Figure 21l-m**) and exhibited an intense red staining after only 12 hours (**Figure 21n-o**). Increased permeability to tetrazolium salts has also been reported for another mutant allele, *ap2-1* (Debeaujon et al., 2000). We also compared dye permeation by dewaxed seeds to non-dewaxed seeds (data not shown). The similar pattern of dye uptake shown in dewaxed seeds indicates that tetrazolium dye permeability is almost entirely dependent on lipid polyester composition and is not dependant on waxes removed by rapid chloroform dipping.

Promoter-YFP reporter analysis of biosynthetic genes suggest different localization of polyester layers in the developing seed coat

In the mature seed coat of *Arabidopsis* the testa arises from the outer integument (oi), which is formed by an outer epidermal layer containing mucilage and displaying a columella structure (oi2), and an inner palisade layer (oi1)

(Beeckman et al., 2000; Western et al., 2000; Windsor et al., 2000). The tegmen originates from a three-layered (ii1, ii1' and ii2) inner integument (ii), but the middle layer (ii1') surrounds only part of the embryo, resulting in only two layers in the zone of the chalazal and micropyle (Beeckman et al., 2000). At maturity oi1, ii2, and ii1' are compressed forming the pigmented layer, with ii1 remaining as a layer of empty thick-walled cells (Beekman et al., 2000). In addition, one or two layers of endosperm remain attached to the seed coat. Because both integuments are epidermal in origin (Schneitz et al., 1995), cuticles can occur in these layers. However, it is unknown how many polyester layers are present and where they are located. A cuticle has been described based on microscopic studies for ii1, facing the endosperm in immature seed coats of *Arabidopsis* (Beekman et al., 2000).

The monomer phenotypes of *gpat5* and *att1* mutants provide evidence that *GPAT5* and *ATT1* are important biosynthetic genes in lipid polyester synthesis in *Arabidopsis* seeds and that there are not redundant genes that can compensate for the monomer phenotypes that occur due to loss of *ATT1* or *GPAT5*. Based on these results, and considering that octadecadiene-1,18-dioate is the major monomer in *Arabidopsis* cutin (Bonaventure et al., 2004; Franke et al., 2005), we assumed that *ATT1* and *GPAT5* can be used as markers for cutin and suberin deposition in seed coats, respectively. Examination of the microarray data from the AtGenExpress project (Schmid et al., 2005) showed that both *ATT1* and *GPAT5* are expressed in seeds. However, as seed coat tissues are an

increasingly minor component of the total seed mass as development proceeds, the gene expression indices for seed coat specific genes become increasingly skewed to low values and do not give an indication of developmentally regulated expression patterns. We hypothesized that the expression profile of the YFP reporter protein under control of *ATT1* or *GPAT5* promoters would reflect the distribution of extracellular lipids in seed coats.

Transcriptional fusions were designed to study the localization and timing of *GPAT5* and *ATT1* expression within the seed coat. The 2-Kb 5' sequence of the *ATT1* gene (*Pro_{ATT1}*) plus the first 10 codons of the first exon was cloned in frame with the *eYFP* gene. Likewise, the *Pro_{GPAT5}::eYFP* construct was made by fusing the 1.6-kb 5' fragment of *GPAT5* (*Pro_{GPAT5}*) plus the first 10 codons. These constructs were utilized to produce stable transgenic Arabidopsis plants, and seeds in different developmental stages were analyzed by confocal laser scanning microscopy (CLSM) (**Figure 22**). When fused to the *ATT1* promoter, the reporter protein is expressed in the inner integument layer facing the endosperm (ii1) (**Figure 22a-e**) in the stages from globular to torpedo. No expression was observed later or in other seed coat integuments. Interestingly, the site of expression co-localizes with the cuticle observed by TEM analysis (Beeckman et al., 2000). By contrast, *GPAT5* expression occurs later in the development over the entire seed coat (**Figure 22f-i**) in cell layers underlying the outer integument (oi2), as visualized after staining of the oi2 cell walls with

Figure 22. Tissue specificity of gene expression in living developing seeds.

GPAT5 and *ATT1* promoter activities in transgenic developing seeds were analyzed by Confocal Laser Scanning Microscopy (CLSM). **(a-e)** Fluorescence images of *Arabidopsis* seeds transformed with *ProATT1::eYFP* and **(f-i)** *ProGPAT5::eYFP* constructs. **(a)** Overlaid optical section of fluorescence and light images of transgenic *Arabidopsis* immature seeds in early-torpedo stage, showing YFP expression in ii1 and background red fluorescence from chloroplasts in neighboring endosperm and embryo; **(b)** YFP fluorescence detected only with the BP505-530 nm emission filter. The *ATT1* promoter activity is clearly limited to the ii1 layer. **(c)** Background fluorescence detected through the LP 650 nm filter **(d)** *ProATT1::eYFP* transgenic seed at higher magnification. **(e)** CLSM extended focus fluorescence image of a developing seeds in early-torpedo stage, compiled from 10 optical sections indicates YFP expression in the ii1 layer. **(f, g)** CLSM extended focus fluorescence image of *ProGPAT5::eYFP* developing seeds at the beginning of the dessication stage. Image **(f)** was compiled from 15 optical sections and shows YFP fluorescence surrounding the embryo. Image **(g)** was compiled from 10 optical sections. The YFP expression is beneath the columella (oi2), now visible because the sample was incubated with propidium iodide. **(h)** An optical section of the seed shown in (g). **(i)** Magnification of a seed section shows *GPAT5* promoter activity in oi1, although it is difficult to assign the fluorescence to a single cell layer at this stage. e: embryo; en: endosperm; ii: inner integument; oi: outer integument; Scale bars = 50 μ m (a-c, e-h) and 20 μ m (d,i). In (g,h,i) the sample was stained with aqueous propidium iodide. All samples were excited at 488 nm, and emission was detected through a BP 505-530 nm (a-f, i) or BP 505-600 nm (g, h) emission filter (YFP fluorescence, green) and LP 650 nm emission filter (autofluorescence and propidium iodide fluorescence, red).

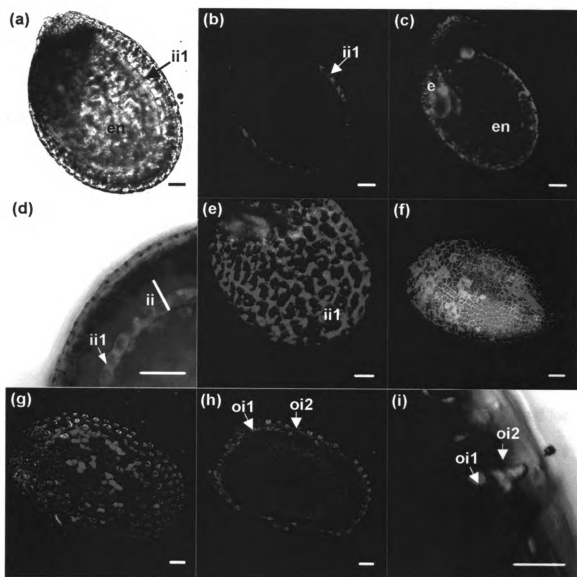


Figure 22.

propidium iodide (**Figure 22g-i**). Our results coincide with the pattern of GUS expression at the beginning of the desiccation stage observed previously by Beisson et al. (2007). At this stage, however, internal cell layers have already started to lose identity, fusing together, and making it difficult to assign YFP expression to a determined integument layer. For this reason, although the optical section shown in **Figure 22i** suggests expression in the cells (oi1) underneath the columella layer, we cannot rule out expression in other layers. As desiccation proceeds and seeds reach maturity, the expression is confined to the chalazal zone of the seed coat (data not shown).

DISCUSSION

Previously we standardized a base-catalyzed transmethylation method for the analysis of monomers from the insoluble lipid polyesters of *Arabidopsis thaliana* and *Brassica napus* seeds (Molina et al., 2006). Over 50 monomers were identified in *Arabidopsis* seeds. *Brassica* seeds had an equally complex monomer composition that was generically similar to that of *Arabidopsis*. A subset of the monomers, namely ferulate, fatty alcohols and C22 and C24 species, were found in the *Brassica* seed coat but not in the embryo, and implied the presence of suberin. Most of the remaining monomers, many of which are found in leaf and stem tissues (Bonaventure et al., 2004; Franke et al., 2005) were present predominantly in the seed coat, with 9,10,18-trihydroxy-octadecenoate being the only monomer highly enriched in the embryo (Molina et

al., 2006). We considered the analysis of *Arabidopsis* seed polyesters to be a useful means to identify mutants in polyester metabolism, yet at the same time, because of the complexity of the seed coat (Haughn and Chaudhury, 2005; Moise et al., 2005; Beeckman et al., 2000), we were not able to interpret the polyester monomer compositions in terms of specific seed coat locations. In this latter context we have applied several methods to gain insights into this question. We have analyzed four *Arabidopsis thaliana* mutants, three of which are for genes known to encode enzymes involved in polyester biosynthesis. The seed analyses validate the depolymerization method as a useful screen for mutants, but more importantly in the context of this paper, the results provide a basis for additional methods to address the issue of seed coat polyester localization. Specifically, it is the confluence of results from a functional transport assay using tetrazolium salts and confocal fluorescence microscopy of transgenic seeds transformed with Promoter::*YFP* constructs, together with the mutant compositions themselves, that lead to the conclusion that suberin and cutin are largely localized to the outer and inner integuments respectively. Additional results from development profiling and seed dissections using *Brassica napus* seeds support the results with *Arabidopsis*. As a practical matter, certain experiments are only feasible with the larger seeded species. However, because of the similarities in polyester composition and seed coat structure between these members of the Brassicaceae, we believe the principal finding for each species are essentially interchangeable.

Seed structure and development

Although the Brassica seed coat reaches its maximum size by stage 2 (**Figure 15**), the deposition of polyesters is not substantial until stage 3, and continues to seed maturity. Presumably the same occurs in Arabidopsis. Thus, unlike the situation in Arabidopsis stems where polyester deposition occurred coincident with epidermal cell expansion (Suh et al., 2005), the deposition of polyesters in Brassica seeds is not coupled to cell expansion. The situation differs for seed wax deposition, which appears to be an earlier event (**Figure 17**). Therefore, in seeds there does not appear to be a coupling of polyester deposition with wax deposition. Because waxes are extracted by rapid chloroform dipping and from hydrated tissues at the earlier stages, we assume that they are indeed a product of the outer layer of the outer integument, but we cannot rule out a contribution from the inner seed coat. Polyester deposition occurs in layers of the testa other than the outermost layer (oi2). One caveat to the above interpretations is that cutan, the insoluble partially aliphatic residue not released by the ester depolymerization reaction (Villena et al., 1999), is not included in the analysis.

The challenge of defining suberin and cutin layers in Arabidopsis seeds is not simply because of their small seed size and the number of layers of the testa, but also because the tissue layers are greatly compressed as seed desiccation proceeds. In addition, we have to distinguish between the testa and the

endosperm-derived aleurone layer of cells. Although we attempted histological staining of maturing seeds with dyes of supposed specificity towards lipids, lignins and suberin, localization of the staining was not definitive. Thus we turned to confocal fluorescence microscopy of transgenic *Arabidopsis* lines expressing YFP fused to promoters of genes involved in polyester synthesis, *ATT1* and *GPAT5*. The spatio-temporal pattern of expression of these two genes is consistent with the role of *ATT1* in the biosynthesis of a polyester layer on the innermost side of the seed coat integuments, and with the function of *GPAT5* in the suberization of the seed coat outer integument during the desiccation phase (**Figure 22**). There are also noteworthy correspondences between detection of *ATT1*promoter::*YFP* reporter activity at the torpedo stage but not later in *Arabidopsis* and the late stage reduction of C18 unsaturated dicarboxylate monomers in *Brassica*, which may imply no late stage biosynthesis; and the later expression of *GPAT5* in *Arabidopsis*, which mirrors the continued accumulation of suberin monomers through *Brassica* seed desiccation.

Suberin monomers are preferentially localized to the outer integument of the seed coat

Polyester monomers which are considered suberin components include fatty alcohols, ferulate and long-chain (> C18) saturated fatty acids, ω -hydroxy fatty acids and α,ω -dioic acids. The chemical analysis of the *ap2-7* mutant places the majority of the fatty alcohols, C18:1 and C18:2 ω -hydroxy fatty acids, C22

and C24 α,ω -dioic acids and ferulate found in *Arabidopsis* seeds in the outer integument. The fact that this mutant is penetrable to the tetrazolium salts suggests that the polyester layer containing these monomers may be a barrier to dye penetration, although it can be argued that the loss of other outer integument structures causes the penetration phenotype. However, this latter argument can be refuted at least in part because the reductions of the C22-C24 suberin aliphatic monomers in *fatB* and *gpat5* mutant lines cause large increases in permeability, confirming that the suberin monomers are a crucial part of the barrier to tetrazolium salt diffusion. The partial compensatory increase observed in C16:0, C18:1, C18:2 ω -hydroxy acids and α,ω -dicarboxylic acids observed in *gpat5* seeds is not enough to recover the impermeable phenotype of wild type seeds, and we cannot be sure of the site of deposition of these compensating monomers. It is also possible that the compensatory increase of monomers with increased unsaturation and reduced chain length, if they are deposited in the suberin layer, may also increase tetrazolium salt permeability. It is not appropriate to expect the quantitative reduction in C22-C24 suberin aliphatic monomers in *fatB* and *gpat5* mutant lines to correlate with the quantitative changes in permeability for several reasons. Firstly, there are some discrete differences in minor components between the two lines, namely that *fatB* seeds also lose C16:0 monomers and C22:0 mono- and di-ols, whereas in *gpat5* seeds some C16 and C18 components increase. Secondly, there may be additional pleiotropic effects, particularly in *fatB*, which is a gene with multiple effects on acyl lipid metabolism (Bonaventure et al., 2003). Thirdly, as shown in **Figure 21c**

and **e**, the *gpat5* and *fatB* mutations influence permeability in different ways. For *gpat5* the tetrazolium molecules primarily enter through the chalazal region whereas in *fatB* seeds permeation occurs throughout the whole seed coat. And fourthly, the data from **Figure 16** suggest that if we can extrapolate from Brassica seeds to Arabidopsis seeds there may be a more complex series of events associated with late-stage suberization in general. The different kinetics might reflect different suberin layers, such as part of the underlying palisade (outer integument, compressed cell layer) or the chalaza.

A second question is the exact location of the suberin-containing polyester layer within the outer integument. Previously, expression of *ProGPAT5::GUS* in Arabidopsis showed that GPAT5 is expressed over the entire seed coat early in seed desiccation but had much more localized expression in the chalazal region late in the seed desiccation (Beisson et al., 2007). The chalazal-localized monomers are synthesized late in the development to create hydrophobic barriers and seal sectors uncovered by the integuments. We have demonstrated that in Brassica seeds the occurrence of the suberin-like monomers is not restricted to the chalaza. This is also consistent with both the expression patterns observed with the *ProGPAT5::YFP* (**Figure 22f-i**) and *ProGPAT5::GUS* constructs (Beisson et al., 2007), and with the *ap2-7* seed polyester phenotype in Arabidopsis. And finally, it should also be noted that the occurrence of suberin in the outer integument is not a trait found in all seeds. The outer seed coat of grapefruit seeds contains no polyester monomers (Espelie, 1980).

The increase in seed coat permeability on reduction of suberin monomers should be compared to the increase of permeability caused by the *transparent testa (tt)* and related mutants (Debeaujon et al., 2000). Most of these mutants are for biosynthetic genes of the flavonoid pathway and result in decreased levels of condensed tannins in the seed coat, particularly in the ii2 layer. This causes the change in pigmentation, which gives the mutants their name. For the *gpat5* mutants we have already noted that the seed coat is slightly darker, but that there are similar levels of soluble and insoluble proanthocyanins in the seed coat (Beisson et al., 2007). Thus the increase in seed coat permeability is unlikely to be a pleiotropic effect on tannin concentrations originating from the *gpat5* mutant. This conclusion is consistent with the results from the *ap2* lines (Debeaujon et al., 2000; and this work), where permeability is enhanced despite negligible change in seed coat color. The seed coat polyester content of the *tt* mutants has not been measured, nor can we quantitatively compare the permeability of polyester and *tt* mutants. It is possible that both polyesters and condensed tannins contribute independently to seed coat permeability. However, as suberin monomers are present largely in oi1, while tannins are present in ii2, the immediate juxtaposition of these two layers might also suggest a degree of interdependence, either directly between the polymers themselves or through interactions between the two layers. These possibilities need to be investigated.

Cutin monomers are preferentially localized to the inner integument of the seed coat

High dicarboxylic acid levels have generally been considered indicative of suberin. However, the presence of high proportions of C16 and C18 dicarboxylic acids in the leaf and stem epidermal layers of *Arabidopsis* (Bonaventure et al., 2004), and the presence of these in the isolated cuticles (Franke et al., 2005), suggest that this generalization is not applicable to *Arabidopsis*. Certainly, octadecadiene-1,18-dioate is not found in other than trace amounts in suberin, and as it is clearly the dominant monomer in isolated cuticles it can best be considered a cutin component.

The chemical analysis of the *ap2-7* mutant places octadecadiene-1,18-dioate largely in a layer underneath the outer integument. The fact that this mutant is extremely penetrable to the tetrazolium salt strongly suggests that the octadecadiene-1,18-dioate-containing polyester layer is a weak barrier to penetration, although it can be argued that a pleiotropic effect of the *ap2-7* mutation might extend beyond the outer integument and cause changes to structures within inner integument. Against this latter argument the large increase in permeability in *fatB* and *gpat5* mutant lines, which also have large reduction of the C22-C24 suberin aliphatic monomers that are major components in polyester layer(s) of the outer integument, support the conclusion that it is the outer integument that is the major polyester barrier to tetrazolium salt diffusion. The

fact that dye penetration is unaffected in seeds of *att1* despite large reductions of C18:1 and C18:2 α,ω -dicarboxylic acids found in this mutant, is completely consistent with the notion that these polyesters are part of a layer underneath the suberized barrier of the outer integument.

The reason for the apparent lack of barrier properties of the octadecadiene-1,18-dioate-containing polyester layer is unknown. It might be a lack of interstitial waxes. The situation appears to contrast with that of leaves, where the cuticle, which contains a octadecadiene-1,18-dioate-rich cutin, is an effective barrier to toluidine blue dye penetration. One possible reason for the poor barrier properties of the octadecadiene-1,18-dioate-containing polyester layer in mature *Arabidopsis* seeds is suggested by the monomer deposition kinetics for *Brassica* seeds over development. Unlike the monomers of groups A and B (**Figure 16**), seed C18:1 and C18:2 α,ω -dicarboxylic acid levels drop by 35% and 75% respectively from their peak at stage 4 to the mature seed. The reason for this drop is obscure, but the loss of monomer density is one simple explanation for dye penetration through this layer. This loss of octadecadiene-1,18-dioate in seeds is itself another difference in comparison to the seed suberin-like monomers. It is also reminiscent of the *Arabidopsis* stem epidermis polyesters (cutin), where the loss of octadecadiene-1,18-dioate occurs later in stem maturation (Suh et al., 2005).

A second question is the definition of the exact location of the octadecadiene-1,18-dioate-containing polyester layer beneath the outer integument. From the *ATT1* reporter activity illustrated in **Figure 22a-e**, *ATT1* expression is only detected in cells of the ii1 layer of the inner integument cells. From this we infer that most of the octadecadiene-1,18-dioate deposition in polyesters also occurs in this layer of cells. This result is consistent with the conclusions reached for the *ap2-7* mutant in seeds and dye penetration assays that this monomer is present largely in the inner integument, and with previous TEM observations with *A. thaliana* seeds, where a cuticle was detected on the inner cell layer of the inner integument facing the endosperm in all developmental stages until maturity (Beeckman et al., 2000). Unlike the situation in the outer integuments, the occurrence of cutin monomers in the inner seed coat which we infer for *Arabidopsis* has a direct parallel with the observation of cutin monomers in the dissected inner seed coat of grapefruit (Espelie et al., 1980).

EXPERIMENTAL PROCEDURES

Plant material

Wild-type *Arabidopsis thaliana* (ecotypes Columbia and Wassilewskija-2) and the mutant lines *fatB*, *gpat5-1*, *gpat5-2*, *att1-1*, *att1-2* and *ap2-7* were grown on a mixture of soil:vermiculite:perlite (1:1:1 v/v/v) under white fluorescent light

(80-100 $\mu\text{E m}^{-2} \text{ s}^{-1}$) in a 18-h-light/6-h-dark photoperiod. The temperature was set at 20-22°C and the relative humidity at 60-70%. Seeds were always stratified four d at 4°C. Homozygous plants of *ap2-7* were cross-pollinated with wild-type pollen to favor fertilization. Despite this, the limited seed yield was not enough for replicate analyses. Seeds of *Brassica napus* cv *Westar* were planted in 30 cm plastic pots in a (2:1 v/v) mixture of soil:vermiculite and grown in an air-conditioned greenhouse under natural light supplemented with lamps to provide 18-h-light/6-h-dark photoperiod.

Lipid analysis

Polyesters. Seed samples were delipidated and dry residues were depolymerized by methanolysis in the presence of sodium methoxide. After acetylation of the CH_2Cl_2 -extractable products, the monomers were analyzed by GC (Molina et al., 2006).

Oil content. Total fatty acid methyl ester (FAME) content was analyzed in each developmental stage of *B. napus* seeds according to Li et al. (2006).

Wax analysis. Waxes were extracted by immersing 0.5 g seeds for 30 s in chloroform (5 ml). N-tetracosane (5 μg) was added as internal standard for quantification, as well as 1-tricosanol (5 μg) and docosanoic acid (5 μg) as controls for derivatization of alcohol and acid functional groups, respectively. The solvent was evaporated under nitrogen and samples were treated with *bis*-N,N-

(trimethylsilyl)-trifluoroacetamide in pyridine (15 min at 100°C) to convert alcohols and carboxylic acids to trimethylsilyl derivatives. Monomers were analyzed by GC (FID) analysis on a DB-5 capillary, using conditions as described by Bonaventure *et al.* (2004). Peak areas (pA.sec) were converted to relative weights by applying FID theoretical correction factors, assuming the FID response is proportional to carbon mass for all carbons bonded to at least one H-atom (Christie, 1991).

Tetrazolium salt penetration assay

Seed samples (50 ± 1 mg each) of *Arabidopsis* wild type and mutants were incubated in 500 μ l 1% aqueous solution of 2,3,5-triphenyltetrazolium chloride (TTC) at 30°C for 1 h, 12 h, 24 h, 48 h, 72 h and 7 d in darkness. After incubation, the samples were washed twice with water, resuspended in 1 ml 95% ethanol and finely ground with mortar and pestle to extract formazans. The final volume was adjusted to 2 ml with 95% ethanol, immediately centrifuged 3 min at 15,000 g and the supernatant recovered. This procedure was performed quickly to avoid reaction of TTC with the embryo cells after seed disruption. Formazan concentration was determined by measuring the absorbance at 485 nm (Candler *et al.*, 1997). Seeds were also observed under dissection microscope. The assay was repeated using seeds that were rinsed for 1 min in chloroform to remove epicuticular waxes.

Construct design and Arabidopsis transformation

The reporter gene, *eYFP* (Accession number CS538989, synthetic construct, Schultz et. al, 2007) was amplified by PCR and cloned into *Xba*I-*Bam*HI-digested pBI101 (Clontech, Palo Alto, CA). The primers used for the amplification were 5' CACACTCTAGA ATGGTGAGCAAGGGCGAG-3' (forward) and 5'-CACACGGATCCTCAGGACTTGTACAGCTCGTCC-3' (reverse), added restriction sites underlined. The 1.6-kb 5' sequence of the GPAT5 DNA, plus 30 bp of the GPAT5 coding region, was amplified by PCR using genomic DNA as template (*PRO_{GPAT5}*) and subcloned in pGEM[®]-T Easy vector (Promega Corporation, Madison, WI) for sequencing. The primers used were 5'-CACACAAGCTTAAAAGCGTTTTAATTAGAGAGA-3' (forward) and 5'-CACACTCTAGACGATGTCGTTCC AGCTT-3' (reverse), introducing *Hind*III and *Xba*I restriction sites (underlined). The *ATT1* promoter sequence was amplified using the primers 5'-CACACAAGCTT GTTTGGCAAACCATCTACAAG-3' (forward) and 5'-CACACTCTAGATACAAGGAGCAT CGTGTTGG-3' (reverse). The fragment included 2-kb upstream of the first ATG and 30 bp of the *ATT1* coding region (*PRO_{ATT1}*), and was subcloned into pGEM[®]-T Easy. All amplifications used a proofreading DNA polymerase (Platinum Pfx, Invitrogen, CA). To generate the *PRO_{GPAT5}::eYFP* and *PRO_{ATT1}::eYFP* constructs, the promoter sequences were released from pGEM[®]-T Easy vectors and ligated into *Hind*III-*Xba*I-digested pBI101-*YFP*, upstream the *YFP* sequence. Both constructs were used for Arabidopsis transformation using the vacuum infiltration method

(Bechtold et al., 1993). Surface-sterilized T₁ seeds of transformed plants were selected on sterile MS medium supplemented with 50 µg/ml kanamycin. Resistant seedlings were transferred to soil for continued growth and T₂ seeds from several individual kanamycin-resistant plants were analyzed by CLSM for YFP expression.

Microscopy

CLSM. Imaging of living, developing transgenic seeds was performed with Zeiss Pascal confocal laser scanning microscope (Carl Zeiss International, Jena, Germany), using a 20X Plan-Neofluar Carl Zeiss objective, numerical aperture (NA) of 0.5. Fluorescence microscopy utilized excitation from a 488-nm argon ion laser line and emission after passing through a BP 505-530 or BP 505-600, and long-pass (LP) 650-nm filter. Individual optical sections were used to create extended focus images with a maximum intensity algorithm using the LSM 5 Pascal (version 3.0) software. Images created with the LP 650-nm filter were digitally colored red, and those created using a BP 505–530 (or BP 505-600) nm emission filter were digitally colored green. Such images were overlaid to derive a two-color image. In some samples, light microscopy was used to co-localize fluorescence and cell layers. When specified, samples were treated with 0.5 mg/ml aqueous propidium iodide (Sigma, St Louis, MO) for 10 min to visualize cell walls. All images were transformed to TIFF format files and processed with Adobe Photoshop Elements 4.0.

Light microscopy. Mature seeds incubated in the tetrazolium salts (see *Tetrazolium Assay* section) were observed with a Leica MZ12.5 light microscope (Leica Microsystems Inc., Bannockburn, IL) coupled to a digital camera.

CHAPTER 4

IDENTIFICATION AND FUNCTIONAL ANALYSIS OF CANDIDATE GENES FOR LIPID POLYESTER BIOSYNTHESIS

Acknowledgements:

I want to acknowledge the following contributions:

-YongHua Li selected homozygous *cyp86A1-1*, *cyp86A1-2*, and *cyp86A4* Arabidopsis lines.

-Orlando Alvarez-Fuentes collaborated with the phylogenetic analysis of the Arabidopsis BAHD gene family shown in Figure 32.

-Dr John Browse provided the *lacs* single and multiple knockout lines.

-Dr Ljerka Kunst provided the *at1g04420* homozygous line.

ABSTRACT

Cutin and suberin are plant-specific lipid polyesters with barrier properties that are essential for the survival of land plants. Because of their complexity and intractability in organic solvents, many aspects of the structure and biosynthesis of these polymers have remained largely unknown. We have started to use the tools available for the plant genetic model, *Arabidopsis thaliana*, and this has facilitated our understanding of a few genes that contribute to the synthesis of monomers and acylglycerols. However, most of the genes required for complex lipid polyesters biosynthesis remain to be discovered using forward and reverse genetics approaches. In this work, I have identified candidate genes for polyester biosynthesis by means of bioinformatics approaches. Specifically, I have taken advantage of 1) publicly available microarray data; 2) a catalog of genes of plant lipid metabolism; and 3) web-based applications for the analysis of transcriptional co-responses. Identified candidate genes belong both to gene families that are known to be involved in lipid polyester biosynthesis and to families that have not previously been shown to have members associated with these processes. Homozygous lines containing T-DNA insertions were obtained for several selected candidate genes, and the lipid polyester phenotype was determined in various tissues of those knockout mutants. Changes in the lipid polyester monomer composition were observed in several of them. Such changes are consistent with the loss of the specific genes represented by each mutant. In particular, I have identified a novel acyl-transferase that, when disrupted, causes

a 95% reduction of ferulate content in suberin monomers released by transesterification. These results verify the efficacy of this approach to identify new genes involved in polyester biosynthesis.

INTRODUCTION

The synthesis of extracellular lipid polyesters, cutin and suberin, involves complex processes where several metabolic pathways act coordinately. Deposition of suberin on the primary cell wall requires synthesis and assembly of metabolites from the phenylpropanoid and lipid pathways, involving a battery of acyl-modifying, acyl-transfer and transport steps. Likewise, cutin aliphatics synthesized by epidermal cells undergo a series of modification, transport and catenation reactions. In both polyesters the sequence of biosynthetic steps remains unknown. Moreover, further modification of cutin and suberin takes place to produce a fraction containing non-ester bonds and therefore cannot be released by typical transmethylation methods. The existence of this non-depolymerizable fractions, cutan and suberan, adds further complexity to the whole picture of extracellular polyesters.

Transcript co-response analysis is a strategy to identify genes under common or related transcriptional control whose transcript levels exhibit simultaneous changes and, therefore, likely function in the same or related physiological pathway (Lisso et al. 2005). Co-expression-based prediction of

gene function followed by phenotypic characterization of insertion lines for selected candidate genes has successfully identified genes in the cellulose biosynthesis pathway (Brown et al., 2005; Persson et al., 2005). Guide-gene approaches have also been applied to unravel pathways closely connected to isoprenoid biosynthesis (Wille et al., 2004), and to identify brassinosteroid-related genes (Lisso et al., 2005) and different Arabidopsis metabolic networks (Wei et al., 2006), although identified candidate genes in these reports still require biochemical characterization. An important limitation of these approaches is that they are dependent on the temporal (i.e. developmental stage) and spatial (i.e. tissue specificity) resolution of the microarray data. For instance, for a transcript that is highly accumulated in a specific developmental stage, such expression will not be reflected in the microarray data if bulk stages are analyzed.

Currently, there are several web-based gene co-expression tools available to the community: “Genevestigator” (Zimmermann P et al., 2004; Zimmermann et al., 2005), “Arabidopsis Coexpression Data Mining Tool” (Jen et al., 2006), AthCor@CSB.DB (Steinhauser et al., 2004), The Botany Array Resource (Toufighi et al., 2005), “Co-expression” at University of Alabama (Wei et al., 2006) and “ATTED-II” (Obayashi et al., 2007). These bioinformatics tools use microarray expression data from different repositories (e.g. AtGenexpress, NASCArray, Gene Expression Omnibus) to evaluate gene co-expression, often quantified by Pearson’s correlation coefficient (Aoki et al., 2007). However, this is

an area under constant progress and not all of the above mentioned data mining tools were developed at the onset of my study.

I have initiated a reverse-genetics approach in *Arabidopsis* to characterize the *in planta* function of candidate genes for polyester synthesis, as part of a general project in the laboratory. Particularly, I have worked with those listed in **Table 7** (see results and discussion). *In silico* approaches require biological knowledge of the system (i.e. lipid polyester synthesis) to select key genes that are used as guide (or 'bait') genes. Candidate genes were identified using genes from the *GPAT* and *CYP86A* plant-specific families as guide genes for co-response analysis. Pairwise correlations were calculated with prioritized genes up-regulated in *Arabidopsis* epidermal microarrays (Suh et al., 2005) and the phellem transcriptome (Soler et al., 2007). Because seeds contain both cutin and suberin, lipid polyester composition analyses were initially conducted in seeds of T-DNA insertion lines for selected genes, unless the studied gene had low seed expression. Pronounced changes were observed in the composition of polyesters of several mutants, consistent with the loss of the specific genes represented by each mutant. These results corroborate the value of this approach to identify new genes involved in the lipid polyester pathway.

RESULTS AND DISCUSSION

Identification of candidate genes for polyester biosynthesis

To elucidate possible players required in the lipid polyester metabolic network, I have based my search on genes whose biological significance in surface lipid metabolism had been demonstrated. *ATT1* (Xiao et al., 2004; Molina et al., 2008) and *GPAT5* (Beisson et al., 2007), which encode polyester-specific enzymes, were selected as bait genes for co-expression analyses. Disruption of the putative ω -hydroxylase gene *ATT1* results in 70% reduction of C16-C18 α,ω -dicarboxylates, the major monomers found in Arabidopsis cuticular polyesters, whereas *GPAT5*, encoding a putative glycerol-3-phosphate acyltransferase, participates in suberin synthesis. Thus, *ATT1* and *GPAT5* can be considered as cutin and suberin markers, respectively.

I examined the timing and tissue specificity of gene expression for members of CYP86A and GPAT families using microarray data from the AtGenExpress project (Schmid et al., 2005). To assess functional relationships between genes of both families, I used the web-based application Gene Correlator, a Genevestigator tool that reveals co-expression between two genes on selected Arabidopsis Affymetrix GeneChip data and generates a linear correlation coefficient (Zimmermann P et al., 2004; Zimmermann et al., 2005). Correlation coefficients, detailed in **Appendix B**, indicated possible association between ω -hydroxylase genes and glycerol-acyltransferase genes. For example, *ATT1* correlates with *GPAT4/GPAT8*, indicating association with cutin synthesis,

while *CYP86A1* correlates with *GPAT5*, and is possibly suberin-related. Recent findings in our lab have demonstrated that, in fact, *GPAT4* and *GPAT8* are required for cutin deposition (Li et al., 2007a), illustrating the value of the proposed strategy to identify new candidates.

To identify other candidate genes for polyester biosynthesis I have searched a catalog of genes of plant lipid metabolism (Beisson et al., 2003) and investigated transcriptomes of *Arabidopsis* epidermis (Suh et al., 2005), and of the suberin-rich phellem (cork) of *Quercus suber* (Soler et al., 2007). Pairwise comparisons of candidates from several gene families with each of the members of the GPAT and CYP86A families were performed (**Appendix B**). Preferred candidate genes are listed in **Table 6**, and putative biosynthetic pathways are illustrated in **Figure 23**. It is important to bear in mind that only one of the possible scenarios for the biosynthetic reactions is illustrated; alternative pathways leading to acylglycerols are discussed in Chapter 5. **Table 6** is divided in two sections, the first one listing genes I wanted to find or confirm are involved in lipid polyester synthesis, and the second is focused on discovery of new gene families. When possible, genes expressed in seeds were selected, as seeds contain both cutin and suberin polyesters (**Appendix C**).

The initial set of guide genes (*ATT1* and *GPAT5*) has continuously contributed to expand and strengthen the list of candidates over time. In this regard, interactions with other members of the lab and their work on

Table 6. Arabidopsis candidate genes selected on basis of gene correlations and/or transcript up-regulation in epidermal or cork microarrays.

Gene families already known to be involved in polyester or cuticle synthesis:				
Gene family	Gene/enzyme names	AGI Number	Putative function	References
Elongase	<i>FDH</i>	At2g26250	β -ketoacyl-CoA synthase, long chain fatty acid elongase	(Lolle et al. 1992; Pruitt et al. 2000; Yephremov et al. 1999)
		At2g46720		
	<i>KCS1</i>	At1g01120		(Todd, 1999)
	<i>CUT1</i>	At1g68530		(Kunst, 2000; Millar, 1999)
	<i>DAISY</i>	At1g04220		(Franke, 2006)
	<i>FATB*</i>	At1g08510	Acyl-ACP thioesterase	(Bonaventure, 2004)
CYP86A	<i>LCR</i> , CYP86A8	At2g45970	P450, fatty acid ω -hydroxylase	(Wellesen, 2001; Duan and Schuler, 2005)
	<i>ATT1</i> CYP86A2	At4g00360		(Xiao, 2004; Duan, 2005)
	CYP86A4	At1g01600		
	CYP86A1	At5g58830		(Li, 2007; Duan and Schuler, 2005)
GPAT	<i>GPAT4</i>	At1g01610	Putative glycerol-3-phosphate acyltransferase	(Zheng, 2003; Li et al., 2007)
	<i>GPAT5</i>	At3g11430		(Beisson et al., 2007; Zheng et al., 2003)
LACS	<i>LACS1</i>	At2g47240	Long-chain acyl-CoA synthetase	(Shockey et al., 2002)
	<i>LACS2</i>	At1g49430		(Schnurr et al., 2004; Shockey et al., 2003; Shockey et al., 2002)
	<i>LACS3</i>	At1g64400		(Shockey et al., 2002)
New candidate gene families				
LPAT	<i>LPAAT4</i>	At1g75020	Lysophosphatidate Acyltransferase	(Kim et al., 2005)
	<i>LPAAT5</i>	At3g18850		
MAG lipase		At2g39400	Monoacylglycerol lipase	
BAHD		At5g41040	Hydroxy-cinnamoyl transferase	(D'Auria, 2006)
		At5g63560		
		At3g48720		
CYP86B	CYP86B1	At5g23190	P450 oxidase	(Watson et al., 2001)
	CYP86B2	At5g08250		

Highlighted genes represent those I have studied. *Indirectly implicated lipid polyester synthesis

Figure 23. Putative pathways for the synthesis of aliphatic polyesters.

Biosynthesis of C16-C18 monomers and their assembly into cutin are shown on the left, and long-chain monomer synthesis and assembly of the aliphatic suberin polymer are shown on the right. Because there is uncertainty regarding the order of biosynthetic steps, one possible scenario is illustrated, where we assume that monomer oxidation occurs after elongation and before esterification to glycerol (or G3P). Similarly, possible sites of monomer activation by LACS homologous are unknown. Likewise, polymerization genes and site(s) remain elusive. Putative Arabidopsis genes are indicated in blue. Synthesis of primary alcohols is not detailed for clarity, but presumably these are produced via the reductive pathway described for waxes. ABC transporters and lipid transporter genes are also omitted. Numbers indicate possible enzymatic activities required in each step: ① Thioesterase; ② CytP450 ω -hydroxylase; ③ ω -hydroxyacid dehydrogenase (NADP); ④ ω -oxoyacid dehydrogenase (NADP); ⑤ Long chain acyl-CoA synthase; ⑥ G3P acyl-transferase; ⑦ Acyl-CoA Reductase; ⑧ β -Ketoacyl-CoA synthase, Fatty acid elongation complex. FA= fatty acid; MAG= monoacylglycerol; OHFA= hydroxy fatty acid; FAE= fatty acid elongation complex; ACP= acyl carrier protein

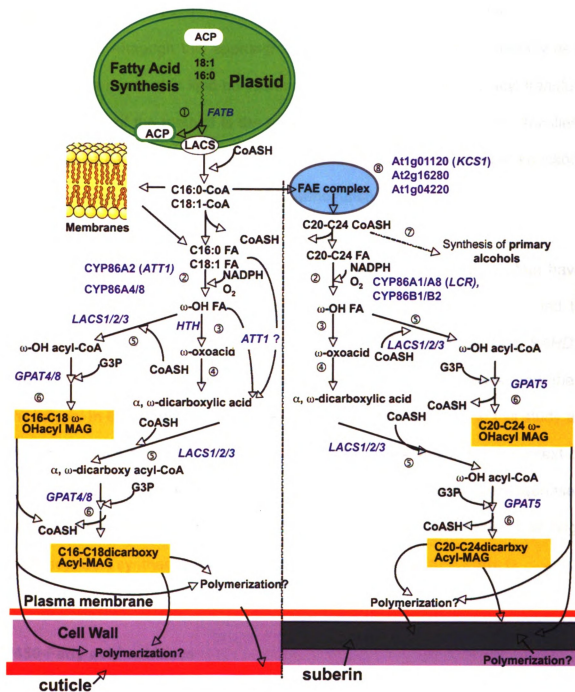


Figure 23.

characterizing GPAT family members have been crucial to define the directions of my project. Although this approach has indeed proven useful to identify new gene families involved in lipid polyester monomer modification and acyl transfer, one weakness of the method is the potential gene redundancy in gene families. Therefore, in certain cases it may be necessary to generate multiple knockout mutants or use other methods to assess gene function.

The goals of this study were to confirm the function of genes that have been suggested to have a role in cuticle synthesis (e.g. *LACERATA*), and to discover gene families not previously associated with this pathway (e.g. *BAHD*). **Table 7** provides a summary of mutants discussed in this work and their phenotype. In the next pages, the different mutants characterized in this study as well as potential candidates for future analyses are discussed in the context of their respective families. In particular, I will focus in P450-monooxygenases involved in monomer modification, Acyl-CoA utilizing acyltransferases, and long-chain acyl-CoA synthases (LACS). Elongases are included **Appendix D**.

P450-Fatty acid oxidases

The activity of several cytochrome P450-dependent fatty acid ω -hydroxylases has been shown *in vitro* (Benveniste et al., 1998; Pinot et al., 1999; Wellesen et al., 2001; Duan and Schuler, 2005; Benveniste et al., 2006). A

Table 7. Summary of mutants characterized in this work.

Gene family	AGI Number	Mutant allele	Polyester monomer phenotype	Permeability phenotype
β -ketoacyl-CoA synthase, FAE	At1g04220 (DAISY)	SALK_033206 C	Seeds: No change in monomer composition/load (Figure 62)	Seeds impermeable to TS
Acyl-ACP thioesterase	At1g08510 (FATB)	<i>fatB</i> -ko T-DNA insertion mutant	Seed: 65-85% <u>reduction</u> in C16 monomers; 45-65% reduction in C20-C24 (Figure 20)	Seeds permeable to TS (Figure 21)
CYP86A Putative cytochrome P450 fatty acid ω -hydroxylase	At2g45970 (LCR) (CYP86A8)	WiscDsLox387 B09 (<i>lcr-2</i>)	Leaf: 20 % <u>reduction</u> total monomers (Figure 30)	Weak leaf permeability to TBO
	At4g00360 (ATT1) (CYP86A2)	EMS mutant (R309C); <i>att1-1</i> SALK_005826; <i>att1-2</i>	Leaf: <u>Reduction</u> in DCAs (70%) and ω -OH acids (variable 0-50%). Stem: 30% <u>reduction</u> in DCAs (Chapter5, Figure7). Seed: <u>Reduction</u> in C18 DCAs (70%) and C16 DCA (30%). 30-45% <u>increase</u> in 18:2 ω -OH acid (Figure 20)	Leaves permeable to TBO (Figure 46); seeds impermeable to TS (Figure 21)
	At1g01600 (CYP86A4)	SALK_073078 (<i>cyp86a4</i>)	Leaves: no change. Stems: DCAs-C16 diol reduced by 30-40% (data not shown) (Figure 31)	Leaves impermeable to TBO
	At4g00360 At1g01600	<i>att1-2/cyp86a4</i>	Stems: 70% reduction total cutin load. (Figure 31)	
	At5g58830 (CYP86A1)	SALK_146813 <i>cyp86A-1</i> SALK_140618 <i>cyp86A-2</i>	Seed: 80% <u>reduction</u> in C16 DCA (<i>cyp86A1-1</i>). Root: 70-90 % <u>decrease</u> in C16:0/C18 α,ω -bifunctional monomers (Figure 27)	Seeds impermeable to TS
GPAT, putative glycerol-3-phosphate acyltransferase	At3g11430	SALK_018117 <i>gpat5-1</i> SALK_142456 <i>gpat5-2</i>	Seed: 90% <u>reduction</u> in C20-C26 FAs; <u>increase</u> in C16-C18 monomers (Chapter 3, Figure 20 ; Beisson et al., 2007)	Seeds permeable to TS (Figure 21)
LACS, Long-chain acyl-CoA synthetase	At2g47240 LACS2	<i>lacs2-1</i> , T-DNA insertion	Leaf: 50% <u>reduction</u> DCAs (Figure 10a). Seed: <u>Reduction</u> in C16/18 DCAs /C14 ω -OH acid (60%), and C22 alcohols (20-40%) (Figures 39-40)	Leaves permeable to TBO
	At1g49430 LACS1	SALK_127291 <i>lacs1-1</i> ; SALK_138782 <i>lacs1-2</i>	Leaf:10-20% <u>reduction</u> 18:2 DCA (Figure 10a). Seed: no change (Figures 39a-40)	Leaves impermeable to TBO
	At1g64400 LACS3	<i>lacs3</i>	Leaf:10-20% <u>reduction</u> 18:2 DCA; 2.5-fold <u>increase</u> C16-Diol (Figure 10a) Seed: <u>increases</u> in most monomers (Figures 39a-40)	
		<i>lacs1-2/lacs2-1</i>	Leaf: 70% monomer load <u>reduction</u> (Figures 39b)	Leaves permeable to TBO
		<i>lacs1-2/lacs2-1/lacs3</i>	Leaf: 83% monomer load <u>reduction</u> (Figures 39b)	
BAHD AcylCoA-utilizing acyltransferase	At5g41040	SALK_048898 SALK_017725	Seed:>95% reduction in ferulate (1.3 mmol/g seeds); loss in OH-containing monomers (Figure 34a)	Seeds permeable to TS after 72 h incubation (Figure 36)

C16-Diol: C16:0 10,16-Dihydroxy Acid; DCA: α,ω -dicarboxylic acid; FA: fatty acid; FAE: fatty acid elongase; TBO: toluidine blue; TS: tetrazolium salts

central issue with these P450s is that their *in vivo* substrates are uncertain and therefore their position in the sequence of reactions is unknown. Members of the CYP86A subfamily are ω -hydroxylases with likely roles in oxidation of lipid polyester aliphatic monomers (the reader is referred to Chapter 5, **Figure 44** for details on microarray expression). As mentioned above, correlation coefficients indicate possible association between putative ω -hydroxylase genes and putative glycerol-acyltransferase genes: *ATT1* correlates with *GPAT4*, and *CYP86A1* with *GPAT5*. This indicates that these enzymes may have evolved different substrate specificities, or that their *in vivo* activity depends exclusively on substrate availability in the cells where they are co-expressed. Decrease in C22:0-C24:0 ω -hydroxy acids and α,ω -dicarboxylic acids were observed in *gpat5* mutants (Beisson et al., 2007), whereas C16 and C18 dicarboxylic acids but not the long chain monomers were affected in *att1* mutants (Beisson et al., 2007; Molina et al., 2008). Given these monomer profiles, investigations in our group have largely been based on the hypothesis that *ATT1* and *GPAT4/GPAT8* may have specificity towards C16-C18 substrates, while *CYP86A1* and *GPAT5* may be more acyl-specific for C22-C24 substrates.

ATT1 (CYP86A2). The recent characterization of the double knockouts *gpat4/gpat8* (Li et al., 2007a) established a role for the GPAT family of acyltransferases in the deposition of cuticular aliphatic monomers. In these mutants, in addition to ~80% reduction in cutin monomers, TEM analysis revealed reduction in the cutin layer on pavement cells and on substomatal

chambers, plus absence of cuticular projections on guard cells. Analysis of *att1* cutin (discussed in detail in Chapter 5) indicated a 70% reduction in leaf cutin monomer load, mainly at the expense of α,ω -dicarboxylic acids (**Figure 47a**, and Molina et al., 2008). Taken together, these results suggest that GPAT4 and GPAT8 are partners of ATT1 in cutin synthesis, as hypothesized on the basis of gene correlations.

Comparison of *GPAT4* and *ATT1* transcript expression patterns using YFP as reporter confirmed that they are specifically expressed in the epidermis (**Figure 24a-e**). Furthermore, these promoter activities are almost exclusively detected in guard cells but not in pavement cells, an observation that led us to hypothesize that the *att1* knockout might lack cuticular ledges, as observed in *gpat4/gpat8*. To test this hypothesis, I used microscopy to visualize lipid features on leaf surfaces (**Figure 25**). When whole leaves were stained with the lipophilic fluorescent dye neutral red (Dubrovsky et al., 2006) and analyzed by CLSM, cuticular ledges were evident in wild-type leaves (**Figure 25a**), but the staining was faint on *att1* guard cells (**Figure 25b**), indicating reduced lipid deposition on *att1* cuticular projections. However, analysis of leaf cross sections at the microscopical (**Figure 25e,f**) and ultrastructural levels (**Figure 25c,d,g**) indicated that cuticular ledges are still present in *att1* stomata (**Figure 25e,g**). Furthermore, in spite of an apparent absence of *ATT1* expression in pavement cells, the ultrastructure of the cutin layer on these cells and on the substomatal chambers is clearly different from wild-type (**Figure 25b-e**). Similar ultrastructural defects

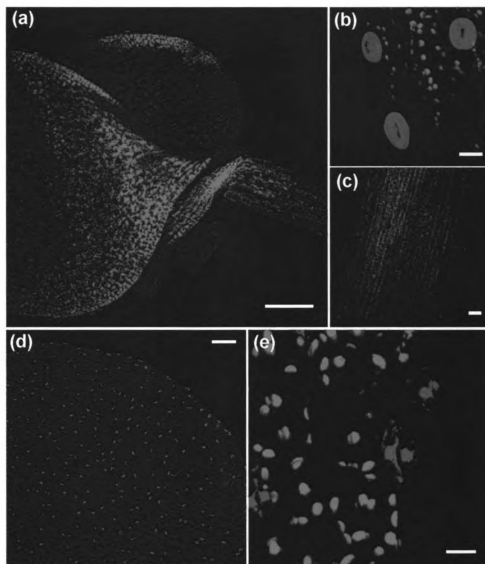


Figure 24. Comparison of *ATT1* and *GPAT4* promoter activities.

CLSM analysis of transgenic Arabidopsis plants transformed with *Pro_{ATT1}::YFP* (**a-c**) and *Pro_{GPAT4}::YFP* (**d-e**) constructs indicates guard cell-specific expression. (**a,b**) YFP expression under the *ATT1* promoter in cotyledons and (**c**) 6-week old stems. (**d,e**) YFP expression under the *GPAT4* promoter in cotyledons. Background red fluorescence corresponds to chlorophyll. Scale bar=200 μ m (**a**), =20 μ m (**b**), =50 μ m (**c**), =100 μ m (**d**), =10 μ m (**e**).

Figure 25. Microscopical analysis of surface lipids in *att1* mutants.

CLSM extended focus confocal images of wild-type (a) and *att1-2* (b) abaxial leaf surfaces stained with the lipophilic fluorescent dye neutral red. The lipid-rich cuticular ledges are strongly stained on wild-type stomata (arrowheads) (a) but the staining is faint in *att1* leaves (b). Insets show lipid features (green). The red chlorophyll background was removed. (c,d) Ultrastructure of the cuticle on pavement cells of wild-type (c) and *att1* (d). (e, f) Light transmission images of wild-type (e) and *att12* (f) leaf guard cells. (g) TEM image of leaf guard cells in *att1-2*. Arrowheads indicate cuticular projections on guard cells (Scale bar=10 μm (a, b), =200 nm (c), =500 nm (d), =5 μm (e, f, g)).

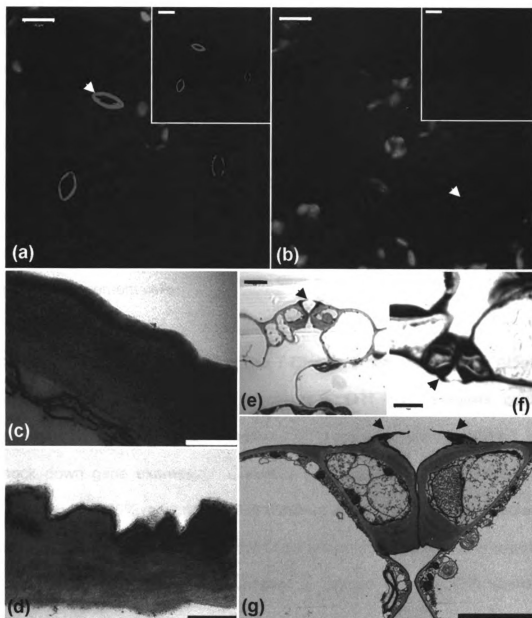


Figure 25.

have been reported earlier by Xiao et al. (2004). Based on these results, it can be reasoned that the preferential guard-cell expression of *ATT1* observed with promoter-YFP construct could be due to lack of other control elements such as 3' UTRs. However, using a gene trap approach, Galbiati et al. (2007) have recently reported that *ATT1* is exclusively expressed in guard cells, a result that was confirmed by RT-PCR in purified guard cells. Therefore, *ATT1* could play a role in modulating stomata activity, as suggested by the authors, or cuticular ledges on guard cells may have a distinctive lipid polyester composition compared to the cuticle on pavement cells.

CYP86A1. Homozygous seeds of two T-DNA insertion alleles of the At5g58860 gene were kindly provided by YongHua Li. RT-PCR analyses confirmed complete gene silencing for *cyp86a1-2* (**Figure 26**), with *cyp86A1-1* having knock down gene expression. Chemical analyses of *cyp86A1* seeds (**Figure 27a**) showed a 75% reduction of C16:0 dicarboxylate and a three-fold increase of trihydroxy C18:1 fatty acid in the *cyp86A1-2* knockout allele but not in *cyp86A1-1*. By comparison, in *att1* seeds (**Chapter 3, Figure 20**) only C18 unsaturated dicarboxylates were affected. It is uncertain if the different phenotypes indicate different substrate specificity and/or different locations of both enzyme products within seed coats. Indeed, these genes are expressed in different seed coat integuments (see below). The reason for the increase in the C18:1 triol fraction is unclear.

Root polyester analysis indicated an overall monomer load reduction of 53% in *cyp86A1-1* and 57% in *cyp86A1-2* compared to WT content. Since analyzed roots were 7-week old, peridermal cells were the main source of

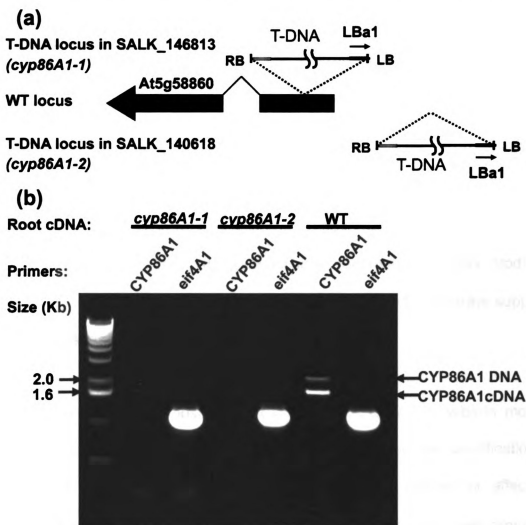


Figure 26. (a) Genomic organization of the *cyp86A1* SALK lines and (b) confirmation of silenced lines by RT-PCR.

(a) Homozygous plants for the T-DNA insertion in *CYP86A1* were isolated for SALK_146813 and SALK_140618 lines and named *cyp86A1-1* and *cyp86A1-2*, respectively. Both lines have a T-DNA insertion in the first exon **(b)** RT-PCR analysis of At5g58860 transcripts (1.8 Kb) isolated from roots of wild type and *cyp86A1* mutants. The *elf4A1* gene was used as load control. RB: T-DNA right border, LB: T-DNA left border; LBa1: T-DNA left border specific primer. The extra band (2.2 Kb) in the WT sample from remnants of genomic DNA .

suberin monomers, with smaller contributions from endodermal suberized cells present in younger lateral roots. Unlike *cyp86A1* seeds, C16:0, C18:0, C18:1, and C18:2 α,ω -bifunctional monomers were reduced by 70-90 % in roots of both *cyp86A1* alleles, plus 20-40% reduction in long-chain monomers (**Figure 27b**). Furthermore, using a gain-of-function approach, Li et al. (2007) have recently shown that ectopic co-overexpression of *CYP86A1* and *GPAT5* in *Arabidopsis* results in increases in a wide chain-length range of dicarboxylate monomers in the depolymerizable fraction of transgenic stems, with more prominent changes in unsaturated fractions (C16:0 and C18:0), a result that agrees with the mutant phenotype. Hence, both loss-of-function and gain-of-function approaches indicated that C16:0 and C18 α,ω -bifunctional monomers are major products of *CYP86A1*. However, such products may vary according to substrate supplies in different tissues and/or expression timing.

These results demonstrate that *CYP86A1* functions in suberin monomer oxidation as suggested by gene correlations. This is the first identification of a cytochrome P450 enzyme involved in suberin. The monomers affected in *cyp86a1* have chain lengths $<C_{20}$, indicating that another P450 likely required for the synthesis of long-chain (C_{22} - C_{24}) α,ω -bifunctional monomers. Such enzyme is unlikely to be a member of the *CYP86A* subfamily. Indeed, a *CYP86B1* homolog is up-regulated in phelloderm. Gene correlations indicate that *Arabidopsis CYP86B1/B2* are co-up-regulated with suberin-synthesizing genes and, therefore, they represent promising candidates for long-chain monomer

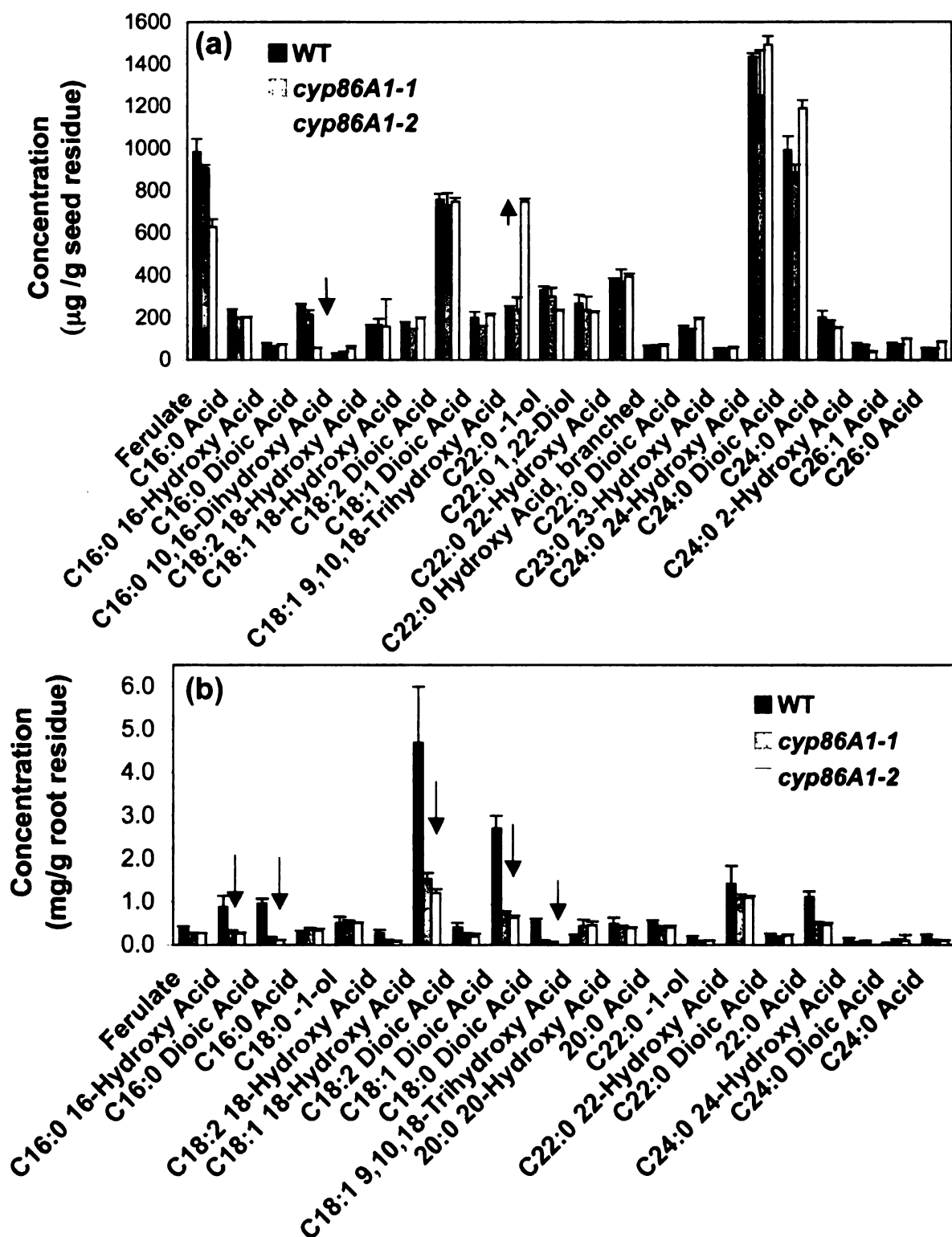


Figure 27. Load and monomer composition of (a) mature seed and (b) 7-week old root polyesters from WT and *cyp86A1* mutants.
Mean and SD for three determinations indicated.

synthesis (**Table 10**, Appendix B). Intriguingly, CYP86B1 is reported to be targeted to the outer envelope of the chloroplast, facing the cytoplasm (Watson et al., 2001). However, the authors, who used in vitro import assays with isolated pea chloroplasts, have not reported control ER-uptake assays to exclude ER localization. If targeted to the plastids, this isoform might: a) be associated to the ER via PLAMs (plastid-associated membranes); or b) oxidize monomers before the elongation step that takes place in the ER-associated FAE complex; or c) not be involved in lipid polyester-related pathways. The functions of CYP86B1 and CYP86B2 in polyester synthesis are currently being investigated in our laboratory.

Examination of stable transgenic Arabidopsis lines expressing *CYP86A1promoter::YFP* fusions revealed an expression pattern reminiscent to that of *GPAT5*, with strong activity in endodermis of young roots (**Figure 28**), peridermal root cells at late stages of secondary growth (**Figure 28b**), and outer seed coat of seeds in the desiccation developmental stage (**Figure 28c-d**). By contrast, *GPAT5* promoter activity in peridermis of old roots was weak (Beisson et al., 2007).

Investigation of cross sections of *cyp86A1* roots, perpendicular to the suberin layers, by TEM confirmed defects in suberin lamellae at the ultrastructural level. Samples were stained according to the procedure described by Heumann (1990) to improve the visualization of suberin (see page 172 for a

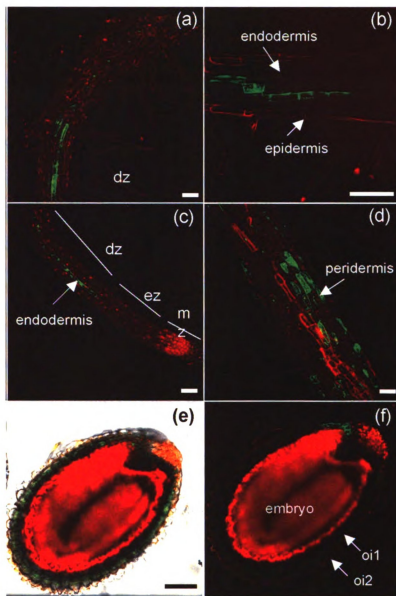


Figure 28. Analysis of eYFP expression in Arabidopsis plants transformed with *ProCYP86A1::eYFP*.

Confocal laser scanning microscopy of stable transgenic plants reveals YFP expression in: (a-c) endodermis of young roots, limited to the specialization zone, but not to the elongation zones or meristem (c); (d) peridermis of 5-week-old roots; (e-f) outer integument (oi1) of seed coats at the beginning of the dissection stage. Seeds and roots were stained with propidium iodide to visualize cell walls. Figure (e) is an overlaid optical section of fluorescence and light images. Scale bar= 50 μm (a, c, d), =100 μm (b, e, f). ez: elongation zone; dz: differentiation zone; mz: meristematic zone; e: embryo; oi: outer integument.

comparison with the conventional staining method). Peridermal cells of 7-week roots from wild-type plants show the typical lamellar structure of suberin depositions on their primary cell walls (**Figure 29a**), but *cyp86A1* presents a more diffuse ultrastructure (**Figure 29b**), with clear reduction of electron opaque bands. According with the model for the macromolecular structure of suberin proposed by (Graça and Santos, 2007), the electron-translucent layers correspond to aliphatic monomers, arranged perpendicularly to the lamellae plane and linked by glycerol. It has been suggested that the thickness of this layer correspond to the length of the alkyl chain (Schmutz et al., 1996). The dark bands seen in TEM images of suberin are postulated to correspond to aromatic-rich domains. In this context, it is difficult to explain the reduction in the electron-dense layers of *cyp86A1* roots since the reductions in aliphatic monomers observed in this mutant are expected to impact the electron-translucent layers. In addition to postulating that dark layers are hydroxycinnamic acid rich, their occurrence could be caused by other polymers (carbohydrates, proteins) or by phase separation within the aliphatic domain. For example, the long-chain saturated aliphatics could associate as a gel phase, phase separating from the unsaturated species, including any esterified aromatics. These more fluid species, possibly including the glycerol backbone, could likely form the electron-rich dark layers. In this scenario, the strong reduction in unsaturated α,ω -bifunctional fatty acids observed in *cyp86A1* roots (**Figure 27b**), may result in a reduction of the osmophilic layers (**Figure 29b**). Therefore, the *cyp86A1*

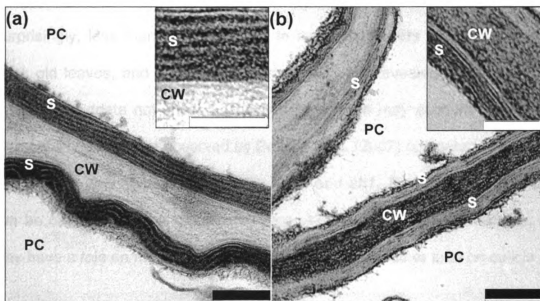


Figure 29. Transmission electron microscopy of suberized peridermal cells in 7-week old roots.

Thin samples cut perpendicularly to the suberin lamellae in wild type (a) and *cyp86A1* (b) root peridermal cells. Samples were stained according to a procedure to enhance contrast of lipids described in Experimental procedures. S: suberin lamellae; CW: cell wall; PC: peridermal cell.

phenotype indicates that the current macromolecular model for suberin needs revision.

CYP86A8 (*LACERATA*). A knockout mutant of the *LACERATA* gene (At2g45970) provided initial evidence that *CYP86A8* is required for cuticle synthesis (Wellesen et al., 2001). Although the phenotypic analysis indicated that *lcr* mutants displayed an organ fusion phenotype, no cutin chemical analyses were reported. Therefore, its exact function is unclear. I have selected another allele for the *lcr* mutation (*lcr-2*), which displayed an organ fusion phenotype (only detected in inflorescences) similar to that described by (Wellesen et al., 2001).

Cutin analyses were carried out in 6-week old *lcr-2* and WT leaves (**Figure 30**). Surprisingly, less than 10% reduction in major monomers was observed in 6-week old leaves, and no monomer reductions were revealed in the younger 4-week old leaves (data not shown). The small reduction may account for the weak permeability phenotype observed by Bessire et al. (2007) compared to the strong permeability phenotypes displayed by *lacs2* and *att1*. The weak leaf phenotype can be caused by gene redundancy (e.g. *ATT1*, *CYP86A4*). Alternatively, *LCR* may have a role on more complex signaling processes rather than on cuticle

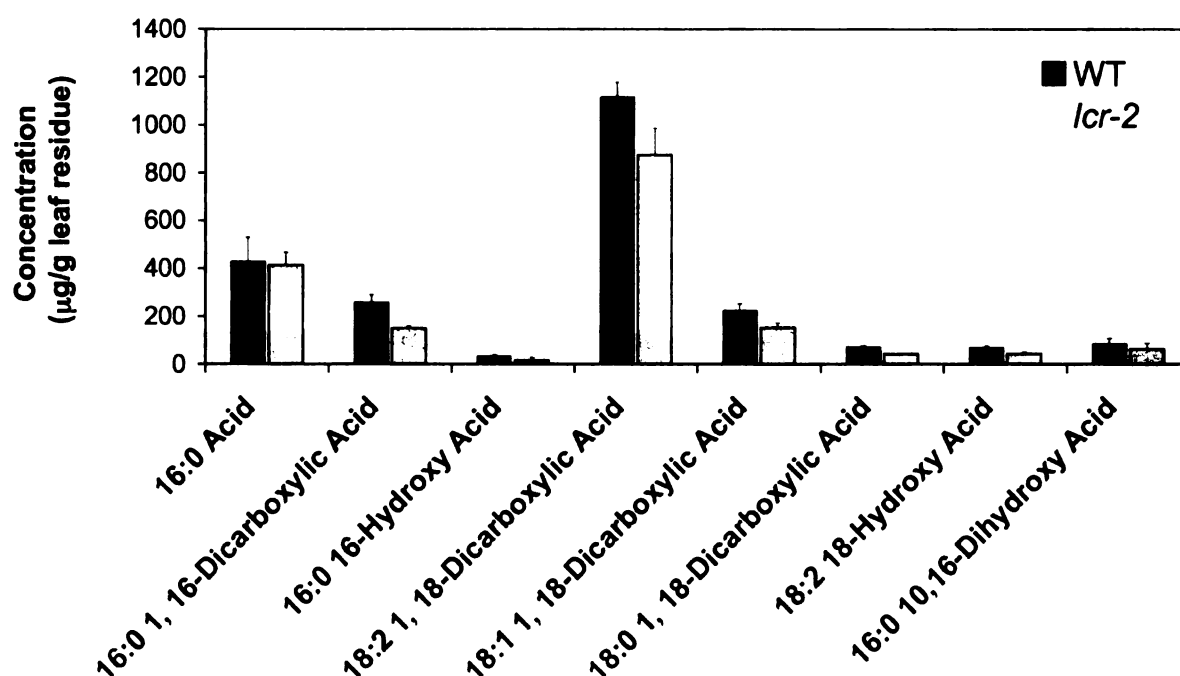


Figure 30. Load and composition of aliphatics realeased by transmethylation of 6-week *lcr-2* mutants and Col0 wild-type leaf residue. Mean of three determinations and SD are indicated.

structure. In fact, organ fusions are observed in *lcr* but not in *att1* (Chapter 5) or *lacs2* (see below), which show stronger cutin reductions. Given its poor co-response with suberin-synthesizing genes, seed and root polyesters were not investigated in this work, but may be analyzed in the future to rule out effects in these organs. In addition, flower cutin need to be determined.

Interestingly, the *hothead* mutant (Kurdyukov et al., 2006b) displayed a phenotype reminiscent to *lcr*. *HOTHEAD* (At1g72970) is proposed to encode an ω -alcohol dehydrogenase that acts downstream LCR in the synthesis of dicarboxylates. In addition to these observations, both *LCR* and *HTH* present high correlation ($r^2=0.513$), suggesting that these genes may encode proteins that are associated with the synthesis of cuticular lipid polyesters. But the biochemical evidence for HTH function remains controversial, and the ω -aldehyde dehydrogenase required to produce the dicarboxylic acid has not been identified thus far. This proposed biosynthetic pathway is discussed in detail in Chapter 5.

CYP86A4. CYP86A4 and CYP86A7 are almost exclusively expressed in flowers, and are highly correlated with each other and with CYP86A8 discussed above. Low levels of *CYP86A4* transcripts are also detected in stems (Schmid et al., 2005). Analysis of a knockout for the At1g01600 gene (encoding CYP86A4) has shown that all C16 monomers, including 10,16-dihydroxy acid, are reduced by 50% in flowers (F. Beisson, unpublished). The mutant is also affected in stem

cutin monomer loads, where it has redundant functions with ATT1 as shown by analysis of double mutants generated in this study (**Figure 31**). Stems of *att1-2/cyp86A4* knockouts show 70% reduction of total monomer loads, whereas single mutants display about 30% decrease. Deepest changes in the double mutant are observed in 10,16-dihydroxy C16:0 acid, and C16/C18:2 dicarboxylates. These observations suggest that CYP86A4 possess a broad specificity of substrates, including saturated C16/C18 and unsaturated C18 monomers. From these data, however, it cannot be inferred that this enzyme functions only as a ω -hydroxylase, or whether it is able to further oxidize the terminal hydroxyl group to carboxylic acid.

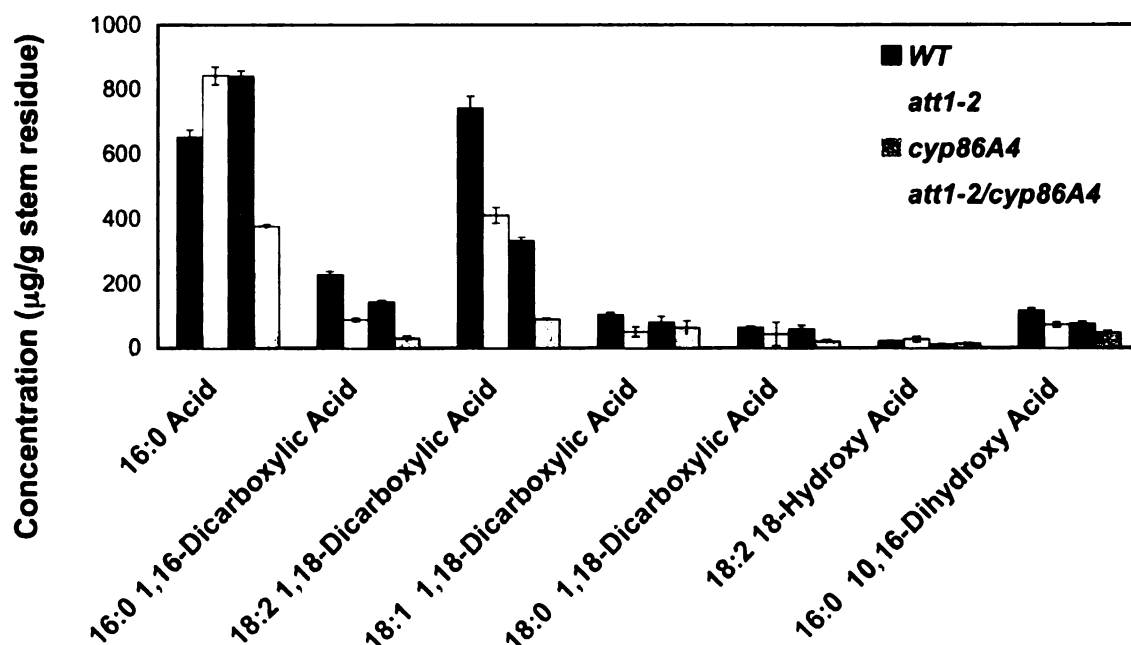


Figure 31. Load and composition of aliphatics realeased by transmethylation of *att1-2* and *cyp86A4* single mutants, *att1-2/cyp86A4* double mutant, and Col0 wild-type stem residues. Mean of three determinations and SD are indicated.

Acyl-CoA-utilizing acyltransferases

Acyltransferases catalyze the acyl transfer from activated acyl-donors to hydroxyl or amine groups on acceptor molecules, to form esters and amides, respectively (St Pierre and De Luca, 2000; D'Auria, 2006). In plants, a subset of these enzymes uses relatively hydrophilic acyl-CoA-activated donors to catalyze acetyl-, malonyl-, benzoyl-, and hydroxycinnamoyl- transfer reactions in the synthesis of secondary metabolites. Identified members of this family are soluble and lack targeting signals, suggesting that these proteins are localized to the cytosol (D'Auria, 2006). Based on the first genes characterized in plants (BEAT, AHCT, HCBT1, DAT), this superfamily is usually called BAHD (St Pierre and De Luca, 2000).

In Arabidopsis, the BAHD superfamily consist of at least 64 genes including pseudogenes (D'Auria and Gershenzon, 2005), most of which have been retrieved from databases by similarity searches. By aligning proteins from different species and performing phylogenetic analysis, D'Auria (2006) classified this family in five clades (I-V), which encode enzymes involved in manolylolation of phenolic glucosides (clade I), in the wax elongation pathway (although it is not clear what is their biochemical function of these enzymes) (clade II), synthesis of volatile esters (clades III, V), acetylation of nitrogen to form amides, and transfer of hydroxy-cinnamoyl- or benzoyl-CoAs (clade V). Only a few Arabidopsis proteins have been included in this analysis, and in an earlier report (St Pierre

and De Luca, 2000). Hence, I have generated a phylogenetic tree including all *Arabidopsis* proteins annotated as members of this family (**Figure 32**).

Because hydroxycinnamoyl esters of ω -hydroxy acids and glycerol have been found in suberin waxes and in fragments released by partial hydrolysis of suberin (Schmutz et al., 1993; Graça and Pereira, 2000; Santos and Graca, 2006), I have looked for putative BAHD hydroxycinnamoyl-CoA acyltransferases in *Arabidopsis*, which may be crucial for suberin synthesis and for anchoring lipid polyesters to the cell wall. Those enzymes belong to clade V according to D'Auria's classification; however, the phylogenetic analysis shown in **Figure 32** suggests higher complexity in terms of groups, which have been designed A-J. For instance, HCT (hydroxycinnamoyl-CoA:shikimate/quinate hydroxycinnamoyl-transferase), one of the handful of *Arabidopsis* proteins of the family that has been biochemically characterized and is known to be involved in synthesis lignin intermediates (Hoffmann et al., 2004, 2005), and CHAT ((Z)-3-hexen-1-ol O-acetyltransferase), fall in a different groups (F and A, respectively). In the reported analysis, both enzymes belong to different subgroups into clade V. It is unclear, however, if these clades represent enzymes with different substrate or acceptor specificity. Initially, I hypothesized that if any of these enzymes catalyzes the formation of hydroxycinnamate esters that anchor polyesters to the cell wall via the aromatic moiety, the corresponding mutants may show absence or reduction of insoluble polyesters and consequent increase of soluble aliphatic polyesters.

Figure 32. Phylogenetic analysis of the Arabidopsis BAHD family.

Protein sequences were aligned using Clustal W. The figure shows the majority-rule consensus tree of 10772 best score trees, generated according to the maximum parsimony principle with PAUP Version 4.0b10. A heuristic bootstrap search was performed with 1000 replicates. Numbers on branches indicate bootstrap values as percentages. Numbers between parentheses correspond to the clades (I-V) described by D'Auria (2006). AACT1: Anthocyanin 5-aromatic acyltransferase1; AT5MAT: O-malonyltransferase; CHAT: AcetylCoA:(Z)-3-hexen-1-ol acetyltransferase); HCT: hydroxycinnamoyl-CoA:shikimate/quinic acid hydroxycinnamoyltransferase; *Cer2*: *Eciferum2*.

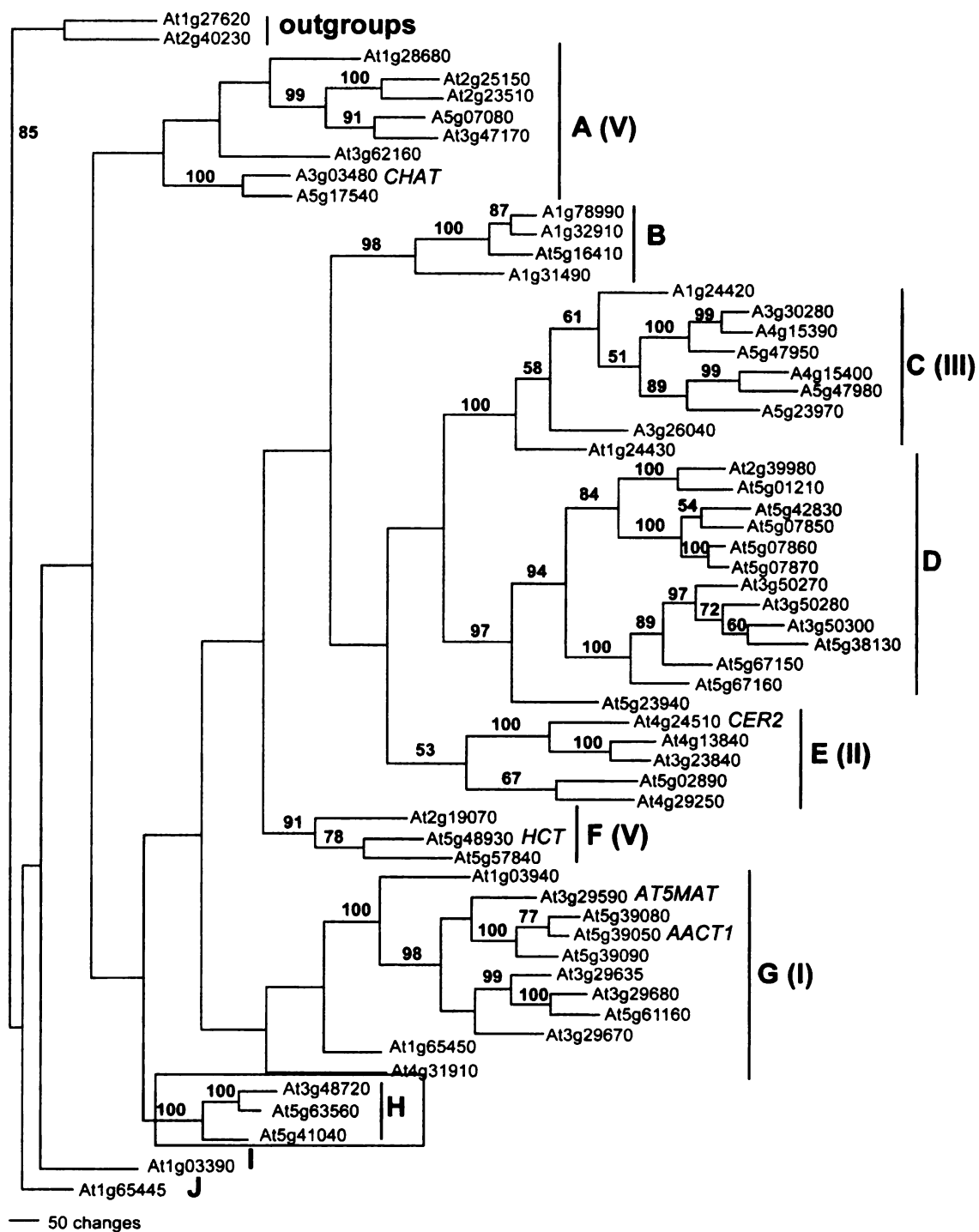


Figure 32.

Pairwise transcript co-expression comparisons were generated with putative hydroxycinnamoyl-CoA acyltransferases. Gene correlations were also performed with selected members of the other groups, such as CER2, which is related to long-chain wax monomer synthesis but its function is unknown (Negruk et al., 1996; Xia et al., 1996). Significant correlations with *GPAT5-CYP86A1* were found in two genes expressed in seeds, corresponding to group H in the Arabidopsis tree, At5g41040 and At5g63560, and therefore they are candidates for suberin synthesis (**Table 6** and **Table 10, Appendix B**). Moreover, transcripts of a gene homologous to At5g41040, have been found to be highly enriched in the phellem transcriptome (Soler et al., 2007). The third member of group H, At3g48720, is expressed in leaves and represented in epidermal microarrays (Suh et al., 2005). At3g48720 shows co-response with *CYP86A2/GPAT8*, indicating possible relation to cutin. Homozygous mutant lines were selected for T-DNA insertion lines of At5g41040 and surface lipids were investigated in these knockouts.

Characterization of at5g41040 knockouts

Two mutant alleles were selected by PCR screening of genomic DNA from segregating populations. These are designed *at5g410401-1* (SALK_048898), and *at5g410401-2* (SALK_017725). Since this gene is expressed in roots and seeds (Schmid et al., 2005), but its expression is negligible in other organs,

mRNA from *at5g41040-1* and wild-type roots was isolated and subjected to RT-PCR. No transcripts of this gene were present in the mutant roots, confirming the homozygosity of this allele (Figure 33).

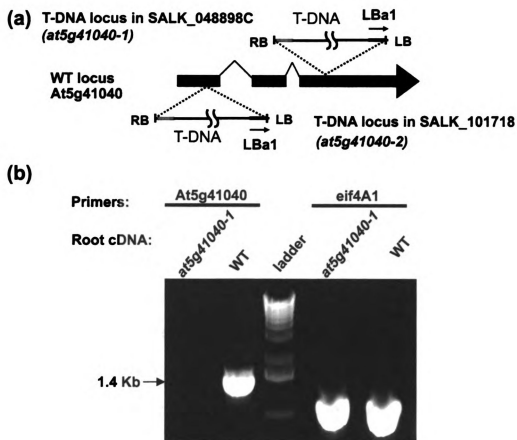


Figure 33. (a) Genomic organization of the *at5g41040* SALK lines and (b) RT-PCR analysis of *At5g41040* transcripts isolated from roots of wild type and *at5g41040-1* mutants.

(a) Homozygous plants for the T-DNA insertion in *At5g41040* were isolated from SALK_101718 heterozygous seeds or obtained from the homozygous collection of ABRC (SALK_048898C). T-DNA insertions are in the first (*at5g41040-2*) and third (*at5g41040-1*) exon (b) The *eIF4A1* gene was used as load control. RB: T-DNA right border, LB: T-DNA left border; LBa1: T-DNA left border specific primer.

Seed polyesters. Monomers released by transesterification (**Figure 34a-b**) revealed an almost complete loss in ferulate in seeds in both alleles (1.55 mmol/g seeds). In addition, the loss in ferulate is correlated with loss in hydroxy-containing monomers (1.34 mmol/g seeds in *at5g41040-1* and 2.25 mmol/g seeds in *at5g41040-2*). This observation suggests that there may be an approximately stoichiometric linkage between these two components; however, the ratio ferulate:OH-monomer is different in the mutants (1:1 and 2:3). These results indicate that At5g41040 encodes an enzyme that a) catalyzes an acyl transfer reaction from feruloyl-CoA to aliphatic hydroxyl groups or b) may act in synthesis of coumaryl-shikimate, an intermediate in the synthesis ferulate (similar to HCT mentioned above). In addition, a compensatory 50 % increase in α,ω -dicarboxylic acid fractions was observed in *at5g41040-1*. An interesting parallel exists with an experiment using inhibitors of synthesis of phenylpropanoids in green cotton fibers (Schmutz et al., 1993), where reduction of hydroxycinnamic acids in suberin was accompanied by decrease of ω -hydroxyalkanoic acids and increase of α,ω -dicarboxylic acids. The total polyester aliphatic content in the *at5g41040-1* allele was the same as wild type (8.89 mmol/g seeds), and reduced only by 10% in *at5g41040-2* (**Figure 34b**). Hence, the loss of ferulate does not impact the insolubility of the suberin polyester, and this raises questions concerning the role of ferulic acid in attaching aliphatics to the cell wall.

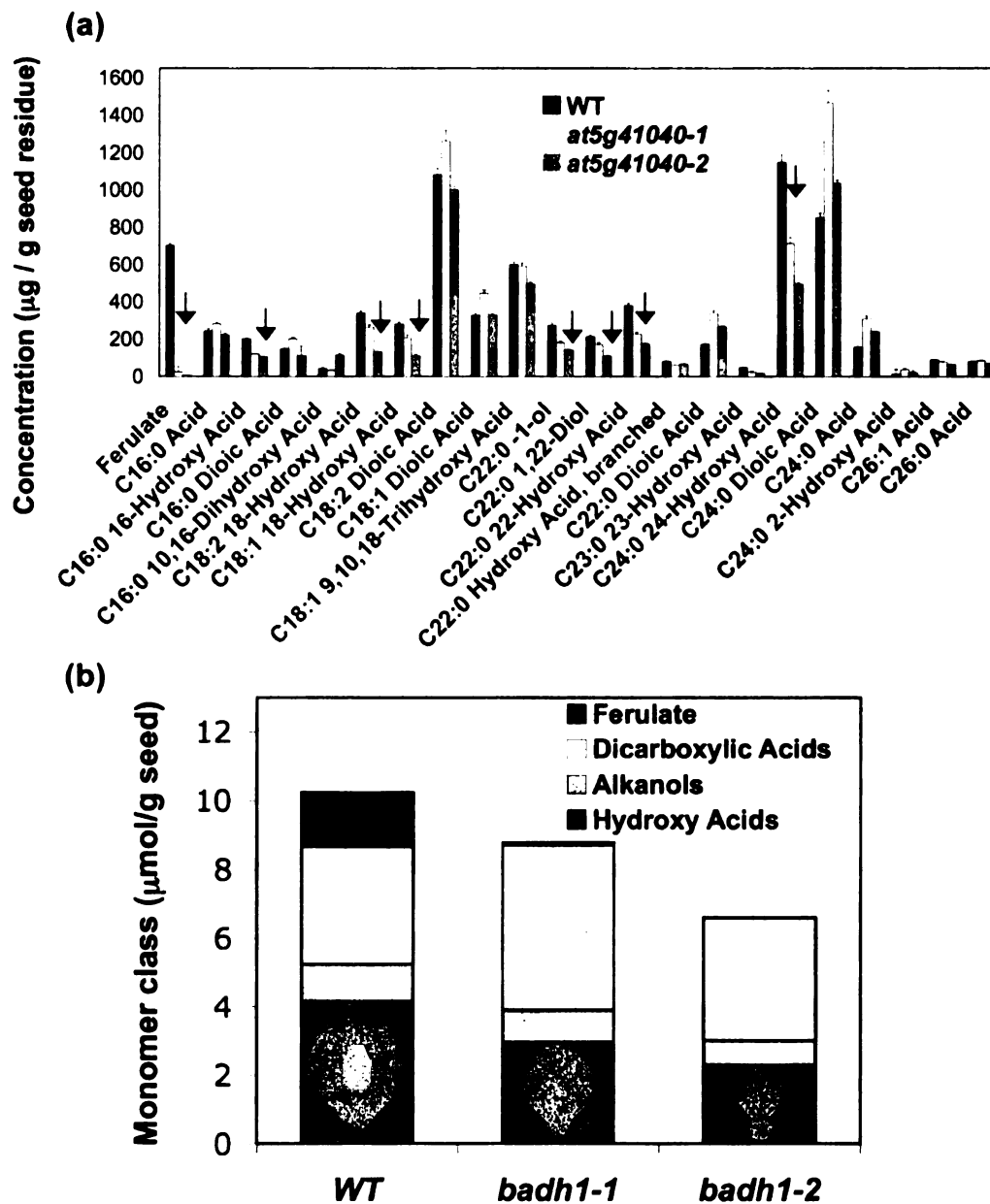


Figure 34. Comparison of seed lipid polyester monomer composition between wild-type and *at5g41040* knockouts.

(a) Detailed monomer load and composition from seeds of *at5g41040* mutants compared to wild-type. Means of triplicate determinations and SD are indicated.

(b) Total monomer loads. Monomers are grouped in four classes.

Although the monomer profile confirms that suberin is affected in *at5g41040* seeds, it is important to bear in mind that the insoluble residue remaining after delipidation is highly complex. Consequently, the ferulate released by transmethylation may represent only a small portion of the total ferulate-derived material. Ferulate may occur in the poly-aromatic domain highly cross-linked, as the anchor molecule of the aliphatic chains attaching them to the cell wall, and also as part of suberin-associated waxes. One possibility that cannot be ruled out is that the ferulate released may be part of trapped waxes, which are not removed in the delipidation steps. Moreover, ferulic acid has been found bridging polysaccharides to lignin (polysaccharide-ester-ferulic acid-ether-lignin) in wheat cell walls (Iiyama et al., 1990; Lam et al., 1992). In this latter scenario, a fraction of the ferulate esterified to cellulose that is not ether-linked to lignin may be released by transmethylation. To understand the nature of the ferulate-esters found in *Arabidopsis* suberin, a series of chemical analyses including investigation of oligomers released by partial depolymerization and determination of cross-linked aromatics are proposed for future research in Chapter 6.

Seed soluble polyester-related lipids. To investigate the soluble lipid fractions in seeds and potential changes in the mutants, I used soluble lipids from the preparation of the delipidated residue. Because seeds have 130-fold more storage lipids than polyesters, if not removed, triacylglycerols would mask the less abundant polyester-related monomers. Therefore, soluble fractions were

pooled, concentrated, transmethyated, and separated by TLC using a non-polar solvent system. Because in these conditions, the R_f of fatty acid methyl esters and alkanes is higher than the R_f s of more polar compounds (i.e. functionalized polyester aliphatic monomers and aromatics), all fractions below the fatty acid methyl ester band were eluted from the silica matrix, derivatized and analyzed by GC (**Figure 35a-b**). By this means, non-polar wax compounds characteristically found in the seed surface were not recovered. Total soluble aliphatic monomer loads were about 10 % of the insoluble fraction, with 0.87 mmol/g WT seeds, 0.77 mmol/g *at5g41040-1* seeds and 0.83 mmol/g *at5g41040-2* seeds. However, when considering loads of different monomer classes (**Figure 35b**), it becomes clear that reductions in ferulate (0.1 mmol/g seeds) in the mutants, correlates with a stoichiometric loss of 1-alkanols (0.11 mmol/g seeds), and a 2.5 fold increase in C22-C24 dicarboxylic acids. This suggests that ferulate was reduced in the wax fraction where it is presumably esterified to primary alcohols. The reason for the increase in dicarboxylates in the soluble fraction, also observed in the polyesters, is unknown. Because the monomers in the soluble fraction (**Figure 35a**) vary in different proportion compared to those in the polyester (**Figure 34a**), it is unlikely that the major contribution to the “soluble” fraction is “particulate” material in suspension. To exclude that possibility, an experiment is underway where the separation step comes first and all fractions except triacylglycerols are recovered from the silica. By this means, if any particulate material is present, it should be retained at the origin.

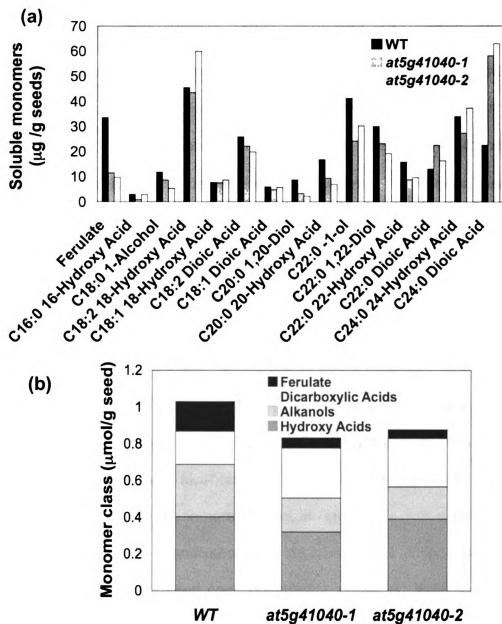


Figure 35. Seed soluble lipid polyester monomers.

(a) Soluble lipid monomers released by transmethylation of total solvent-extracted lipids. Triacylglycerols were removed before GC analysis. (b) Total soluble loads, grouped in four monomer classes.

Seed permeability to tetrazolium salts. Consistent with their polyester phenotype, *at5g41040-2* seeds showed increased permeability to tetrazolium salts compared to wild-type seeds. However, this trait was only visible when seeds were incubated with dye for three days (**Figure 36 a-d**), whereas in other mutants altered in suberin monomer loads (Beisson et al., 2007; Molina et al., 2008) the permeability phenotype becomes evident after shorter incubation times. Embryos were evenly stained, indicating that the seed coat permeability is uniformly affected all over the seed. This is comparable to the permeability pattern displayed by *fatB* seeds, and suggests that even a 12 % reduction in total suberin hydroxy-acids and alkanols affects the passage of the dye. The permeability phenotype was less perceptible in seeds of *at5g41040-1* incubated for the same time length (data not shown). Since ferulate is equally reduced in both alleles, but only *at5g41040-1* shows a dicarboxylate compensation for the missing hydroxy-acids and alcohols, this observation suggests that it is the reduction in the aliphatic monomers but not in ferulate itself that renders more permeable seeds. These analyses also imply that the *At5g41040* gene is expressed over the entire seed coat, presumably in the oi1 layer as shown for *GPAT5* (Chapter 3, **Figure 22**) and *CYP86A1* (**Figure 28e-f**) expression. This assumption needs to be confirmed, and transgenic lines have been generated to study *At5g41040*-promoter activity using YFP and GUS reporters.

Root polyesters and waxes. Investigation of lipid polyesters in 6-week old roots (**Figure 37a**) indicated that ferulate is also reduced in root suberin

monomers released by transesterification. However, ferulate represents only 3 % (w/w) of total root lipid polyester load and the aliphatic monomers, specifically the hydroxy-containing ones, do not seem to vary as observed in seeds. Nevertheless, minor changes in monomer loads may be masked because of the high variation usually observed in root polyester analysis caused by root anatomical complexity and mixed developmental stages.

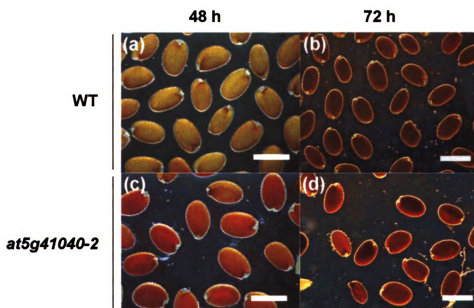


Figure 36. Seed coat permeability to tetrazolium salts.

Seeds of WT (a, b) and *at5g41040-2* (c,d) incubated with tetrazolium salts for 48 h (a, c) and 72 h (b, d). Scale bars= 0.5 mm.

Endogenous root waxes contain alkyl hydroxycinnamate esters, predominantly coumarate and caffeate, with ferulate in minor proportion (Li et al., 2007b). Waxes extracted from roots by quick chloroform dipping (Figure 37b) showed that there is a two-fold increase in the total wax

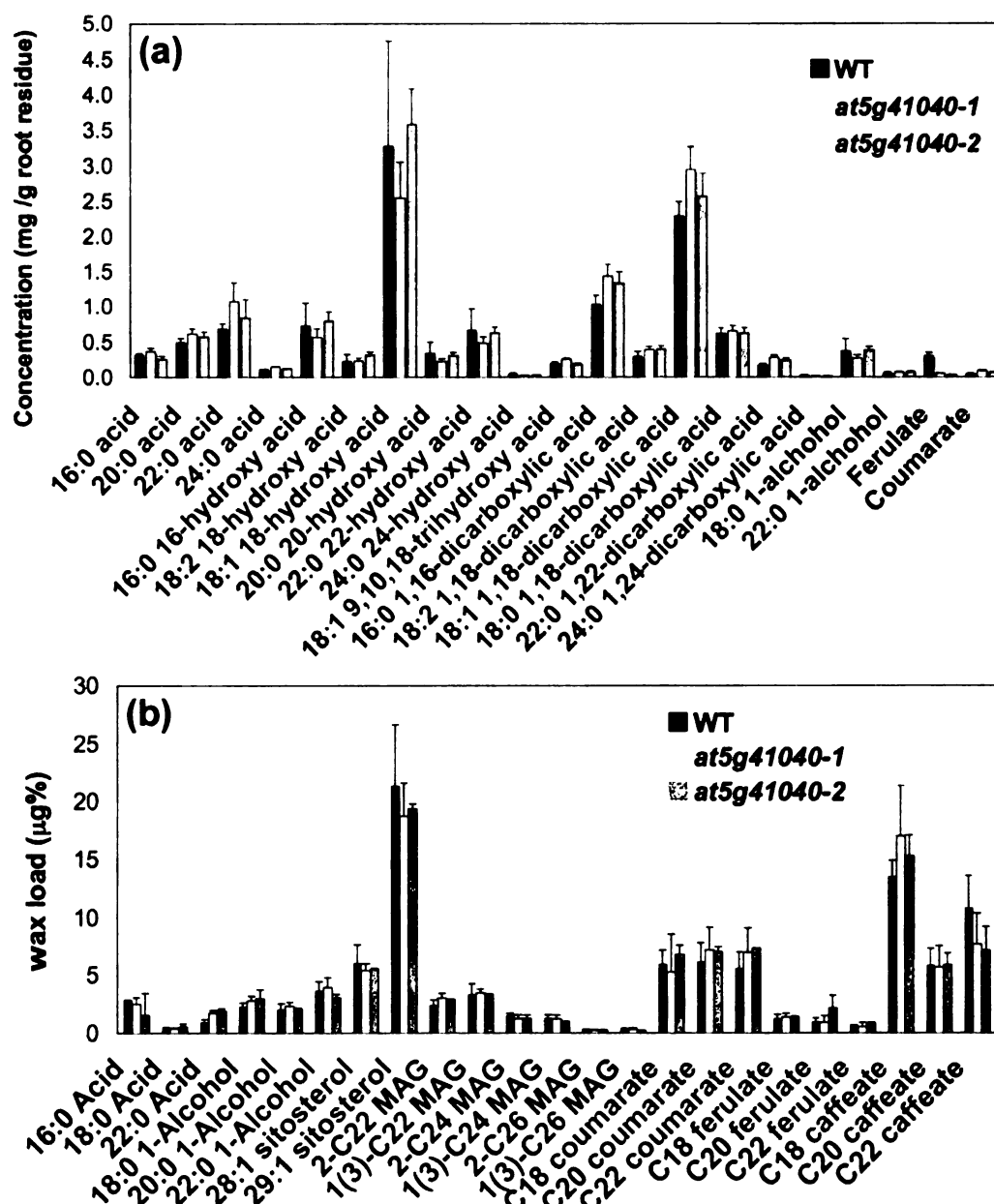


Figure 37. Root polyester and wax phenotypes.

(a) Load and monomer composition of 6-week old root polyesters in wild-type (WT) and *at5g41040* mutants. (b) Composition and content of chloroform-extracted root waxes, expressed as $\mu\text{g} \%$ respect to total monomer load for each line. Means of triplicate determinations and SD are indicated.

load of *at5g41040-2* (460 mg/gfw) compared to wild-type roots (220 mg/gfw). It is unclear if such difference is because of biomass variances. The relative amount of individual wax compounds in the mutants was indistinguishable from wild-type (**Figure 37c**). These results indicated that the synthesis of alkyl ferulates of 1-alkanols is not affected in root suberin waxes. By comparison, the suberin-specific transferase GPAT5 has been shown to participate in the deposition of both suberin waxes and polyester, indicating possible metabolic association between extractable and insoluble components of suberin (Li et al., 2007b). The *gp5* mutant showed reduction of aliphatic suberin monomers and of monoacylglycerol (MAGs) in waxes. But in *at5g41040* roots, feruloyl-esters are not reduced in the waxes, suggesting that alkyl-ferulates are not precursors of the insoluble ferulate that is released by transmethylation. In addition, the presence of ferulate and caffeate esters of 1-alkanols indicates that the At5g41040 gene product is unlikely to function in the synthesis of caffeoyl-CoA and its downstream product feruloyl-CoA (similar to HCT, encoded by At5g48930). However, this evidence is not enough to rule out such function, because redundant enzymes can be present in roots.

Taken together, the root phenotypes imply that: a) the At5g41040 gene product is involved in the deposition of ferulate that is released by transmethylation; b) the enzyme is not responsible for the synthesis of alkyl-hydroxycinnamates present in waxes, either because it is not expressed in the tissues where waxes are synthesized, or because it does not have the correct

specificity, or because a redundant gene (At5g63560?) can completely compensate; b) At5g41040 is not a ferulate biosynthetic gene, unless a redundant enzyme compensates its function in roots. To test these possibilities, the biochemical function of the At5g41040-encoded protein need to be studied (see Chapter 6).

Ultrastructural analysis of root peridermal cells. I next explored the ultrastructure of the *at5g41040* mutant and wild-type roots. Roots were chosen instead of seeds because Arabidopsis seeds are too small, and have highly compacted seed coats, making problematic all sample preparation steps for TEM analysis as well as subsequent observation of the specimen. Arabidopsis root suberin (Franke et al., 2005) presents the characteristic lamellar distribution described in other species, such as green cotton fibers (Yatsu et al., 1983), potato (Bernards, 2002), and cork (Graça and Santos, 2007). Based on its appearance and chemical composition, models have been depicted for this polymer (described in Chapter 1, and also discussed in page 148). Considering these models, and the biochemical phenotype of *at5g41040* roots, I hypothesized that the reduction in ferulate may be reflected in changes in the electron-opaque bands. **Figure 38** shows the results obtained for thin sections from 6-week old roots. Samples for TEM were stained using a standard protocol (**Figure 38a-b**) and also a modified technique to enhance the contrast of lipid features (**Figure 38c-d**) (Heumann, 1990). No changes were observed in the fine structure of suberin deposited in peridermal cells of the mutant (**Figure 38b,d**), compared to

wild-type (**Figure 38a,c**). This observation implies that the ferulate released by transmethylation does not contribute to the ultrastructure of root peridermal suberin. Because ferulate may be released from endodermal cells of younger roots, these also need to be analyzed by TEM.

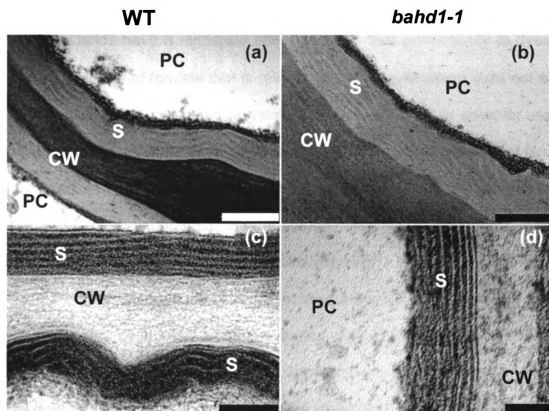


Figure 38. Transmission electron micrographs of *Arabidopsis* roots in the later stages of secondary thickening.

The fine structure of suberin in the mutant alleles is similar to the wild-type. Note the higher contrast observed in the lamellar structure shown in figures (c) and (d) compared to (a) and (b). Samples (c) and (d) were treated with hydrogen peroxide before the staining procedure (Heumann, 1990). Scale bar =200 nm (a,b), =100 nm (c), =50 nm (d). CW: cell wall; PC: peridermal cell; S: suberin

In summary, the initial characterization of *at5g41040* mutants reported here, indicates that: i) disruption of *At5g41040* results in reduction of ferulate released by transmethylation of suberin polyester and/or suberin waxes in seed coat residues; ii) ferulate might be ester-linked to 1-alkanols and ω -hydroxy acids in seed coats; iii) the complete loss of ferulate, and reductions in 1-alkanols and ω -hydroxy acids have a moderate effect on seed coat permeability to dyes; iv) the complete loss of ferulate that is released by transmethylation does not affect the insolubility of the polyester (suggesting that ferulate plus its acceptor are not crucial for the attachment of the aliphatics to the cell wall); v) the loss of ferulate in roots does not affect the ultrastructure of suberized peridermal cells (but might have an effect on endodermal cells of younger roots). The *at5g41040* knockout constitutes the first example of an Arabidopsis mutant affected in the deposition of an aromatic component of suberin. As discussed in Chapter 6, further experiments will be focused on understanding the function of the protein encoded by *At5g41040* using a gain of function approach and yeast expression assays. This is of particular interest since no genes capable of catalyzing the transfer of feruloyl-CoA have previously been identified.

Long chain acyl-CoA synthetases (LACS)

LACS enzymes catalyze the activation of free fatty acids to acyl-CoAs. Of nine isoforms of *LACS* that are found in the Arabidopsis genome (Shockey et al., 2002), *LACS1*, *LACS2*, and *LACS3* are specifically up-regulated in stem

epidermis (Suh et al., 2005). *LACS2* is expressed in fast growing tissues including seeds, and has been proposed to catalyze the synthesis of ω -hydroxy fatty acyl-CoA in the cutin biosynthetic pathway (Schnurr et al., 2004) (**Figure 23**). Recent investigations of several *lacs2* alleles have confirmed its role in leaf cutin metabolism (Bessire et al., 2007). Because this gene seems to act downstream of the chloroplast-export site (Schnurr et al., 2004), it may be involved in the activation of P450-fatty substrates and/or P450-fatty acid products (**Figure 23**).

Leaf lipid polyesters in lacs single, double and triple mutants. Lipid polyester analyses of *lacs* mutants were conducted to evaluate the impact of these mutations on cutin and suberin composition, as part of a joint effort with John Browse's group. Leaf total lipid polyester monomer loads were reduced by 30% in *lacs2-1*, in agreement with (Bessire et al., 2007) (**Figure 39a**), and consistent with its increased permeability to toluidine blue (data not shown). Specifically, all dicarboxylate fractions were reduced by 50%. Only 10-20% reductions of 18:2 DCA were observed in *lacs1* or *lacs3*, and this reduction did not affect the cuticle permeability to toluidine blue dye. In addition, *lacs3-1* presented a 5-fold increase in 10,16-dihydroxyplamitic acid. A common finding in all *lacs* was that ω -hydroxy fatty acids were largely unaffected, or even increased, in leaf cutin.

Further investigation of double and triple mutants suggested partially redundant functions for *LACS2*, *LACS1* and *LACS3* in cutin synthesis (**Figure 39b**). Both double (*lacs2-1/lacs1-2*) and triple (*lacs2-1/lacs1-2/lacs3-1*) knockouts presented stronger cutin phenotypes than the parental lines, with 70% and 83% total monomer load reductions, respectively. Strikingly, even multiple mutants reflected changes in dicarboxylic acids but not in ω -hydroxy acids, with only a minor reduction in C18:2 ω -hydroxy acid in the triple knockout. Homozygous plants of multiple mutants were dwarf and sterile, but it is unclear whether this pleiotropic phenotype is produced exclusively by defects in *LACS* genes, or because the genetic background of the *lacs2-1* is Col-0 *glabrous-1*. Indeed, two different groups have recently reported the isolation of additional *lacs2* alleles in Col-0 wild-type background (Bessire et al., 2007; Tang et al., 2007). Unlike the *lacs2-1* allele reported by Schnurr et al. (2004), which displays a dwarf phenotype in certain growth conditions, these plants show normal size. Regardless of size differences, the cutin composition reported by Bessire et al. (2007) confirmed a defective cuticle in *lacs2-2* and *lacs2-3* alleles.

Seed lipid polyesters in *lacs* single mutants. Seed chemical analyses were performed on single knockouts (**Figure 40**), which showed a lipid polyester phenotype consistent with the one in leaves. In *lacs2-1* seeds, C16 /C18 α,ω -dicarboxylates were reduced by 60%, with less pronounced effects on C24 ω -hydroxy acid (35%), C22 1-alkanol (40%) and C22 α,ω -diol (20%). Conversely, *lacs1-2* and *lacs3-1* mutants did not display monomer reductions in seeds.

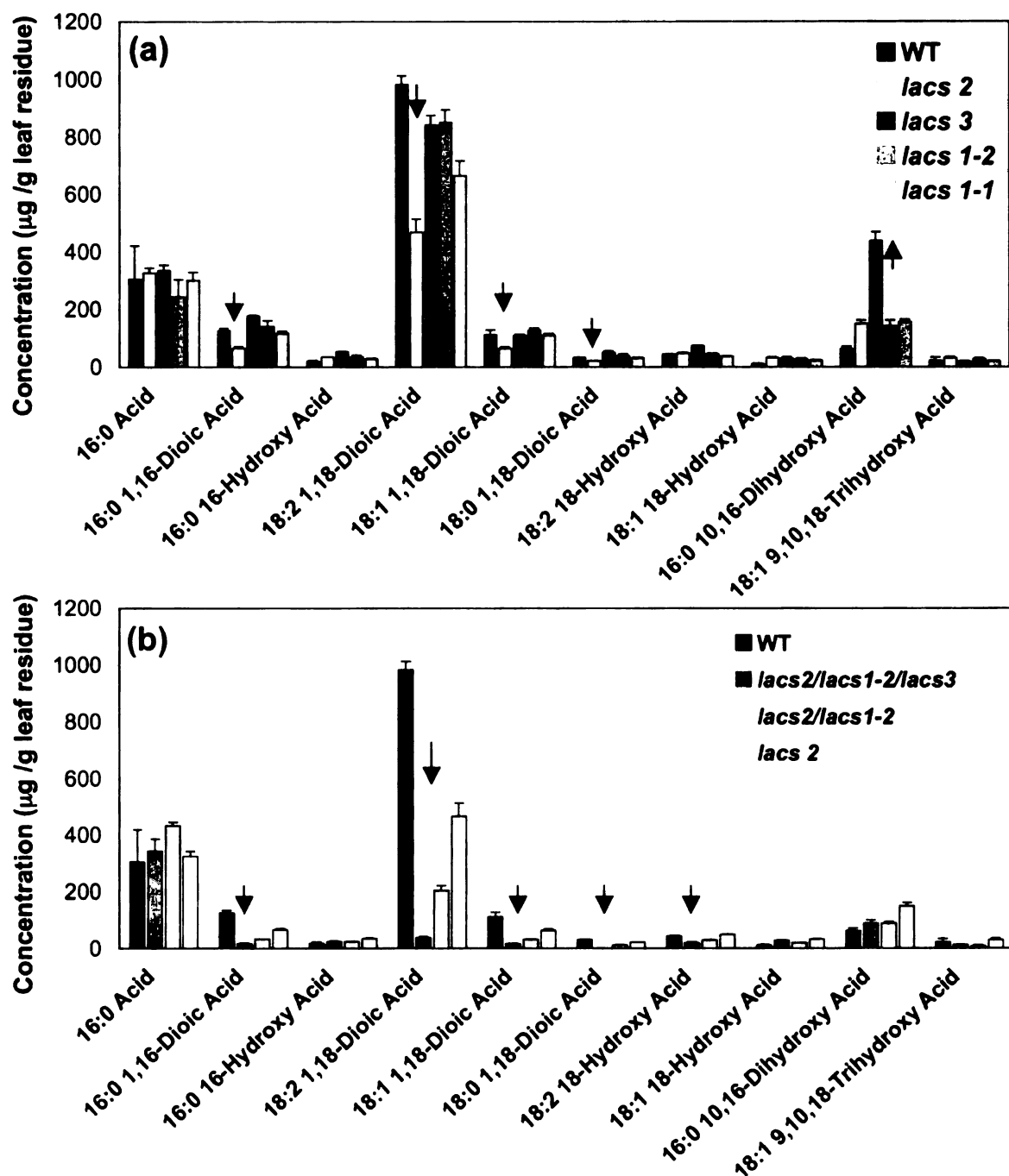


Figure 39. Lipid polyester monomer load and composition in leaves of *lacs* single (a) and multiple (b) mutants.

GC analysis of acetylated monomers released by NaOMe-catalyzed transmethylation (mean with SD, n=3). Homozygous plants of double (*lacs2/lacs1-2*) or triple (*lacs2/lacs1-2/lacs3*) mutants were selected from a *lacs2* segregating population homozygous for *lacs1-2* or *lacs1-2/lacs3* on the basis of their small size and permeability to TBO.

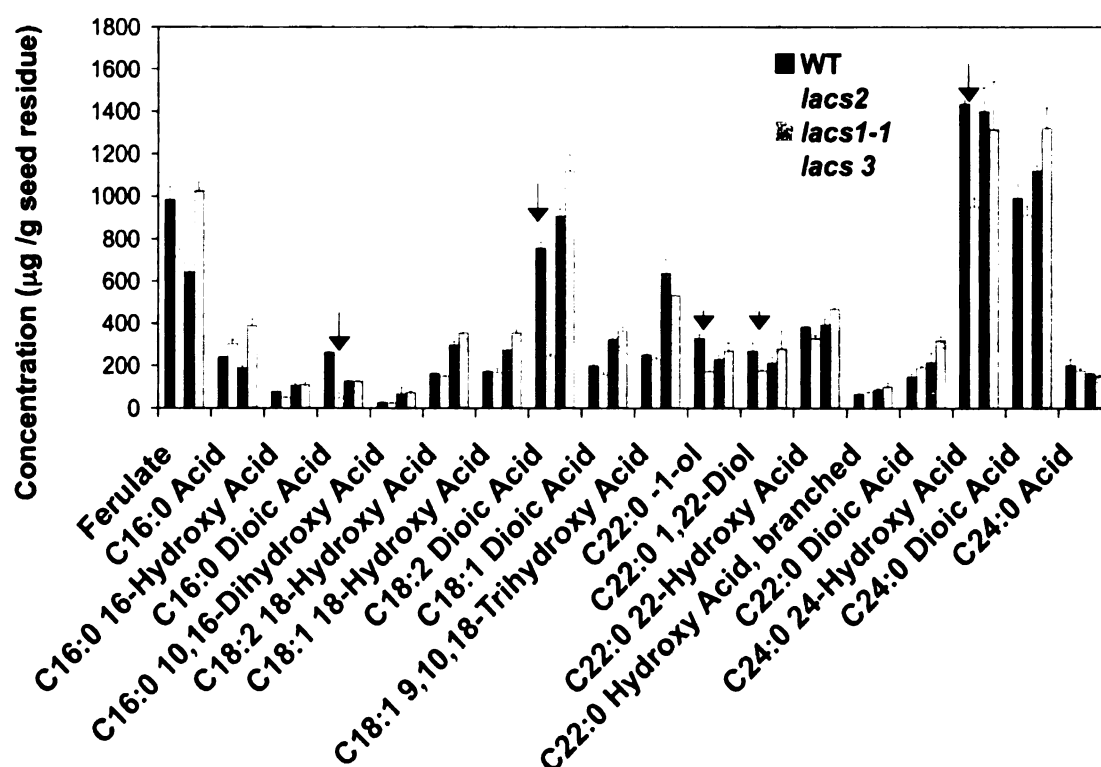


Figure 40. Seed lipid polyester monomer load and composition in wild-type and *lacs2*, *lacs1-2* and *lacs3* knockouts.

Data are reported for the mean of triplicate determinations \pm SD.

Hence, these results suggest that *LACS2* functions in Arabidopsis lipid polyester synthesis by activating intermediates in lipid polyester synthesis in leaves and seeds, confirming its role in both cutin and suberin deposition. *LACS1* and *LACS3* have partially redundant functions with *LACS2* in leaves. From these data, however, the substrate specificity for *lacs* cannot be inferred. Moreover, *in vitro* assays performed with recombinant LACS proteins expressed in *E. coli*

indicated that LACS2 can use both palmitate (16:0) and 16-hydroxypalmitate as substrates (Schnurr et al., 2004).

Other gene families

Analysis of *Arabidopsis* epidermis and *Quercus suber* cork transcriptomes highlight the potential importance of other gene families not fully discussed in the present work. In particular, one of the up-regulated families of acyl-transferases or hydrolases may include a so far uncharacterized “polyester synthase” responsible for the assembly of polyester chains. The recent identification and characterization of the GPAT family indicates that these intracellular acyl-transferases are crucial for cutin and suberin aliphatic polyester deposition (Beisson et al., 2007; Li et al., 2007a; Li et al., 2007b), providing *in planta* evidence for their role in acyl-transfer to a glycerol-based acceptor, and for their involvement in cutin synthesis. Other acyl-transferases listed by Suh et al. (2005), such as the 1-acylglycerol-3-P acyltransferase LPAT5 (Kim et al., 2005), may be also involved in cutin synthesis.

Monoacylglycerol lipases, patatin-like acyl-hydrolases, lysophospholipases (one of which, *BDG*, has been characterized by Kurdyukov et al., 2006a) (**Table 6**), are up-regulated in stem epidermis (Suh et al., 2005). These enzymes catalyze reversible reactions and could have a function either in synthesis or remodeling of the polyesters. Mutants for preferred candidates have

been selected and the characterization of surface lipids has been performed in leaves and stems (Deborah Dos Santos and Isabel Molina, unpublished results). Moreover, transcripts of the GDSL-motif lipase/hydrolase family are abundant in cork phelloderm and in transgenic *Arabidopsis* plants overexpressing the transcription factor *WIN1* (*WAX INDUCER1*) (Kannangara et al., 2007). A related GDSL protein isolated from *Agave Americana* has been proposed as a putative extracellular hydrolase involved in cutin synthesis (Reina et al., 2007), but this hypothesis awaits biochemical and genetics confirmation. The possible function of GDSL lipases in *Arabidopsis* polyesters is currently being investigated by reverse genetic approaches in our lab.

CONCLUSIONS

I have generated a list of candidate genes for lipid polyester synthesis, which includes gene families whose members are known to function or likely to function in lipid polyester function, and gene families of unknown function. From the first group, using a loss-of-function approach, I have demonstrated that CYP86A1 is involved in ω -oxidation of suberin aliphatics, that LACS1 and LACS3 have partially redundant functions with LACS2 in cutin monomer activation, and that LACS2 also participates in suberin synthesis in seeds. Regarding the group of uncharacterized gene families, I have found three candidate genes for suberin/cutin that belong to the BAHD family. The involvement of one of these, At5g41040, in suberin synthesis has been demonstrated by biochemical analyses

of knockout mutants. To our knowledge, this is the first suberin mutant defective in a hydroxy-cinnamic derived monomer, and the first gene of the BAHD family that has been associated to lipid polyester synthesis.

Several breakthroughs have been achieved in the last five years in identification of genes for cutin and suberin biosynthesis. The work described in this chapter and its continuation will help to continue the search for candidate genes using a systematic approach taking advantage of the constantly developing data mining bioinformatics tools.

EXPERIMENTAL PROCEDURES

Plant materials and growth conditions

Growth conditions. Arabidopsis wild-type plants, and mutants (Col-0 background) were stratified for four days at 4°C and grown with 16-/8-h light/dark photoperiod under 80 to 100 $\mu\text{mol}\cdot\text{m}^{-2}\cdot\text{s}^{-1}$ light conditions at 23°C and 40 to 60% RH. Transgenic seeds were stratified and germinated on MS (Murashige and Skoog, Gibco) plates supplemented with 5% sucrose, 1x B5 vitamins, and 50 mg/L kanamycin. For young root analyses, seeds were grown on vertical agar plates.

Plant material. Arabidopsis Col-0 wild-type plants were used for all transformation experiments, as well as for lipid polyester analyses. Knockout lines used in this work were: *at1g01600* (SALK_073078) and *at5g58860* (SALK_146813 and SALK_140618), provided by Y. Li; *at1g04220* (SALK_033206C), provided by L. Kunst, and *lacs1-1* (SALK_127291), *lacs1-2* (SALK_138782), *lacs3-1*, *lacs 2-1* (T-DNA insertion line 1-1#100), *lacs1-2/lacs2* and *lacs1-2/lacs2/lacs3*, all *lacs* provided by J. Browse's lab. Heterozygous *at5g41040* (SALK_048898 and SALK_017725) and *lcr* (WiscDsLox387B09) seeds stocks were obtained from the Arabidopsis Biological Resource Center (ABRC) seed collection (<http://www.biosci.ohiostate.edu>).

Bioinformatics

Co-response analyses. The Gene Correlator tool (<https://www.genevestigator.ethz.ch>) was used to evaluate gene coexpression over more than 2,000 chips in the database. Twenty-two K (ATH1) array chips from different sources (NASC, ArrayExpress, AtGenExpress TAIR) were selected. All annotation categories (anatomy, development, and stress) were included, but arrays for specific experiments were not chosen. Pearson's correlation is given as a score for the measure of linear relationship. Plots were performed selecting log₂(n) scale to ensure linearity (co-response values are detailed in **Table 10, Appendix B**). Because of the large number of arrays selected, a relatively low threshold value (0.1) was considered a significant

correlation, with high correlations correlation coefficients ranging between 0.4-0.6.

Sequence alignment and tree construction. Deduced protein sequences of the Arabidopsis BAHD family were retrieved in FASTA format from the GenBank database and a multiple alignment was created by ClustalX (Thompson et al., 1997) using the default settings. Phylogenetic trees were evaluated according to the maximum parsimony principle with PAUP 4.0b10 (Swofford, 2000), using two proteins (encoded by At1g27620 and At2g40230 loci) as outgroups. The best score tree is shown in **Figure 32**. A heuristic bootstrap search was performed with 1,000 replicates, 100 random addition replicates per bootstrap replicate. Bootstrap values lower than 50% are not shown.

Mutant isolation

Single mutants. T-DNA insertion mutant information was obtained from the SIGnAL website at <http://signal.salk.edu>. The insertional line WiscDsLox387B09 has a pDs-Lox T-DNA insert in the exon of AT2G45970 (*LACERATA*) gene. To select homozygous plants for such insertion, plants from those seeds were screened by PCR using the gene-specific primer pair LCR-F and LCR-R, and the T-DNA left border primer of pDs-Lox (p745) (primers listed in **Table 8**). Two allelic mutants for At5g41040 were selected from SALK_048898 and SALK_017725 (Alonso et al., 2003) T-DNA insertion lines. Gene specific primers

to identify the wild type gene were BAHD1-F1 and BAHD1-R1 (**Table 8**). To check for the insertion, the primer set used was BAHD1-R2, specific for the 3' UTR gene sequence, and the T-DNA left border-specific primer Lba1. **Figure 33** shows a scheme representing the genetic structures of the *at5g41040* mutant alleles.

Generation of *att1-2/cyp86a4* double mutants. Parental lines were crossed to each other. F₁ plants were selfed, and F₂ seeds planted. Plants of F₃ generation were tested by PCR using the *ATT1*-specific primers (ATT1-F and ATT1-R), *CYP86A4*-specific primers (A4-F and A4-R), and the T-DNA-specific Lba1 primer.

Reverse Transcription Polymerase Chain Reaction (RT-PCR)

RNA was isolated from 100 mg of 3-week old Arabidopsis roots using the RNeasy Plant Mini Kit (Qiagen, Valencia, CA), following manufacturer's instructions (including the optional steps of heating sample in buffer RLT for 3 min at 56°C, and extra spin step following addition of wash buffer). Membranes were eluted with 30 µl of Rnase-free water. SuperScript III Reverse Transcriptase (Invitrogen) was used to synthesize the first-strand cDNA from 2 µl-aliquots of RNA, following manufacturer's protocol. Two-µl aliquots of the RT reactions were used as template for PCRs. Primers used for amplification of At5g41040 gene (BAHD-F2 and BAHDR-3) and At5g58860 cDNA (CYP86A1-F and CYP86A1-R)

are listed in **Table 8**. PCRs were also performed for the housekeeping eukaryotic translation initiation factor 4A (*eIF4A*), which was used as a loading control. Amplification conditions were as follows: 95°C for 2 minutes, followed by 30 cycles of 30 sec at 95°C, 30 sec at 55°C, 2 min at 72°C, with a final extension step at 72°C for 10 min.

Table 8. Primer sequences used in work described in Chapter 4.

	Primer Name	Primer sequence (5' – 3')
T-DNA homozygous selection primers	LBa1	TGGTTCACGTAGTGGGCCATCG-3'
	p745	AACGTCCGCAATGTGTTATTAAGTTGTC
	ATT1-F	ATGTCTCCAACACGATGCTCC
	ATT1-R	CGTTGCATTTTCCGTAAAGAA
	A4-F	AAATATCCAATGCCATGCTTCT
	A4-R	TAAACCACTGCAACTCCCGTAT
	LCR-F	ATTTCCACTGCTCTAATGATTCTTT
	LCR-R	TCATTGACGACGTTAGATTTACACT
	BAHD1-F	GTGCTGTTTTCTCCATTTGG
	BAHD1-R	GCCAGATATTTGTATTTTGTCTG
	BAHD1-R2	CCAACCTGATGAACTTGTAATGTAA
RT-PCR primers	CYP86A1-F	CACAATCTCTCCACAGAACAAAAG
	CYP86A1-R	CATAGAATAAAGTAGGTTGTTCTTAAAC
	BAHD1-F2	GACAACAACAACAACATCAAAG
	BAHD1-R3	CACTACATGGTCAAGATTGGGTTT
Cloning primers	A1-Pro-F	cacac <u>gtcgac</u> AATCCTGGGCAACGATGACT (<i>Sall</i>)
	A1-Pro-R	cacac <u>tctaga</u> GCCGGTTAAGATAGAGTTTAGAGC (<i>XbaI</i>)
	G4-Pro-F	cacac <u>aagctt</u> AACCTTCATTGTTGCATCTTGG (<i>HindIII</i>)
	G4-Pro-R	cacac <u>tctaga</u> AGGAAACTTCGGCTCTTCT (<i>XbaI</i>)

YFP reporter construct design and plant transformation

Construct design procedures were similar to those described in Chapter 3 for *ATT1* and *GPAT5* transcriptional fusions (p. 122). Briefly, the 2-kb 5' sequences of CYP86A1 DNA and of GPAT4 DNA, plus 5' 30 bp of their respective coding regions were amplified by PCR using the following primer pairs A1-Pro-F/A1-Pro-R (for CYP86A1 promoter), and G4-Pro-F/G4-Pro-R (for GPAT4 promoter). All amplifications used a proofreading DNA polymerase (Platinum Pfx, Invitrogen). PCR fragments were subcloned in pGem[®]-T Easy vector (Promega) for sequencing. To generate pBI-*Promoter*_{CYP86A1}::YFP and pBI-*Promoter*_{GPAT4}::YFP, promoter fragments were released from pGem[®]-T Easy and ligated into pBI101-eYFP digested *Sal*I-*Xba*I (for CYP86A1 promoter) or *Hind*III-*Xba*I (for GPAT4 promoter), to fuse the promoter sequences in frame to the 5' end of the YFP sequence in pBI-YFP. These binary plasmids were introduced into *Agrobacterium tumefaciens* strain C58C1 by electroporation. Arabidopsis Col-0 wild-type transformation was performed by the vacuum infiltration method (Bechtold et al., 1993). Confocal laser microscopy analysis is described in Chapter 3 p. 126.

Transmission electron microscopy

Leaf or root samples of about 1mm² size were fixed with 2.5% glutaraldehyde/2% paraformaldehyde in 0.1 M cacodylate buffer. Immediately after immersing the specimens into the fixation solution, vacuum was applied until no floating material remained, followed by 2 h incubation at RT, and ON incubation at 4°C in the same solution. Postfixation with 1% buffered osmium tetroxide was performed ON at 4°C, followed by dehydration through a graded acetone series with a 10% increment (20 min in each incubation). Samples were infiltrated with Poly/Bed 812 resin in six steps, with increasing resin concentration. After placing in silicone moulds, embedded samples were polymerized for 24 h at 60°C. Silver-gold ultrathin sections were prepared with a diamond knife on a Power Tome_XL microtome (Boeckeler Instruments, Tucson, AZ), placed on copper-mesh grids, and stained with 2% uranyl acetate (15 min) in 50 and Reynold's lead citrate (10 min). Alternatively, root samples were pre-incubated in 10% hydrogen peroxide for 10 min, followed by staining with 10% uranyl acetate in methanol for 8 min, and lead citrate for 10 min. This procedure enables to enhance the contrast of both cutin and suberin (Heumann, 1990). Specimens were examined with a JEOL 100CX transmission electron microscope, and images processed with Adobe Photoshop CS2.

Determination of lipid polyester monomers: See Chapter 2, p. 81-82 for procedures.

Test of permeability to tetrazolium salts: See Chapter 3, p. 126 for procedures.

CHAPTER 5

***IN PLANTA* HETEROLOGOUS EXPRESSION APPROACH TO UNDERSTAND THE FUNCTION OF CYP86A PROTEINS**

Aknowledgement

I would like to thank Dr Jan Jaworski for providing the following material generated in his laboratory: clones of *PH1* cDNA and *PH1* promoter, anti-PH1 antibody, and petunia PH1-RNAi lines.

ABSTRACT

Hydroxylated fatty acid monomers are major constituents of plant lipid polyesters. Although several enzymes can catalyze in-chain aliphatic hydroxylation in plants, only cytochrome P450s are known to introduce the hydroxyl group in the omega position of fatty acids. In this chapter, I describe an *in planta* heterologous expression strategy toward understanding the function of a ω -hydroxylase, CYP86A2 (ATT1). The *att1* mutant was reported to have a thinner, highly permeable cuticle with lower content of cutin monomers compared to wild-type (Xiao et al., 2004). Using an improved method for cutin analysis, I have shown that C18:2, C18:1 and C16:0 dicarboxylates are specifically affected in *att1*, but an expected significant reduction in ω -hydroxylated monomers was not observed. To study the function of this enzyme *in planta*, two approaches were taken. First, the *att1* mutant was complemented with the cDNA sequence corresponding to a confirmed fatty acid ω -hydroxylase from petunia (petunia hydroxylase-1, PH1). However, the complemented plants failed to even partially recover the wild-type leaf impermeability phenotype and monomer composition. Second, in an attempt to increase improving the ω -hydroxy fatty acid content in tobacco stigma, I also overexpressed ATT1 in this organ. Stigma exudates provide a soluble polyester synthesis system, which may reveal biochemistry related to cutin biosynthesis. However, transgenic tobacco plants did not show increased production of ω -hydroxylated monomers in stigmas. The interchange of these two orthologous plant genes was expected to complement the *att1*

mutant and increase the production of tobacco stigma polyesters. The presented evidence questions the role of CYP86A2 (ATT1) as a simple ω -hydroxylase. Possible reactions catalyzed by this enzyme are discussed.

INTRODUCTION

Cytochrome P450 enzymes constitute one of the largest superfamilies of enzyme proteins. The Arabidopsis genome contains 272 cytochrome P450 genes, which catalyze a wide range of substrate oxidations (Werck-Reichhart et al., 2002). Monooxygenases involved in catalysis of hydroxylation steps are complexes of a heme-protein-dependent oxidase and a NADPH-cytochrome P450 reductase. They use molecular oxygen to produce the functionalized substrate and a molecule of water (Schuler and Werck-Reichhart, 2003). In spite of the critical roles played by the plant P450 superfamily, a functional analysis of these genes is difficult to approach for several reasons. Obstacles include the size of the family and the high degree of duplication and divergence of the genes, low abundance of transcripts, specific cellular expression, expression in response to stresses, and requirement of a co-localized electron transfer protein (Schuler and Werck-Reichhart, 2003). As a result, only a few P450 gene products have been biochemically characterized using heterologous expression systems, and even less have been related to specific functions *in planta*. Moreover, gene redundancy complicates reverse genetic analyses in certain

P450 subfamilies. In those cases antisense approaches are promising alternative tools to assign functions.

Plant fatty acid omega-hydroxylases

Hydroxylated fatty acids are major constituents of plant lipid polyesters such as cutin, suberin, and those found in stigma exudates of solanaceous plants. In-chain and terminal hydroxyl functions in fatty acids are fundamental for assembling the polyester network, which in large part is based on ester bonds between carboxyl and hydroxyl groups (Kolattukudy, 1980a). In plants, hydroxylation at the ω -position is catalyzed by cytochrome-P450-dependant enzymes, most of them belonging to the CYP86 and CYP94 subfamilies (Benveniste et al., 1998; Tijet et al., 1998; Pinot et al., 1999; Le Bouquin et al., 2001; Duan and Schuler, 2005; Benveniste et al., 2006; Rupasinghe et al., 2007). The reaction catalyzed is exemplified in **Figure 41**.

It is important to note that there are almost no publications supporting the proposed catalytic functions of CYP86 and CYP94 enzymes *in vivo*. Almost all *in vitro* activities were obtained by expression in yeast or insect cells rather than plants (Pinot et al., 1992; Benveniste et al., 1998; Cabello-Hurtado et al., 1998; Benveniste et al., 2006). Only one report has confirmed ω -hydroxylation *in planta* (Han et al., 2005). Moreover, there are no reports in the literature showing accumulation of ω -hydroxylated products in transgenic plants overexpressing

P450 genes, with exception of the ectopic co-expression of CYP86A1 and GPAT5, which resulted in major accumulation of dicarboxylates and small increases in ω -hydroxylated cutin monomers (Li et al., 2007a). This co-expression study was undertaken in our laboratory well after I initiated this project and was influenced by the negative results presented in this chapter.

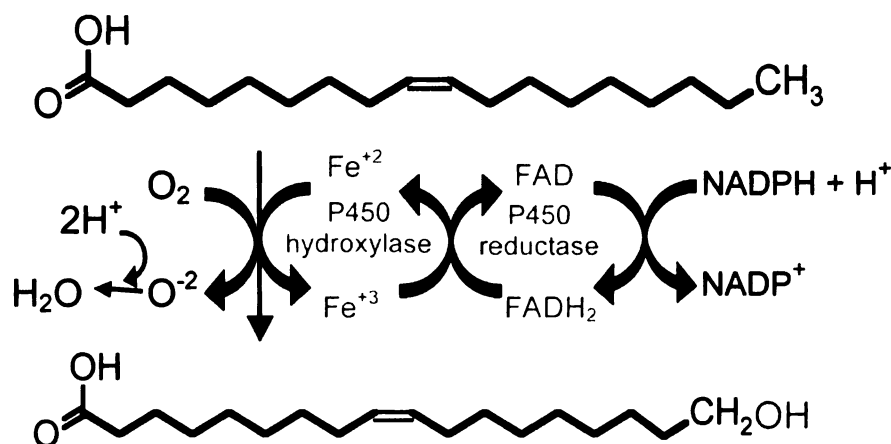


Figure 41. Schematic representation of the enzymatic reaction catalyzed by plant ω -hydroxylases.

The introduction of a hydroxyl function at the terminal methyl group of fatty acids requires molecular oxygen and a FAD/FMN-containing P450 reductase that transfers electrons from NADPH.

A phylogenetic analysis of potentially orthologous ω -hydroxylases from various organisms is illustrated in **Figure 42**. The group of plant CYP86A, CYP94A and CYP94B subfamilies has a common ancestor with fungal and mammalian sequences, whereas the group comprised of CYP78A, CYP72B and CYP703A derives from a plant-specific ancestor and is related to synthesis and metabolism of secondary metabolites. The Arabidopsis CYP86A subfamily contains five genes encoding proteins with fatty acid ω -hydroxylase functions

Figure 42. Phylogenetic tree for fatty acid ω -hydroxylases from plants and other kingdoms.

The tree was generated using the bioinformatics tools available at www.Phylogeny.fr. Sequence alignment was performed with Muscle, PhyML-aLRT was used for phylogenetic analysis, and Tree Dyn for tree drawing (Felsenstein, 1989; Guindon and Gascuel, 2003; Edgar, 2004; Anisimova and Gascuel, 2006; Chevenet et al., 2006). The following sequences of fatty acid ω -hydroxylases were aligned: Arabidopsis (CYP94B, CYP94C1, and CYP86A and CYP86B subfamilies), *V. sativa* (CYP94A1, CYP94A2), *N. tabacum* (CYP94A5), *P. hybrida* (PH1, CYP92B1, CYP703A1, CYP75A1), *Z. mays* (CYP78A1), *Candida tropicalis* (CYP52A2), *Candida maltosa* (CYP52A4), and rat (CYP4a1), human (CYP4A11, CYP4B1, CYP4F2). The biochemically-characterized plant fatty acid ω -hydroxylase subfamilies CYP86A and CYP94 have a common ancestor with mammalian and fungal sequences; the less-characterized CYP92B, CYP703A, and CYP78A proteins have a common ancestor with the plant-specific group related to synthesis of secondary metabolites (CYP88A4, CYP73A5, CYP84A1, CYP83A1, CYP98A3). (Figure legend adapted from Duan and Schuler, 2005).

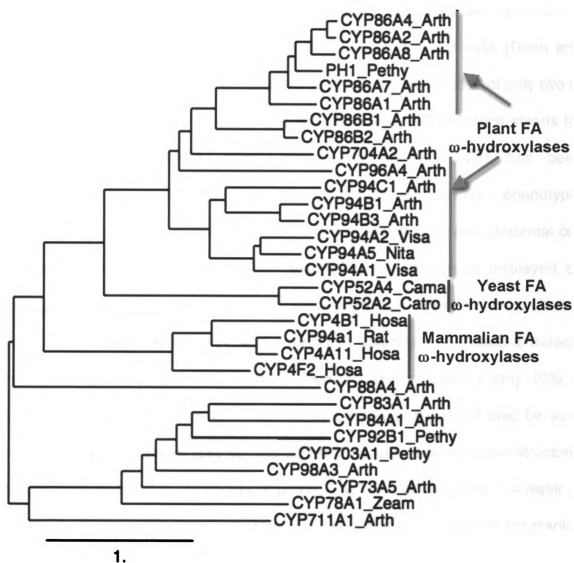


Figure 42.

(Figure 42). Their functions have been biochemically demonstrated by heterologous expression in yeast (Benveniste et al., 1998; Wellesen et al., 2001; Benveniste et al., 2006; Rupasinghe et al., 2007) and insect cells (Duan and Schuler, 2005; Rupasinghe et al., 2007). The physiological function of only two of these proteins, CYP86A8 (LACERATA) and CYP86A2 (ATT1) (which stands for *aberrant induction of type three genes*, Xiao et al., 2004), has been demonstrated in planta. The *lcr* mutant displayed a pleiotropic phenotype, including organ fusion, pollen germination on the leaf surface, and abnormal cell morphology (Wellesen et al., 2001), resembling the phenotype displayed by transgenic Arabidopsis expressing the cutinase gene of *Fusarium solani* (Sieber et al., 2000). Although the *lcr* organ fusion phenotype might be related to defects in the cuticle layer, *lcr-2* cutin monomer loads were reduced by only 10% in expanding leaves (Chapter 4). Thus, the fusion phenotype could also be as a consequence of a lack of lipid derived signal molecules, altered cutan structure, or a localized alteration during development that was not detected in 4-week or 6-week leaf samples analyzed. On the other hand, the *att1* mutant did not display organ fusions, but had a thinner, more permeable cuticle with lower content of cutin monomers compared to wild type plants (Xiao et al., 2004). Since different monomer classes with various chain lengths were affected, from this analysis the specific enzyme function of ATT1 could not be clearly identified.

Soluble lipid polyesters from “wet” stigmas

The so-called “wet” stigmas of certain solanaceous plants such as petunia and tobacco are covered with a sticky exudate during receptive periods. By contrast, “dry” type stigmas lack such exudates. This fluid contains a large amount of lipids, of which approximately 80% are polyesters (Matsuzaki et al., 1983a). Stigma lipid polyesters are polyacylglycerols containing ω -hydroxy fatty acids. Although they contain similar monomers to cutin (**Figure 43**), stigma polyesters have the experimental advantage of solubility in organic solvents. C18:1 and C18:2 are the major ω -hydroxy fatty acids found in stigmas of solanaceous species. Petunia stigmas contain 96% ω -hydroxy fatty acids, while tobacco stigmas contain 60% ω -hydroxy fatty acids (Koiwai and Matsuzaki, 1988). Recent studies performed using gel permeation chromatography showed that the petunia polyester fraction has about 50 acyl groups per molecule, whereas in tobacco stigmas 5-6 acyl groups per molecule are found (Chapter 1, **Figure 7**) (Wang et al., 2003). Little is known about their biosynthesis.

Bioinformatics screening of an expressed sequence tag (EST) database from petunia stigma identified six putative P450 genes (PH1- PH6). Of these, the most abundant clone in the cDNA library (30 ESTs) was PH1 (petunia hydroxylase-1). Transgenic petunia plants transformed with RNAi constructs for the PH1 gene showed a dry stigma phenotype and arrested biosynthesis of ω -hydroxy fatty acids, demonstrating that PH1 is a key P450 FA ω -hydroxylase in petunia stigmas (Han et al., 2005). Phylogenetic analysis indicated that PH1 is closely related to the cutin hydroxylases CYP86A of Arabidopsis (**Figure 42**)

Figure 43. Structural comparison of soluble and insoluble lipid polyesters.
(a) Structure of one of the possible isomers of polyhexaacyl glycerol, TAG (6), found in stigmas of *Nicotiana tobaccum*. No free hydroxyl groups are present in these structures, which are end-capped with an unsubstituted fatty acid. **(b)** A hypothetical arrangement of monomers that could be found in a ω -hydroxy fatty acid-rich cutin. Primary ester bonds are dominant, with some secondary ester bonds from mid-chain hydroxylated monomers. R: aliphatic polyester.

(Han et al., 2005), and CYP86A2 (ATT1) is its closest orthologous (see **Figure 48** in Results section). The work described in this paragraph has been performed by the group of J. Jaworski who collaborated with the Ohlrogge/Pollard laboratory in the stigma polyester project.

The occurrence of ω -hydroxy fatty acids in both extracellular cutin and stigma lipid polyesters raised an interesting question: Are insoluble (i.e. cutin) and soluble plant lipid polyesters synthesized by similar pathways? To better understand cutin biosynthesis and, in parallel, to test the hypothesis that stigma exudates constitute a “soluble polyester system” to study cutin biosynthesis, the role of a key enzyme involved in cutin biosynthesis in Arabidopsis leaves, ATT1, was studied by a transgenic approach. First, the petunia ω -hydroxylase (PH1) was expressed in Arabidopsis *att1* knockout mutants in order to rescue the wild type phenotype. Second, the “cutin” gene (ATT1) was over-expressed in stigmas of Nicotiana tobaccum. Based on the in planta evidence of these enzyme functions, and on the fact that these proteins share 84% sequence similarity, I tested the hypothesis that a cutin hydroxylase can hydroxylate stigma polyester monomers and, conversely, a stigma hydroxylase can use leaf cutin fatty acids as substrates. Moreover, I speculated that the MW of oligomers that are found in tobacco polyesters may be limited by ω -hydroxy fatty acid production, and that their MW could be increased in transgenic tobacco plants that overexpress ATT1.

As will be shown in the next sections, the above described strategy resulted in negative results. It is important to bear in mind that such results were obtained before our knowledge on genes involved in polyester synthesis evolved. Indeed, these negative outcomes were useful to design further experiments. We know now that cytochrome P450s need to be coexpressed with GPATs (glycerol-3-phosphate-acyltransferases) to accumulate polyesters in transgenic plants (Li et al., 2007a), and that LACS (long-chain acylCoA synthetases) are necessary for substrate activation during polyester biosynthesis (see Chapter 4 for details). However, available data are insufficient to assign substrate specificity to these enzymes. It is equally uncertain whether CYP86A monooxygenases are able to catalyze all oxidation steps to produce dicarboxylic acids. The combination of the mentioned negative results with this new evidence helped me shape new ideas on how CYP86A enzymes may function *in vivo*. The hypothesis of the existence of a “metabolon” for polyester synthesis will be discussed.

RESULTS

Characterization of *Arabidopsis att1* mutants

Comparison of transcript profile from microarray data (Schmid et al., 2005) and RT-PCR (Duan and Schuler, 2005) has shown that members of the *Arabidopsis* CYP86A subfamily are differentially expressed, as illustrated in

Figure 44. CYP86A1 is mostly expressed in roots and seeds, and thus, this gene would not be expected to have a function in leaf or stem cutin biosynthesis. Indeed, I have shown that it oxidizes C16-C18 fatty acid substrates in root suberin (Chapter 4). CYP86A4 and CYP86A7 are highly represented in flowers, although significant levels of CYP86A4 transcripts are also found in shoot apex, leaves and stems. CYP86A2 (*ATT1*) and CYP86A8 (*LACERATA*) transcripts are broadly found in all plant organs, although *CYP86A2* transcripts 4-fold more abundant in average. The physiological significance of these two genes in cuticle biosynthesis has been demonstrated (Wellesen et al., 2001; Xiao et al., 2004). The lipid polyester phenotype has been reported for *att1*, where the cutin matrix was affected. However, because of experimental issues (i.e. sample oxidation), the values of individual monomer loads reported by Xiao et al. were incorrect and, thus, it was not possible to assign a function to the disrupted gene. This article was published before more reliable protocols for Arabidopsis cutin analysis were available, emphasizing the importance of well-standardized methodologies for lipid polyester analysis to understand gene functions. Since the most abundant ω -hydroxylase transcripts in leaf and stem correspond to At4g00360 (*ATT1*) (compared to the other genes in the subfamily), it is the strongest candidate gene for stem and leaf cutin biosynthesis. Hence, work described in this chapter was mainly focused on functional characterization of this member of the CYP86A subfamily.

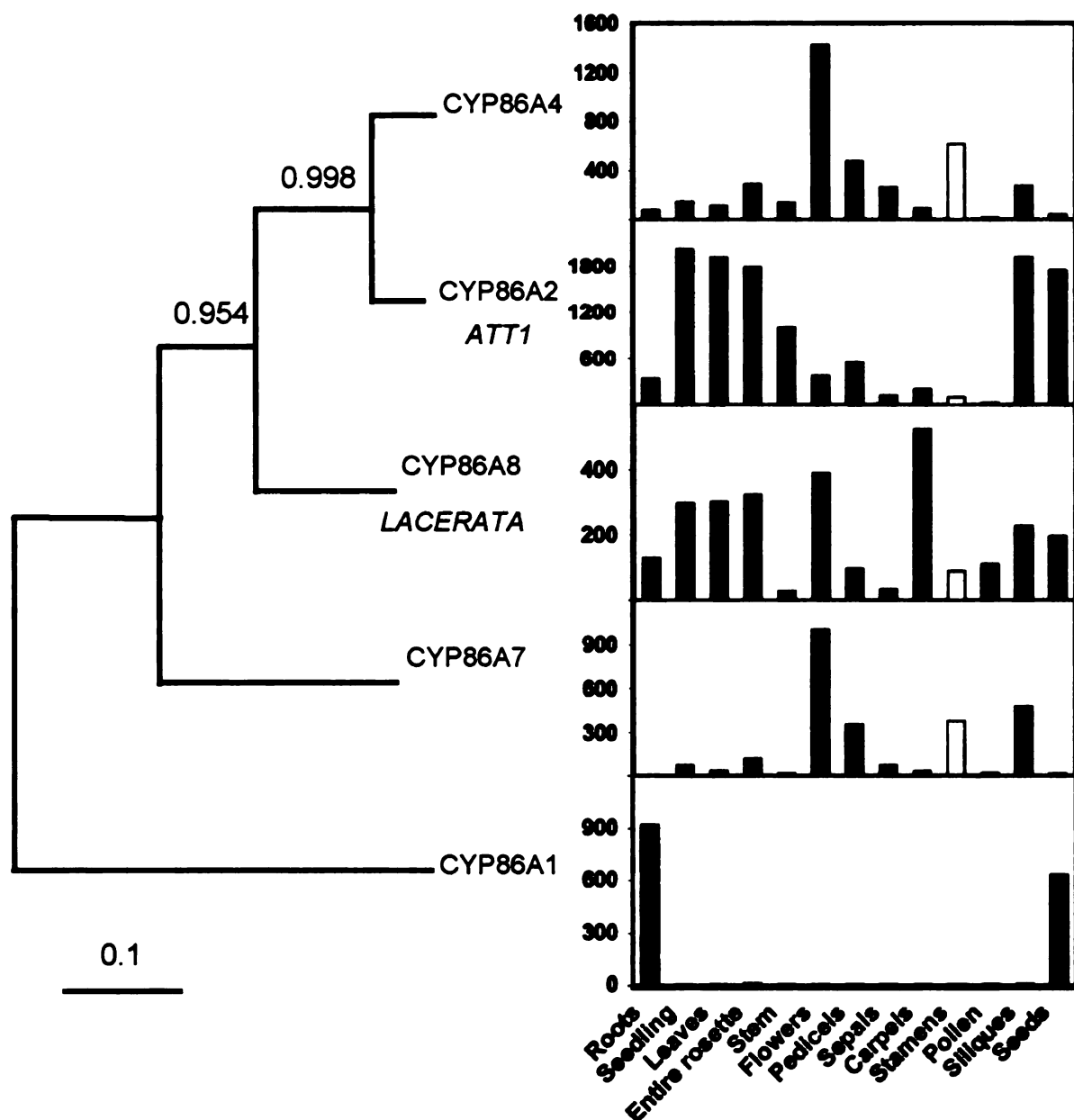


Figure 44. Expression analysis of the Arabidopsis CYP86A subfamily.

Phylogenetic tree was calculated as explained in Figure 42. Charts showing gene expression levels in various tissues (right) were generated from microarray data obtained from the AtGenExpress project (Schmid et al., 2005).

Confirmation of *att1-2* knockout by RT-PCR. Because *Arabidopsis* cuticles are extremely thin and fragile, I used recently developed methods to study lipid

polyester monomers that bypass the cuticle isolation step (Bonaventure et al., 2004; this study, Chapter 2). The two *att1* alleles used in this study were kindly provided by Dr. Jian-Min Zhou (NIBS, Beijing, China). The *att1-1* mutant obtained by ethyl methanesulfonate mutagenesis has a substitution in R309 to C in the second exon (Figure 45a), as demonstrated by gene sequencing (Xiao et al., 2004). The T-DNA tagged mutant, *att1-2* (SALK_005826), has an insertion in the second exon of the At4g00360 gene. Gene silencing in *att1-2* was confirmed by reverse transcriptase-mediated PCR. As shown in Figure 45b, no expression was observed in leaves and stems of *att1-2* mutant, whereas it was highly expressed in wild-type tissues.

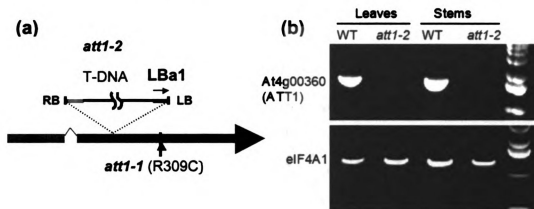


Figure 45. (a) Schematic representation of the genomic organization of *att1* mutants and (b) RT-PCR from leaves and stems of *att1-2* and WT plants.

(a) Schematic representation of the structure of the At4g00360 gene showing the T-DNA insertion in the second exon (*att1-2*) and the non-synonymous substitution in aminoacid 309 of the EMS mutant (*att1-1*). Adapted from (Xiao et al., 2004). (b) RT-PCR analysis of *ATT1* transcripts in leaves and stems of wild type and *att1-2* mutant. The *eIF4A1* gene was used as load control. RB: T-DNA right border, LB: T-DNA left border, LBa1: T-DNA left border specific primer.

Permeability of *att1* seedlings to aqueous TBO. The higher permeability of *att1* cuticles was confirmed by toluidine blue test (TBO test) (Tanaka et al., 2004). Plants with discontinuous or defective cuticle can be rapidly visualized by staining for two minutes in an aqueous solution of toluidine blue (TBO), as schematized in **Figure 46a**. When the dye crosses the cuticular barrier, it reacts

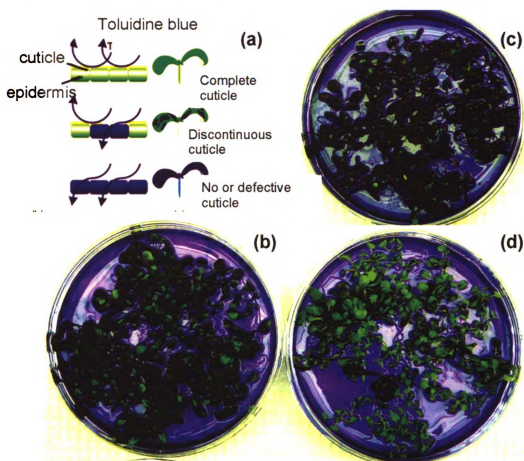


Figure 46. Permeability of *att1* cuticles to toluidine blue.

(a) Scheme showing three possible patterns of permeability to aqueous toluidine blue (modified from Tanaka et al., 2004). Wild type seedlings are not stained after 2 min exposure to an aqueous solution of the dye **(d)**, while the highly permeable phenotype shown by *att1-2* **(b)** and *att1-1* **(c)** seedlings is consistent with a defective cuticle.

with cell walls (as well as with other cellular components), which results in blue coloration. *att1-2* (**Figure 46b**) and *att1-1* (**Figure 46c**) were completely permeable to the dye, consistent with a defective cuticle, whereas wild-type plants remained green (**Figure 46d**).

Lipid polyester monomer analysis in att1 leaves and stems. To investigate the lipid monomer fractions that were specifically affected by the *att1* mutation, analyses of non-extractable lipid polyesters were carried out using NaOMe-catalyzed transesterification, as previously described for seed analysis (Chapter 2, (Molina et al., 2006)). In *att1-1* and *att1-2* leaf residue, all fractions of dicarboxylic acids (C16, C18:2, C18:1, and C18:0) were lower than in wild type leaf residue (**Figure 47a**) (Molina et al., 2008). However, a significant decrease in the corresponding ω -hydroxy-fatty acid fractions was not observed. A reduction in these components had been anticipated given that the putative catalytic function of the enzyme is ω -fatty acid hydroxylation (**Figure 41**). The phenotype observed in stems of *att1* lines was similar, but the reduction of C18:2 dioic acid (50%) was not as strong as in leaves (70%) (**Figure 47b**). Furthermore, as presented in Chapter 3 (**Figure 20**), the monomer profile obtained by analysis of delipidated seeds clearly showed a three fold reduction in C18:1 and C18:2 dioic acids, accompanied by a concomitant increase in C18:2 ω -hydroxy fatty acid and no change in C18:1 ω -hydroxy fatty acid. However, such increases should be interpreted with caution because seed lipid polyesters have several contributions. In particular, the *ap2* phenotype suggested that C18:2 and C18:1 ω -hydroxy

acids are predominantly located in the outer integument, whereas reduction of dicarboxylic acids in *att1* likely occurs in the ii1 layer (Chapter 3). As discussed in Chapter 3, and below, together these data raise questions about the catalytic function of CYP86A2. From the mutant phenotype it is not possible to assign a specific function to the enzyme, although my observations indicated that CYP86A2 is involved in the synthesis of C18 unsaturated and, in minor degree, C16 saturated dicarboxylic acids. Possible reactions catalyzed by ATT1 are schematized in **Figure 47c**. The cutin phenotype seems to be consistent with ATT1 functioning as an ω -oxidase downstream the ω -hydroxylase, this last being highly regulated by product accumulation because no increase of ω -hydroxylated monomers is observed (**Figure 47c-reaction ii'**). However, situations where ATT1 is just ω -hydroxylase (i) or both ω -hydroxylase/ ω -oxidase (iii) are also possible if another ω -hydroxylase compensates for the reduced ω -hydroxylated monomers, thereby masking any reduction in ω -hydroxylated monomers caused by the *att1* mutation.

Seed coat analyses demonstrated that this gene is not likely to be related to suberin synthesis (Chapter 3, and Molina et al., 2008). This is also sustained by determinations of lipid polyester monomers in three-week old roots, where no differences were observed between *att1* alleles and wild-type monomer profiles (data not shown).

Figure 47. Comparison of the monomer composition after depolymerization of solvent-extracted *Arabidopsis thaliana* wild-type and *att1* mutants by NaOMe-catalyzed transmethylation.

(a) Monomer content in five-week old leaves. (b) Monomer content in five-week old stems. The means of triplicate determinations \pm SD are reported (c) Schematic view of possible reactions catalyzed by ATT1 (left) and expected monomer changes compared to wild-type (right). Both monomer classes are reduced if ATT1 is just ω -hydroxylase (i) or acts as ω -hydroxylase and ω -oxidase (iii). ω -hydroxy fatty acids are accumulated and dioic acid reduced if ATT1 oxidates ω -hydroxy fatty acids to dicarboxylates (ii), but no change in the substrate (ω -hydroxy fatty acids) is expected if the upstream hydroxylase is regulated by product accumulation (ii'). Further complexities of this view are detailed in the Discussion section. (a) and (b) are part of a publication (Molina et al., 2008).

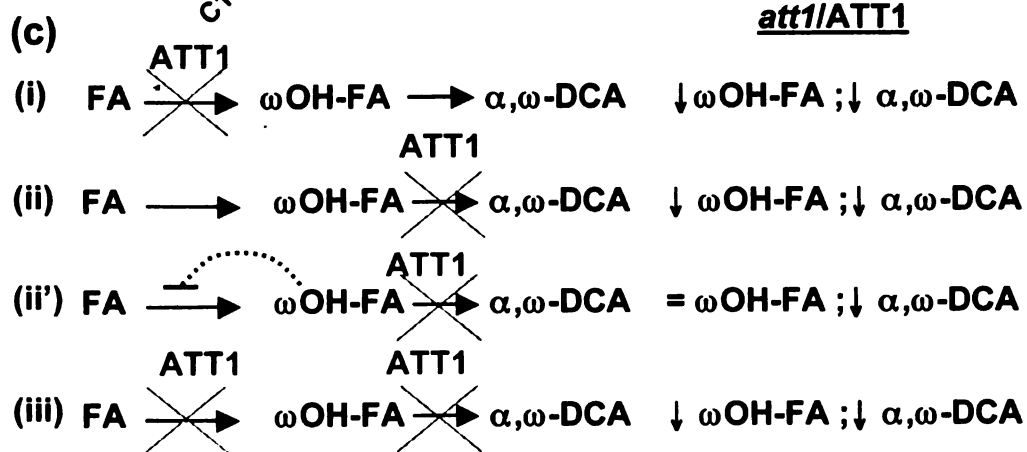
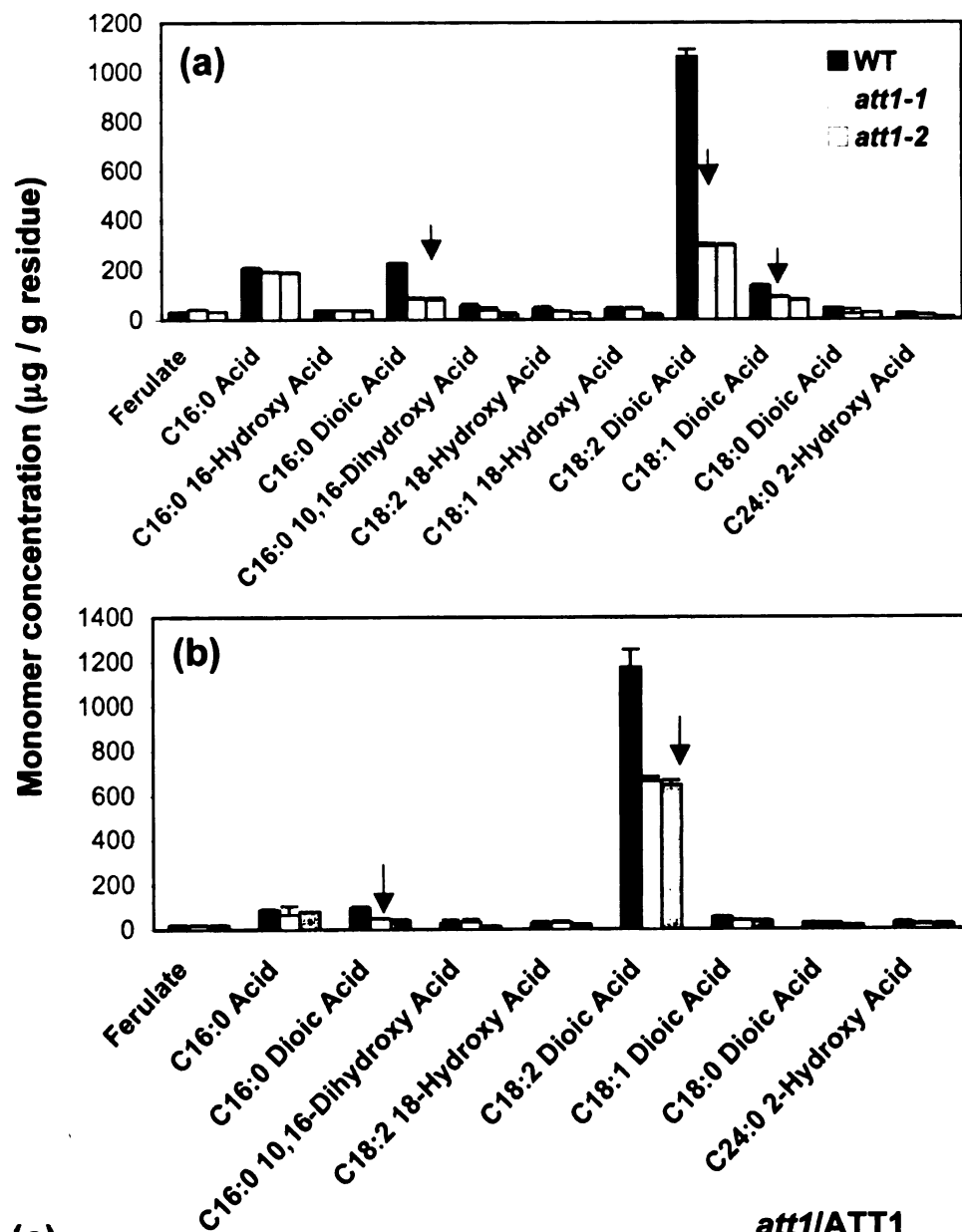


Figure 47.

Complementation of *att1* mutants with the ω -hydroxylase PH1 from *Petunia* stigmas

In an effort to better understand possible relationships between cutin and stigma polyester biosynthetic pathways, a complementation experiment to transform PH1 into *att1* lines was designed. As discussed above, the ability of CYP86A2 to catalyze hydroxylation of the terminal methyl of aliphatic monomers with variable chain lengths has been studied *in vitro*. Because a closely related ω -hydroxylase, PH1, has been found by the Jaworski laboratory to be required to produce lipid polyester monomers in stigma exudates of *petunia*, it was hypothesized that this enzyme could rescue *att1* mutants. Both *Arabidopsis* CYP86A2 and *petunia* PH1 proteins are composed of 533 aa, sharing 71.8% identity and 83.8% similarity (**Figure 48**). Interestingly, they also have PEST domains (PEST find score >5, <https://emb1.bcc.univie.ac.at/toolbox/pestfind/pestfind-analysis-webtool.htm>), which are associated with targeting to degradation and subsequent short half life (Rogers S. et al., 1986; Rechsteiner and Rogers, 1996).

Constructs were designed to express PH1 in epidermis (under the control of the epidermis-specific *Cer6* promoter) (Hooker et al., 2002) or ectopically (under the control of the CaMV35S promoter) (**Figure 49**). The *att1-1* mutant was transformed with pBI-based vectors (**Figure 49a-b**), carrying kanamycin resistance gene, and *att1-2* with pCambia-based vectors, carrying hygromy

PH1 1 S [REDACTED] AIP [REDACTED] NLEHIL [REDACTED] PH1 E
ATT1 1 G [REDACTED] AVF [REDACTED] NIEHMLT [REDACTED] ATT1 Q
consensus RAC GTYQTCICAiPFLArKqGLVTVTCDPKNiEHILK RFDNYPKGPTWQAVFHD LG

PH1 [REDACTED] VCGK [REDACTED]
ATT1 [REDACTED] NNYE [REDACTED]
consensus GIFNSDGDWLFQRKTAALEFTTRTLRQAMGRWVNraIK RfCPiLE AQ q PVDLQD

SRS1 PST (PH1)

PH1 [REDACTED] P [REDACTED] ELPENNFATS [REDACTED] IMPFVWKL [REDACTED]
ATT1 [REDACTED] TRCAGLEENGFSASAFI [REDACTED] ILRFLWR [REDACTED]
consensus LILRLTFDNICGLAFGKD T P LPEN Fat FDRATEatL RfImPEFvWkLKK LG

SRS2

PH1 [REDACTED] KQVINMTD [REDACTED] NHQNG [REDACTED] E [REDACTED]
ATT1 [REDACTED] SRG [REDACTED] ILGILDA [REDACTED] SQRES [REDACTED] E [REDACTED]
consensus LGLEVSL SL vD Ym VINTRK ELL G QrHDDLlSRFMKKKeqSYSD FL

SRS3

PH1 [REDACTED] LVSSNER EEP [REDACTED] T [REDACTED] NIT [REDACTED] KLE
ATT1 [REDACTED] T [REDACTED] ED [REDACTED] SV [REDACTED] T [REDACTED] S [REDACTED]
consensus HVALNFIILAGRDTSSVALSWFFWLvss P VEeKiL EICtiL ETRG D S W EPL

SRS4 PST (ATT1)

PH1 [REDACTED] Y [REDACTED] NIT [REDACTED] ST [REDACTED]
ATT1 [REDACTED] SV [REDACTED] AA [REDACTED]
consensus FeEVD LmYLKAALSETLRLYSPVPEDSKHvi DD LPDGTfVPAGS iTYSiY GRM

SRS5 Heme Binding

PH1 [REDACTED] QVQ [REDACTED] T [REDACTED] F [REDACTED] H [REDACTED] K [REDACTED]
ATT1 [REDACTED] VNH [REDACTED] Q [REDACTED] G [REDACTED] L [REDACTED] T [REDACTED]
consensus K WGEDCLEFKPERWmS D KF D fRfVAFNAGPRICLGKDLAYLQMKsIAAAVL

↑

PH1 [REDACTED] LVM [REDACTED] TP [REDACTED] T [REDACTED] LAKIEKFGKVE [REDACTED] CAGEHHLI
ATT1 [REDACTED] LV [REDACTED] HK [REDACTED] EVMKSLVPKERND-VVVLNGKC
consensus LRHRL VAPGHKVEQKMSLTfFMK GLvmNV RDL il i kes N

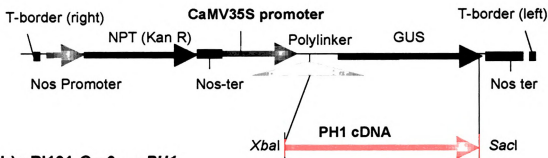
SRS6

PH1 N [REDACTED] HQP [REDACTED] NGIA [REDACTED] --- 553
ATT1 G [REDACTED] GEG--V [REDACTED] AAV [REDACTED] 553
consensus GI gsiAVNg Avav

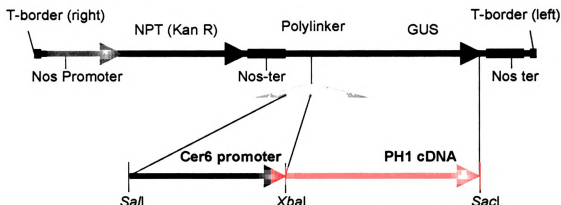
Figure 48. Deduced amino acid sequence alignment of *Arabidopsis thaliana* CYP86A2 (ATT1) and *Petunia hybrida* PH1 omega-hydroxylases.

The alignment was performed using ClustalW. Conserved residues are denoted in black. Substrate recognition sequences (SRS1-SRS6) are indicated in red (according to Duan and Schuler, 2005). The P450-signature motif is marked with a dotted blue rectangle. This motif contains the Cys residue that binds the heme-iron ligand (arrow). PESTs sequences were found in both proteins (green boxes).

(a) pBI121-CAMV35S_{Pro}::PH1



(b) pBI101-Cer6_{Pro}::PH1



(c) pCambia-Cer6_{Pro}::PH1 and pCambia-CAMV35S_{Pro}::PH1

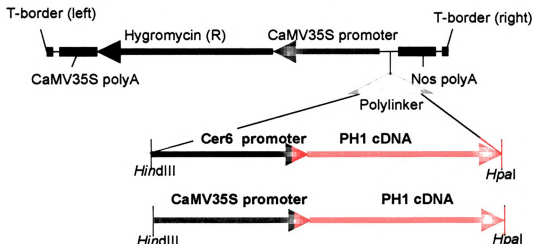


Figure 49. Binary constructs for complementation of Arabidopsis *att1* mutants with petunia ω -hydroxylase (PH1) cDNA.

(a) pBI101-Cer6_{Pro}::PH1 for *att1-1* transformation. **(b)** pBI121-CaMV35S_{Pro}::PH1 for *att1-1* transformation **(c)** pCambia-Cer6_{Pro}::PH1 and pCambia-CaMV35S_{Pro}::PH1 for *att1-2* transformation. See Experimental procedures for cloning details.

resistance gene (because *att1-2* plants might be kanamycin resistance) (**Figure 49c**), The toluidine blue test was used as an initial screen of T₁ antibiotic resistant plants. Several independent antibiotic-resistant lines in the *att1-1* genetic background (n>20) for each construct were screened for recovery of the wild-type impermeable phenotype. Less transgenic lines were recovered, and therefore screened, from transformed plants with *att1-2* background. Only four of them, all having *att1-1* background, were apparently less permeable to TBO compared to control plants (transformed with an empty vector).

Lipid polyester phenotype of transgenic lines

Selected plants (T₂) were subjected to chemical lipid polyester analysis (**Figure 50**) to detect any effect caused by PH1 hydroxylase on monomer production. Polyester monomers in leaves were released by NaOMe catalyzed transesterification and analyzed by GC on a DB-5 column. Dicarboxylic acid fractions in PH1-complemented lines remained the same as in the controls, except for one line transformed with the *35S_{Pro}::PH1 construct* (pBI121-*CaMV35S_{Pro}::PH1* in Figure 50), which shows one-fold increase in 18:2 dicarboxylic acid (but not C16:0 or C18:1) respect to the content of the empty vector control. Furthermore, despite the proposed catalytic role played by PH1, no increases in ω -hydroxy FAMES were observed. These data suggest that PH1

is not able to complement ATT1. However, from the above polyester composition results it cannot be concluded

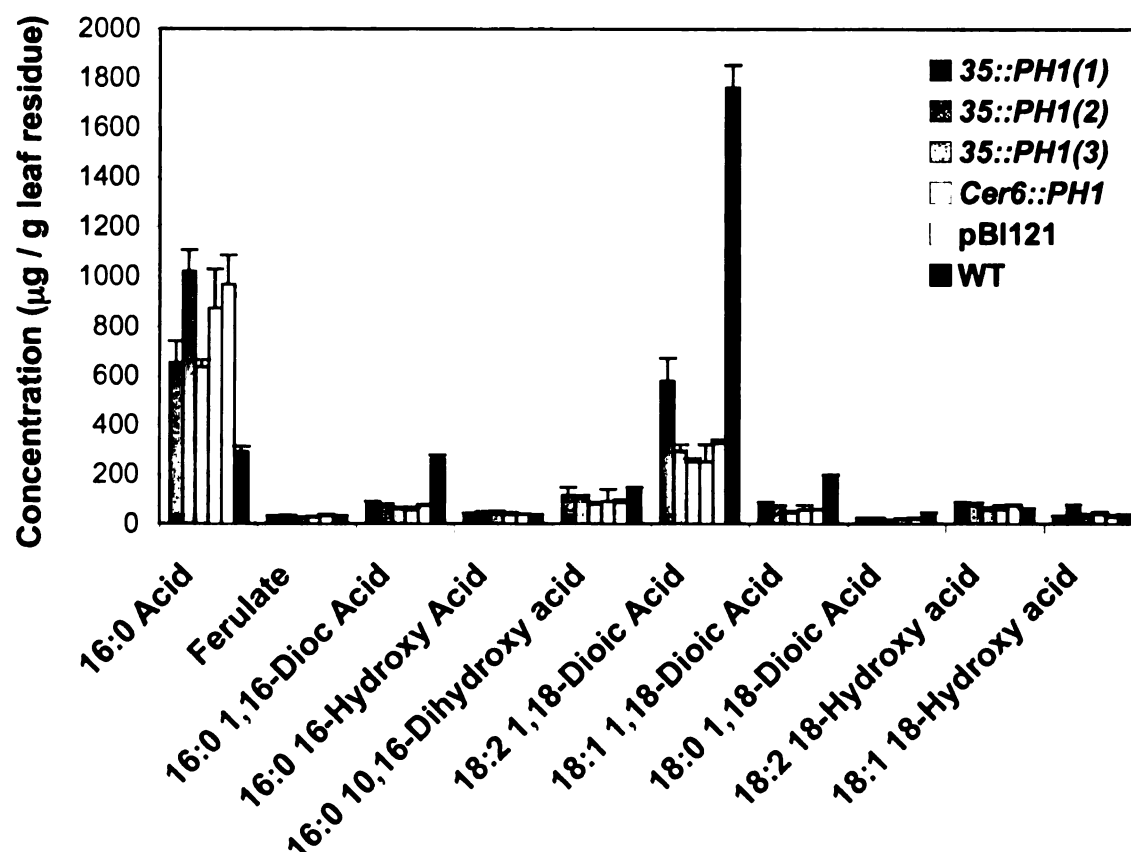


Figure 50. Lipid polyester phenotype of PH1-transformed *att1-1* lines. Solvent-extracted leaf residues were depolymerized by NaOMe catalyzed transmethylation and analyzed by GC. pBI121 corresponds to *att1-1* mutant transformed with empty vector, used as negative control. A wild-type Arabidopsis Col0 control is also included. The means of triplicate determinations \pm SD are reported

that the petunia gene was translated to a functional enzyme, and that the enzyme was stable in the transformed mutants. In fact, a western blot analysis of roots from several transgenic lines developed with an anti-PH1 polyclonal antibody did not detect the protein (data not shown). This observation cannot be taken as a categorical result because the reactivity of the antibody to PH1 was

low and would possibly not detect low levels of the recombinant protein. Assuming that PH1 was expressed as a functional enzyme in tobacco stigmas, these results suggest that it did not complement the dye permeation or the low dicarboxylic acid content of the disrupted At4g00360 (*ATT1*) gene. As shown in Chapter 4, *ATT1* is specifically expressed in guard cells (**Figure 24**). Since the promoters used for PH1 expression were *Cer6* and 35S, one reason for the lack of complementation is that these promoters are not specific enough to make the cuticular projections on guard cell hydrophobic. In other words, if guard cells are the main point of entry of the toluidine blue solution, this would explain why all transgenic lines remained permeable.

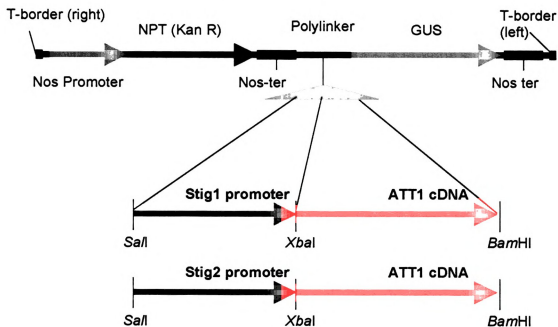
Over-expression of At4g00360 (*ATT1*) in stigmas of *Nicotiana tabacum*

Transgenic tobacco plants were generated as described in Materials and Methods, using pBI- and pCambia-based binary constructs to specifically overexpress At4g00360 (*ATT1*) in stigmas (**Figure 51**). The stigma-specific promoters Stig1 from tobacco (Goldman et al., 1994), or Stig2 (PH1 promoter, obtained from J. Jaworski) from petunia were fused upstream the *ATT1* cDNA sequence. For each construct, including empty vector controls, 20 transgenic lines were produced. Only stigmas in the stage immediately prior to flower opening were harvested for lipid analysis. Since an increase in ω -hydroxylated monomers was expected, presumably as part of higher molecular weight

Figure 51. Binary constructs used for overexpression of At4g00360 (ATT1) in stigmas of *Nicotiana tabacum*.

The Arabidopsis cDNA was over-expressed under control of the stigma specific tobacco promoter (Stig1; Goldman et al., 1994), or the petunia stigma specific *PH1* promoter (Stig 2) **(a)** pBI101-based constructs **(b)** pCambia-based constructs. See Materials and Methods for cloning details.

(a) pBI 101- based constructs



(b) pCambia- based constructs

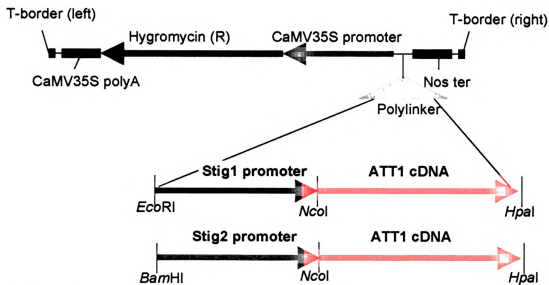


Figure 51.

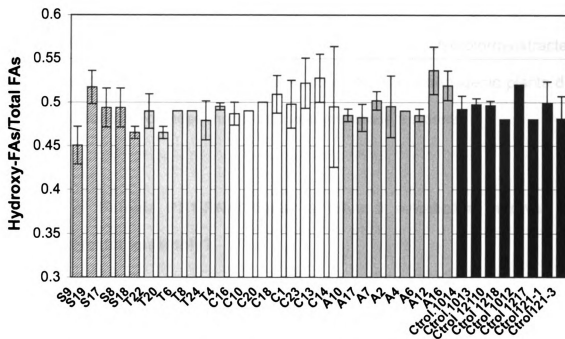


Figure 52. Lipid analysis in whole stigmas of tobacco transgenic lines.

Total fatty acid methyl esters were analyzed by direct methylation of whole stigmas, and the ratio of ω -hydroxy fatty acids to total fatty acid was plotted to visualize any possible changes in ω -hydroxy fatty acid content in transgenic lines. S: pBI-*Stig1_{Pro}::ATT1*; T: pBI-*Stig2_{Pro}::ATT1*; C: pCambia-*Stig1_{Pro}::ATT1*; A: pCambia-*Stig2_{Pro}::ATT1*; Controls: empty vector transformed lines. For each line, the mean of at least triplicate determinations \pm SD is reported.

estolides such as those found in petunia stigma exudates (see **Figure 7** in Chapter 1), total FAMES were determined by direct transmethylation. The ratio of ω -hydroxy fatty acids to total FAMES was calculated for the different transgenic lines, and results from some of the transgenic plants analyzed at least in triplicate are shown in **Figure 52**. No significant effect on the amount of ω -hydroxy fatty acid monomers was observed in ATT1-expressing lines compared to controls (t test, $P = 0.23-0.47$). Because of the uncertainty about ATT1-oxidation products discussed above, dicarboxylic acids could be potentially found in the transgenic

stigmas. Dicarboxylates are not commonly found among stigma polyester monomers. Investigation of monomers released from both chloroform-extracted (soluble) and remaining stigma (insoluble) polyesters from transgenic plants did not show production of these monomers in any of these fractions.

Analysis of Petunia PH1-RNAi lines. Is there a metabolon involved in stigma polyester assembly?

As noted above, there are no reports on ω -hydroxy acid-accumulation in transgenic plants overexpressing cytochrome P450 genes. Also, the mostly negative results on over-expression of cytochrome P450 enzymes reported in this chapter, raised new questions: What is the biochemical reaction catalyzed by ATT1?, Are these enzymes part of protein complexes that need to be co-expressed with other genes? If that were true, does this putative complex include a still unknown polyester synthase?. To begin to address these issues, I have used PH1-RNAi petunia lines to test the idea of cooperating enzymes organized into a macromolecular complex for polyester assembly.

As found in other biological systems, polyester-synthesizing enzymes may be physically bound together in a meta-structural unit, or metabolon (Winkel, 2004). The hypothesis of a closely integrated molecular unit could explain problems with overexpression of P450 genes. Identifying such a protein complex or membrane domain would help discover additional gene products, as well as

define how the assembly occurs. In addition to the experiments described above, I have overexpressed ATT1 in wild-type Col-0 background using three different promoters: *CaMV 35S* for ectopic expression, and *Cer6* and *ATT1* for epidermis-specific expression. None of the transgenic lines transformed with these constructs showed changes in monomer load/composition (data not shown). Moreover, J. Jaworski's group has done control experiments where (i) ATT1 did not restore hydroxy fatty acid formation in PH1 RNAi lines of petunia, and (ii) where PH1 over-expression in tobacco did not change hydroxy fatty acid content of the stigma polyester. Although there is no direct evidence for its existence, the above results are consistent with a metabolon view of polyester assembly and, therefore, I have tested this hypothesis as described below.

Three petunia PH1 RNAi lines (available from Jaworski lab), which show different degrees of reduction in ω -hydroxylated monomer content, and wild-type petunia stigmas, have been used to address the question: Does the size (MW) of the petunia stigma polyester change as the amount of hydroxy-fatty acid is reduced by RNAi titration? To test the metabolon hypothesis, I have performed TLC analysis of solvent-extracted polyesters from stigmas of the mentioned petunia lines and wild-type tobacco, to look for oligomers at low hydroxy-fatty acid content. Two possible outcomes are illustrated in **Figure 53**. If the size of the polyester does not change when less hydroxylated monomers are available (constant size, **Figure 53d**), then the hydroxylase is likely part of a metabolon

(**Figure 53c**). However, if the size is a function of hydroxylated monomer availability the results shown in **Figure 53b** are predicted.

Analysis of hydroxy fatty acids relative to total fatty acids (**Figure 54a**) confirmed the reduction in hydroxylated monomers in the PH1 RNAi lines. TLC results illustrated in **Figure 54b** show that, when less ω -hydroxylated monomers are available (mid-content line), the profile is similar to that of tobacco with the estolides usually present in wild-type petunia (~50 acyl groups/molecule) being replaced by shorter oligomers ($\text{TAG}_{(n)}$). The high-content line is undistinguishable from the wild-type petunia in both monomer ratio (**Figure 54a**) and TLC profile (**Figure 54b**). In the low-content line, the 90% reduction in hydroxylated monomers is reflected in an almost complete disappearance of estolides of glycerolipids. In this line, the dominant lipids are triacylglycerol, α,α -diacylglycerol and α,β - diacylglycerol. Interestingly, α,α -diacylglycerols are rare in other biological systems. Their accumulation in the PH1-RNAi lines suggests that a different type of acyl-transferase is involved in the synthesis of these atypical diacylglycerols. These results suggest that shorter polyesters are synthesized when less monomers are available. This is consistent with a non-mentabolon view of the system (**Figure 53a,b**).

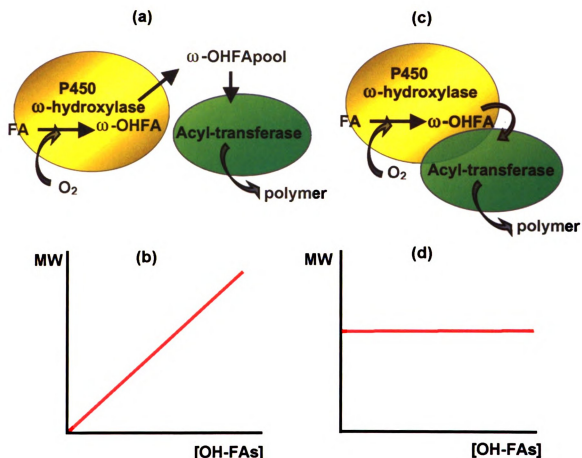


Figure 53. Analysis of poly-hydroxy fatty acids in petunia RNAi lines to test the "metabolon" hypothesis:

If the P450 enzyme acts independently of other functions (a), larger polyesters should be found in the exudates when the concentration of ω -hydroxylated monomers increase (b); if the enzyme is part of a metabolon (c), the size of the polymer is expected to be independent of the amount of ω -hydroxylated monomers available (d). For simplicity, the P450 reductase necessary to reduce the P450 enzyme is not shown

Figure 54. Analysis of solvent-extracted stigma lipids of petunia PH1 RNAi lines.

(a) Percentage of hydroxy fatty acids (OH FAs) in total fatty acids determined by transmethylation and GC analysis of released monomers from stigma lipids. **(b)** TLC analysis of solvent-extracted lipids from stigmas of Petunia RNAi lines. Three transgenic lines with high, intermediate, and low hydroxy fatty acid content were compared to petunia and tobacco wild-type stigma lipids. Standards: triolein (C18:1 triacylglycerol); Diolein ($\alpha\alpha$: C18:1 1,3 diacylglycerol; $\alpha\beta$: C18:1 1(3),2 diacylglycerol).

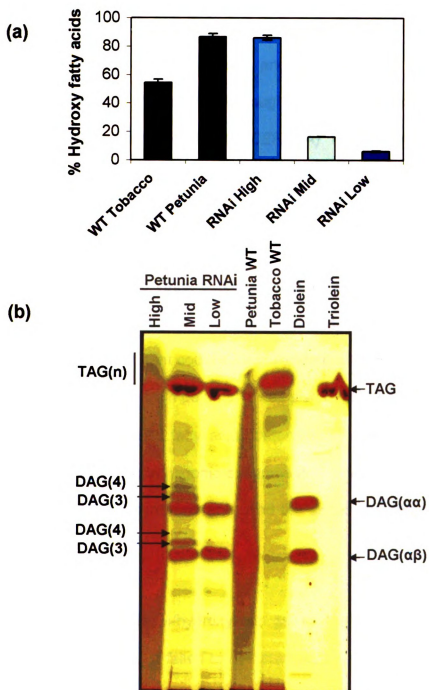


Figure 54.

DISCUSSION

The activity of several Arabidopsis P450 ω -hydroxylases has been previously demonstrated by expression in yeast and insect cells (Benveniste et al., 1998; Wellesen et al., 2001; Duan and Schuler, 2005; Benveniste et al., 2006; Rupasinghe et al., 2007). Although the physiological significance of CYP86A2 (*ATT1*) and CYP86A8 (*LACERATA*) has been shown *in planta* (Wellesen et al., 2001; Xiao et al., 2004), only *att1* has been biochemically analyzed and reported to have altered lipid polyester composition. In the study of Xiao et al (2004) a 70% reduction in total lipid polyester monomers was observed and, together with *in vitro* yeast expression data the conclusion was made that *ATT1* encodes a fatty acid omega hydroxylase. Based on this conclusion, it was expected that the *att1* mutant could be complemented by PH1 (Han et al., 2005), which is a ω -hydroxylase from petunia. It was also hypothesized that ATT1 would improve the ω -hydroxylated fatty acid content when overexpressed in tobacco stigmas. These very first transgenic experiments in this project were oriented to test ideas on polyester synthesis and used the simple concept of expression of reciprocal genes.

When the petunia ω -hydroxylase gene, *PH1*, was overexpressed in Arabidopsis *att1* mutants, it failed to complement the dye permeability mutation. Analysis of lipid monomer loads indicated no change in the transgenic lines relative to the mutant phenotype. These observations suggest that PH1 is not enough to rescue the phenotype and a downstream activity may also be

necessary. However, this result could also be as a consequence of instability of the enzyme in *Arabidopsis*, because the protein could not be detected in the transgenic plants by western blot (data not shown). Both PH1 and ATT1 proteins contain PEST sequences (**Figure 48**), an indication they may have a short half-life. Cytochrome P450s are highly regulated proteins; if not recognized by the new host or if they do not have their binding partners are likely degraded. Another explanation is that neither 35S nor *Cer6* promoters, although both known to be expressed in epidermis, may not be strong enough in guard cells to allow the proper synthesis of hydrophobic ledges that block the entrance of water through stomatal pores.

Attempts to use ATT1 to increase the amount of ω -hydroxy fatty acids in tobacco stigmas (and also the size of the estolides) were equally unsuccessful, despite the use of two different promoters and vectors for the overexpression. Unfortunately, specific antibodies to detect the transgenic protein by western blot were not available and I could not corroborate its presence. A number of reasons can explain the failure of the complementation approaches, such as incompatibility between species, enzyme requirements (i.e. co-localization of an electron transfer partner such as NADPH P450 reductase), protein instability, or requirement for co-overexpressing other upstream/downstream proteins (Schuler and Werck-Reichhart, 2003). Another plausible explanation arises from modeling of tobacco stigma lipid polyester biosynthesis (Mike Pollard, unpublished results). In a model that best explains the product distribution of ω -hydroxy fatty acid

monomer polymerization in tobacco stigmas, the rate-limiting step is not the hydroxylation rate, but is elsewhere downstream of this reaction (e.g. acyl-transfer step, chain termination step). Hence, an increase in omega-hydroxylase activity would not affect the accumulation/length of polyesters. Furthermore, in this scenario, a transient increment in ω -hydroxy fatty acid monomers, which are not rapidly incorporated to a growing chain, might be quickly degraded by mechanisms designed to prevent accumulation of toxic fatty acids in the cells. Nevertheless, because this model was built considering a simple chemical polymerization process, it may not reflect the complexity of living cells.

Despite close similarity between ATT1 and PH1, expression experiments failed in both directions. This is a significant observation about P450s being highly controlled. However, the failure of the PH1 complementation may be because the correct promoter (i.e. ATT1 promoter) was not used.

What is the biochemical reaction catalyzed by ATT1?

Both over-expression in tobacco stigma and complementation of *att1* approaches failed to yield a chemical phenotype. These results emphasize that we do not have a clear answer to the question: what is the actual reaction catalyzed by ATT1? I have shown that the *att1* mutation specifically affects the deposition of 18:2 DCA, 18:1 DCA and 16:0 DCA in leaves, stems, and also in seeds. Surprisingly, levels of ω -hydroxy fatty acids remained comparable to wild

type in leaf and stem, although the C18:2 ω -hydroxy fatty acid fraction was somewhat higher in seed compared to wild type. These are not the results that would be expected if ATT1 only catalyzes omega-hydroxylation, as depicted in **Figure 47c-i**. Taken together, the lipid polyester phenotype observed in various tissues of *att1* mutants suggested that the catalytic function of the enzyme may not be simply omega-hydroxylation of cutin monomers. My results were also not in agreement with the data reported previously (Xiao et al., 2004), which showed that a wide range of monomers was affected. Thus, the data presented did not provide clear evidence to confirm that the *in vivo* catalytic activity of ATT1 is just fatty acid ω -hydroxylation.

This question has different aspects. It is not clear what is the oxidation reaction actually catalyzed by ATT1; and substrates (whether free fatty acids or other acyl chains) as well as acyl chain-length specificity are not defined. These uncertainties are illustrated in **Figure 55** that places ATT1 in the context of biosynthesis of an acyl-glycerol, a putative building block of Arabidopsis cutin.

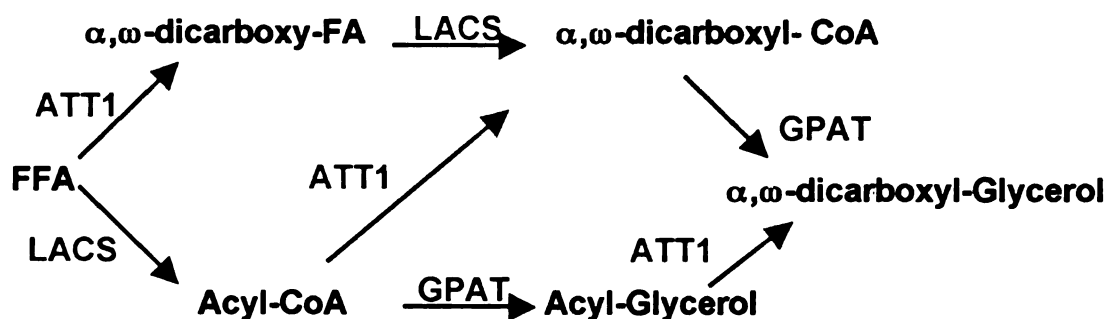


Figure 55. Possible biosynthetic pathways for the synthesis of acyl-glycerol units.

Biochemical data is insufficient to determine substrates and products for CYP86A (ATT1), LACS, and GPAT in the synthesis of lipid polyesters. Synthesis of one possible type of building block is shown (α,ω -dicarboxyl-glycerol), which is predominant in Arabidopsis lipid polyesters. Intermediate steps from fatty acid to dicarboxylate are not shown. Note that only one scenario was considered in Figure 7c (free fatty acid substrates for all steps). FFA: free fatty acid; LACS: long chain acyl-CoA synthetase; GPAT: glycerol-3-phosphate acyltransferase; ATT1: CYP86A2 (cytochrome P450 fatty acid oxidase).

Several lines of evidence indicate that ATT1 might not just act as a simple ω -hydroxylase. First, *att1* lipid polyester analysis demonstrated a decrease in dicarboxylic acid fraction without change in the corresponding ω -hydroxylated monomers (Figure 47, Molina et al., 2008). Second, attempts to complement the *att1* mutant with a well-characterized ω -hydroxylase (PH1) were unsuccessful. Third, *ATT1* overexpression in tobacco stigmas did not result in an increased content of ω -hydroxy fatty acids in the exudates. Likewise, a control experiment performed by J. Jaworski's group showed that transgenic tobacco stigmas overexpressing PH1 did not accumulate hydroxylation products compared to wild-type stigmas (data not shown). Additional evidence comes from *in vitro* assays. Expression in yeast microsomes revealed that CYP86A2 (ATT1) has high activity

towards C14:0 free fatty acid substrates, which have no demonstrated physiological function in plants (e.g. cutin or glycerolipid synthesis). In addition, compared to other ω -hydroxylases of the CYP94, and CYP96 subfamilies, ATT1 had the lowest activity towards C18:1 free fatty acids (Benveniste et al, 2006). Expression in insect cells showed that CYP86A2 (ATT1), as well as the rest of the CYP86A members, are able to catalyze hydroxylation in the omega position of lauric acid (C12:0) (Duan and Schuler, 2005), and oleic acid (C18:1) (Rupasinghe et al., 2007). Based on above described *in vitro* experiments it is generally assumed that the preferred substrate for p450s are free fatty acids, but substrates such as acyl-glycerols have not been tested in such studies.

According to the results presented in this chapter, two hypothetical pathways leading to dicarboxylic acids are proposed (**Figure 56**). CYP86A2 function could likely be related to tobacco CYP94A5 (Le Bouquin et al., 2001), or Arabidopsis CYP94C1 (Kandel et al., 2007). These monooxygenases catalyze the complete set of reactions leading to the oxidation of a terminal methyl group to the carboxyl function (**Figure 56 a**). Another recent example found in the literature suggests that animals have two parallel mechanisms co-existing for omega-oxidation of fatty acids: a NADPH-driven pathway, where one (or more) P450(s) are involved in ω -hydroxylation of docosanoic acid (C22:0) and subsequent oxidation to C22:0 dicarboxylic acid, and a NAD⁺-driven pathway, where production of C22:0 dicarboxylic acid is catalyzed by dehydrogenases.

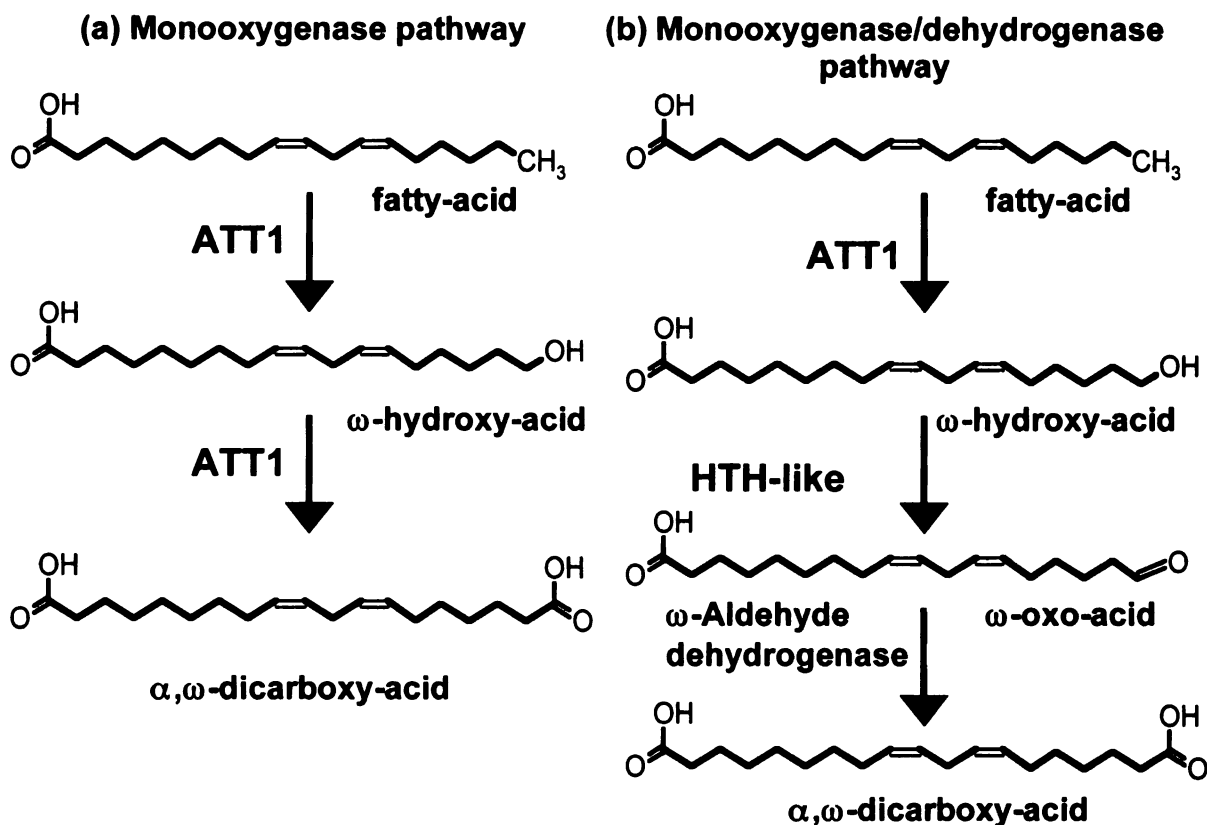


Figure 56. Hypothetical reactions catalyzed by CYP86A2 (ATT1) in the route of biosynthesis of dicarboxylic acids in Arabidopsis epidermal cells.

(a) Illustrates a metabolic route involving only P450 monooxygenases (ATT1). (b) A P450 hydroxylase (ATT1) catalyzes only the ω-hydroxylation step. Further oxidations are catalyzed by an ω-hydroxy acid dehydrogenase (HOTH-12-like) and ω-aldehyde dehydrogenase (no genes identified so far) (Kurdyukov et al., 2006b).

An alternative route for the oxidation of terminal hydroxyl functions has been recently suggested in Arabidopsis epidermal cells (Kurdyukov et al., 2006b) (**Figure 56 b**). The authors have characterized an organ fusion mutant, *hth-12*, which is apparently unable to oxidize ω-hydroxy fatty acids to ω-oxo fatty acids. The transposon mutant presented a chemical phenotype with 24% reduction in α,ω-dicarboxylic acids, 25% increase in levels of ω-hydroxy fatty acids, and accumulation of an ω-oxo acid in leaf residues. However, ω-oxo acid is not a

major cutin monomer, and the authors did not provide a MS spectrum supporting its chemical structure. It is proposed that *HOTHEAD* (*HTH*) encodes a dehydrogenase that oxidizes alcohols to aldehydes, thereby acting downstream of the ω -hydroxylation step catalyzed by CYP86A8 (*LCR*), although this remains a speculation since *in vitro* evidence is not provided. However, there is some evidence in the literature for the existence of this pathway in suberin synthesis. Early biochemical experiments have shown that a ω -hydroxy fatty acid dehydrogenase is required for the synthesis of α,ω -dicarboxylic acids in wound-healing potato tubers (Agrawal and Kolattukudy, 1977). If an ω -alcohol dehydrogenase acts coordinately with *ATT1* towards producing dicarboxylates (**Figure 56b**), a high transcript co-response between both genes would be expected. In fact, *LCR* and *HTH* are highly correlated ($r^2 = 0.513$) (Zimmermann et al., 2005). Pairwise correlations with five Arabidopsis putative long-chain fatty acid ω -alcohol dehydrogenases described by Kurdyukov (2006), included in the *HTH* clade, showed that At3g56060 is co-upregulated with *ATT1* ($r^2 = 0.369$). In addition, this gene is up-regulated in stem epidermis (Suh et al., 2005).

The hypothesis that cytochrome P450s are part of metabolic units devoted to polyester synthesis in wet stigmas was not supported by analysis of petunia lines with reduced amounts of PH1 and ω -hydroxylated monomers (**Figure 54**). Ectopic over-expression of *ATT1* (data not shown) and CYP86A1 (Li et al., 2007a) in wild-type Arabidopsis did not result in changes in lipid polyester composition or load. In fact, my results helped the lab to realize that more than

one gene might be required to observe accumulation of ω -oxidated monomers in cutin. Only when CYP86A1 was co-expressed with the acyl-transferase GPAT5, cutin oxygenated monomers increased by 80%. Furthermore, overexpression of either GPAT4 or GPAT8 resulted in increases in C16 and C18 cutin monomers. Taken together, these results imply that acyl-transfer to a glycerol-based substrate is the limiting step in polyester synthesis in *Arabidopsis* (Li et al., 2007a).

In conclusion, although the different approaches used in this work failed to explain the ATT1 catalytic function *in planta*, my observations question its role as a simple ω -hydroxylase. The same question may apply to other members of CYP86A, such as CYP86A1 discussed in Chapter 4 and by Li et al. (2007a). However, analysis of *cyp86A1* roots showed a clear reduction of both ω -hydroxy fatty acids and α,ω -dioic acids. More research is needed not only to understand this particular enzyme function, but also to demonstrate whether cutin and polyesters found in stigma exudates are synthesized by similar pathways. Suggestions for future investigations are discussed in Chapter 6.

EXPERIMENTAL PROCEDURES

Binary constructs for tobacco transformation

Amplification of DNA fragments. Full-length stigma specific promoter sequences, *Stig1* (from *Nicotiana tabacum*) (Goldman et al., 1994) and *Stig2* (from *Petunia hybrida*, generously provided by Dr. Jan Jaworsky), and At4g00360 cDNA (from clone BX827611 in pCMV Sport6, obtained from The National Center of Plant Genomic Resources, Toulouse, France) were PCR amplified with the proofreading polymerase Pfu Turbo (Stratagene, La Jolla, CA, USA) and the primer pairs were designed to introduce restriction sites for cloning into pBI101 (Clontech, Palo Alto, CA) and pCambia 1390 (CAMBIA, Canberra, Australia), as detailed in **Table 9**. Amplification products were run on a 1% agarose gels and purified using the Qiaquick Gel Isolation Kit (Quiagen, Valencia, CA). PCR conditions were as follows: 95°C for 5 minutes, followed by 30 cycles of 30 sec at 95°C, 30 sec at 51 to 55°C (depending on the T_m of the primer pairs), 2 min at 72°C, with a final extension step at 72°C for 10 min.

Ligation and transformation reactions. Amplified DNA fragments were subcloned into pGEM[®]-T Easy vector (Promega Corporation, Madison, WI) using T4 DNA ligase supplied with the kit. Positive and background controls were prepared in parallel. The reactions (20 µl final volume) were incubated overnight

at 10°C, after which 10µl of each were used to transform 50 µl DH5α competent cells. Transformation was performed by heat shock and bacteria were plated onto LB/Ampicillin/IPTG/X-Gal plates.

Plasmid extraction and sequencing. White bacterial colonies were picked and grown overnight at 37°C with agitation in 5 ml Luria broth supplemented with Ampicillin (100 µg/ml). Recombinant plasmids were purified using Wizard® Plus SV Minipreps DNA purification system (Promega). Insertion of the PCR product into the plasmid was verified by digestion of 1 µl of recombinant plasmid followed by agarose gel electrophoresis.

DNA inserts in recombinant plasmids were sequenced on both strands using Applied Biosystems cycle sequencing technology (Applied Biosystems, Foster City, CA), and sequences were determined on an ABI PRISM® 3100 Genetic AnalyzerB. Primers used for sequencing were Sp6 (5'-ATTAGGTGACACTATAG-3'), T7 (5'-TAATACGACTCACTATAGGG-3'), and internal specific primers for the At4g00360 cDNA sequence (5'TGCGGTTTAGCATTCGGTA 3' and 5'CCTCTCCGGTTTGAATTCC 3'). Sequence data were analyzed using Clustal W program.

Cloning in binary vectors. *Stig 1* and *Stig 2* promoters were released from pGemT easy using the created restriction sites and subcloned in pCambia 1390

and pBI101 digested with the same enzyme pairs. Ligation products were purified as described above, and digested to introduce the At4g00360 cDNA fragment. Final constructs are schematized in **Figure 41**.

Table 9. Oligonucleotides for amplification of stigma-specific promoters and *ATT1* cDNA.

DNA fragment	Binary vector			
	pBI101		PCambia 1390	
	Primer pair	Added restriction site	Primer pair	Added restriction site
Stig1 promoter	5'cacacg <u>tcgac</u> CCCGA GCTGTATATGTTTGC A 3' 5'cacact <u>ctaga</u> CATGGT TTGATACTGGTGGTT TC3'	<i>Sall</i> <i>Xbal</i>	The promoter sequence was released by digestion with <i>EcoRI</i> and <i>NcoI</i> restriction enzymes.	
Stig2 promoter	5'cacact <u>ctaga</u> CTTTTA ATAACACCAACTTCC TGT3' 5'cacacg <u>tcgac</u> CATGC AGAAAACTACAGTTT ACTAAT 3'	<i>Xbal</i> <i>Sall</i>	5'cacacc <u>atgg</u> CTTTT AATAACACCAACT TCCTGT 3' 5'cacacg <u>gatcc</u> AGAA AACTACAGTTTAC TAATTTTTTTTT3'	<i>NcoI</i> <i>BamHI</i>
At4g00360 cDNA	5'cacact <u>ctaga</u> TTTTTG GAAACACCATTTTCAT A 3' 5'cacacg <u>gatcc</u> AACAAA AACAAATCAAACCTTC TTTA 3'	<i>Xbal</i> <i>BamHI</i>	5'cacacc <u>atgg</u> TTTTT GGAAACACCATTT CATA3' 5'cacag <u>ttaac</u> AACAA AAACAATCAAACCT TTCTTTA3'	<i>NcoI</i> <i>HpaI</i>

Binary constructs for complementation of *att1* mutants

Four constructs were designed to express PH1 in Arabidopsis *att1* mutants under the control of the constitutive *CaMV35S* promoter or the epidermis specific *Cer 6* promoter (Hooker et al., 2002). The full length *PH1* coding region was kindly provided by Dr Jan Jaworski (Donald Danforth Plant Science Center, St. Louis, Missouri). This sequence was amplified by PCR using 5'cacacttctagaATGGAAGTATCAACAACATGATGATTG 3' (*Xba*I restriction site underlined) and 5' cacacgagctcTCAAGCAGCAATCCCATTACT 3' (*Sac*I restriction site underlined) primers. The *Cer6* promoter was amplified by PCR from Arabidopsis genomic DNA using 5' cacac gtcgac TCTTCGATATCGGTTGTTGACG 3' (*Sal*I restriction site underlined) and 5'cacac tctaga CGTCGGAGAGTTTTAATGTATAATTG 3' (*Xba*I restriction site underlined) primers. The final constructs for *att1-1* transformation were as follows: *PH1* was introduced into pBI121 binary vector, which contained the 35S promoter, by releasing the GUS sequence using *Xba*I and *Sac*I restriction sites (pBI121-*PH1*), and *Cer6* promoter and *PH1* cDNA were cloned into pBI101 using *Sal*I/*Xba*I and *Xba*I/*Sac*I, respectively (pBI-*Cer6_{Pro}*-*PH1*). For *att1-2* transformation, constructs were designed in pCambia 1390 vector as follows: pBI121-*PH1* and pBI101- *Cer6_{Pro}*-*PH1* were digested with *Sac*I, and the sticky ends were filled with T4 polymerase to convert them to blunt ends. Upon digestion with *Hind*III, the cassette was released and cloned into pCambia1390

digested with *Hind*III and *Hpa*I. Cloning procedure was as described above for constructs for tobacco transformation. Constructs are schematized in **Figure 49**.

***Agrobacterium* transformation**

Binary plasmids were introduced by electroporation into electro-competent *Agrobacterium tumefaciens* strain LBA4404 (for tobacco transformation) or strain C58Cl (for *Arabidopsis* transformation). Cultures were grown for 5-6 h in liquid YEP without antibiotics at 30°C with shaking. Transformed colonies were selectively grown in YEP plates containing 50 µg/ mL Rifampicin, 25 µg/ mL Gentamycin and 50 µg/ mL Kanamycin for C58Cl, and 50 µg/ mL Rifampicin , 25 µg/ mL Streptomycin and 50 µg/ mL Kanamycin for LBA4404.

Generation of transgenic tobacco lines by *Agrobacterium* transformation

Agrobacterium cultures were incubated on YEP plates for 3 days. Liquid selection medium (10 ml) was directly poured onto the plate surface to make a suspension. The bacterial culture was used to incubate tobacco leaf disks (grown in sterility on MS medium) for 5-10 min. Explants were briefly dried on sterile filter paper and then incubated on regeneration medium at room temperature for 2 days in the dark. All these steps were performed in a sterile transfer hood. Leaf disks were then transferred to selection medium plates and incubated in a growth room at 25°C with a 16/8 h light/dark cycle, changing the

plates for fresh ones every 2 weeks. Shoots visible after 2-3 weeks, were transferred to root inducing medium. When roots were formed (after 1-2 weeks), seedlings were carefully transferred to soil and grown in a greenhouse. Media compositions were as follows: MS agar (1L): 4.3 g MS salt, 10 g sucrose, 1 mL B5 vitamins 1000x, pH5.7 (with KOH); B5 vitamins 1000X (10 mL): 1g Myo-inositol, 0.1 g Thiamine-HCl, 10 mg Nicotinic acid and 10 mg Pyridoxine-HCl; Regeneration medium (500 mL): 2.15 g MS salt, 5 g sucrose, 3.5 g Phytagar, 0.5 mL, B5 vitamins 1000x, 0.5 mg BAP and 0.05 mg NAA; Selection medium: regeneration medium plus 250 µg/mL Carbenicillin and 100 µg/mL Kanamycin (pBI constructs) or 10 µg/mL Hygromycin (pCambia constructs). Rooting medium: MS agar plus antibiotics.

Transformation of *A. thaliana att1* mutants

Arabidopsis plants were transformed using the vacuum infiltration method (Bechtold et al., 1993). Transformed plants were selected on the basis of kanamycin resistance (for pBI constructs) or hygromycin resistance (for pCambia constructs).

Reverse Transcription Polymerase Chain Reaction (RT-PCR)

RNA was isolated from approximately 10 mg of leaf or stem tissue using the RNeasy Plant Mini Kit (Qiagen, Valencia, CA). Manufacturer's instructions

were followed, including the optional steps of heating sample in Buffer RLT for 3 min at 56°C, and extra spin step following addition of wash buffer. Membranes were eluted with 30 µl of RNase-free water.

Aliquots of RNA (10 µl) were used as template for reverse transcription polymerase chain reaction (RT-PCR). SuperScript III Reverse Transcriptase (Invitrogen) was used to synthesize the first-strand cDNA, following manufacturer's protocol. Sample was RNaseH treated for 20 minutes at 37°C following the reverse transcription reaction. A 2 µl aliquot of the RT reaction was used as template in PCR with. Primers used for amplification of the At4g00360 gene were as follows: ATGTCTCCAACACGATGCTCC (forward); CGTTGCATTTTCCGTTAAGAA (reverse). Amplification conditions were as follows: 95°C for 2 minutes, followed by 30 cycles of 30 sec at 95°C, 30 sec at 56°C, 2 min at 72°C, with a final extension step at 72°C for 10 min.

Stigma fatty acid analysis

Tobacco stigmas were carefully harvested with forceps to avoid contamination with pollen. Samples containing 5 stigmas were placed into screw capped tubes and stored at -80°C until analysis. Lipids were determined by direct methylation, adding 1 ml of 5% (v/v) sulphuric acid in methanol plus 0.5 ml of chloroform as a co-solvent. The following internal standards were used: 200 µg

of C17:0 TAG, 200 µg squalane and 200 µg pentadecalactone (15:0 15OH). The reaction was incubated at 80°C for 2 hours. To extract FAMES, 1.5 ml 0.9% NaCl (wt/vol. aq) and 3 ml hexane were added to each tube and centrifuged 5 min at 2000 rpm, repeating the hexane extraction once more. Anhydrous sodium sulphate was added pooled extracts, which were finally evaporated under nitrogen. Samples were acetylated by reacting with 0.1 ml pyridine plus 0.1 ml acetic anhydride at 60-70°C for 1 hour and analyzed by GC on a DB23 column.

Cutin analysis

Hydrogenolysis with LiAlH₄ was performed using the method described by Bonaventure et al. (2004). Analysis by NaOMe catalyzed transmethylation is described in Chapter 2 (p. 81).

Analysis of Petunia RNAi stigma lipids

Petunia PH1 RNAi lines were provided by J. Jaworski (Han et al., 2005). Stigma samples (10 each, ~30-40 mg) were solvent-extracted in four sequential steps: isopropanol (twice), chloroform:methanol (2:1), and chloroform:methanol (1:2). Pooled extracts were dried under nitrogen stream and dissolved in chloroform. Equal sample loads (250 µg) and standards (100 µg) were separated by TLC on K6 silica plates (Whatman, Clifton, PA). The plate was developed with

chloroform/1.5% (v/v) methanol, and lipids were detected by exposure to iodine vapors. Triolein (1mg/ml) and diolein (1mg/ml) were used as standards. For GC analysis, samples (100 μ g each) were transmethylated as explained above for stigma lipid analysis.

CHAPTER 6

CONCLUSIONS AND FUTURE DIRECTIONS

Plant extracellular lipid polyesters serve many fundamental functions, such as protection against pathogens and predators, maintenance of organ identity, and control of water, gas, and solute exchange. Despite their importance, the structure, biosynthesis and genetics of these essential polymers have received minor attention in plant biology, mainly because of their complexity and the lack of chemical analytical techniques. The completion of the Arabidopsis genome sequence, the availability of approaches to gene discovery, and the continuous development of new technologies, have stimulated research in this field during the last few years. The work presented in this dissertation used multidisciplinary approaches. Major outcomes of my research work are the development of an analytical method to characterize the composition of seed extracellular lipid polyesters, which was further combined with microscopical approaches to localize polyester features in seed tissues. In addition, this work contributed to our understanding of several genes (and enzymes) involved in lipid polyester biosynthesis. Results from this basic research are expected to impact future research on the plant surface. One long-term goal of this field is to manipulate the composition of plant polyesters. Research in Arabidopsis will likely be applicable to crops that are close relatives such as *B. napus*, and also to many

other crops such as the family of solanaceous plants, which includes tomato and potato. Potential agricultural applications include improvement of drought tolerance, pathogen resistance, and modification of seed germination and dormancy. Because plant lipid polyesters are biodegradable, prospective industrial and medical applications are promising (Benitez et al., 2004). For instance, genetic manipulation will help understand the physical properties that make the cuticle such an excellent barrier to gas and water exchange, a basic knowledge that may be applied to design artificial films with improved properties (Bargel et al., 2006). Understanding how fatty acid-derived monomers (i.e. ω -hydroxy acids and α,ω -dicarboxylic acids) are synthesized and assembled is crucial to produce commodity polymers in biological systems (Dodds and Gross, 2007).

Conclusions on seed lipid polyester characterization

In Chapters 2 and 3 the lipid polyester composition of seeds and the distribution of polyesters within different tissues and layers of the seed were presented. Major conclusions that can be drawn from the investigations described in those chapters are:

- The seeds of *Arabidopsis* and *B. napus* contain the major polyester monomers found in leaf and stem cutins, as well as a large proportion of monomers that are characteristic of suberin.

- Suberin monomers are specifically located in seed coats; cutin monomers are found both in seed coat and embryo.
- Suberization is not restricted to the chalazal zone but occurs over the entire seed coat.
- Deposition of suberin-like monomers occurs late in the time-course of seed development.
- The suberized layer is associated with the outer integument, whereas a cutin-like polyester layer is associated with the inner integument.

Figure 57 summarizes some of these conclusions.

This work introduced a quantitative and reproducible method for the analysis of lipid polyester monomers in seeds of *Arabidopsis thaliana* and *Brassica napus*, and this method can probably be extended to other species. Moreover, it reports for first time the characterization of lipid polyesters in seeds of these species, providing evidence for the presence of both cutin and suberin monomers as part of the complex mixture of polyester monomers released after chemical depolymerization of delipidated tissues. As shown in **Figure 57a**, surface lipids constitute only 1% of the total lipid content in seeds. For this reason, an exhaustive delipidation step is required before polyester analysis.

Because the other site where a substantial amount of suberin is produced is the root, and roots are extremely fragile and thin, many plants are needed for

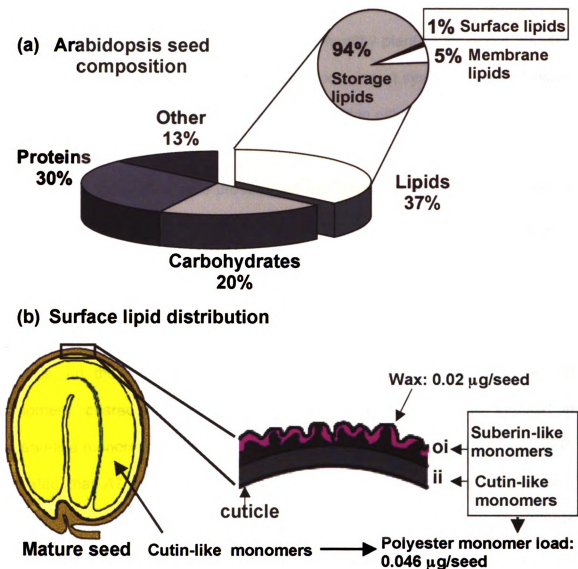


Figure 57. Surface lipid load and distribution in *Arabidopsis thaliana* seeds.

(a) Lipid polyesters and chloroform-extractable waxes constitute only 1% of the total seed lipid loads. Storage lipid and protein values were obtained from Li et al., 2006. Percentage of membrane glycerolipids relative to total lipids is from Ohlogge and Browse, 1995. Content of surface lipids is from this work. (b) Distribution of extracellular lipids in seeds. Values of total polyester monomers and distribution between seed coat and embryo are from Chapter 2. Distribution of polyester monomers within seed coat layers and wax compositions summarize results from Chapter 3. oi: outer integument; ii: inner integument.

screening. I have shown that only 100 mg seeds can be used for a single GC analysis. Therefore, considering that a single healthy plant yields about 300-400 mg seeds, this new method provides a more convenient system to apply forward and reverse genetics screening for genes involved in either or both polyesters.

In fact, the method was proven useful to identify compositional changes in mutant lines for three genes and these changes are consistent with the loss of specific genes that function in cutin and/or suberin biosynthesis. *Att1* seeds had lower amounts of C18 unsaturated dicarboxylic acids than wild-type seeds, and the same phenotype was observed in leaves and stems. Seeds of *gpat5* mutants, on the other hand, had reduced loads C20-C26 fatty acid-derived monomers, characteristic of suberin. And *fatB* seeds were also affected in suberin-like monomers. Further investigation of transcriptional fusions with YFP, indicated that *ATT1* expression is limited to the innermost layer of the inner integument (ii1), and *GPAT5* to the outer integument. I then compared patterns and kinetics of dye uptake by these mutant seeds. In previous publications, uptake of tetrazolium salts has been used to assess seed permeability, but results were reported qualitatively as micrographs. In this work, I have adapted a method often used to measure cell viability, to semi-quantitatively evaluate dye uptake over time. Only the mutants affected in suberin (i.e. *fatb* and *gpat5*) showed increased permeability to tetrazolium salts. Such permeability was not modified by removal of chloroform-extractable waxes, which demonstrates lipid polyesters but not extractable waxes constitute a barrier to the dye permeability.

The polyester analysis was also applied to immature seeds, mature seed parts, and to *ap2*, a mutant that lacks a differentiated outer integument. These determinations revealed that there is a complex pattern of monomer deposition over development, that suberin is not only confined to the chalazal end of the seed coats, as observed for example in grapefruit seeds (Espelie, 1980), and that suberin monomers are preferably localized to the outer integument. In summary, it is the confluence of evidence from chemical analyses, functional transport assays on mutants, and confocal fluorescence microscopy of transgenic seeds transformed with promoter:YFP constructs that allowed to conclude that a suberized layer is localized at the outer integument, whereas a cutin-like layer is present at the inner integument facing the embryo (**Figure 57b**).

Directions for further research on seed coat extracellular lipids

What is the physiological relevance of seed coat lipid polyesters? As it has been shown in Chapter 3, reduced suberin monomer loads affect the seed coat permeability to tetrazolium dyes (**Figure 21**). However, it is uncertain the increased permeability to dyes observed in *fatB* and *gpat5* mutants can be extrapolated to permeability to water. Attempts for measuring permeability to water were unsuccessful because the water-holding capacity of the mucilage layer impedes the measurement of small variations in seed weight upon incubation in high humidity conditions (data not shown). In addition, although one

would expect that reduced polyesters would reduce seed dormancy, dormancy was released more slowly in the *gpat5* mutants (Beisson et al., 2007). Hence, future studies should focus on investigating the role of lipid polyesters in dormancy and germination, which have agronomic significance. Perhaps the analysis of different seed coat mutants altered in lipid polyester loads, and seeds of transgenic plants accumulating seed coat polyesters, will help to understand how variations in seed coat lipid layers affect seed coat dormancy and germination under different conditions.

Are seed coat lipid polyesters altered in transparent testa mutants? As discussed in Chapter 3, increased permeability to dyes has also been observed in *transparent testa (tt)* and related mutants (Debeaujon et al., 2000). These mutants present decreased levels of condensed tannins in the ii2 layer of the seed coat, with a concomitant change in pigmentation. However, in seeds of lipid polyester mutants *gpat5* (Beisson et al., 2007), *fatB*, *ap2* lines (Debeaujon et al., 2000; and this work), dye permeability is enhanced despite negligible change in seed coat color. Because the seed coat polyester content of the *tt* mutants has not been measured, it needs to be investigated. It is possible that both polyesters and condensed tannins contribute independently to seed coat permeability.

Conclusions on the role of P450 monooxygenases on lipid polyester monomer modification

Cytochrome P450 enzymes of the CYP86A subfamily are known to play a fundamental role in the synthesis Arabidopsis lipid polyester monomers. Chapter 4 presents the characterization of several knockout mutants of this subfamily. In Chapter 5 a different approach is taken to study the function of CYP86A2 *in planta*. Major conclusions drawn from the presented evidence are:

- CYP86A1 is the first cytochrome P450 enzyme shown to have a function in suberin monomer oxidation.
- The *cyp86A2 (att1)* mutation impacts cutin dicarboxylic acid but not ω -hydroxy acid loads.
- Overexpression of CYP86A genes fails to accumulate oxygenated fatty acid monomers in wild-type plants.
- CYP86A2 may not catalyze just a fatty acid ω -hydroxylation reaction.
- CYP86A2 is strongly expressed in guard cells.

CYP86A1 and suberin. In Chapter 4 I have characterized two *cyp86A1* mutant alleles. These presented reduced loads of C16-C18 α,ω -bifunctional monomers in roots, and of C16 dicarboxylic acid in seeds. These results, in combination with the phenotype of transgenic plants co-overexpressing CYP86A1 and GPAT5 (Li et al., 2007a), suggested that major CYP86A1 products *in vivo* are saturated C16 and C18 dicarboxylic acids. This finding was unexpected because *CYP86A1* and *GPAT5* are highly correlated, and the *gpat5* phenotype suggests that GPAT5 transfers long-chain acyl moieties to the glycerol-based backbone, leading to the hypothesis that the CYP86A1 oxidase

would modify long chain monomers. Hence, a long-chain acyl oxidase remains to be identified.

Results on reporter expression show *CYP86A1* promoter activity in root endodermis and peridermis and outer integument of seed coats, similar to *GPAT5* transcripts. These observations are consistent with a suberin-synthesizing gene. Moreover, *cyp86A1* suberin lamellae had reduced dark bands, a result that was not anticipated for a mutant with reduced content of aliphatic monomers. The ultrastructure of *cyp86A* root suggests that the existing macromolecular model for suberin needs revision.

CYP86A2 and cutin. Although the current assumption is that CYP86A2 catalyzes the ω -hydroxylation step leading to synthesis of cutin precursors, results in the present work show evidence questioning this assumption. Furthermore, possible reactions catalyzed by this enzyme are discussed by comparison with plant (Le Bouquin et al., 2001; Kurdyukov et al., 2006) and animal (Sanders et al., 2005) biosynthetic pathways that lead to dicarboxylic acids. For instance, CYP86A2 could catalyze the whole pathway from the fatty acid to the dicarboxylic acid product, as biochemically demonstrated for tobacco CYP94A5. It also could function downstream of the ω -hydroxylation step, as part of a p450-mediated oxidation pathway where several monooxygenases lead to production of dicarboxylic acids.

Analysis of *ATT1* promoter activity using YFP as reporter led to an intriguing observation: the reporter is mainly expressed in guard cells. This result is unlikely to be an artifact caused by improper construct design, because a similar expression pattern has been recently reported using a gene-trap strategy (Galbiati et al., 2007). Lipids on *att1* guard cell ledges are reduced, as shown by confocal fluorescence microscopy in Chapter 4, but such projections are not missing, as shown by TEM. Does the *ATT1* expression in guard cell imply different cutin composition than cutin on pavement cells? More research is needed in order to understand the possibly different spatial distribution of surface lipids on epidermal cells (see below).

Directions for further research on P450 monooxygenases

What is the reaction catalyzed by ATT1? This is a fundamental question in Arabidopsis cutin biogenesis, since C18:2 dioic acid is the major cutin monomer in Arabidopsis (Bonaventure et al., 2004; Franke et al., 2005) and *B. napus* (Bonaventure et al., 2004; Molina et al., 2006). Overexpression of single P450 genes, *ATT1* (in this work) and *CYP86A1* (in Li et al., 2007a), did not result in compositional changes in wild-type plants. This suggests that future work to address the role of *ATT1* should include co-overexpression of *ATT1* and a *GPAT* gene (i.e. *GPAT4*) both in Arabidopsis leaves and in tobacco stigmas. The polyester phenotype of Arabidopsis transgenic plants is expected to be similar to that of plants overexpressing *GPAT5* and *CYP86A1*, presumably with higher

loads of C18 unsaturated dicarboxylic acids. By itself, this result will not explain the catalytic function of ATT1 in full, but I suggest a similar experiment using PH1 and the petunia homolog of GPAT4. If different monomers are incorporated in lipid polyesters of both transgenic plants, that may imply different functions of these P450s. For example, ATT1/GPAT4-overexpressors may accumulate more dicarboxylates in the polyesters, whereas PH1/GPAT4 polyesters may be enriched in ω -hydroxylated monomers compared to non-transgenic plants. And finally, if co-overexpression of ATT1 and GPAT4 in tobacco stigmas is pursued, it may help clarify the catalytic role of ATT1, as stigmas represent a different biosynthetic context and downstream enzymes potentially required for producing dicarboxylic acids in Arabidopsis cutin may not be present in this system. If these experiments are undertaken, it would be useful to produce anti-ATT1 antibodies to corroborate the presence of the transgenic protein.

If an ω -alcohol dehydrogenase acts coordinately with ATT1 towards producing dicarboxylates, as proposed by (Kurdyukov et al., 2006), the corresponding mutant should have a reduced content of dicarboxylic acid monomers in leaves. I believe that, before pursuing mutant analysis for other candidates, the role of HOTHEAD in cutin synthesis should be proven *in vitro*. Once the activity is confirmed, the best candidate for a loss-of-function approach is At3g56060, a gene within the HTH clade that is co-upregulated with ATT1 and is up-regulated in stem epidermis (Suh et al., 2005).

Why is ATT1 preferentially expressed in guard cells? To unravel possible compositional differences between surface lipids on pavement cells and on guard cells, the application of novel techniques may be required. In this regard, laser desorption/ionization time-of-flight (LDI-TOF) mass spectrometry has been applied to intact plant surfaces to analyze waxes (Sluszný et al., 2005), although the application of this method to polymeric material such as cutin may require overcoming major experimental issues (i.e. lack of analyte volatility). Raman microspectroscopy offers another sophisticated technique to determine surface compounds at the level of resolution of a confocal microscope. It has been used to determine the spatial distribution of triterpenoids in waxes on leaf surfaces (Yu et al., 2007). However, a potential limitation of this technique is that the spectra of different aliphatic molecules may not be distinct enough to detect different distribution of 18:2 dicarboxylate, which I hypothesize may be preferentially localized in guard cell cuticular ledges. Finally, scanning electron microscopy (SEM) combined with energy dispersive X-ray (EDX), may represent an alternative to distinguish compositional differences *in situ*. Although the unsaturated fatty acids *per se* cannot be revealed by this method, if the sample is pre-treated with bromine the Br atoms added to the double bonds would make the detection possible.

Conclusions on preliminary characterization of a mutant of the BAHD family involved in suberin synthesis

One major focus of my research work was to discover new gene families involved in lipid polyester biosynthesis. In Chapter 4, I used bioinformatics approaches for candidate gene identification, and characterized knockout mutants of selected candidate genes. In particular, I have identified three genes that constitute a separate clade in the BAHD family of acylCoA-utilizing acyltransferases. No members of this family have previously been demonstrated to have a function in cutin or suberin biogenesis. The main contributions of this work can be summarized as follows:

- An acyl-CoA transferase of the BAHD family (encoded by *At5g41040*) is involved in ferulate deposition in *Arabidopsis* suberin.
- The loss of ferulate does not impact the insolubility of the suberin polyester, and this raises questions concerning cross-linking between ferulate and aliphatics.
- Loss of ferulate correlates with approximately stoichiometric losses of ω -hydroxy fatty acids plus fatty alcohols.

From the initial characterization of *at5g41040* mutants reported in Chapter 4, we learned that disruption of *At5g41040* results in an almost complete loss of ferulate released by transmethylation of seed and root residues, and that it might be esterified to 1-alkanols and ω -hydroxy acids in seed coat suberin. These losses may slightly influence seed coat permeability to dyes. Although suberin models suggest that aliphatic chains are linked to ferulate via its carboxyl end, and it is further cross linked to the cell wall aromatic polymers or sugars, the fact

that aliphatics are recovered from the insoluble fraction suggests that ferulate plus its acceptor are not crucial for the attachment of the aliphatics to the cell wall. Likewise, the loss of ferulate in root suberin does not affect aliphatic monomer deposition on peridermal suberized cell walls or their ultrastructure, but it might affect the ultrastructure of endodermal cells of younger roots. Therefore, these need to be studied by TEM.

To our knowledge, this is the first suberin mutant defective in a hydroxycinnamic derived monomer, and the first gene of the BAHD family that has been associated to lipid polyester synthesis.

Directions for further research on acylCoA-utilizing acyltransferases

What is the function of the At5g41040 gene product? The mutant phenotype suggests that the At5g41040 gene encodes a feruloyl-CoA transferase (**Figure 58**) catalyzing the feruloylation of aliphatic monomers (i.e. ω -hydroxy fatty acids and 1-alkanols). If the proposed function is demonstrated, this will be an important finding because no genes encoding proteins with such function have been identified thus far. Furthermore, because cellulosic biomass is foreseen as substantial alternative source of fuels, there is an increasing interest in understanding how ferulate esters occurring in cell walls are synthesized, since ferulic acid bound to cellulose and lignin is a significant factor

that makes cell wall polysaccharides recalcitrant to hydrolysis (Fazary and Ju, 2007).

Further experiments will be focused on addressing this question, using a gain of function approach and *in vitro* assays. Some of these experiments are underway. Transgenic plants to overexpress the gene under its native promoter, and also under the *CaMV* 35S promoter have already been generated. When T₂ plants are obtained, both waxes and insoluble polyester fractions will be investigated. For example, any accumulation of ferulate esters in the wax fraction will give clues on the enzyme function *in vivo*. Such strategy has been used with GPAT5, whose ectopic overexpression resulted in accumulation of monoacylglycerols in stem waxes (Li et al., 2007b). To study the enzymology of this protein, an approach similar to that used for the characterization of other enzymes of the BAHD family, such as tobacco HCT (Hoffmann et al., 2003) will be likely successful. The Arabidopsis cDNA will be expressed in *E. coli* as a recombinant protein fused to glutathione S-transferase or His-tag for easy affinity purification. Enzyme activity can be evaluated using feruloyl-CoA (and other hydroxy-cinnamoyl-CoA thioesters), and different acceptors (1-alkanols and ω -hydroxy fatty acids of variable chain length). Reaction products can be further analyzed by HPLC coupled to an UV detector. Alternatively, radiolabeled acceptors can be used and the products separated by TLC and evaluated by autoradiography.

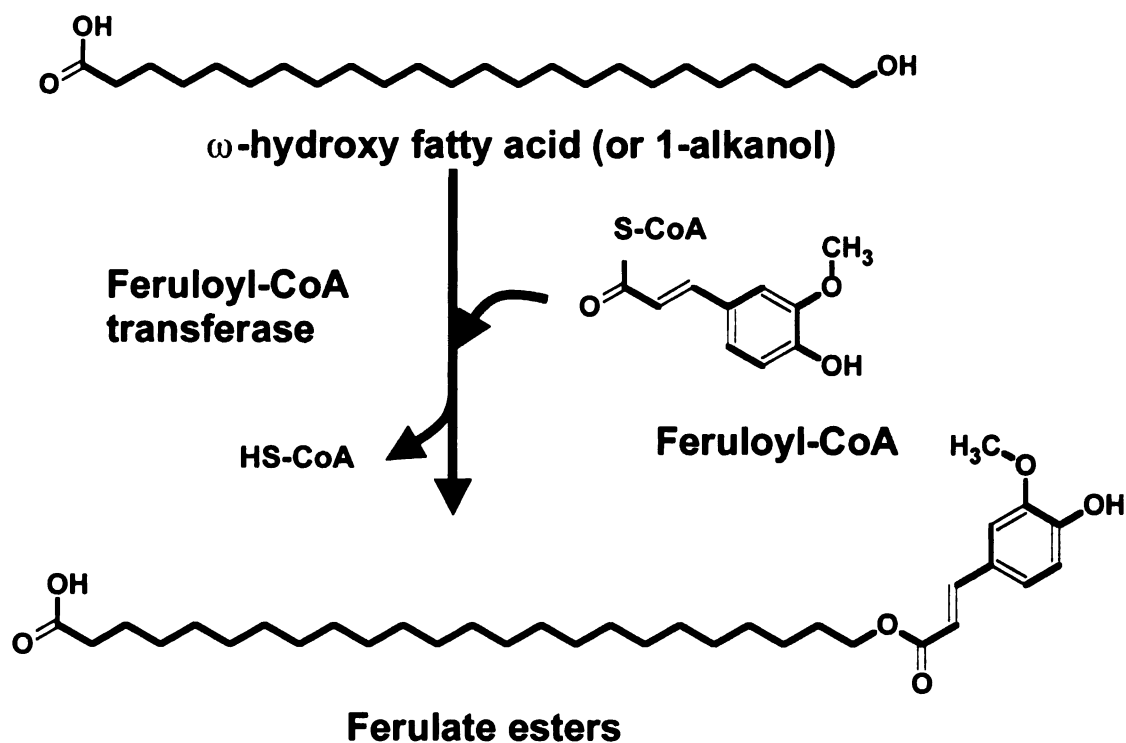


Figure 58. Schematic diagram of the proposed enzymatic reaction catalyzed by enzyme encoded by At5g41040.

What is the origin of the ferulate released by transmethylation? The transmethylation process is applied to the bulk of insoluble residue remaining after delipidation. Consequently, the ferulate released by transmethylation may:

- a) represent only a small portion of the total ferulate-derived material (the cross-linked molecules cannot be released by this process);
- b) be part of the insoluble polyester, and/or of trapped waxes that remained after exhaustive delipidation;
- and c) be esterified to cellulose that is not ether-linked to lignin, since ferulic acid has been found bridging polysaccharides to lignin (polysaccharide-ester-ferulic

acid-ether-lignin) in wheat cell walls (Iiyama et al., 1990; Lam et al., 1992). To understand the nature of the ferulate-esters found in Arabidopsis suberin, future biochemical analyses need to be focused on partial depolymerization assays (e.g. calcium hydroxide-catalyzed methanolysis) and further characterization of the released oligomers by GPC and ESI/MS/MS, and possibly NMR. Such studies should be performed in both wild-type and *at5g41040* seeds to identify ferulate esters that are absent or reduced in the knockout. Determination of total cross-linked aromatics (e.g. by alkaline nitrobenzene oxidation) in the transmethylation residue in wild-type and knockout will help identify load changes in cross-linked aromatics. Such aromatics may be reduced if the BAHD transferase links ferulate to an acyl acceptor that is readily cross-linked (glycerol, glycoprotein, polysaccharide or tyramine). In summary, these analyses may shed light on the so far uncharacterized suberin-aromatic composition in Arabidopsis, the nature of the ferulate-esters reduced in the mutant, and the identification of anchor molecules responsible for polyester insolubility.

How does the lack of ester-bound ferulate impact the ultrastructure of suberin? My results on TEM analysis of root peridermis show no correlation between the loss of ferulate and the ultrastructure of the suberin lamellae, which has a wild-type appearance. This result may imply that ester-bound ferulate does not contribute to the dark bands, as suggested by current models. However, the reduced ferulate may affect endodermal cells of younger roots, which were not included in this study. Therefore, these also need to be analyzed by TEM. Although I choose roots because sample preparation and subsequent analysis is

easier, TEM also needs to be performed in seeds where ferulate is a major suberin compound.

Other BAHD candidate genes. Also included in my research for the near future are the characterization of mutants of the other two genes in clade H (**Figure 32**), At5g63560 (co-expressed with At5g41040, see **Table 10, Appendix B**), and At3g48720, which is up-regulated in leaves and correlates with *ATT1* and *GPAT4*. I have generated homozygous T-DNA insertion lines, and analyses are underway. In particular, it will be interesting to obtain a double mutant *at5g41040/at5g63560* to assess gene redundancy.

In conclusion, the use of forward and reverse genetic approaches in *Arabidopsis* have facilitated our understanding of genes involved in the biogenesis of plant lipid polyesters. However, polyester size, the nature of its insolubility, and polyester assembly are aspects that still remain unknown. The recent demonstration that lipid polyesters can be engineered in this plant, which have unusual ultrastructure and altered functional properties (Li et al., 2007a) indicates that *Arabidopsis* will continue to provide a useful system to address these issues. In addition, new technological developments are making possible investigations that were not even dreamed to accomplish in the past. For instance, with the availability of fast, affordable new sequencing technologies and improved methods for plant transformation, it is now feasible to use genetic approaches in the classical plant models for the study of lipid polyesters, such as

potato for suberin. In the next decade, accomplishments will depend on the creativity of the scientists devoted to unravel the complex processes underlying the biosynthesis of plant lipid polyesters.

APPENDICES

APPENDIX A

ADDITIONAL COMPONENTS RELEASED BY TRANSMETHYLATION OF *B. NAPUS* AND *ARABIDOPSIS* DELIPIDATED SAMPLES

Present in the depolymerization products when *Arabidopsis* or *Brassica* stem, leaf and seed tissues were exhaustively extracted and transmethylated were a lignan and two diterpene acids. These were most noticeable for the isolated embryos of *Brassica* seeds. The lignan gave a bis-TMSi derivative on silylation, with diagnostic MS ions (m/z (rel. int.)) at 502 $[M]^+$ (100) and 487 $[M-Me]^+$ (18) (**Figure 59a**). On acetylation diagnostic MS ions were noted for a bis-acetyl derivative at 442 $[M]^+$ (18), at 400 $[M-CH_2CO]^+$ (33) and 358 $[M-2CH_2CO]^+$ (100) (**Figure 59b**). The data suggest a lignan of molecular formula $C_{20}H_{22}O_2$ and rule out lignans with a lactone functional group between the phenyl rings. The data suggest a lignan such as 8,8'-pinoresinol (**Figure 59, inset**). The diterpene acids were tentatively identified as methyl abiet-8-en-18-oate ($C_{21}H_{34}O_2$) and methyl abieta-8,11,13-trien-18-oate (methyl dehydroabietate, $C_{21}H_{30}O_2$) on the basis of mass spectral comparisons. Diagnostic ions were the expected $[M]^+$, $[M-Me]^+$ and $[M-Me-HOAc]^+$ peaks, the latter being the base peak (**Figure 60**).

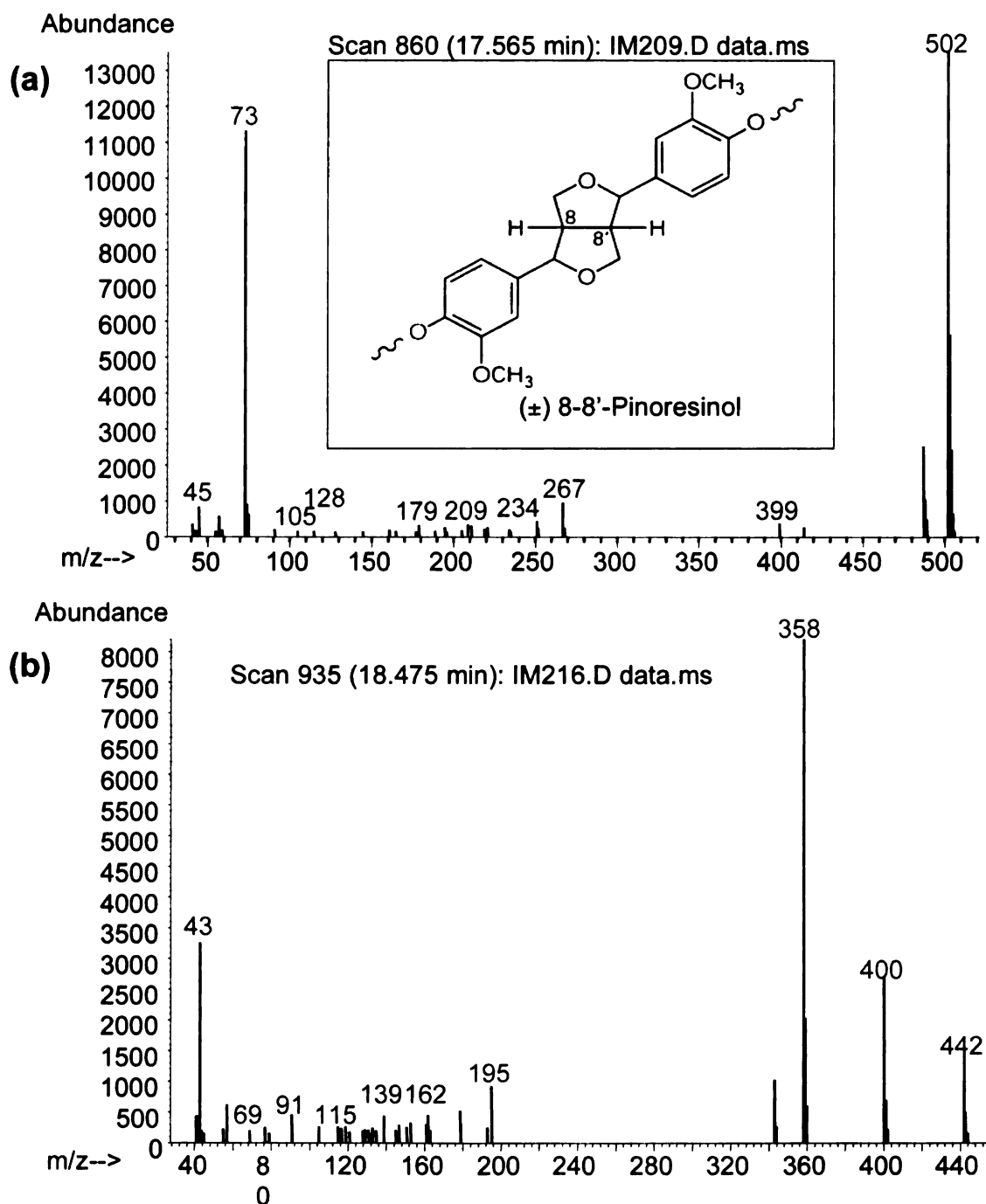


Figure 59. MS spectra of the lignan molecule released by transesterification of seed residues.

(a) Bis-TMSi derivative. **(b)** Acetyl derivative. **Inset:** Estructure of 8-8' Pinoresinol.

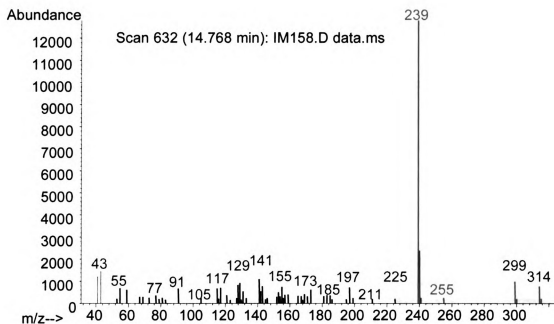


Figure 60. MS spectrum of 1-Phenanthrenecarboxylic acid, tetradecahydro-1, 4a-dimethyl-7-(1-methylethyl)-, methyl ester.

This compound was identified by searching on NIST02 Mass Spectral Library

APPENDIX B

CORRELATED EXPRESSION BETWEEN LIPID POLYESTER RELATED GENES AND CANDIDATE GENES

Table 10. Pearson pairwise correlation coefficients (r^2) between bait genes and candidate genes for lipid polyester synthesis

Bait and candidate genes ▼	Bait genes								
	At5g58860 (CYP86A1)*	At3g11430 (GPAT5)*	At1g63710 (CYP86A7)	At2g45970 (CYP86A8)	At1g01600 (CYP86A4)	At1g01610 (GPAT4)	At2g38110 (GPAT6)	At4g00360 (CYP86A2)	At4g00400 (GPAT8)
At2g45970 (CYP86A8; LCR)	0.032	0.024	0.148	1	0.357	0.129	0.129	0.135	0.331
At4g00360 (CYP86A2; ATT1)	0.023	0.002	0.001	0.135	0.005	0.324	0.002	1	0.386
At5g58860 (CYP86A1)	1	0.509	0.044	0.032	0.019	0.048	0.056	0.023	0
At1g63710 (CYP86A7)	0.044	0.007	1	0.148	0.303	0.091	0.305	0.001	0.143
At1g01600 (CYP86A4)	0.019	0.025	0.303	0.357	1	0.264	0.26	0.05	0.056
At5g23190 (CYP86B1)	0.498	0.426	0.062	0.007	0.015	0.012	0.016	0.003	0.048
At5g08250 (CYP86B2)	0.237	0.426	0.007	0	0.005	0.011	0.053	0.002	0.013
At1g12740 (CYP87A2)	0.337	0.207	0.089	0.002	0.007	0.008	0.002	0	0.016
At3g11430 (GPAT5)	0.509	1	0.007	0.024	0.025	0.042	0.159	0.002	0.004
At1g01610 (GPAT4)	0.048	0.042	0.091	0.474	0.264	1	0.131	0.324	0.296
At4g00400 (GPAT8)	0	0.004	0.143	0.331	0.056	0.296	0.028	0.386	1
At2g38110 (GPAT6)	0.056	0.159	0.305	0.129	0.26	0.131	1	0.02	0.028
At2g47240 (LACS1)	0.09	0.045	0.387	0.181	0.148	0.129	0.175	0.054	0.177
At1g49430 (LACS2)	0.043	0.054	0.207	0.338	0.424	0.448	0.424	0.03	0.095

Table 10. (Continued)

Bait and candidate genes ▼	Bait genes								
	At5g58860 (CYP86A1)*	At3g11430 (GPAT5)*	At1g63710 (CYP86A7)	At2g45970 (CYP86A8)	At1g01600 (CYP86A4)	At1g01610 (GPAT4)	At2g38110 (GPAT6)	At4g00360 (CYP86A2)	At4g00400 (GPAT8)
At1g64400 (LACS3)	0.006	0.002	0	0	0.002	0.07	0.008	0.332	0.072
At1g01120 (KCS1)	0.072	0.054	0.019	0.307	0.115	0.587	0.037	0.481	0.278
At2g16280	0.023	0.028	0.095	0.226	0.019	0.151	0	0.296	0.429
At1g04220 (DAISY)	0.223	0.303	0.007	0.099	0.18	0.234	0.153	0.017	0.002
At2g15090	0.021	0.032	0.215	0.326	0.169	0.234	0.023	0.107	0.34
At4g34520 (FAE1)	0.012	0.029	0.001	0.005	0	0.003	0.002	0.01	0.022
At4g34250	0.044	0.008	0.046	0.278	0.139	0.161	0.006	0.194	0.221
At2g26250 (FDH)	0.013	0.009	0.175	0.368	0.193	0.495	0.047	0.304	0.369
At1g68530 (CUT1)	0.05	0.023	0.174	0.162	0.041	0.3	0.026	0.458	0.447
At1g75020 (LPAAT4)	0.032	0.024	0.103	0.091	0.141	0.009	0.01	0.035	0.036
At3g63200	0.132	0.069	0.018	0.358	0.23	0.261	0.078	0.028	0.103
At1g64670 (BDG)	0.008	0.008	0.162	0.475	0.255	0.35	0.022	0.127	0.357
At5g41040	0.66	0.502	0.077	0.022	0.016	0.044	0.012	0.017	0.004
At5g63560	0.726	0.529	0.058	0.011	0.006	0.017	0.064	0.006	0.01
At1g65450	0.05	0.001	0.494	0.098	0.176	0.026	0.31	0.007	0.082
At3g48720	0.071	0.124	0.041	0.013	0.013	0.059	0.019	0.387	0.28
At3g14680 (CYP72A14)	0.563	0.297	0.187	0.003	0	0	0.006	0.01	0.03
At3g14650 (CYP72A11)	0.062	0.03	0.085	0.119	0.005	0.16	0.006	0.41	0.33
At3g14610 (CYP72A7)	0.347	0.274	0.117	0.008	0.003	0.011	0	0.18	0.124
At3g14690 (CYP72A15)	0.02	0.02	0.016	0.008	0.009	0.02	0.004	0.184	0.03

Pairwise correlations were calculated using the Gene-correlator application at the Genevestigator website (<https://www.genevestigator.ethz.ch/>) (Zimmermann et al., 2004; Zimmermann et al., 2005). Scores for linear relationships between the expression of two genes are tabulated (Pearson's correlation). Shadowed boxes indicate significant correlations.

APPENDIX C

DEVELOPING SEEDS MICROARRAY EXPRESSION DATA

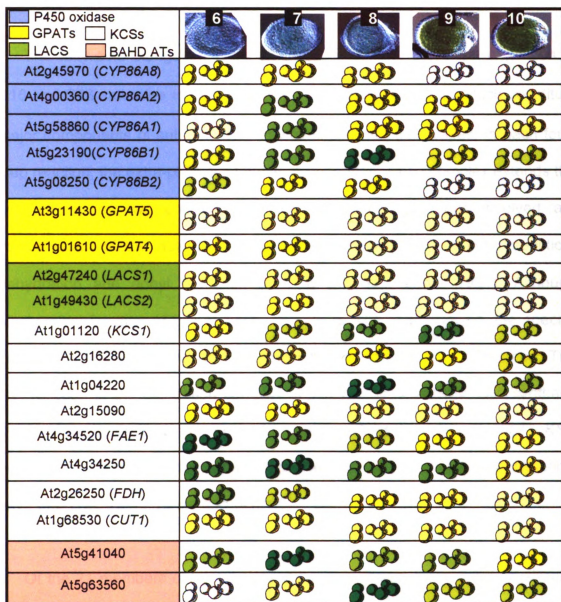


Figure 61. Gene expression in Arabidopsis developing seeds for selected candidate genes.

Data source: AtGenExpress; expression visualization tool. (<http://arabidopsisgfp.ueb.cas.cz>). Numbers represent seed stages used to extract the RNA for the RNA developmental series: 6, mid torpedo to late torpedo; 7, late torpedo to early walking-stick; 8, walking-stick to early curled cotyledons; 9, curled cotyledons to early green cotyledons; 10, green cotyledons.

APPENDIX D

FATTY ACID ELONGASES

The fatty acid elongation complex is responsible for the chain extension of C16 and C18 saturates to very long chain fatty acids (C₂₀-C₃₄), which constitute major components of suberin, suberin waxes and cuticular waxes. In each four-step reaction, the extra-plastidial fatty acid elongation (FAE) complex extends the acyl chains by two carbons. The four enzymatic reactions involved are condensation of the acyl-CoA substrate and malonyl-CoA, β -keto reduction, dehydration and enoyl reduction (Fehling and Mukherjee, 1991). Although biochemical function of this enzyme complex is well characterized, the specific function of individual genes in lipid polyester synthesis is less understood. The first reaction in the elongation complex is initiated by a ketoacyl-CoA synthase (KCS), the rate limiting enzyme in the complex (Millar and Kunst, 1997). *KCS* mutants potentially affected in wax composition, but not in suberin aliphatics, have been reported (Franke and Schreiber, 2007).

Of the 21 members comprising the KCS gene family, several are expressed in seeds (listed in **Table 6** and **Appendix C**). Of these, *KCS1* (At1g01120), At2g16280, *FAE1*, At1g04220, *CUT1*, At2g15090, *FDH*, At4g34520, and At4g34250 transcripts are highly represented in seeds (**Appendix C**). *KCS1* and *CUT1* are known to be involved in wax biosynthesis (Todd et al., 1999; Kunst et

al., 2000), although a role in suberin monomer extension cannot be excluded. *FAE1* was shown to function in storage triacyl glycerols (Kunst et al., 1992; James et al., 1995). Analysis of *fae1* seeds (Chapter 2) indicated that the effect of the mutation on seed polyester monomers is minimal. This particular example serves as a control for our data mining analysis, since correlation coefficients indicate no co-response of *FAE1* with surface lipid-related genes ($r^2 < 0.03$ for all bait genes) (**Appendix B**). *FIDDLEHEAD* (At4g34520) (Yephremov et al., 1999; Pruitt et al., 2000) is epidermis-specific and it is expressed in the inner integument of the seed coat (Efremova et al., 2004). It is uncertain if it is involved in biosynthesis of polyester aliphatics or waxes or both. Very long chain fatty acids (C₂₀-C₃₄) are present in waxes but not in cutin, therefore, could be involved in synthesis of waxes and/or signal molecules. Gene correlations indicate co-upregulation with *GPAT4*, *GPAT8*, *CYP86A8* and *CYP86A2*. This implies co-regulation with cutin genes, an observation that excludes a role in suberin, and provides an example that correlations do not reflect biosynthetic association in all cases.

At1g04220 is potentially associated with suberin synthesis based on its correlation with *GPAT5/CYP86A1*, and heterologous expression assays have established that it is capable of elongating C18 and C20 fatty acids (Trenkamp et al., 2004). I have conducted seed polyester analysis of *at1g04220* knockout mutant (kindly provided by L. Kunst) (**Figure 60**). The lack of phenotype in seeds may be because of gene redundancy or because it participates in elongation of

suberin wax components, which are extracted during the delipidation steps and not analyzed here. Despite poor correlation with suberin genes, other *KCS* genes are highly expressed in seeds (**Appendix C**). One candidate is the enzyme encoded by At2g16280, which synthesizes C22 and C24 products when expressed in yeast (Paul et al., 2006). This gene might become up-regulated in conditions where At1g04220 is silenced, explaining the absence of phenotype in *at1g04220*. While performing this analysis, the characterization of root lipid

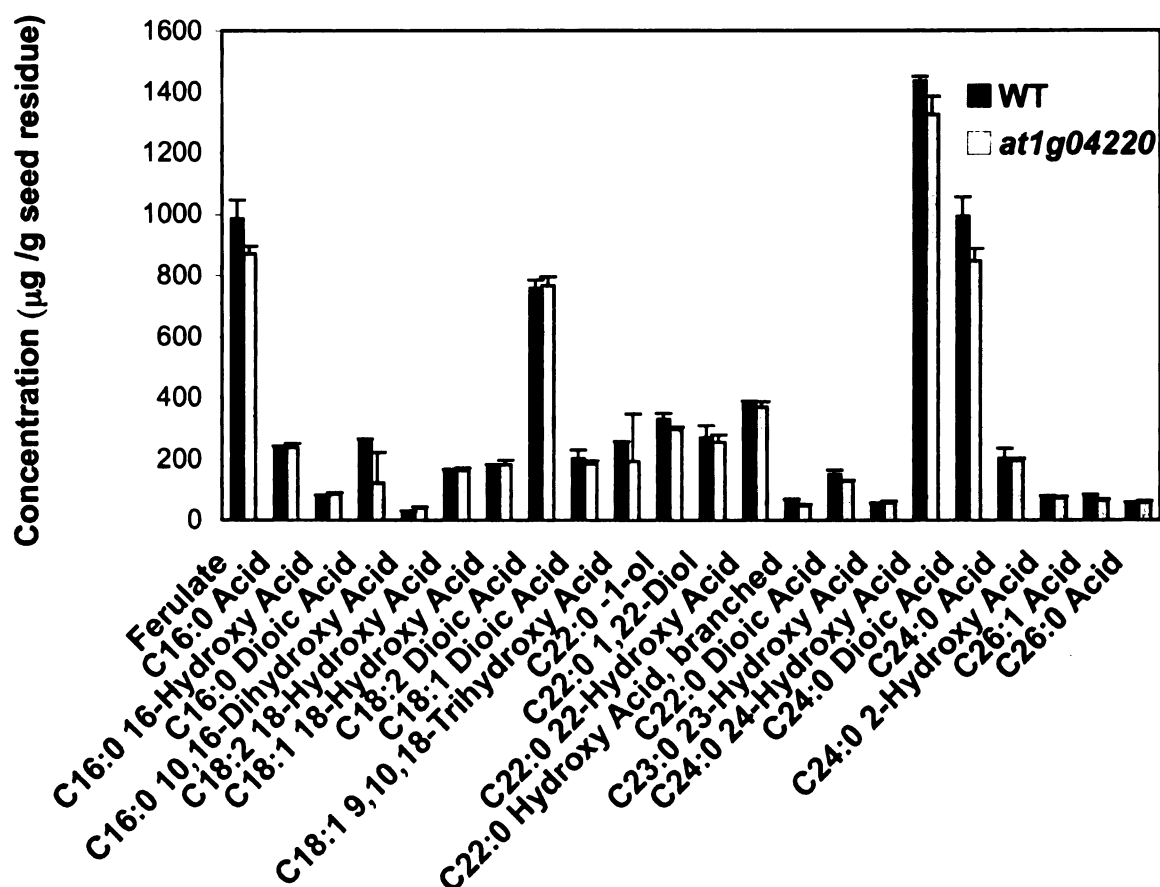


Figure 62. Load and monomer composition of seed polyesters from WT and *at1g04220* mutant.

Values are reported as the mean of three determinations \pm SD

polyesters in a transposon mutant allele of this gene was communicated in a meeting (Franke et al., 2006). The authors found reduced suberin long-chain (>C20) fatty acids derivatives and abnormal root growth. Seed lipids polyesters were not reported.

Further analyses in other knockout mutants of uncharacterized KCS genes and other genes in the elongation complex were not attempted in this work for a number of reasons. First, a major focus of this research was to discover new gene families involved in lipid polyesters, and the KCS family is not one of them. Second, the FAE complex genes are studied by other groups interested in wax or suberin synthesis. Third, saturated long chains are common to several biosynthetic pathways (suberin, cutin, and sphingolipids), therefore, these enzymes can act in more than one pathway thus complicating any attempt to assign specific functions.

LITERATURE CITED

- Agrawal, V.P. and Kolattukudy, P.E.** (1977) Biochemistry of suberization. ω -Hydroxyacid oxidation in enzyme preparations from suberizing potato tuber disks. *Plant Physiology*, **59**, 667-672.
- Agrawal, V.P. and Kolattukudy, P.E.** (1978) Purification and characterization of a wound-induced omega-hydroxyfatty acid:NADP oxidoreductase from potato tuber disks (*Solanum tuberosum* L.). *Arch Biochem Biophys*, **191**, 452-465.
- Aharoni, A., Dixit, S., Jetter, R., Thoenes, E., van Arkel, G. and Pereira, A.** (2004) The SHINE clade of AP2 domain transcription factors activates wax biosynthesis, alters cuticle properties, and confers drought tolerance when overexpressed in Arabidopsis. *Plant Cell*, **16**, 2463-2480.
- Albert, S., Delseny, M. and Devic, M.** (1997) BANYULS, a novel negative regulator of flavonoid biosynthesis in the Arabidopsis seed coat. *Plant Journal*, **11**, 289-299.
- Alonso, J.M., Stepanova, A.N., Leisse, T.J., Kim, C.J., Chen, H., Shinn, P., Stevenson, D.K., Zimmerman, J., Barajas, P., Cheuk, R., Gadrinab, C., Heller, C., Jeske, A., Koesema, E., Meyers, C.C., Parker, H., Prednis, L., Ansari, Y., Choy, N., Deen, H., Geralt, M., Hazari, N., Hom, E., Karnes, M., Mulholland, C., Ndubaku, R., Schmidt, I., Guzman, P., Aguilar-Henonin, L., Schmid, M., Weigel, D., Carter, D.E., Marchand, T., Risseuw, E., Brogden, D., Zeko, A., Crosby, W.L., Berry, C.C. and Ecker, J.R.** (2003) Genome-wide insertional mutagenesis of *Arabidopsis thaliana*. *Science*, **301**, 653-657.
- Anisimova, M. and Gascuel, O.** (2006) Approximate likelihood-ratio test for branches: A fast, accurate, and powerful alternative. *Systematic Biology*, **55**, 539-552.
- Aoki, K., Ogata, Y. and Shibata, D.** (2007) Approaches for extracting practical information from gene co-expression networks in plant biology. *Plant Cell Physiol*, **48**, 381-390.
- Ballard, L.A.T.** (1973) Physical barriers to germination. *Seed Science and Technology*, 185-303.
- Bargel, H., Koch, K., Cerman, Z. and Neinhuis, C.** (2006) Structure-function relationships of the plant cuticle and cuticular waxes - a smart material? *Funct Plant Biol*, **33**, 893-910.

- Bechtold, N., Ellis, J. and Pelletier, G.** (1993) *In planta* Agrobacterium-mediated gene transfer by infiltration of adult *Arabidopsis thaliana* plants. *C. R. Acad. Sci. Paris, Life Sciences*, **316**, 1194-1199.
- Beeckman, T., De Rycke, R., Viane, R. and Inze, D.** (2000) Histological study of seed coat development in *Arabidopsis thaliana*. *Journal of Plant Research*, **113**, 139-148.
- Beisson, F., Koo, A.J.K., Ruuska, S., Schwender, J., Pollard, M., Thelen, J.J., Paddock, T., Salas, J.J., Savage, L., Milcamp, A., Mhaske, V.B., Cho, Y.H. and Ohlrogge, J.B.** (2003) *Arabidopsis* genes involved in acyl lipid metabolism. A 2003 census of the candidates, a study of the distribution of expressed sequence tags in organs, and a Web-based database. *Plant Physiology*, **132**, 681-697.
- Beisson, F., Li, Y.H., Bonaventure, G., Pollard, M. and Ohlrogge, J.B.** (2007) The acyltransferase GPAT5 is required for the synthesis of suberin in seed coat and root of *Arabidopsis*. *Plant Cell*, **19**, 351-368.
- Benítez, J., García-Segura, R. and Heredia, A.** (2004) Plant biopolyester cutin: a tough way to its chemical synthesis. *Biochim Biophys Acta*, **1674**, 1-3.
- Bent, A.F., Kunkel, B.N., Dahlbeck, D., Brown, K.L., Schmidt, R., Giraudat, J., Leung, J. and Staskawicz, B.J.** (1994) RPS2 of *Arabidopsis thaliana*: a leucine-rich repeat class of plant disease resistance genes. *Science*, **265**, 1856-1860.
- Benveniste, I., Saito, T., Wang, Y., Kandel, S., Huang, H.W., Pinot, F., Kahn, R.A., Salaun, J.P. and Shimoji, M.** (2006) Evolutionary relationship and substrate specificity of *Arabidopsis thaliana* fatty acid omega-hydroxylase. *Plant Science*, **170**, 326-338.
- Benveniste, I., Tijet, N., Adas, F., Philipps, G., Salaun, J.P. and Durst, F.** (1998) CYP86A1 from *Arabidopsis thaliana* encodes a cytochrome P450-dependent fatty acid omega-hydroxylase. *Biochemical and Biophysical Research Communications*, **243**, 688-693.
- Bernards, M.** (2002) Demystifying suberin. *Canadian Journal of Botany*, **80**, 227-240.
- Bernards, M. and Razem, F.** (2001) The poly(phenolic) domain of potato suberin: a non-lignin cell wall bio-polymer. *Phytochemistry*, **57**, 1115-1122.
- Bernards, M.A., Fleming, W.D., Llewellyn, D.B., Priefer, R., Yang, X.L., Sabatino, A. and Plourde, G.L.** (1999) Biochemical characterization of the suberization-associated anionic peroxidase of potato. *Plant Physiology*, **121**, 135-145.

Bernards, M.A. and Lewis, N.G. (1992) Alkyl ferulates in wound healing potato tubers. *Phytochemistry*, **31**, 3409-3412.

Bernards, M.A. and Lewis, N.G. (1997) Induced phenylpropanoid metabolism in suberizing potato tubers. *Plant Physiology*, **114**, 2-2.

Bernards, M.A., Lopez, M.L., Zajicek, J. and Lewis, N.G. (1995) Hydroxycinnamic acid-derived polymers constitute the polyaromatic domain of suberin. *Journal of Biological Chemistry*, 7382-7386.

Bernards, M.A., Summerhurst, D.K. and Razem, F.A. (2004) Oxidases, peroxidases and hydrogen peroxide: The suberin connection. *Phytochemistry Reviews*, **3**, 113-126.

Berridge, M.V., Tan, A.S., McCoy, K.D. and Wang, R. (1996) The biochemical and cellular basis of cell proliferation assays that use tetrazolium salts. *Biochemica*, **4**, 15-20.

Bessire, M., Chassot, C., Jacquat, A.C., Humphry, M., Borel, S., Petetot, J.M., Metraux, J.P. and Nawrath, C. (2007) A permeable cuticle in Arabidopsis leads to a strong resistance to Botrytis cinerea. *EMBO J*, **26**, 2158-2168.

Bewley, J.D. (1997) Seed germination and dormancy. *Plant Cell*, **9**, 1055-1066.

Bird, D., Belsson, F., Brigham, A., Shin, J., Greer, S., Jetter, R., Kunst, L., Wu, X., Yephremov, A. and Samuels, L. (2007) Characterization of Arabidopsis ABCG11/WBC11, an ATP binding cassette (ABC) transporter that is required for cuticular lipid secretion. *Plant Journal*.

Blee, E. and Schubert, F. (1993) Biosynthesis of Cutin Monomers - Involvement of a Lipoxygenase Peroxygenase Pathway. *Plant Journal*, **4**, 113-123.

Body, D.R. (1984) Branched-chain fatty acids. In *CRC Handbook of Chromatography, Lipids* (H.K., M. ed, pp. 24`-275.

Boesewinkel, F. and Bouman, F. (1995) Seed structure and functions. In *Seed development and germination* (Galili, J.K.a.G. ed. New York: Marcel Dekker, Inc., pp. 1-24.

Bonaventure, G., Belsson, F., Ohlrogge, J. and Pollard, M. (2004) Analysis of the aliphatic monomer composition of polyesters associated with Arabidopsis epidermis: occurrence of octadeca-cis-6, cis-9-diene-1,18-dioate as the major component. *Plant Journal*, **40**, 920-930.

Bonaventure, G., Salas, J.J., Pollard, M.R. and Ohlrogge, J.B. (2003) Disruption of the FATB gene in Arabidopsis demonstrates an essential role of saturated fatty acids in plant growth. *Plant Cell*, **15**, 1020-1033.

- Boom, A., Damste, J.S.S. and de Leeuw, J.W.** (2005) Cutan, a common aliphatic biopolymer in cuticles of drought-adapted plants. *Org Geochem*, **36**, 595-601.
- Borchert, R.** (1974) Wound-Induced DNA-Synthesis as a Prerequisite for De Novo Synthesis of Certain Isoperoxidases in Potato. *Plant Physiology*, 60-60.
- Borchert, R.** (1978) Time Course and Spatial-Distribution of Phenylalanine Ammonia-Lyase and Peroxidase-Activity in Wounded Potato-Tuber Tissue. *Plant Physiology*, **62**, 789-793.
- Broun, P., Poindexter, P., Osborne, E., Jiang, C.Z. and Riechmann, J.L.** (2004) WIN1, a transcriptional activator of epidermal wax accumulation in Arabidopsis. *Proc Natl Acad Sci U S A*, **101**, 4706-4711.
- Brown, D.M., Zeef, L.A., Ellis, J., Goodacre, R. and Turner, S.R.** (2005) Identification of novel genes in Arabidopsis involved in secondary cell wall formation using expression profiling and reverse genetics. *Plant Cell*, **17**, 2281-2295.
- Cabello-Hurtado, F., Batard, Y., Salaun, J.P., Durst, F., Plnot, F. and Werck-Reichhart, D.** (1998) Cloning, expression in yeast, and functional characterization of CYP81B1, a plant cytochrome P450 that catalyzes in-chain hydroxylation of fatty acids. *Journal of Biological Chemistry*, **273**, 7260-7267.
- Cai, X., Davis, E.J., Ballif, J., Liang, M., Bushman, E., Haroldsen, V., Torabinejad, J. and Wu, Y.** (2006) Mutant identification and characterization of the laccase gene family in Arabidopsis. *Journal of Experimental Botany*, **57**, 2563-2569.
- Candler, J.W., Abrams, S.R. and Bartels, D.** (1997) The effect of ABA analogs on callus viability and gene expression in *Craterostigma plantagineum*. *Physiolgia Plantarum*, **99**.
- Chevenet, F., Brun, C., Banuls, A.L., Jacq, B. and Christen, R.** (2006) TreeDyn: towards dynamic graphics and annotations for analyses of trees. *BMC Bioinformatics*, **7**, 439.
- Christie, W.W.** (1982) A simple procedure for rapid transmethylolation of glycerolipids and cholesteryl esters. *Journal of Lipid Research*, **23**, 1072-1075.
- Christie, W.W.** (1991) Gas chromatographic analysis of fatty acid methyl esters with high precision. *Lipid Technology*, **3**, 97-98.
- Christie, W.W.** (2003) *Lipid Analysis, Isolation, Separation, Identification and Structural Analysis of Lipids, Third Ed* Bridgewater, UK: Oily Press.

Clerkx, E.J.M., Blankestijn-De Vries, H., Ruys, G.J., Groot, S.P.C. and Koornneef, M. (2004) Genetic differences in seed longevity of various *Arabidopsis* mutants. *Physiol Plantarum*, **121**, 448-461.

Cochrane, M.P. (1983) Morphology of the Crease Region in Relation to Assimilate Uptake and Water-Loss During Caryopsis Development in Barley and Wheat. *Aust J Plant Physiol*, **10**, 473-491.

Cominelli, E., Sala, T., Calvi, D., Gusmaroli, G. and Tonelli, C. (2007) Over-expression of the *Arabidopsis* AtMYB41 gene alters cell expansion and leaf surface permeability. *Plant Journal*.

Corner, E.J.H. (1976) *The seeds of Dicotyledons*. Cambridge, London, New York, Melbourne: Cambridge University Press.

Cresti, M., Keijzer, C.J., Tiezzi, A., Ciampolini, F. and Focardi, S. (1986) Stigma of *Nicotiana* - Ultrastructural and Biochemical-Studies. *Am J Bot*, **73**, 1713-1722.

Croteau, R. and Kolattuk.Pe (1973) Enzymatic-Synthesis of a Hydroxy Fatty-Acid Polymer, Cutin, by a Particulate Preparation from *Vicia-Faba* Epidermis. *Biochemical and Biophysical Research Communications*, **52**, 863-869.

D'Auria, J.C. (2006) Acyltransferases in plants: a good time to be BAHD. *Current Opinion in Plant Biology*, **9**, 331-340.

D'Auria, J.C. and Gershenzon, J. (2005) The secondary metabolism of *Arabidopsis thaliana*: growing like a weed. *Current Opinion in Plant Biology*, **8**, 308-316.

Dean, B.B. and Kolattukudy, P.E. (1976) Synthesis of suberin during wound-healing in jade leave, tomato fruit, and bean pods. *Plant Physiology*, **58**, 411-416.

Dean, B.B. and Kolattukudy, P.E. (1977) Biochemistry of Suberization - Incorporation of [1-C-14]Oleic Acid and [1-C-14]Acetate into Aliphatic Components of Suberin in Potato-Tuber Disks (*Solanum-Tuberosum*). *Plant Physiology*, **59**, 48-54.

Debeaujon, I. and Koornneef, M. (2000) Gibberellin requirement for *Arabidopsis* seed germination is determined both by testa characteristics and embryonic abscisic acid. *Plant Physiology*, **122**, 415-424.

Debeaujon, I., Leon-Kloosterziel, K.M. and Koornneef, M. (2000) Influence of the testa on seed dormancy, germination, and longevity in *Arabidopsis*. *Plant Physiology*, **122**, 403-413.

del Rio, J.C., Rodriguez, I.M. and Gutierrez, A. (2004) Identification of intact long-chain p-hydroxycinnamate esters in leaf fibers of abaca (*Musa textilis*) using

gas chromatography/mass spectrometry. *Rapid Commun Mass Spectrom*, **18**, 2691-2696.

Dodds, D.R. and Gross, R.A. (2007) Chemistry. Chemicals from biomass. *Science*, **318**, 1250-1251.

Duan, H. and Schuler, M.A. (2005) Differential expression and evolution of the Arabidopsis CYP86A subfamily. *Plant Physiology*, **137**, 1067-1081.

Dubrovsky, J.G., Guttenberger, M., Saralegui, A., Napsucialy-Mendivil, S., Voigt, B., Baluska, F. and Menzel, D. (2006) Neutral red as a probe for confocal laser scanning microscopy studies of plant roots. *Ann Bot-London*, **97**, 1127-1138.

Edgar, R.C. (2004) MUSCLE: multiple sequence alignment with high accuracy and high throughput. *Nucleic Acids Res*, **32**, 1792-1797.

Efremova, N., Schreiber, L., Bär, S., Heldmann, I., Huijser, P., Wellesen, K., Schwarz-Sommer, Z., Saedler, H. and Yephremov, A. (2004) Functional conservation and maintenance of expression pattern of *FIDDLEHEAD*-like genes in Arabidopsis and Antirrhinum. *Plant Molecular Biology*, **56**, 821-837.

Eglinton, G. and Hunneman, D.H. (1968) Gas Chromatographic-Mass Spectrometric Studies of Long Chain Hydroxy Acids .I. Constituent Cutin Acids of Apple Cuticle. *Phytochemistry*, **7**, 313-&.

Esau, K. (1977). In *Anatomy of seed Plants*. New York: John Wiley & Sons.

Espelie, K.E., Davis, R.W. and Kolattukudy, P.E. (1980) Composition, ultrastructure and function of the cutin- and suberin-containing layers in the leaf, fruit peel, juice-sac and inner seed coat of the grapefruit (*Citrus paradisi* Macf.). *Planta*, **149**, 498-511.

Espelie, K.e., Dean, B.B. and Kolattukudy, P.e. (1979) Composition of lipid-derived polymers from different anatomical regions of several plant species. *Plant Physiology*, **64**, 1089-1093.

Espelie, K.E., Franceschi, V.R. and Kolattukudy, P.E. (1986) Immunocytochemical Localization and Time Course of Appearance of an Anionic Peroxidase Associated with Suberization in Wound-Healing Potato-Tuber Tissue. *Plant Physiology*, **81**, 487-492.

Espelie, K.E. and Kolattukudy, P.E. (1979) Composition of the aliphatic components of suberin of the endodermal fraction from the first internode of etiolated *Sorghum* seedlings. *Plant Physiology*, **63**, 433-435.

- Espelie, K.E. and Kolattukudy, P.E.** (1985) Purification and characterization of an abscisic acid-inducible anionic peroxidase associated with suberization in potato (*Solanum tuberosum*). *Archives of Biochemistry and Biophysics*, **240**, 539-545.
- Fang, X., Qiu, F., Yan, B., Wang, H., Mort, A. and Stark, R.** (2001) NMR studies of molecular structure in fruit cuticle polyesters. *Phytochemistry*, **57**, 1035-1042.
- Fazary, A.E. and Ju, Y.H.** (2007) Feruloyl esterases as biotechnological tools: current and future perspectives. *Acta Bioch Bioph Sin*, **39**, 811-828.
- Fehling, E. and Mukherjee, K.D.** (1991) Acyl-CoA elongase from a higher plant (*Lunaria annua*): metabolic intermediates of very-long-chain acyl-CoA products and substrate specificity. *Biochim Biophys Acta*, **1082**, 239-246.
- Felsenstein, J.** (1989) PHYLIP -- Phylogeny Inference Package (Version 3.2). *Cladistics* **5**: 164-166, 5.
- Franke, R., Briesen, I., Höfer, R. and Schreiber, L.** (2006) FAE genes encoding β -ketoacyl-CoA-synthases involved in root suberin biosynthesis. In *17th International Symposium on Plant Lipids*, Michigan State University, East Lansing, Michigan pp. 46.
- Franke, R., Briesen, I., Wojciechowski, T., Faust, A., Yephremov, A., Nawrath, C. and Schreiber, L.** (2005) Apoplastic polyesters in Arabidopsis surface tissues-A typical suberin and a particular cutin. *Phytochemistry*, **66**, 2643-2658.
- Franke, R. and Schreiber, L.** (2007) Suberin - a biopolyester forming apoplastic plant interfaces. *Curr Opin Plant Biol*, **10**, 252-259.
- Galbiati, M., Simoni, L., Pavesi, G., Cominelli, E., Francia, P., Vavasseur, A., Nelson, T., Bevan, M. and Tonelli, C.** (2007) Gene trap lines identify Arabidopsis genes expressed in stomatal guard cells. *Plant Journal*, Postprint; doi:10.1111/j.1365-3113.2007.03371.x.
- Ghanati, F., Morita, A. and Yokota, H.** (2005) Deposition of suberin in roots of soybean induced by excess boron. *Plant Science*, **168**, 397-405.
- Gil, A.M., Lopes, M.H., Neto, C.P. and Callaghan, P.T.** (2000) An NMR microscopy study of water absorption in cork. *Journal of Materials Science*, **35**, 1891-1900.
- Goldman, M.H.S., Goldberg, R.B. and Mariani, C.** (1994) Female Sterile Tobacco Plants Are Produced by Stigma-Specific Cell Ablation. *Embo Journal*, **13**, 2976-2984.

- Graça, J. and Pereira, H.** (2000a) Diglycerol alkenedioates in suberin: building units of a poly(acylglycerol) polyester. *Biomacromolecules*, **1**, 519-522.
- Graça, J. and Pereira, H.** (2000b) Suberin structure in potato periderm: glycerol, long-chain monomers, and glyceryl and feruoyl dimers. *Journal of Agricultural and Food Chemistry*, **48**, 5476-5483.
- Graça, J. and Santos, S.** (2006a) Glycerol-derived ester oligomers from cork suberin. *Chem Phys Lipids*, **144**, 96-107.
- Graça, J. and Santos, S.** (2006b) Linear aliphatic dimeric esters from cork suberin. *Biomacromolecules*, **7**, 2003-2010.
- Graça, J. and Santos, S.** (2007) Suberin: a biopolyester of plants' skin. *Macromolecular Biosciences*, **7**, 128-135.
- Graça, J., Schreiber, L., Rodrigues, J. and Pereira, H.** (2002) Glycerol and glyceryl esters of omega-hydroxyacids in cutins. *Phytochemistry*, **61**, 205-215.
- Guindon, S. and Gascuel, O.** (2003) A simple, fast, and accurate algorithm to estimate large phylogenies by maximum likelihood. *Syst Biol*, **52**, 696-704.
- Han, J., Ng, S., Li, J., King, A. and Jaworski, J.** (2005) Silencing cytochrome P450 monooxygenases of stigmas in *Petunia hybrida*. In *2005 Biochemistry and Molecular Biology of Plant Fatty Acids and Glycerolipids Symposium*. Stanford Sierra Conference center, Fallen Leaf Lake, CA.
- Haughn, G. and Chaudhury, A.** (2005) Genetic analysis of seed coat development in Arabidopsis. *Trends in Plant Science*, **10**, 472-477.
- Heller, S.R. and Milne, G.W.A.** (1978) EPA/NIH Mass Spectral Data Base. *US Dept. Commerce, National Bureau of Standards*.
- Heredia, A.** (2003) Biophysical and biochemical characteristics of cutin, a plant barrier biopolymer. *Biochimica and Biophysica Acta*, **1620**, 1-7.
- Heumann, H.G.** (1990) A Simple Method for Improved Visualization of the Lamellated Structure of Cutinized and Suberized Plant-Cell Walls by Electron-Microscopy. *Stain Technology*, **65**, 183-187.
- Hoffmann, L., Besseau, S., Geoffroy, P., Ritzenthaler, C., Meyer, D., Lapierre, C., Pollet, B. and Legrand, M.** (2004) Silencing of hydroxycinnamoyl-coenzyme A shikimate/quinate hydroxycinnamoyltransferase affects phenylpropanoid biosynthesis. *Plant Cell*, **16**, 1446-1465.
- Hoffmann, L., Besseau, S., Geoffroy, P., Ritzenthaler, C., Meyer, D., Lapierre, C., Pollet, B. and Legrand, M.** (2005) Acyltransferase-catalysed p-

coumarate ester formation is a committed step of lignin biosynthesis. *Plant Biosystems*, **139**, 50-53.

Hoffmann, L., Maury, S., Martz, F., Geoffroy, P. and Legrand, M. (2003) Purification, cloning, and properties of an acyltransferase controlling shikimate and quinate ester intermediates in phenylpropanoid metabolism. *Journal of Biological Chemistry*, **278**, 95-103.

Hoffmann-Benning, S., Klomparens, K. and Kende, H. (1994) Characterization of growth-related osmophilic particles in corn coleoptiles and deepwater rice internodes. *Ann Bot-London*, **74**, 563-572.

Holloway, P.J. (1984) Cutins and suberins, the polymeric plant lipids. In *CRC Handbook of chromatography, Lipids* (H.K., M. ed, pp. 321-345.

Hooker, T.S., Millar, A.A. and Kunst, L. (2002) Significance of the expression of the CER6 condensing enzyme for cuticular wax production in Arabidopsis. *Plant Physiology*, **129**, 1568-1580.

Iiyama, K., Lam, T.B.T. and Stone, B.A. (1990) Phenolic-Acid Bridges between Polysaccharides and Lignin in Wheat Internodes. *Phytochemistry*, **29**, 733-737.

Imai, H., Ohnishi, M., Kinoshita, M., Kojima, M. and Ito, S. (1995) Structure and Distribution of Cerebroside Containing Unsaturated Hydroxy Fatty-Acids in Plant-Leaves. *Biosci Biotech Bioch*, **59**, 1309-1313.

James, D.W., Jr., Lim, E., Keller, J., Plooy, I., Ralston, E. and Dooner, H.K. (1995) Directed tagging of the Arabidopsis FATTY ACID ELONGATION1 (FAE1) gene with the maize transposon activator. *Plant Cell*, **7**, 309-319.

Jeffree, C.E. (1996) Structure and ontogeny of plant cuticles. In *Plant Cuticles* (G Kerstiens, e. ed. Oxford, UK: BIOS Scientific Publishers . pp. 33–82.

Jen, C.H., Manfield, I.W., Michalopoulos, I., Pinney, J.W., Willats, W.G., Gilmartin, P.M. and Westhead, D.R. (2006) The Arabidopsis co-expression tool (ACT): a WWW-based tool and database for microarray-based gene expression analysis. *Plant Journal*, **46**, 336-348.

Johann, H. (1942) Origin of the suberized semipermeable membrane in the caryopsis of maize. *J. Agr. Res.*, **64**, 275-282.

Kandel, S., Sauveplane, V., Compagnon, V., Franke, R., Millet, Y., Schreiber, L., Werck-Reichhart, D. and Pinot, F. (2007) Characterization of a methyl jasmonate and wounding-responsive cytochrome P450 of Arabidopsis thaliana catalyzing dicarboxylic fatty acid formation in vitro. *FEBS J*, **274**, 5116-5127.

Kannangara, R., Branigan, C., Liu, Y., Penfield, T., Rao, V., Mouille, G., Hofte, H., Pauly, M., Riechmann, J.L. and Broun, P. (2007) The transcription factor WIN1/SHN1 regulates Cutin biosynthesis in *Arabidopsis thaliana*. *Plant Cell*, **19**, 1278-1294.

Kim, H.U., Li, Y. and Huang, A.H. (2005) Ubiquitous and endoplasmic reticulum-located lysophosphatidyl acyltransferase, LPAT2, is essential for female but not male gametophyte development in *Arabidopsis*. *Plant Cell*, **17**, 1073-1089.

Koiwai, K. and Matsuzaki, T. (1988) Hydroxy and normal fatty acid distribution in stigmas of *Nicotiana* and other plants. *Phytochemistry*, **27**, 2827-2830.

Kolattukudy, P. (1984) Biochemistry and function of cutin and suberin. *Canadian Journal of Botany*, 2918-2933.

Kolattukudy, P. (1993) Cuticle and suberin- Extracellular-matrix unique to plants *J Cell Biochem*, 12-12.

Kolattukudy, P. (1996) Biosynthetic pathways of cutin and waxes, and their sensitivity to environmental stresses. In *Plant cuticles - an integrated functional approach* (Kerstiens, G., ed. ed. Oxford, UK: BIOS Scientific Publishers Ltd., pp. 83-108.

Kolattukudy, P.E. (1977) Lipid polymers and associated phenols, their chemistry, biosynthesis, and role in pathogenesis. In *The Structure, Biosynthesis, and Degradation of Wood* (FA Loewus, V.R., eds ed. New York.: Plenum Press, pp. 185–246.

Kolattukudy, P.E. (1980a) Biopolyester Membranes of Plants: Cutin and Suberin. *Science*, **208**, 990-1000.

Kolattukudy, P.E. (1980b) Cutin, suberin, and waxes. In *The Biochemistry of Plants. A Comprehensive Treatise*. (Stumpf PK., e. ed. London: Academic Press, pp. 571–645.

Kolattukudy, P.E. (1981) Structure, Biosynthesis, and Biodegradation of Cutin and Suberin. *Annu Rev Plant Phys*, **32**, 539-567.

Kolattukudy, P.E. (2001a) Polyesters in higher plants. *Advances in Biochemical Engineering/Biotechnology* **71**, 1-49.

Kolattukudy, P.E. (2001b) Cutin from Plants in Biopolymers (Wiley-VCH ed. Munster, Germany, pp. 1-35.

Kolattukudy, P.E., Croteau, R. and Walton, T.J. (1975) Biosynthesis of Cutin - Enzymatic Conversion of Omega-Hydroxy Fatty-Acids to Dicarboxylic-Acids by Cell-Free-Extracts of *Vicia-Faba* Epidermis. *Plant Physiology*, **55**, 875-880.

Kolattukudy, P.E. and Espelie, K.E. (1985) Biosynthesis of cutin, suberin, and associated waxes. In *Biosynthesis and biodegradation of wood components* (Higuchi, T. ed. Orlando, Fla., pp. 161-207.

Kolattukudy, P.E., Walton, T.J. and Kushwaha, R.P. (1973) Biosynthesis of the C18 family of cutin acids: omega-hydroxyoleic acid, omega-hydroxy-9,10-epoxystearic acid, 9,10,18-trihydroxystearic acid, and their delta12-unsaturated analogs. *Biochemistry*, **12**, 4488-4498.

Kunst, L., Clemens, S. and Hooker, T. (2000) Expression of the wax-specific condensing enzyme CUT1 in Arabidopsis. *Biochem Soc Trans*, **28**, 651-654.

Kunst, L., Samuels, A.L. and Jetter, R. (2005) The plant cuticle: formation and structure of epidermal surfaces. In *Plant lipids- Biology, utilisation and manipulation* (Murphy, D. ed. Oxford, UK: Blackwell, pp. 270-302.

Kunst, L., Taylor, D.C. and Underhill, E.W. (1992) Fatty-Acid Elongation in Developing Seeds of Arabidopsis-Thaliana. *Plant Physiology and Biochemistry*, **30**, 425-434.

Kurdyukov, S., Faust, A., Nawrath, C., Bar, S., Voisin, D., Efremova, N., Franke, R., Schreiber, L., Saedler, H., Metraux, J.P. and Yephremov, A. (2006a) The epidermis-specific extracellular BODYGUARD controls cuticle development and morphogenesis in Arabidopsis. *Plant Cell*, **18**, 321-339.

Kurdyukov, S., Faust, A., Trenkamp, S., Bar, S., Franke, R., Efremova, N., Tietjen, K., Schreiber, L., Saedler, H. and Yephremov, A. (2006b) Genetic and biochemical evidence for involvement of HOTHEAD in the biosynthesis of long-chain alpha-omega-dicarboxylic fatty acids and formation of extracellular matrix. *Planta*, 1-15.

Lam, T.B.T., Iiyama, K. and Stone, B.A. (1992) Cinnamic Acid Bridges between Cell-Wall Polymers in Wheat and Phalaris Internodes. *Phytochemistry*, **31**, 1179-1183.

Lapierre, C., Monties, B. and Rolando, C. (1986) Preparative Thioacidolysis of Spruce Lignin - Isolation and Identification of Main Monomeric Products. *Holzforschung*, **40**, 47-50.

Le Bouquin, R., Skrabs, M., Kahn, R., Benveniste, I., Salaun, J.P., Schreiber, L., Durst, F. and Pinot, F. (2001) CYP94A5, a new cytochrome P450 from *Nicotiana tabacum* is able to catalyze the oxidation of fatty acids to the omega-alcohol and to the corresponding diacid. *European Journal of Biochemistry*, **268**, 3083-3090.

Lepiniec, L., Debeaujon, I., Routaboul, J.M., Baudry, A., Pourcel, L., Nesi, N. and Caboche, M. (2006) Genetics and biochemistry of seed flavonoids. *Annu Rev Plant Biol*, **57**, 405-430.

- Lequeu, J., Fauconnier, M., Chammaï, A., Bronner, R. and Blée, E.** (2003) Formation of plant cuticle: evidence for the occurrence of the peroxygenase pathway. *Plant Journal*, **36**, 155-164.
- Li, Y., Beisson, F., Koo, A.J., Molina, I., Pollard, M. and Ohlrogge, J.** (2007a) Identification of acyltransferases required for cutin biosynthesis and production of cutin with suberin-like monomers. *P Natl Acad Sci USA*, **104**, 18339-18344.
- Li, Y., Beisson, F., Ohlrogge, J. and Pollard, M.** (2007b) Monoacylglycerols are components of root waxes and can be produced in the aerial cuticle by ectopic expression of a suberin-associated acyltransferase. *Plant Physiology*, **144**, 1267-1277.
- Li, Y., Beisson, F., Pollard, M. and Ohlrogge, J.** (2006) Oil content of Arabidopsis seeds: the influence of seed anatomy, light and plant-to-plant variation. *Phytochemistry*, **67**, 904-915.
- Lisso, J., Steinhäuser, D., Altmann, T., Kopka, J. and Müssig, C.** (2005) Identification of brassinosteroid-related genes by means of transcript co-response analyses. *Nucleic Acids Res*, **33**, 2685-2696.
- Liu, Z.H., Shao, M., Cai, R.X. and Shen, P.** (2006) Online kinetic studies on intermediates of laccase-catalyzed reaction in reversed micelle. *J Colloid Interface Sci*, **294**, 122-128.
- Lolle, S.J., Cheung, A.Y. and Sussex, I.M.** (1992) Fiddlehead: an Arabidopsis mutant constitutively expressing an organ fusion program that involves interactions between epidermal cells. *Dev Biol*, **152**, 383-392.
- Lu, F.C. and Ralph, J.** (1997) DFRC method for lignin analysis. 1. New method for beta aryl ether cleavage: Lignin model studies. *Journal of Agricultural and Food Chemistry*, **45**, 4655-4660.
- Ma, F., Cholewa, E., Mohamed, T., Peterson, C.A. and Gilzen, M.** (2004) Cracks in the palisade cuticle of soybean seed coats correlate with their permeability to water. *Annals of Botany*, **94**, 213-228.
- Ma, F. and Peterson, C.** (2003) Current insights into the development, structure, and chemistry of the endodermis and exodermis of roots. *Canadian Journal of Botany*, **81**, 405-421.
- Markham, J.E., Li, J., Cahoon, E.B. and Jaworski, J.G.** (2006) Separation and identification of major plant sphingolipid classes from leaves. *Journal of Biological Chemistry*, **281**, 22684-22694.
- Martin, J.T. and Juniper, B.E.** (1970) *The cuticles of plants* New York: St. Martins Press.

Matsuzaki, T., Koiwai, A. and Kawashima, N. (1983a) Isolation of Tetraacyl, Pentaacyl, Hexaacyl and Heptaacyl Glycerides From Stigmas of *Nicotiana-Tabacum*. *Agr Biol Chem Tokyo*, **47**, 77-82.

Matsuzaki, T., Koiwai, A. and Kawashima, N. (1983b) Changes in Stigma-Specific Lipids of Tobacco Plant During Flower Development. *Plant and Cell Physiology*, **24**, 207-213.

Metz, J.G., Pollard, M.R., Anderson, L., Hayes, T.R. and Lassner, M.W. (2000) Purification of a Jojoba Embryo Fatty Acyl-Coenzyme a Reductase and Expression of Its Cdna in High Erucic Acid Rapeseed. *Plant Physiology*, **122**, 635-644.

Millar, A.A. and Kunst, L. (1997) Very-long-chain fatty acid biosynthesis is controlled through the expression and specificity of the condensing enzyme. *Plant J*, **12**, 121-131.

Mohan, R., Bajar, A.M. and Kolattukudy, P.E. (1993) Induction of a tomato anionic peroxidase gene (tap1) by wounding in transgenic tobacco and activation of tap1/GUS and tap2/GUS chimeric gene fusions in transgenic tobacco by wounding and pathogen attack. *Plant Mol Biol*, **21**, 341-354.

Moire, L., Schmutz, A., Buchala, A., Stark, R.E. and Ryser, U. (1999) Glycerol is a suberin monomer. New experimental evidence for an old hypothesis. *Plant Physiology*, **119**, 1137-1146.

Moise, J.A., Han, S., Gudynaite-Savitch, L., Johnson, D.A. and Miki, B.L.A. (2005) Seed coats: Structure, development, composition, and biotechnology. *In Vitro Cell Dev-Pl*, **41**, 620-644.

Molina, I., Bonaventure, G., Ohlrogge, J. and Pollard, M. (2006) The lipid polyester composition of *Arabidopsis thaliana* and *Brassica napus* seeds. *Phytochemistry*, **67**, 2597-2610.

Molina, I., Ohlrogge, J. and Pollard, M. (2008) Lipid polyester deposition and localization in developing seeds of *Brassica napus* and *Arabidopsis thaliana*. *Plant J*,

Monties, B. (1989) Lignins. *Methods in Plant Biochemistry*, **1**, 113-157.

Mosle, B., Finch, P., Collinson, M.E. and Scott, A.C. (1997) Comparison of modern and fossil plant cuticles by selective chemical extraction monitored by flash pyrolysis gas chromatography mass spectrometry and electron microscopy. *J Anal Appl Pyrol*, **40-1**, 585-597.

Murphy, R.C. (1993) Mass spectroscopy of lipids. In *Handbook of Lipid Research* (Snyder, F. ed. New York: Plenum Press.

Nakaune, S., Yamada, K., Kondo, M., Kato, T., Tabata, S., Nishimura, M. and Hara-Nishimura, I. (2005) A vacuolar processing enzyme, delta VPE, is involved in seed coat formation at the early stage of seed development. *Plant Cell*, **17**, 876-887.

Nawrath, C. (2002) The biopolymers cutin and suberin. In *The Arabidopsis Book* (Somerville, C.R. and Meyerowitz, E.M. eds). Rockville, MD, doi: 10.1199/tab.0021, www.aspb.org/publications/arabidopsis/: American Society of Plant Biologists, pp. 1-14.

Nawrath, C. (2006) Unraveling the complex network of cuticular structure and function. *Current Opinion in Plant Biology*, **9**, 281-287.

Negruk, V., Yang, P., Subramanian, M., McNevin, J.P. and Lemieux, B. (1996) Molecular cloning and characterization of the CER2 gene of *Arabidopsis thaliana*. *Plant Journal*, **9**, 137-145.

Obayashi, T., Kinoshita, K., Nakai, K., Shibaoka, M., Hayashi, S., Saeki, M., Shibata, D., Saito, K. and Ohta, H. (2007) ATTED-II: a database of co-expressed genes and cis elements for identifying co-regulated gene groups in *Arabidopsis*. *Nucleic Acids Research*, **35**, D863-D869.

Ohlrogge, J. and Browse, J. (1995) Lipid biosynthesis. *Plant Cell*, **7**, 957-970.

Ohnishi, M., Ito, S. and Fujino, Y. (1983) Characterization of Sphingolipids in Spinach Leaves. *Biochimica Et Biophysica Acta*, **752**, 416-422.

Panikashvili, D., Savaldi-Goldstein, S., Mandel, T., Ylifar, T., Franke, R.B., Hofer, R., Schreiber, L., Chory, J. and Aharoni, A. (2007) The *Arabidopsis* DESPERADO/AtWBC11 Transporter is Required for Cutin and Wax Secretion. *Plant Physiology*.

Paul, S., Gable, K., Beaudoin, F., Cahoon, E., Jaworski, J., Napier, J.A. and Dunn, T.M. (2006) Members of the *Arabidopsis* FAE1-like3-ketoacyl-CoA synthase gene family substitute for the Elop proteins of *Saccharomyces cerevisiae*. *Journal of Biological Chemistry*, **281**, 9018-9029.

Penfield, S., Meissner, R.C., Shoue, D.A., Carpita, N.C. and Bevan, M.W. (2001) MYB61 is required for mucilage deposition and extrusion in the *Arabidopsis* seed coat. *Plant Cell*, **13**, 2777-2791.

Persson, S., Wei, H.R., Milne, J., Page, G.P. and Somerville, C.R. (2005) Identification of genes required for cellulose synthesis by regression analysis of public microarray data sets. *P Natl Acad Sci USA*, **102**, 8633-8638.

Pesacreta, T.C. and Hasenstein, K.H. (1999) The internal cuticle of *Cirsium horridulum* (Asteraceae) leaves. *Am J Bot*, **86**, 923.

Pinot, F., Benveniste, I., Salaun, J.P., Loreau, O., Noel, J.P., Schreiber, L. and Durst, F. (1999) Production in vitro by the cytochrome P450CYP94A1 of major C-18 cutin monomers and potential messengers in plant-pathogen interactions: enantioselectivity studies. *Biochemical Journal*, **342**, 27-32.

Pinot, F., Salaun, J.P., Bosch, H., Lesot, A., Mioskowski, C. and Durst, F. (1992) Omega-Hydroxylation of Z9-Octadecenoic, Z9, 10-Epoxystearic and 9,10-Dihydroxystearic Acids by Microsomal Cytochrome P450 Systems from *Vicia-Sativa*. *Biochemical and Biophysical Research Communications*, **184**, 183-193.

Pollard, M., Beisson, F., Li, Y. and Ohlrogge, J. (submitted) Building lipid barriers: structure and biosynthesis of cutin and suberin. *Trends in Plant Science*.

Pruitt, R.E., Vielle-Calzada, J.P., Ploense, S.E., Grossniklaus, U. and Lolle, S.J. (2000) FIDDLEHEAD, a gene required to suppress epidermal cell interactions in *Arabidopsis*, encodes a putative lipid biosynthetic enzyme. *P Natl Acad Sci USA*, **97**, 1311-1316.

Rashotte, A.M., Jenks, M.A. and Feldmann, K.A. (2001) Cuticular waxes on *eceriferum* mutants of *Arabidopsis thaliana*. *Phytochemistry*, **57**, 115-123.

Ray, A.K., Chen, Z.J. and Stark, R.E. (1998) Chemical depolymerization studies of the molecular architecture of lime fruit cuticle. *Phytochemistry*, **49**, 65-70.

Ray, A.K. and Stark, R.E. (1998) Isolation and molecular structure of an oligomer produced enzymatically from the cuticle of lime fruit. *Phytochemistry*, **48**, 1313-1320.

Rechsteiner, M. and Rogers, S.W. (1996) PEST sequences and regulation by proteolysis. *Trends Biochem Science*, **21**, 267-271.

Reina, J.J., Guerrero, C. and Heredia, A. (2007) Isolation, characterization, and localization of AgaSGNH cDNA: a new SGNH-motif plant hydrolase specific to *Agave americana* L. leaf epidermis. *Journal of Experimental Botany*, **58**, 2717-2731.

Reina, J.J. and Heredia, A. (2001) Plant cutin biosynthesis: the involvement of a new acyltransferase. *Trends in Plant Science*, **6**, 296-296.

Riederer, M. and Schreiber, L. (2001) Protecting against water loss: analysis of the barrier properties of plant cuticles. *Journal of Experimental Botany*, **52**, 2023-2032.

Rogers S., Wells R. and M, R. (1986) Amino Acid Sequences Common to Rapidly Degraded Proteins: The PEST Hypothesis. *Science*, **234**, 364-368.

Rupasinghe, S.G., Duan, H. and Schuler, M.A. (2007) Molecular definitions of fatty acid hydroxylases in *Arabidopsis thaliana*. *Proteins-Structure Function and Bioinformatics*, **68**, 279-293.

Ryser, U. (1992) Ultrastructure of the Epidermis of Developing Cotton (*Gossypium*) Seeds - Suberin, Pits, Plasmodesmata, and Their Implication for Assimilate Transport into Cotton Fibers. *Am J Bot*, **79**, 14-22.

Salas, J.J. and Ohlrogge, J.B. (2002) Characterization of substrate specificity of plant FatA and FatB acyl-ACP thioesterases. *Arch Biochem Biophys*, **403**, 25-34.

Sanders, R.J., Ofman, R., Valianpour, F., Kemp, S. and Wanders, R.J. (2005) Evidence for two enzymatic pathways for omega-oxidation of docosanoic acid in rat liver microsomes. *J Lipid Res*, **46**, 1001-1008.

Santos, S. and Graca, J. (2006) Glycerol-omega-hydroxyacid-ferulic acid oligomers in cork suberin structure. *Holzforschung*, **60**, 171-177.

Schmid, M., Davison, T.S., Henz, S.R., Pape, U.J., Demar, M., Vingron, M., Schölkopf, B., Weigel, D. and Lohmann, J. (2005) A gene expression map of *Arabidopsis* development. *Nature Genetics*, **37**, 501-506.

Schmutz, A., Buchala, A.J. and Ryser, U. (1996) Changing the Dimensions of Suberin Lamellae of Green Cotton Fibers with a Specific Inhibitor of the Endoplasmic Reticulum-Associated Fatty Acid Elongases. *Plant Physiology*, **110**, 403-411.

Schmutz, A., Jenny, T., Amrhein, N. and Ryser, U. (1993) Caffeic Acid and Glycerol Are Constituents of the Suberin Layers in Green Cotton Fibers. *Planta*, **189**, 453-460.

Schneitz, K., Hülskamp, M. and Pruitt, R. (1995) Wild-type ovule development in *Arabidopsis thaliana*: a light microscope study of cleared whole-mount tissue. *The Plant Journal*, **7**, 732-749.

Schnurr, J., Shockey, J. and Browse, J. (2004) The acyl-CoA synthetase encoded by LACS2 is essential for normal cuticle development in *Arabidopsis*. *Plant Cell*, **16**, 629-642.

Schreiber, L., Franke, R. and Hartmann, K. (2005) Effects of NO₃ deficiency and NaCl stress on suberin deposition in rhizo- and hypodermal (RHCW) and endodermal cell walls (ECW) of castor bean (*Ricinus communis* L.) roots. *Plant Soil*, **269**, 333-339.

Schuler, M.A. and Werck-Reichhart, D. (2003) Functional genomics of P450s. *Annual Review of Plant Biology*, **54**, 629-667.

Shao, S., Meyer, C.J., Ma, F., Peterson, C.A. and Bernards, M.A. (2007) The outermost cuticle of soybean seeds: chemical composition and function during imbibition. *Journal of Experimental Botany*, **58**, 1071 - 1082.

Sherf, B.A., Bajar, A.M. and Kolattukudy, P.E. (1993) Abolition of an Inducible Highly Anionic Peroxidase-Activity in Transgenic Tomato. *Plant Physiology*, **101**, 201-208.

Shockey, J.M., Fulda, M.S. and Browse, J.A. (2002) Arabidopsis contains nine long-chain acyl-coenzyme A synthetase genes that participate in fatty acid and glycerolipid metabolism. *Plant Physiology*, **129**, 1710-1722.

Sieber, P., Schorderet, M., Ryser, U., Buchala, A., Kolattukudy, P., Metraux, J.P. and Nawrath, C. (2000) Transgenic Arabidopsis plants expressing a fungal cutinase show alterations in the structure and properties of the cuticle and postgenital organ fusions. *Plant Cell*, **12**, 721-738.

Sluszný, C., Yeung, E.S. and Nikolau, B.J. (2005) In-Situ probing of the biotic-abiotic boundary of plants by laser desorption/ionization time-of-flight mass spectrometry. *J Am Soc Mass Spectrom*, **16**, 107-115.

Soler, M., Serra, O., Molinas, M., Huguet, G., Fluch, S. and Figueras, M. (2007) A genomic approach to suberin biosynthesis and cork differentiation. *Plant Physiology*, **144**, 419-431.

Soliday, C.L. and Kolattukudy, P.E. (1977) Biosynthesis of Cutin - Omega-Hydroxylation of Fatty-Acids by a Microsomal Preparation from Germinating Vicia-Faba. *Plant Physiology*, **59**, 1116-1121.

Soliday, C.L., Kolattukudy, P.E. and Davis, R.W. (1979) Chemical and ultrastructural evidence that waxes associated with the suberin polymer constitute the major diffusion barrier to water vapor in potato tuber (*Solanum tuberosum* L.). *Planta*, **146**, 607-614.

Sperling, P., Franke, S., Luthje, S. and Heinz, E. (2005) Are glucocerebrosides the predominant sphingolipids in plant plasma membranes? *Plant Physiology and Biochemistry*, **43**, 1031-1038.

St Pierre, B. and De Luca, V. (2000) Evolution of acyltransferase genes: origin and diversification of the BAHD superfamily of acyltransferases involved in secondary metabolism. In *Recent Advances in Phytochemistry* (Romeo JT, I.R., Varin L, De Luca V. ed: Elsevier Science Ltd., pp. 285-315.

Steinhauser, D., Usadel, B., Luedemann, A., Thimm, O. and Kopka, J. (2004) CSB.DB: a comprehensive systems-biology database. *Bioinformatics*, **20**, 3647-3651.

Suh, M.C., Samuels, A.L., Jetter, R., Kunst, L., Pollard, M., Ohlrogge, J. and Belsson, F. (2005) Cuticular lipid composition, surface structure, and gene expression in *Arabidopsis* stem epidermis. *Plant Physiology*, **139**, 1649-1665.

Swofford, D.L. (2000) *Phylogenetic Analysis Using Parsimony (*and Other Methods)*. Version 4. (Associates, S. ed. Sunderland, Massachusetts).

Tanaka, T., Tanaka, H., Machida, C., Watanabe, M. and Machida, Y. (2004) A new method for rapid visualization of defects in leaf cuticle reveals five intrinsic patterns of surface defects in *Arabidopsis*. *Plant Journal*, **37**, 139-146.

Tang, D.Z., Simonich, M.T. and Innes, R.W. (2007) Mutations in LACS2, a long-chain acyl-coenzyme a synthetase, enhance susceptibility to avirulent *Pseudomonas syringae* but confer resistance to *Botrytis cinerea* in *Arabidopsis*. *Plant Physiology*, **144**, 1093-1103.

Thompson, J.D., Gibson, T.J., Plewniak, F., Jeanmougin, F. and Higgins, D.G. (1997) The CLUSTAL_X windows interface: flexible strategies for multiple sequence alignment aided by quality analysis tools. *Nucleic Acids Research*, **25**, 4876-4882.

Thompson, W.W., Platt-Alola, K. and Koller, W. (1979) Ultrastructure and development of the trichomes of *Larrea* (*Creosote bush*). *Bot Gaz*, **140**, 249-260.

Tijet, N., Helvig, C., Plnot, F., Le Bouquin, R., Lesot, A., Durst, F., Salaun, J.P. and Benveniste, I. (1998) Functional expression in yeast and characterization of a clofibrate-inducible plant cytochrome P-450 (CYP94A1) involved in cutin monomers synthesis. *Biochemical Journal*, **332** (Pt 2), 583-589.

Todd, J., Post-Belittenmiller, D. and Jaworski, J.G. (1999) *KCS1* encodes a fatty acid elongase 3-ketoacyl-CoA synthase affecting wax biosynthesis in *Arabidopsis thaliana*. *Plant Journal*, **17**, 119-130.

Toufighi, K., Brady, S.M., Austin, R., Ly, E. and Provar, N.J. (2005) The Botany Array Resource: e-Northern, Expression Angling, and promoter analyses. *Plant Journal*, **43**, 153-163.

Trenkamp, S., Martin, W. and Tietjen, K. (2004) Specific and differential inhibition of very-long-chain fatty acid elongases from *Arabidopsis thaliana* by different herbicides. *P Natl Acad Sci USA*, **101**, 11903-11908.

Tulloch, A.P. (1964) Gas liquid chromatography of the hydroxy-, acetoxy- and oxo-stearic acid methyl esters. *Journal of the American Oil Chemists' Society* **41**, 833-836.

- Van Caesele, L., Mills, J.T., Sumner, M. and Gillespie, R.** (1981) Cytology of Mucilage Production in the Seed Coat of Candle Canola (*Brassica-Campestris*). *Canadian Journal of Botany-Revue Canadienne De Botanique*, **59**, 292-300.
- Van Caesele, L., Mills, J.T., Sumner, M. and Gillespie, R.** (1982) Cytological study of palisade development in the seed coat of Candle canola. *Canadian Journal of Botany*, **60**, 2469-2475.
- Villena, J.F., Dominguez, E., Stewart, D. and Heredia, A.** (1999) Characterization and biosynthesis of non-degradable polymers in plant cuticles. *Planta*, **208**, 181-187.
- Vogt, E., Schonherr, J. and Schmidt, H.W.** (1983) Water permeability of periderm membranes isolated enzymatically from potato tubers (*Solanum tuberosum* L.). *Planta*, **158**, 294-301.
- Walton, T.J. and Kolattukudy, P.E.** (1972) Determination of the structures of cutin monomers by a novel depolymerization procedure and combined gas chromatography and mass spectrometry. *Biochemistry*, **11**, 1885-1896.
- Wang, G., Cho, Y., Keifer, J., Ohlrogge, J. and Pollard, M.** (2003) The structure and biosynthesis of the lipid polyesters in stigma exudates of tobacco and petunia. In *2003 Biochemistry and Molecular biology of Plant Fatty Acids and Glycerolipids Symposium*. June 4-5, 2003. Fallen Leaf Lake, CA.
- Watson, C.J.W., Froehlich, J.E., Josefsson, C.A., Chapple, C., Durst, F., Benveniste, I. and Coolbaugh, R.C.** (2001) Localization of CYP86B1 in the outer envelope of chloroplasts. *Plant and Cell Physiology*, **42**, 873-878.
- Wei, H., Persson, S., Mehta, T., Srinivasasainagendra, V., Chen, L., Page, G.P., Somerville, C. and Loraine, A.** (2006) Transcriptional coordination of the metabolic network in Arabidopsis. *Plant Physiology*, **142**, 762-774.
- Wellesen, K., Durst, F., Pinot, F., Benveniste, I., Nettesheim, K., Wisman, E., Steiner-Lange, S., Saedler, H. and Yephremov, A.** (2001) Functional analysis of the LACERATA gene of Arabidopsis provides evidence for different robes of fatty acid omega-hydroxylation in development. *P Natl Acad Sci USA*, **98**, 9694-9699.
- Werck-Reichhart, D., Bak, S. and Paquette, S.M.** (2002) Cytochromes P450. In *The Arabidopsis Book* (Somerville, C. and Meyerowitz, E.M. eds). Rockville, MD, doi: 10.1199/tab.0021, www.aspb.org/publications/arabidopsis/: American Society of Plant Biologists.
- Werker, E.** (1997) *Seed anatomy* Berlin, Stuttgart.
- Western, T.L., Burn, J., Tan, W.L., Skinner, D.J., Martin-McCaffrey, L., Moffatt, B.A. and Haughn, G.W.** (2001) Isolation and characterization of

mutants defective in seed coat mucilage secretory cell development in arabidopsis. *Plant Physiology*, **127**, 998-1011.

Western, T.L., Skinner, D.J. and Haughn, G.W. (2000) Differentiation of mucilage secretory cells of the Arabidopsis seed coat. *Plant Physiology*, **122**, 345-355.

Wille, A., Zimmermann, P., Vranova, E., Furholz, A., Laule, O., Bleuler, S., Hennig, L., Prelic, A., von Rohr, P., Thiele, L., Zitzler, E., Gruissem, W. and Buhlmann, P. (2004) Sparse graphical Gaussian modeling of the isoprenoid gene network in Arabidopsis thaliana. *Genome Biology*, **5**, -.

Windsor, J.B., Symonds, V.V., Mendenhall, J. and Lloyd, A.M. (2000) Arabidopsis seed coat development: morphological differentiation of the outer integument. *Plant Journal*, **22**, 483-493.

Winkel, B.S. (2004) Metabolic channeling in plants. *Annual Review of Plant Biology*, **55**, 85-107.

Winkel-Shirley, B. (2001) Flavonoid biosynthesis. A colorful model for genetics, biochemistry, cell biology, and biotechnology. *Plant Physiol*, **126**, 485-493.

Wolters-Arts, M., Van der Weerd, L., Van Aelst, A.C., Van der Weerd, J., Van As, H. and Mariani, C. (2002) Water-conducting properties of lipids during pollen hydration. *Plant Cell Environ*, **25**, 513-519.

Xia, Y., Nikolau, B.J. and Schnable, P.S. (1996) Cloning and characterization of CER2, an Arabidopsis gene that affects cuticular wax accumulation. *Plant Cell*, **8**, 1291-1304.

Xiao, F., Goodwin, S., Xiao, Y., Sun, Z., Baker, D., Tang, X., Jenks, M. and Zhou, J. (2004) Arabidopsis CYP86A2 represses Pseudomonas syringae type III genes and is required for cuticle development. *EMBO Journal*, **23**, 2903-2913.

Yatsu, L.Y., Espelie, K.E. and Kolattukudy, P.E. (1983) Ultrastructural and chemical evidence that the cell wall of green cotton fibers is suberized. *Plant Physiology*, **135**, 521-524.

Yeats, T.H. and Rose, J.K. (2007) The biochemistry and biology of extracellular plant lipid-transfer proteins (LTPs). *Protein Science*.

Yephremov, A., Wisman, E., Huijser, P., Huijser, C., Wellesen, K. and Saedler, H. (1999) Characterization of the FIDDLEHEAD gene of Arabidopsis reveals a link between adhesion response and cell differentiation in the epidermis. *Plant Cell*, **11**, 2187-2201.

- Yu, M.M., Schulze, H.G., Jetter, R., Blades, M.W. and Turner, R.F. (2007)** Raman microspectroscopic analysis of triterpenoids found in plant cuticles. *Appl Spectrosc*, **61**, 32-37.
- Zee, S.Y. and O'Brien, T.P. (1970)** Studies on the ontogeny of the pigment strand in the caryopsis of wheat. *Australian Journal of Biological Science*, **23**, 1153-1171.
- Zheng, Z., Xia, Q., Dauk, M., Shen, W., Selvaraj, G. and Zou, J. (2003)** Arabidopsis AtGPAT1, a member of the membrane-bound glycerol-3-phosphate acyltransferase gene family, is essential for tapetum differentiation and male fertility. *Plant Cell*, **15**, 1872-1887.
- Zimmermann P, Hirsch-Hoffmann M, Hennig L and W, G. (2004)** GENEVESTIGATOR. Arabidopsis Microarray Database and Analysis Toolbox. . *Plant Physiology*, **136**, 2621-2632.
- Zimmermann, P., Hennig, L. and Grissem, W. (2005)** Gene-expression analysis and network discovery using Genevestigator. *Trends Plant Science*, **10**, 407-409.

MICHIGAN STATE UNIVERSITY LIBRARIES



3 1293 02956 8130